CR-120811

VON KARMAN CENTER

SNAP-8 DIVISION

ENGINEERING SUPPORT DOCUMENTATION FOR THE SNAP-8 TURBINE ALTERNATOR ASSEMBLY (LeRC UNIT 4/1)

VOLUME VI

MECHANICAL DESIGN SUPPORT FOR THE SNAP-8 PRE-PROTOTYPE ALTERNATOR (P/N 094162)

A REPORT TO

NATIONAL AERONAUTICS AND SPACE ADMINISTRATION

REPORT NO. 2954 / NOVEMBER 1965 / COPY NO. 3

FACILITY FORM 602

N71-75717 (ACCESSION NUMBER) (THRU)

335 (PAGES) NONE (CODE)

CR-120811 (NASA CR OR TMX OR AD NUMBER) (CATEGORY)

OCT 1971
RECEIVED
NASA STI FACILITY
INPUT BRANCH

AEROJET GENERAL TIRE GENERAL

AEROJET-GENERAL CORPORATION

AZUSA, CALIFORNIA

ENGINEERING SUPPORT DOCUMENTATION FOR THE

SNAP-8 TURBINE ALTERNATOR ASSEMBLY
(LeRC UNIT 4/1)

VOLUME VI: MECHANICAL DESIGN SUPPORT FOR THE
SNAP-8 PREPROTOTYPE ALTERNATOR (P/N 094162)

A REPORT TO

NATIONAL AERONAUTICS AND SPACE ADMINISTRATION

REPORT NO. 2954 DECEMBER 1965

AEROJET-GENERAL CORPORATION
A SUBSIDIARY OF THE GENERAL TIRE & RUBBER COMPANY

CONTRACT FULFILLMENT STATEMENT

This report is submitted as partial fulfillment of National Aeronautics and Space Administration Contract Number 5-417. This volume, Volume VI, is one of six plus an index that comprise the complete report.

MECHANICAL DESIGN SUPPORT FOR THE

SNAP-8 PREPROTOTYPE ALTERNATOR (P/N 094162)

CONTENTS

		PAGE
I.	INTRODUCTION	I-1
II.	ROTOR DESIGN	II-1
III.	BEARING DESIGN	III-1
IV.	SEAL DESIGN	IV-1
V.	FITS AND CLEARANCES, TABLE	V-1
VI.	FIELD COIL FIT	VI-1
VII.	WEIGHT	VII-1
VIII.	MATERIALS	VIII-1
IX.	INSTRUCTION MANUAL	IX-1

I. INTRODUCTION

This volume contains the mechanical design details for the SNAP-8 Preprototype Alternator, P/N 094162, accomplished by the DCM&G Department of the General Electric Company in Erie, Pa. Four (4) of these alternators were built, one of which is installed on TAA P/N 093000-5, S/N A-2, and located at the NASA Lewis Research Center in Cleveland, Ohio.

Included are design calculations for the rotor and complete bearing and seal reports. Tables of fits and clearances, weights and materials used in the mechanical design and construction of this alternator are also a part of this design file.

A complete description, principal of operation, instruction for handling and storage, inspection, maintenance, disassembly, cleaning and testing, generator constants and illustrations are compiled in an instruction manual.

II. ROTOR DESIGN

A. Moment of Inertia of Rotor

B. Shaft Fit

C. Quill Shaft Design

D. Balance Stability of the Rotor

GENERAL ELECTRIC

REV NO.	TITLE: MOMENT OF INERTIA OF ROTOR	CONT ON SHEET 2 SH NO. 1
CONT ON SHEET SH NO.	FIRST MADE FOR SNAP 8 JCM 391 A1	

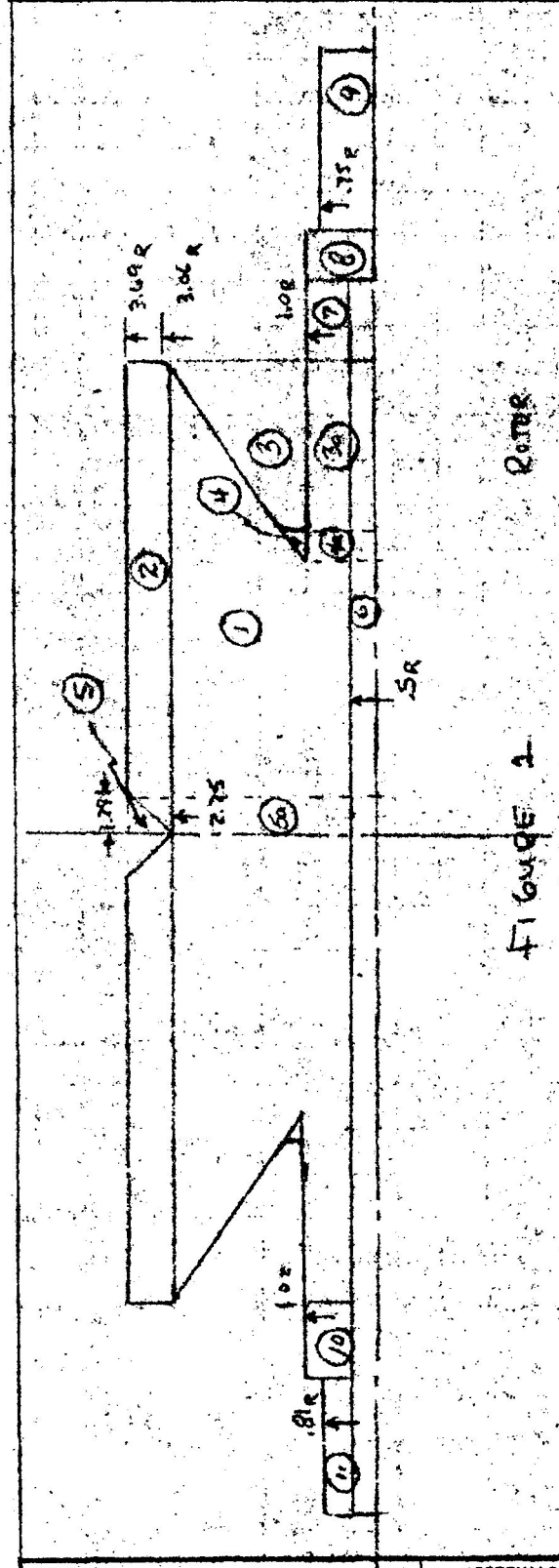

FIGURE 1

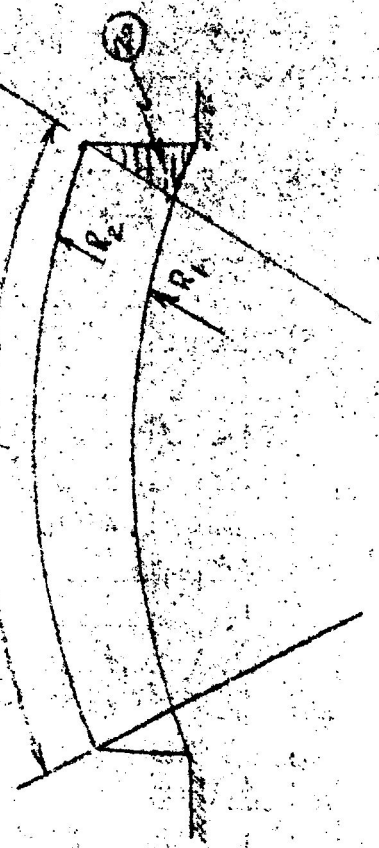

ROTOR END VIEW

FIGURE 2

MADE BY P. S. Yaski	APPROVALS	DIV. OR DEPT.	II 2
ISSUED 8/12/63		LOCATION	CONT ON SHEET SH NO.

VOLUMES ARE OBTAINED FROM WEIGHT CALCULATION

MOMENT OF SECTION (1)

VOLUME = 109.2 in^3

WEIGHT = (109.2 in^3 X .284 lbs/in^3) = 30.8 lb

MOMENT OF INERTIA = $\frac{W D^2}{8}$

where W = WEIGHT

D = OD of SECTION (1)

MOMENT OF INERTIA = $\frac{(30.8)(5.5)^2}{8}$

= 116.2 $lb\text{-}in^2$

MOMENT OF SECTION (2) PLUS (2a)

VOLUME = 30.6 in^3

ADD V_{2a} = 5.75 in^3

∴ TOTAL VOLUME = 36.35 in^3

∴ TOTAL WEIGHT = 36.35 (.284) = 10.3 lb

MOMENT = $\frac{W}{8}(D_1^2 + D_2^2)$

where

D_1 = OUTSIDE DIAMETER

D_2 = INSIDE DIAMETER

$$\text{MOMENT} = \frac{10.3}{8}\left(7.38^2 + 5.5^2\right)$$

$$= \frac{10.3}{8}\left(54.5 + 30.2\right)$$

$$= \frac{10.3}{8}\left(84.7\right) = 109 \ \text{lb}\cdot\text{in}^2$$

MOMENT of SECTION (3)

$$\text{VOLUME} = 1.0472\ h\left(R_1^2 + R_1R_2 + R_2^2\right)$$

(FRUSTUM of CONE)

(INCLUDES (3a))

where R_1 = OUTSIDE RADIUS $R_1 = 3.06$
R_2 = INSIDE RADIUS $R_2 = 1.06$
h = WIDTH $h = 2.44$

$$\text{VOLUME} = 1.047\,(2.44)\left(3.06^2 + (3.06)(1.06) + 1.06^2\right)$$

$$= (1.047)(2.44)(9.36 + 3.24 + 1.12)$$

$$= 1.047\,(2.44)(13.72)$$

$$= 35 \ \text{in}^3$$

$$\text{WEIGHT} = 35\ (.284) = 9.95 \ \text{lb}$$

$$\text{MOMENT} = \frac{3\,w\left(R_1^5 - R_2^5\right)}{10\left(R_1^3 - R_2^3\right)}$$

where R_1 = OUTSIDE RADIUS $R_1 = 3.06$
R_2 = INSIDE RADIUS $R_2 = 1.06$

$$\text{MOMENT} = \frac{3(9.95)(3.06^5 - 1.06^5)}{10(3.06^3 - 1.06^3)}$$

$$= \frac{3(9.95)(268 - 1.331)}{10(28.65 - 1.19)}$$

$$= \frac{3(9.95)(266.7)}{10(27.46)}$$

$$= 29 \text{ lb-in}^2$$

SUBTRACT MOMENT of (3a)

$$\text{VOLUME} = \pi R^2 h$$
$$= \pi (1.06)^2 (2.44)$$
$$= \pi (1.12)(2.44)$$
$$= 8.61 \text{ in}^3$$

$$\text{WEIGHT} = 8.61 (.284) = 2.44 \text{ lb}$$

$$\text{MOMENT of (3a)} = \frac{1}{2} WR^2 = \frac{WD^2}{8}$$

$$= \frac{1}{2}(2.44)(1.06^2)$$

$$= 1.368 \text{ lb-in}^2$$

∴ MOMENT of SECTION (5)

$$= 29 - 1.368 = 27.632 \text{ lb-in}^2$$

MOMENT OF SECTION (4)

VOLUME = $1.047\, h\, (R_1^2 + R_1 R_2 + R_2^2)$ $\quad R_1 = 1.47$, $R_2 = 1.06$, $h = .5$

(INCLUDES (4a)) $= 1.047(.5)\left[1.47^2 + 1.06(1.47) + 1.06^2\right]$

$= 1.047(.5)(2.16 + 1.56 + 1.12)$

$= 1.047(.5)(4.84) = 2.53 \text{ in}^3$

WEIGHT $= 2.53\,(.284) = .718$ lb

MOMENT $= \dfrac{3\,w\,(R_1^5 - R_2^5)}{10\,(R_1^3 - R_2^3)}$ $\quad R_1 = 1.47$, $R_2 = 1.06$

$= \dfrac{3(.718)(1.47^5 - 1.06^5)}{10(1.47^3 - 1.06^3)}$

$= \dfrac{3(.718)(6.96 - 1.331)}{10(3.18 - 1.19)}$

$= \dfrac{3(.718)(5.63)}{10(1.99)} = .609$ lb-in^2

SUBTRACT MOMENT OF (4a)

VOLUME $= \pi R^2 h - \pi(1.06^2)(.5)$

$= 1.76 \text{ in}^3$

WEIGHT = 1.76 (.284) = .5 lb

MOMENT = $\frac{WR^2}{2} = \frac{WD^2}{8}$

$= \frac{.5\,(1.06^2)}{2} = .28$ lb-in^2

∴ MOMENT of (4) = .609 − .28 = .329 lb-in^2

MOMENT OF SECTION (5)

VOLUME = $\pi R^2 h$

$= \pi\,(3.69)^2\,(1.29)$

$= \pi\,(13.6)(1.29) = 55.2$ in^3

WEIGHT = 55.2 (.284) = 15.68 lb

MOMENT = $\frac{WR^2}{2} = \frac{15.68\,(3.69)^2}{2}$

$= \frac{15.68}{2}\,(13.6) =$

$= 106.6$ lb-in^2

SUBTRACT MOMENT OF (5a)

VOLUME = $1.047\,h\,(R_1^2 + R_1R_2 + R_2^2)$ $R_1 = 3.69$, $R_2 = 2.75$, $h = 1.29$

$$\text{VOLUME} = 1.047\,(1.29)\left(3.69^2 + 2.75(3.69) + 2.75^2\right)$$

$$= 1.047\,(1.29)\,(13.6 + 10.16 + 7.56)$$

$$= 1.047\,(1.29)\,(31.32) = 42.2 \text{ in}^3$$

$$\text{WEIGHT} = 42.2\,(.284) = 12 \text{ lb}$$

$$\text{MOMENT} = \frac{3\,w\,(R_1^5 - R_2^5)}{10\,(R_1^3 - R_2^3)} \qquad R_1 = 3.69 \quad R_2 = 2.75$$

$$= \frac{.3\,(12)\,(3.69^5 - 2.75^5)}{(3.69^3 - 2.75^3)}$$

$$= \frac{.3\,(12)\,(682 - 157)}{(50.2 - 13.6)}$$

$$= \frac{3.6\,(525)}{36.6} = 51.6 \text{ lb-in}^2$$

MOMENT of (5) $= 106.6 - 51.6 = 55$ lb-in^2

MOMENT of SECTION (6)

$$\text{VOLUME} = 3.6 \text{ in}^3$$

$$\text{WEIGHT} = 3.6\,(.284) = 1.021 \text{ lb}$$

$$\text{MOMENT} = \frac{1}{2} WR^2 = \frac{1.021\,(.5)^2}{2} = .128 \ \text{lb-in}^2$$

TOTAL MOMENT OF ROTOR MINUS SHAFT EXTENSIONS

MOMENTS OF INERTIA OF A SECTION MAY BE ADDED OR SUBTRACTED PROVIDED THE MOMENT IS TAKEN WITH RESPECT TO THE SAME AXIS

ADD MOMENTS	SUBTRACT MOMENTS
$M_1 = 116.2$	$M_3 = 27.632$
$M_2 = 109.0$	$M_5 = 55.0$
$M_4 = .329$	$M_6 = .128$
225.529	82.76

TOTAL MOMENT, = 142.769

DUE TO SYMMETRY DOUBLE THE ABOVE FIGURE

TOTAL MOMENT MINUS SHAFT ENDS = 142.77(2) = 285.54 lb-in²

SHAFT ENDS

MOMENT OF SECTION (7)

VOLUME = 2.66

WEIGHT = 2.66 (.284) = .755

$$\text{MOMENT} = \frac{1}{2} w (R_1^2 + R_2^2) \qquad R_1 = 1, \quad R_2 = .5$$

$$= \frac{1}{2}(.755)(1 + .25)$$

$$= \frac{.755(1.25)}{2} = .472 \text{ lb-in}^2$$

MOMENT OF SECTION (8)

VOLUME = 2.75 in^3

WEIGHT = .78 lb

$$\text{MOMENT} = \frac{1}{2} w R^2 = \frac{.78}{2}(1)^2 = .39 \text{ lb-in}^2$$

MOMENT OF SECTION (9)

VOLUME = 5.06 in^3

WEIGHT = 1.438

$$\text{MOMENT} = \frac{1}{2} w R^2 = \frac{1.438}{2}(.75)^2$$

$$= .719(.562) = .404 \text{ lb-in}^2$$

GENERAL ELECTRIC

REV NO.	TITLE	CONT ON SHEET 11 SH NO.
CONT ON SHEET SH NO.	MOMENT OF INERTIA OF ROTOR	
	FIRST MADE FOR SNAP 8	

MOMENT OF SECTION (10)

VOLUME = 3.53
WEIGHT = 1.001

$$\text{MOMENT} = \frac{1}{2} w (R_1^2 + R_2^2) \qquad R_1 = 1, \; R_2 = .5$$

$$= \frac{1.001}{2}(1^2 + .5^2)$$

$$= \frac{1.001}{2}(1.25) = .626 \text{ lb-in}^2$$

MOMENT OF SECTION (11)

VOLUME = 3.81
WEIGHT = 1.081

$$\text{MOMENT} = \frac{1}{2} w (R_1^2 + R_2^2) \qquad R_1 = .81, \; R_2 = .5$$

$$= \frac{1}{2}(1.081)(.81^2 + .5^2)$$

$$= .5405(.656 + .25)$$

$$= .5405(.906) = .49 \text{ lb-in}^2$$

MADE BY P.S. Naski	APPROVALS	DIV. OR DEPT.	II 11
ISSUED 8/22/63		LOCATION	CONT ON SHEET SH NO.

GENERAL ELECTRIC

REV. NO.

CONT ON SHEET SH NO.

TITLE MOMENT OF INERTIA OF ROTOR

FIRST MADE FOR SNAP 8

CONT ON SHEET F SH NO. 12

TOTAL MOMENT OF INERTIA OF ROTOR WITH RESPECT TO AXIS OF ROTATION.

MOMENT MINUS SHAFT ENDS	=	285.54
M_7	=	.472
M_8	=	.39
M_9	=	.404
M_{10}	=	.626
M_{11}	=	.49

TOTAL MOMENT — 287.922 lb-in²

$$\frac{287.922 \text{ lb-in}^2}{144 \text{ in}^2/\text{ft}^2 \quad 32.2 \text{ ft/sec}^2} = .0621 \text{ lb-ft-sec}^2$$

MADE BY P.S. NASK

ISSUED 8/12/63

APPROVALS

DIV. OR DEPT.

LOCATION

CONT ON SHEET

SH NO.

ne. deflection of the hub of the rotor will be determined by shrinking the spline in the rotor.

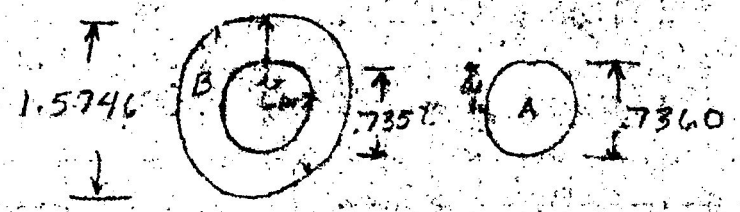

According to Timoshenko, a cylinder subjected to internal pressure, as the case of B, the radial deflection at the inner surface is:

$$(u)_{r=a} = \frac{a P_i}{E}\left(\frac{a^2+b^2}{b^2-a^2} + \mu\right)$$

For a cylinder subjected to external pressure, as is the case of A, the radial deflection is:

$$(u)_{r=a} = -\frac{a P_o}{E}\left(\frac{a^2}{a^2} - \mu\right)$$ for a solid cylinder

The increase in the outer cylinder + the decrease in the inner cylinder must be equal to δ

where $\delta = \frac{.7360 - .7352}{2} = .0004$

and $P_i = P_o = P$ for this case

Therefore

$$\delta = (U)_{r=\omega} - (U)_{r=\omega}$$

$$\delta = \frac{\omega P}{E}\left(\frac{\omega^2+b^2}{b^2-\omega^2} + \cancel{\mu}\right) + \frac{\omega P}{E}(1-\cancel{\mu})$$

solving for P

$$P = \frac{E\delta}{\omega\left(1+\frac{\omega^2+b^2}{b^2-\omega^2}\right)} = \frac{E\delta(b^2-\omega^2)}{2\omega b^2}$$

$$P = \frac{30\times10^6\ \#/in^2\ (.0009\ in)\left[(1.5746)^2-(.7352)^2\right] in^2}{\cancel{2}\ \frac{(.7352)(1.5746)^2}{\cancel{2}\ \cancel{4}}\ in^3\ (4)}$$

$P = 1.28\times10^4$ psi - This is the internal pressure of the inner shaft of the rotor

Now the radial deflection in the O.D of the rotor shaft will be calculated

Using Roark's Eq on pg 276, Case 27

$$\Delta b = P\frac{b}{E}\left[\frac{2\omega^2}{b^2-\omega^2}\right]$$

$$\Delta b = \frac{1.28\times10^4\ psi}{30\times10^6\ psi}\ \frac{(1.5746)\ in}{2}\left[\frac{2(.7352)^2}{\cancel{4}\left[(1.5746)^2-(.7352)^2\right]}\right]$$

$$\Delta b = 2.55\times10^{-4} = .000166$$

The stress concentration factor due to a keyway in the shaft & rotor shaft will be determined

Rotor shaft

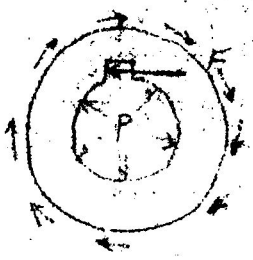

The stresses produced in this shaft are due to
1) The interference fit between spline & outer shaft
2) The Force of the 3/16 in² Key
3) The stress concentration factor due to Keyway.

Due to case 1 the maximum stress occurs at the inner surface:

$D_o = 1.575$, $D_i = .735 + 2\left(\frac{3}{32}\right) \overset{+.04}{} = .963$

From Roark pg 276 Case 27

$$S_{z(max)} = 1.28 \times 10^4 \text{ psi} \frac{\left[\frac{(1.575)^2 + (.963)^2}{4}\right]^{2.39}}{\left[\frac{(1.575)^2 - (.963)^2}{4}\right]^{1.55}} = 2.80 \times 10^4 \text{ psi}$$

Case 1: $S_{z(max)} = 28{,}000$ PSI at inner surface - tension

Due to case 2: The Force will be determined on the keyway, due to the key

$$W = \frac{80\ KW}{.87\ eff} = 92\ KW$$

$$T = \frac{63{,}025\ (hp)}{n}$$

$$\therefore\ T = \frac{63{,}025\ (1\ hp)\ (92\ KW)}{12{,}000\ rpm\ (.746\ KW)} = 648\ in\text{-}lb$$

$$T = \frac{648\ in\text{-}\#}{12\ in/ft} = 54\ ft\text{-}\#$$

Now the distance from the center of the shaft at which the force acts is r

where $r = \frac{.735}{2} + \frac{3/32}{2} = .414\ in$

The Force is

$$F = \frac{648\ in\text{-}\#}{.414\ in} = 1570\ \#$$

Use a key length of 3 7/8 in.

$\therefore$ The Force will be acting over a length of 3 7/8" and this will be assumed as the portion in tension for a worst case.

Now looking at the stressed keyway as if it were rolled out

GENERAL ELECTRIC

REV NO.	TITLE SNAP-8	CONT ON SHEET	SH NO. 5
Aug 27, 1963			
CONT ON SHEET / SH NO.	FIRST MADE FOR Stress concentration in shaft		

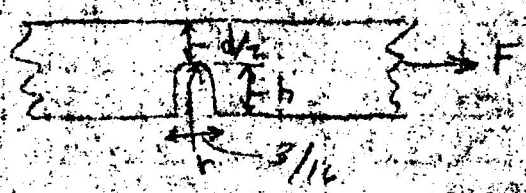

Using a value of $h = 3/32 + .02$, $d/2 = \frac{1.575 - .863}{2} = .306''$

$S = \frac{F}{A} = \frac{1570\ \#}{3.875\ in(.306\ in)} = 1320\ psi$ - tension

The total stress acting on this member in tension is:

$S_T = 1320 + 28{,}000 = 29{,}320\ psi$

Now this will be increased as the stress concentration factor covered by Case III is considered

Consider a corner radius:

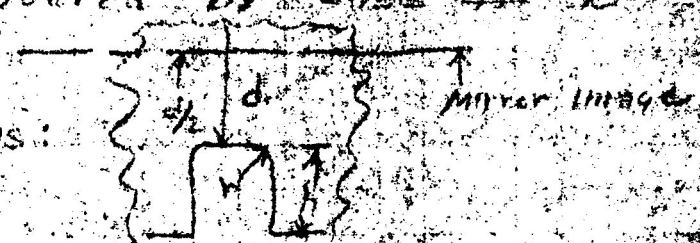

From Roark - pg 392, case 2 in tension:
Consider only half of this case as shown above:

$d = 2(.306) = .612\ in$, $h = .114\ in$

Assume $r = .05$, $\therefore \frac{h}{r} = \frac{.114}{.05} = 2.28$, $\frac{r}{d} = \frac{.05}{.612} = .082$

$K \approx 2.77$ by iteration

$\therefore S_T = 29{,}320\ psi\ (2.77) = 81{,}000\ psi$ Tension

MADE BY	APPROVALS	DIV. OR DEPT.	II 17
ISSUED		LOCATION	CONT ON SHEET / SH NO.

Since the stresses are high, a means of reduction in the key way height will be made.

Minimum limiting dimensions are shown:

$$d/2 + r + 3/64 = \frac{1.5746 - .7352}{2}$$

$$d/2 + r = .3728$$

$$h = r + .0469$$

In order to reduce these stresses, it is advisable to keep d/2 as large as possible and also keep r large.

as $\frac{h}{r} \to 0$ and $\frac{r}{d} \to \infty$, $K \to 1$

$$\therefore \frac{h}{r} = 1 + \frac{.0469}{r}$$

let $r = .05$

$$\frac{h}{r} = 1 + \frac{.0469}{.05} = 1.94 \quad ,$$

$$d = 2(.3728 - r) \quad , \quad d = .6456$$

$$r/d = \frac{.05}{.6456} = .0775$$

From Roark:

$K \approx 2.80$

Referring to pg. 3

Due to case 1

$D_i = 1.575 - .646 = .929$

$S_{2(max)} = 1.28 \times 10^4 \text{ psi} \dfrac{[(1.575)^2 + (.929)^2]}{4[(1.575)^2 - (.929)^2]} = 26,900 \text{ psi}$

This will appear high:

Now let $r = .07$, $d = 2(.3728 - .07) = .6056$

$r/d = \dfrac{.07}{.1456} = .108$

$\dfrac{h}{r} = 1 + \dfrac{.0469}{.07} = 1.67$

$K \approx 2.4$

Due to case 1

$D_i = 1.575 - .6056 = .969$

$S_2 = 1.28 \times 10^4 \text{ psi} \dfrac{[(1.575)^2 + (.969)^2]}{4[(1.575)^2 - (.969)^2]} = 28,600 \text{ psi}$

Now looking at a .0004 fit, and referring to the previous analysis

$P = 1.28 \times 10^4 \left(\frac{.0002}{.0004}\right) = 6.4 \times 10^3$ psi – internal pressure

Radial deflection in OD of rotor shaft

$\Delta b = .000166 \left(\frac{.0002}{.0004}\right) = .000083$ in.

Now analyzing the following keyway slot.

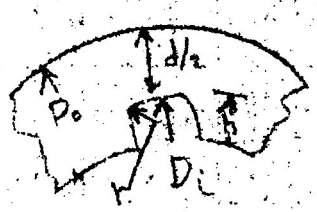

$D_o = 1.575$

let $r = 1/32 = .0313$

let $h = \frac{1}{16} \pm \frac{1}{64} + r$

$h = .0782 + .0313 = .1095$

$D_i = .735 + 2(.1095) = .954$ in

$S_{2(max)} = 6.4 \times 10^3 \dfrac{\left[(1.575)^2 + (.954)^2\right]}{\left[(1.575)^2 - (.954)^2\right]} = 1.385 \times 10^4$ psi

$d/2 = \frac{1.575 - .954}{2} = .310$

Stress due to Force of Key.

$$S = \frac{F}{A} = \frac{1570\ \#}{3.875(.31)\ in^2} = 1310\ psi - Tension$$

Total Stress

$$S_T = 1310 + 13{,}850 = 15{,}160\ psi$$

Stress concentration Factor

$$\frac{h}{r} = \frac{.1095}{.0313} = 3.5$$

$$\frac{r}{d} = \frac{.0313}{.310(2)} = .05$$

From Roark: $K \approx 3.12$

Therefore

$$S_T = 15{,}160\ psi\ (3.12) = 47{,}250\ psi$$

GENERAL ELECTRIC

REV NO.	TITLE	CONT ON SHEET 2 SH NO. 1
	QUILL SHAFT DESIGN	
CONT ON SHEET SH NO.	FIRST MADE FOR SNAP 8	

GIVEN: RATINGS FOR GENERATOR
60 KW
88 KVA
.75 PF
FOR PEAK VALUE
120 KW
176 KVA

MOD. OF ELASTICITY = 29×10^6 PSI
YIELD STRENGTH = 90×10^3 PSI

THE GENERATOR HAS AN EFFICIENCY OF 85%

PROBLEM: DESIGN SHAFT FOR A DEFLECTION OF 2#/.010" AND A MAXIMUM SHEARING STRESS OF 40000 PSI.

$$\Delta_{MAX} = \frac{P L^3}{3 E I}$$

WHERE
Δ_{MAX} = DEFLECTION (IN)
L = LENGTH OF SHAFT
P = lbs
E = MOD OF ELASTICITY
I = MOMENT OF INTERIA
$= \frac{\pi r^4}{4}$
r = RAD. OF SHAFT

$$\frac{L^3}{I} = \frac{(.01)(3)\ 29 \times 10^6}{2}$$

$$\frac{L^3}{r^4} = 29 \times 10^4 \left(\frac{3}{2}\right)\left(\frac{\pi}{4}\right)$$

$$= 34.15 \times 10^4$$

MADE BY P.S. NASK 7/10/63	APPROVALS	DIV. OR DEPT.	II 22
ISSUED		LOCATION	CONT ON SHEET SH NO.

TABLE 1:

r (in)	r^4	L^3	L (in)
.2	.0016	546	8.17
.3	.0081	2.76×10^3	14.04
.375	.01875	6.74×10^3	18.9
.4	.0256	8.74×10^3	20.6
.5	.0625	21.35×10^3	27.7
.6	.1296	44.3×10^3	35.4

∴ FOR A 3/8 IN RADIUS SHAFT (.375) THE LENGTH OF THE SHAFT COULD BE 18.9 IN

CHECKING THE MAXIMUM SHEAR

$$\tau = T \frac{J}{r}$$

J = POLAR MOMENT
τ = SHEARING STRESS

$$J = \frac{\pi d^4}{32}$$

$$T = \frac{\tau \pi d^4}{c(32)} = \frac{\tau \pi (16) r^3}{32}$$

WITH THE OUTPUT OF THE GENERATOR UNDER MAX. CONDITIONS AS 100 KW (DOUBLE LOAD)

THE EQUIVALENT INPUT TO THE GENERATOR

$$\frac{100}{.85} = 141 \text{ KW}$$

CONVERSION TO Hp $\qquad$ 1 KW = 1.341 Hp

$$\therefore \; 141(1.341) = 189.1 \text{ Hp}$$

$$Hp = \frac{2\pi T N}{33\,000} \qquad N = 12000 \text{ RPM}$$

$$T = \frac{(Hp)\; 33 \times 10^3}{2\pi N}$$

$$T = \frac{(189.1)(33) \times 10^3}{6.28\,(12) \times 10^3} = 83 \text{ ft-lbs}$$

USING

$$T = \frac{\tau \pi r^3}{2}$$

WHERE THE ASSUMPTION OF $\tau_{MAX} = 40 \times 10^3$ psi WAS MADE

$$r^3 = \frac{T\,(2)}{\tau \pi}$$

$$= \frac{83\,(2)(12)}{(\pi)(40 \times 10^4)} = 15.88 \times 10^{-3}$$

$$\therefore \; r = .255 \text{ in} \qquad \text{with } 40\,000 \text{ psi}$$

GENERAL ELECTRIC

REV NO.	TITLE	CONT ON SHEET 5	SH NO. 4
	QUILL SHAFT DESIGN		
CONT ON SHEET SH NO.	FIRST MADE FOR SNAP 8		

USING RADIUS of .375 in

$$\sigma = \frac{T(z)}{\pi r^3}$$

$\sigma = 12080$ psi

USING RADIUS of .5 in

$\sigma = 5070$

∴ Quill shaft will have .690" diameter for 17 inch length

MADE BY P. Nasi 7/10/63	APPROVALS	DIV. OR DEPT.	II 25
ISSUED		LOCATION	CONT ON SHEET SH NO.

Sheet 5

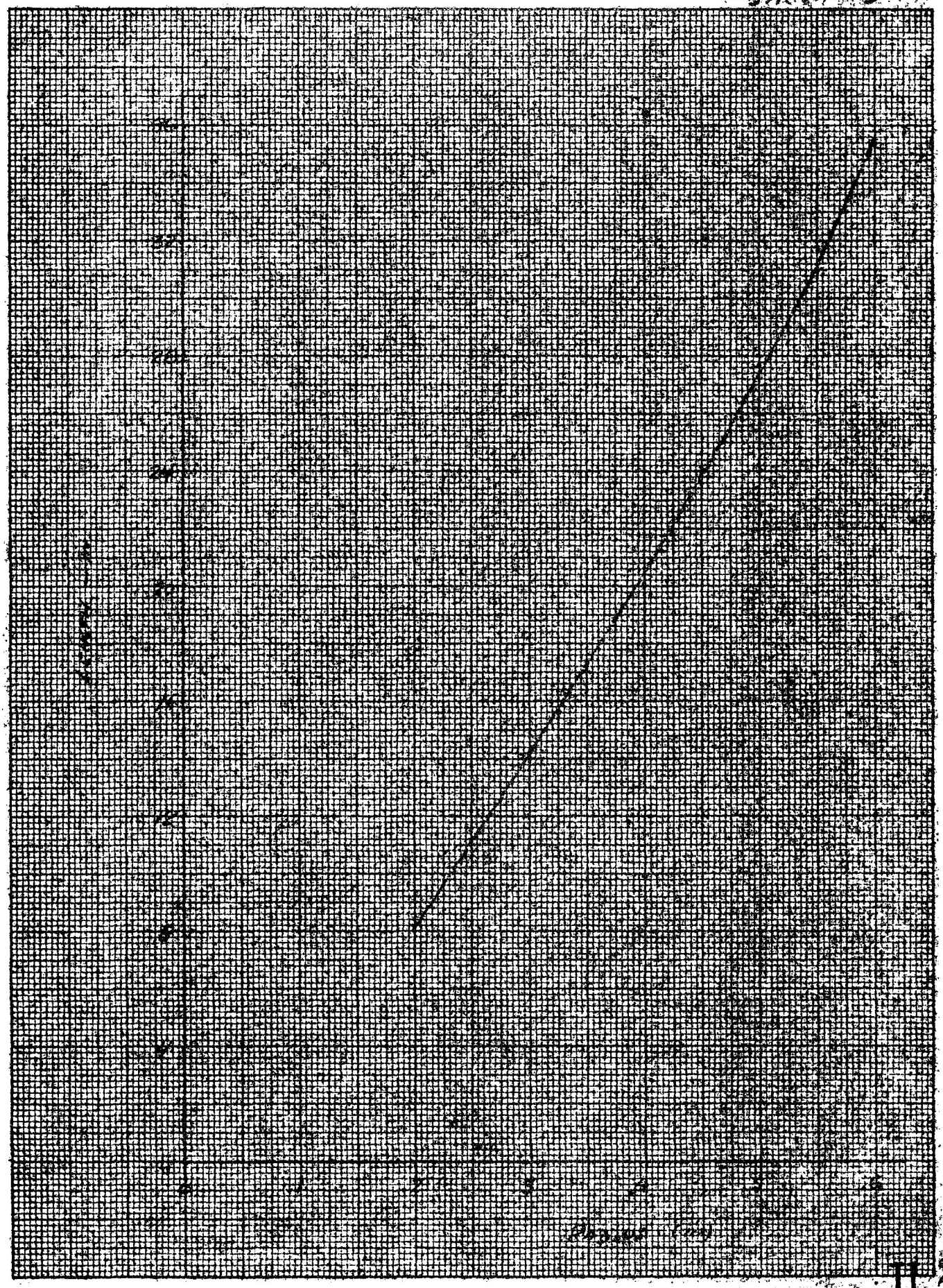

II-D

GENERAL ELECTRIC

SNAP-8

ENGINEERING MEMO

EM NO. E-4-49

RECEIVED
JUN 12 1964
ROTATING MACHINERY

TO: P. H. Hudson/G. Olye
AEROJET GENERAL CORP.
Azusa, California

COPIES: Standard Distribution

DATE: May 28, 1964
PAGE NO. 1 OF 2 PAGES

SUBJECT: AGC LETTER 932:IV:0281
DATED 22 APRIL 1964

This EM is written in reply to the first three items of the subject letter.

1. The balance stability of the rotor after heat treating is verified by spinning the heat treated and balanced rotor for five minutes at 18,000 RPM, 550°F. This is a 50% overspeed condition. After spin testing, the balance of the rotor is checked. No change in balance has been observed in any rotor tested to date.

   The 18,000 RPM overspeed spin test induces stresses in the rotor of 2.25 times those experienced during normal operation at 12,000 RPM. The rotor pole diameters have been measured before and after spin testing and no change in dimension has been observed in any rotor tested to date.

   The maximum calculated stress is only 19,700 psi at 12,000 RPM. This stress occurs at the center hole of the rotor where the yield strength is estimated to be in excess of 70,000 psi at operating temperature.

   At the stress level and temperature at which the rotor operates, creep is not a problem even for annealed carbon steel. The SNAP 8 rotor, therefore, should not have any problem in maintaining stable dimensions for 10,000 hours.

2. The seal weld joint design for the prototype generator has been changed from the design proposed at the February 26, 1964 Design Review. The new design has a trepanned weld preparation on the ADE end shield which will require a minimal heat input to achieve the weld and will absorb distortion caused by welding. The DE seal weld design has also changed in coordination with Aerojet and is comparable with the pre-prototype design as far as dimensional stability is concerned.

II 27

GENERAL ELECTRIC

SNAP-8

ENGINEERING MEMO

EM NO. E-4-49

TO:

COPIES:

SUBJECT:

DATE: May 28, 1964

3. The only damage which has occurred to generator parts during disassembly has been scoring and galling of diameters having tight fits. This has been overcome by the application of a lubricant to these diameters during assembly of the generator. The screw seal collars have been redesigned to permit them to be removed as individual pieces before bearing removal, thereby reducing the removal force required when the bearing is removed. Fixtures are in use which eliminate the requirement that force be transmitted through the bearing balls during disassembly. Inspection of parts after disassembly has not revealed any distortion caused by disassembly procedures.

S. J. Bellows
Aerospace Motor and Generator Product Engineering
Building 3-64B Extension 3153

Reviewed by R. H. Guedet

Reviewed by W. R. David, Jr.

jmb

OLD

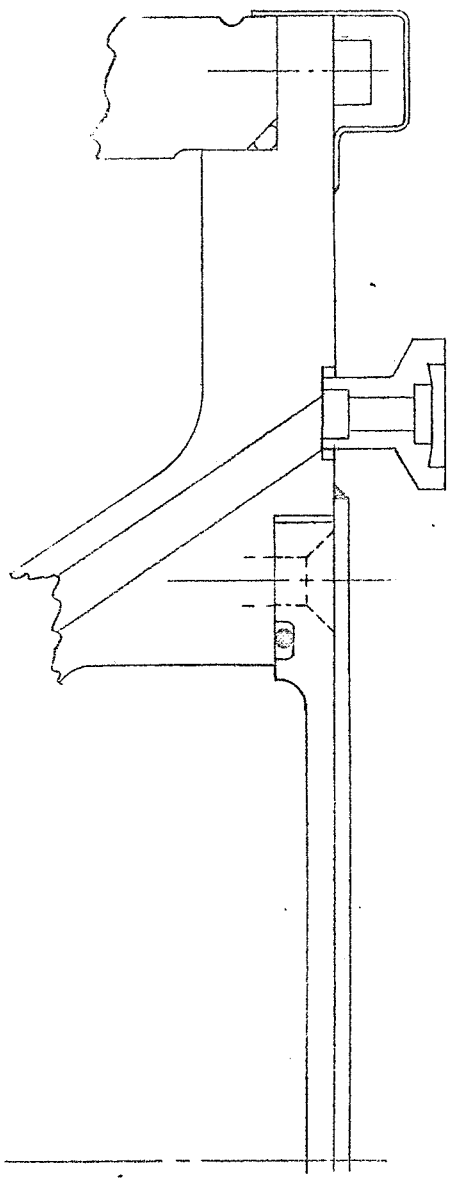

PRESENT

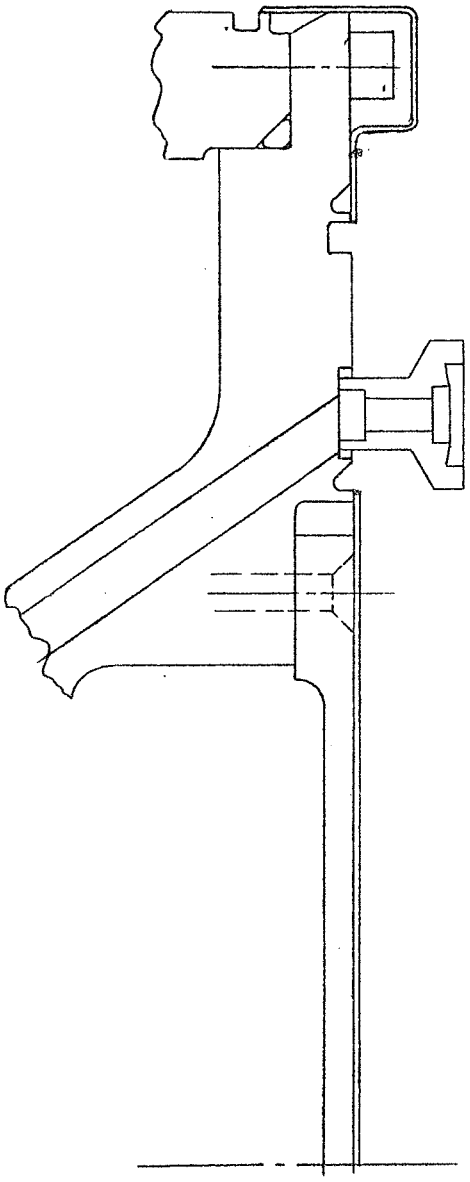

A. [illegible]
[illegible] 1964

II 29

III. BEARING DESIGN

A. AGC Specification 10206, Bearing, Ball, Angular Contact, 40 mm Bore

B. Bearing Evaluation and Critical Speed Calculations for the SNAP-8 Alternator, by J. M. McGrew, General Electric Report No. 64GL125, dated 31 August 1964

C. Bearing Forces Due to Magnetic Eccentricity

AEROJET-GENERAL CORPORATION

CODE IDENT. NO. 70143

AGC-10206A
11 November 1964
Superseding
AGC-10206
28 June 1963

DEVELOPMENT

PRODUCT SPECIFICATION

BEARING, BALL, ANGULAR CONTACT, 40 mm BORE

1. SCOPE

1.1 This specification establishes the requirements for a light series, 40 millimeter (mm) bore, single row, angular contact ball bearing, hereinafter referred to as the bearing.

2. APPLICABLE DOCUMENTS

2.1 Department of Defense documents.- Unless otherwise specified, the following documents, listed in the issue of the Department of Defense Index of Specifications and Standards in effect on the date of invitation for bids, shall form a part of this specification to the extent specified herein.

SPECIFICATIONS

Military

MIL-L-6085	Lubricating Oil, Instrument, Aircraft, Low Volatility
MIL-I-6868	Inspection Process, Magnetic Particle
MIL-H-6875	Heat Treatment of Steels, Aircraft Practice, Process for

STANDARDS

Military

MIL-STD-10	Surface Roughness, Waviness, and Lay
MIL-STD-105	Sampling Procedures and Tables for Inspection

MIL-STD-130	Identification Marking of U.S. Military Property

(Copies of documents required by contractors in connection with specific procurement functions should be obtained as indicated in the Department of Defense Index of Specifications and Standards.)

2.2 Other documents.- Unless otherwise specified, the following documents, of the issue in effect on the date of invitation for bids, shall form a part of this specification to the extent specified herein.

SPECIFICATIONS

Society of Automotive Engineers

AMS 4616	Silicon Bronze

(Copies of AMS specifications may be obtained from the Society of Automotive Engineers, 485 Lexington Avenue, New York 17, N. Y.)

STANDARDS

Anti-Friction Bearing Manufacturers Association (AFBMA)

Section No. 3	Bearing Tolerances
Section No. 4	Ball and Roller Bearing Standard Gaging Practices
Section No. 10	Standards for Balls

(Copies of AFBMA standards may be obtained from the Anti-Friction Bearing Manufacturers Association, Inc., 60 East 42nd Street, New York 17, N. Y.)

2.3 Aerojet-General Corporation documents.- Unless otherwise specified, the following documents of the latest issue in effect, shall form a part of this specification to the extent specified herein.

SPECIFICATION

AGC-10354	Steel, Bearing, AISI M50, Requirements for

STANDARD

ASD 5215	Marking, Methods of

DRAWING

095355	Bearing, Ball, Angular Contact

3. REQUIREMENTS

3.1 Deviations.- Deviations from the requirements of this specification and the applicable documents shall not be permitted unless written authorization has been granted to the supplier by the Aerojet-General Corporation (AGC) cognizant engineer. Deviations specified in the procurement documents (see 6.2) shall constitute such authorization.

3.2 Materials.- The materials used in the manufacture of the bearing shall be of the highest available quality, consistent with the requirements of maximum fatigue life.

3.2.1 Rings and balls.- The inner and outer rings and the balls shall be made of consumable electrode vacuum remelted AISI M-50 high speed steel in accordance with Specification AGC-10354. The rings of each bearing shall be fabricated from material processed in a single heat. Similarly, the balls of each bearing shall be fabricated from material processed in a single heat. Each bearing serial number and the corresponding material heat numbers shall be recorded and certified by the supplier (see 4.5). Classification of the material as to melt type and number of vacuum remelt cycles shall be specified in the procurement document (see 6.2).

3.2.1.1 Heat treatment.- The rings and balls shall be uniformly through hardened and triple tempered to 63 through 65 on the Rockwell C scale in accordance with Specification MIL-H-6875 and the best commercial practice for high-grade aircraft and missile bearings. The heat treatment procedure shall be such that the microstructure shall be homogeneous and the amount of retained austenite shall be a minimum consistent with the specified hardness.

III 4

3.2.2 Separator.- The ball separator shall be made of Iron-Silicon-Bronze material in accordance with Specification AMS-4616, or equivalent.

3.3 Design.- The basic design of the bearing shall be a single-row, angular contact ball bearing, separable under hand pressure, with the low, non-thrust shoulder in the inner ring, and with an outer-ring-piloted ball separator of one-piece construction. Dimensions shall be in accordance with Drawing 095355 and as specified herein.

3.3.1 Size and internal geometry.- The basic size and internal geometry of the bearing shall be as follows:

(a)	Basic size: Bore 40 mm (1.5748 inch) Outside diameter 80 mm (3.1496 inches) Width 18 mm (0.7087 inch)	
(b)	Number of balls - 13	
(c)	Nominal ball diameter - 15/32 inch	
(d)	Inner race curvature (nominal)	52%
(e)	Outer race curvature (nominal)	53%
(f)	Initial contact angle (reference)	16 degrees
(g)	Separator configuration	See 3.3.1.1

3.3.1.1 Separator configuration.- The basic design of the ball separator shall be a one-piece, light-weight construction, piloted on the inside diameter of the outer ring. The ball-spacing portion of the separator shall extend below the pitch circle of the bearing. The design shall permit jet impingement of lubricant directly on the low, non-thrust shoulder of the inner ring and on the ball area below the

bearing pitch circle, and shall not unduly restrict lubricant flow through the bearing. Neither side of the separator shall extend beyond the ring faces when maximum working clearances are taken up in either axial direction. Additional specific design and piloting features, dimensions, tolerances, clearances, concentricities, roundness, surface roughness, and method of fabrication shall be specified by the supplier. A drawing of the separator defining the configuration, all nominal dimensions, and the material shall be submitted to the AGC cognizant engineer for approval prior to fabrication.

3.3.2 Tolerances.- Except as otherwise specified herein and on Drawing 095355, tolerances shall be in accordance with the Annular Bearings Engineers Committee (ABEC) Class 7, as specified in AFBMA Standard, Section No. 3.

(a) Inner ring maximum radial run-out: 0.0001 inch (see 4.3.5.1)

(b) Outer ring maximum radial run-out: 0.00015 inch (see 4.3.5.2)

(c) Ball tolerances shall be equivalent to Grade 5 as specified in AFBMA Standard, Section No. 10

(d) Roundness of inner ring bore, outer ring outside diameter, inner ring raceway, and outer ring raceway: each within 0.0001 inch

(e) Inner race curvature radius: $\pm$ 0.001 inch

(f) Outer race curvature radius: $\pm$ 0.002 inch

(g) Bore and outside diameter taper, maximum: 0.0001 inch of diameter per inch of length

3.3.3 Radial play.- The bearing internal diametral clearance (radial play) shall be 0.0016 through 0.0021 inch under a reversing gage load of $5\frac{1}{2}$ pounds (see 4.3.5.4).

3.3.4 Raceway depths.- The depths of the inner and outer ring ball raceways, and the dimensions related to the low shoulder on the inner ring, shall be specified by the supplier. These dimensions shall be forwarded to the AGC cognizant engineer prior to fabrication for the purpose of coordinating the design of bearing accessory components.

3.3.5 Surface Roughness.- Surface roughness shall be as specified on Drawing 095355, in accordance with Standard MIL-STD-10, and as follows:

(a) Balls: Equivalent to Grade 5 as specified in AFBMA Standard, Section No.10

(b) Inner and outer raceways: Maximum 4 root mean square (rms) microinches

3.3.6 Gaging temperature.- The dimensions and tolerances specified herein and on Drawing 095355 apply at a gaging temperature of $68^{\circ} \pm 5^{\circ}F$.

3.4 Marking and Identification.-

3.4.1 Eccentricity.- The high points of eccentricity of the inner and the outer rings shall be legibly marked with a 1/16 inch diameter burnished spot on that side of the bearing which is opposite to the side having the low, non-thrust shoulder.

3.4.2 Identification of bearing.- The bearing shall be permanently and legibly marked for identification in accordance with Standard MIL-STD-130 using Method C of Standard ASD5215. The identification data applied to the bearing shall be as follows:

(a) AGC Drawing Number 095355, together with revision letter, if any

(b) AGC serial number (see 6.2)

(c) Manufacturer's part number

(d) Manufacturer's name or symbol

(e) Bore and outside diameter calibration code symbol (see 4.4)

3.5 Workmanship.- The workmanship shall be in accordance with the best commercial practice used in the manufacture of high quality, precision bearings for aircraft and missile applications. The bearing shall be free from tool marks, nicks, chatter waves, rust, grinding scratches, pits, or any other defects that may adversely affect its serviceability.

4. QUALITY ASSURANCE PROVISIONS

4.1 Inspection responsibility.- Unless otherwise stated in the procurement document, the supplier shall perform all tests, inspections, examinations and measurements specified herein. The supplier may utilize his own or any other inspection facilities acceptable to AGC. Inspection records of all examinations, measurements and tests shall be certified by the supplier and furnished to AGC with delivery of each bearing (see 4.5). AGC reserves the right to witness any of the inspections performed by the supplier, and to repeat any such inspections at any other test facility or commercial laboratory.

4.2 Test Requirements.-

4.2.1 Ambient conditions.- Unless otherwise specified, all dimensional inspections, examinations and tests shall be performed in air-conditioned, clean surroundings and under the following ambient conditions:

a. Temperature: $68^{\circ} \pm 5^{\circ}F$

b. Relative humidity: 50 percent maximum

All measurements shall be made after the gaging equipment and parts to be measured have been brought to the temperature of the room in which the measurements are to be made.

4.2.2 Acceptance tests.- The bearing shall be subjected to the tests specified in 4.3 to determine conformance to this specification and applicable documents. The methods and procedures shall conform to the best commercial practice used in the quality control and inspection of precision aircraft and missile bearings. Additional tests as deemed necessary shall be left to the discretion of the supplier.

4.3 Test methods.-

4.3.1 Magnetic inspection.- The inner and outer rings of each bearing shall be inspected prior to assembly in accordance with Specification MIL-I-6868.

4.3.2 Balls.- Prior to assembly, each ball shall be non-destructively inspected for surface defects using optical, electronic, or similar methods applicable to precision ball manufacture. Balls having pits, cracks, grind marks, seams, rust, or any other surface blemishes or defects shall be rejected.

4.3.3 Examination of component.- The bearing shall be visually examined, by microscopic means if necessary, for conformance to this specification and applicable documents with respect to dimensions, identification, workmanship, cleanliness, and surface defects. The examination shall be performed on all parts prior to assembly and, to the extent practicable, on the bearing assembly.

4.3.4 Sampling tests.- Tests as specified in (a) through (e) of this paragraph shall be made, employing appropriate sampling methods and acceptable quality levels in accordance with Standard MIL-STD-105.

These sampling procedures shall be submitted to AGC for review, a minimum of two weeks prior to implementation.

(a) The hardness of the balls and the inner and outer race rolling contact areas shall be determined with a standard hardness tester using the Rockwell "C" scale (see 3.2.1.1). Balls and rings used for hardness testing shall not be used in any bearing. All samples used for hardness testing shall be packaged separately, appropriately identified and shipped to AGC with their respective bearing assembly lots.

(b) The surface roughness of balls, rings, and races, shall be measured in accordance with Standard MIL-STD-10 (see 3.3.5) and Drawing 095355.

(c) Ball dimensions, sphericity and size variation shall be measured in accordance with the requirements for Grade 5 balls as specified in AFBMA Standard, Section No. 10.

(d) Inner and outer race curvature radii shall be measured (see 3.3.1 and 3.3.2).

(e) The initial contact angle of the bearing shall be measured after assembly using the indirect method whereby the ratio of separator revolutions to either inner or outer ring revolutions is determined either manually or in an appropriate fixture. An axial thrust load not to exceed 5 pounds shall be applied uniformly to the bearing during the measurement.

4.3.5 Individual tests.- Unless otherwise specified, each bearing shall be measured as specified in 4.3.5.1 through 4.3.5.5 in accordance with AFBMA Standard, Section No. 4. Applicable dimensions and tolerance requirements are specified in 3.3.1, 3.3.2, 3.3.3, 3.3.4 and on Drawing 095355. Prior to testing, the bearing shall be lubricated with light oil in accordance with Specification MIL-L-6085.

4.3.5.1 Inner ring.-

(a) Bore diameter (see 4.4)

(b) Width

(c) Width variation

(d) Radial run-out (use co-axial load method)

(e) Groove run-out with reference side

(f) Reference side run-out with bore

(g) High shoulder diameter

(h) Low shoulder diameter (at side)

(i) Bore roundness

(j) Raceway roundness

(k) Bore taper

4.3.5.2 Outer ring.-

(a) Outside diameter (see 4.4)

(b) Width

(c) Width variation

(d) Radial run-out (use co-axial load method)

(e) Groove run-out with reference side

(f) Outside cylindrical surface run-out with reference side

(g) Shoulder diameter

(h) Outside diameter roundness

(i) Raceway roundness

(j) Outside diameter taper

4.3.5.3 Ring flushness.- The flush condition of the sides of one ring with respect to the corresponding sides of the other ring shall be measured in accordance with Drawing 095355.

4.3.5.4 Radial play.- The bearing internal diametral clearance (radial play) shall be measured using a reversing measuring load of $5\frac{1}{2}$ pounds. The bearing shall be mounted with its axis in a horizontal position and with one of its rings supported to prevent movement. The unsupported ring shall be permitted to float both axially and radially while the specified reversing measuring load moves this member upward and downward. Radial play shall be the total diametrical movement of the unsupported ring when the specified load is reversed, and shall be the average of readings taken at different relative angular positions of the inner ring, outer ring, and balls, with sufficient travel between readings to provide a full rotation of the set of balls.

4.3.5.5 Vibration and noise test.- The over-all functional quality of balls and races shall be determined for each bearing using a vibration and noise tester specified by the supplier. Smoothness of operation, absense of rolling-contact surface defects, and cleanliness of the bearing shall be judged, and acceptance or rejection specified, in accordance with the supplier's (or his designated testing laboratory's) quality standards for reliable, high-grade aircraft and missile bearings.

4.4 Calibration.- The bore and outside diameter of each bearing shall be calibrated or classified for the purpose of selective fitting with the shaft and housing. The bore and outside diameter tolerances shall each be divided into four equal increments and a calibration code established with appropriate symbols designating each calibration group. Data permitting interpretation of the code shall be furnished to AGC with each shipment of bearings.

4.5 Inspection documentation.- The results of all acceptance tests and inspections shall be recorded on data sheets utilizing a format selected by the supplier. At least two certified reproducible copies of the data sheets shall be delivered to AGC with each bearing. The data sheets shall contain, as a minimum, the following:

(a) This specification number, issue, and date.

(b) Drawing Number (095355), title, revision, and date.

(c) AGC serial number of bearing tested

(d) Respective heat numbers of material used for the balls and the rings (see 3.2.1).

(e) Manufacturer's part number

(f) Record of all inspections and tests performed, including those specified under 4.3 and 4.4

(g) Manufacturer's inspection signatures

(h) Signature of AGC-designated representative, if inspection is witnessed.

5. PREPARATION FOR DELIVERY

5.1 Cleaning, preservation and packaging.- Cleaning, preservation and packaging shall be in accordance with the supplier's best commercial practice for precision aircraft and missile bearings.

III 11

5.1.1 Packaging after test.- Each bearing assembly shall be cleaned, treated with preservative, and packaged in a sealed container immediately after completion of the final test. The packaged bearing shall then be processed through a final demagnetization in three axes.

5.2 Packing for delivery.- The packaged bearings shall be packed in a manner to ensure carrier acceptance and safe delivery at destination. Any bearing improperly cleaned, or damaged as a result of improper packaging or packing, may be rejected by AGC. Inspection data sheets (see 4.5) shall be packed with each bearing in a manner to ensure ready and proper identification.

5.3 Marking for shipment.- Marking for shipment shall be at the discretion of the supplier. Markings shall be adequate to ensure proper handling and delivery at destination and shall comply with all applicable carrier regulations.

6. NOTES

6.1 Intended use.- The bearing covered by this specification is intended for use as a component in the turbine-alternator assembly of a nuclear power conversion system.

6.1.2 Nominal operating conditions.- The nominal operating conditions and requirements for the bearing will be in accordance with (a) through (m) of this paragraph.

(a)	Shaft speed	12,000 RPM
(b)	Life, minimum	10,000 hours
(c)	Duty	Continuous
(d)	Reliability, minimum	99.5%
(e)	Spring preload, axial	60 lb
(f)	External thrust load	40 lb
(g)	Radial load	50 lb
(h)	Maximum temperature	300°F
(i)	Lubrication method	Multiple jet
(j)	Lubricant	Organic fluid (3 to 10 centistokes at 210°F)
(k)	Lubricant temperature	210°F

(l) Lubricant flow rate 200 lb/hr/bearing

(m) Radiation dose levels in 10,000 hours:

Fast neutrons	5×10^{12} nvt
Gamma	5×10^{7} rads (c)

6.2 Ordering data.- The procurement document should include the following:

(a) Title, number and date of this specification

(b) Title, number and date of the applicable specification control drawing (see 2.3), including revision letter, if any

(c) Classification of ring and ball material in accordance with Specification AGC-10354.

(d) Deviations, exceptions, or alternates permissible, if any

(e) Responsibility for inspections, if other than supplier

(f) Bearing serialization requirements

(g) AGC receiving inspection requirements

6.3 Precedence.- In the event of conflict between the contract, this specification, and any applicable documents, the following order of precedence shall apply:

(a) The contract

(b) The specification control drawing (see 2.3)

(c) This specification

(d) Other applicable documents (see Section 2)

6.4 Oral statements.- No oral statement by any person shall be allowed to modify or otherwise affect in any manner or degree any part of this specification or any document referred to herein.

Authorized for Release:

R. A. Martin, Head
Specification and Standards
SNAP-8 Division
Von Karman Center

TECHNICAL INFORMATION SERIES

GENERAL ELECTRIC

ADVANCED TECHNOLOGY LABORATORIES

AUTHOR	SUBJECT	NO. 64GL125
J. M. McGrew	Bearings	DATE 8/31/64
TITLE Bearing Evaluation and Critical Speed Calculations for the SNAP-8 Alternator		G.E. CLASS II
		GOVT. CLASS None
REPRODUCIBLE COPY FILED AT G.E. TECHNICAL DATA CENTER BLDG. 5, SCHENECTADY, N. Y.		NO. PAGES 83

SUMMARY

The bearings of the SNAP-8 alternator are evaluated for the loads and operating conditions anticipated for the SNAP-8 power system. The results of the evaluation indicate that the bearings have adequate capacity to meet the 10,000 hour life requirement with 99.5 percent reliability. Computations using calculated bearing stiffness show that the alternator first critical speed is almost twice running speed.

Initial tests indicate a time dependent deterioration of the oil specified for this application. Decision on the use of this oil should be delayed until the cause of this deterioration is determined.

KEY WORDS

Bearing, Alternator, Critical Speed

INFORMATION PREPARED FOR Aerospace Motor and Generator Engineering

TESTS MADE BY H. E. Marx

AUTHOR J. M. McGrew J.M. McGrew

COMPONENT Bearing Laboratory, G. R. Fox, Manager G.R. Fox

APPROVED H. Stern, Manager, Fluids Engineering, MEL H Stern

III 14

Acknowledgement

Acknowledgement is made to Mr. J. E. Lake, who performed the spline and fit calculations and to Mr. R. E. Lee, Jr., and Dr. E. R. Booser, who evaluated the lubricant and bearing materials.

TABLE OF CONTENTS

	Page
NOMENCLATURE	iv
TABLES	vii
FIGURES	viii
I. INTRODUCTION	1
II. BEARING EVALUATION	2
A. Bearing Type and Geometry	2
1. General Information	2
2. Race Curvature	5
3. Contact Angle and Diametral Clearance	6
4. Reduction in Contact Angle due to Press Fit	6
5. Increase in Free Contact Angle due to Preload	6
6. Speed Ratio	9
B. Materials	11
1. Lubricant, Dow ET-378	11
2. Bearing Material	13
C. Bearing Capacity	13
1. Dynamic Capacity	13
2. Static Capacity	14
D. External Loads	14
1. Rotor Weight	15
2. Residual Unbalance	15
a. Balancing Speed	16
b. Unbalance due to Ball Bearing	16
c. Unbalance due to Temperature and Centrifugal Loading Effects	17
3. Magnetic Pull Forces	17
4. Spline Loads	19
E. Shock Loading	20
F. Internal Bearing Loads	20
1. Gyroscopic Moment	20
2. Centrifugal Loads	22

III 16

G. Selection of Preload 23

H. Bearing Equivalent Load 23

1. Parallel Axis Displacement 24
2. Cocked Rotor 25
3. Calculation of Equivalent Load 28

J. Bearing Load Distribution 31

K. Bearing Life 34

L. Other Factors Affecting Bearing Life 36

M. Bearing Mounting and Fits 37

1. Mounting 37
2. Fits 38

N. Bearing Computer Evaluation 40

P. Selection of Preload Spring 58

III. ALTERNATOR CRITICAL SPEEDS 59

IV. OPERATING EXPERIENCE 71

A. Introduction 71

B. Bearing Failure 71

C. Lubricant Deterioration 76

V. CONCLUSIONS AND RECOMMENDATIONS 79

REFERENCES 80

III 17

NOMENCLATURE

A	axial deflection factor
B	total curvature
c	rotor radial clearance
C	basic dynamic capacity
C_o	basic static capacity
d	ball diameter
D	distance between race curvature centers or race diameter
e	rotor eccentricity
E	pitch circle diameter
f	bearing factor
f_c	dynamic bearing factor
f_o	static bearing factor
$\mathcal{F}$	race curvature
F	force
$\mathcal{J}$	load distribution parameter
g_o	gravitational acceleration
G	angular momentum of ball = $I\omega_n$
i	number of rows of balls
I	ball mass moment of inertia
k	spring stiffness
ℓ	length between force and bearing
L	bearing span or bearing life
M	moment or mass of ball
n	number of balls
N	shaft rotational speed, rpm
P	bearing equivalent load
P_o	ball load
P_s	probability of survival

Nomenclature (Continued)

r	radius
R	bearing reaction
T	thrust preload
W	rotor weight
P_D	diametral clearance
ΔP_D	change in diametral clearance
U	unbalance
V	bearing rotation factor
X	bearing radial factor
Y	bearing thrust factor
β	contact angle
δ	deflection
ϵ	eccentricity ratio
μ	coefficient of friction
ω	angular velocity
ψ	angular extent of loaded zone

SUBSCRIPTS

a	axial
b	ball
c	centrifugal
d	diameter
E	electromagnetic
i	inner race
max.	maximum
min.	minimum
o	outer race or initial condition
r	radial
x	x direction
y	y direction
U	unbalance

III 20

LIST OF TABLES

Table No.		Page
1.	Bearing Specification	2
2.	R. C. Rig Test Life	12
3.	Effect of Bearing Material on Fatigue Life	37
4.	Shaft and Housing Fits	40
5.	BEST Program Print Out	44-45
6.	Computer Solution - Case 1	46-47-48
7.	Computer Solution - Case 2	49-50-51
8.	Computer Solution - Case 3	52-53-54
9.	Computer Solution - Case 4	55-56-57
10.	Summary of Bearing Stiffness	62
11.-17.	Rotor Mode Shapes for Various Bearing Stiffnesses	64-70

LIST OF FIGURES

Figure No.		Page
1.	Cut-Away Drawing of Alternator	3
2.	Bearing Dimensions	4
3.	Free Contact Angle vs Diametral Clearance	7
4.	Reduction in Diametral Clearance and Contact Angle vs Interference	8
5.	Contact Angle and Axial Deflection vs Spring Preload	10
6.	Magnetic Pull Forces vs Eccentricity	18
7.	Illustration of Gyroscopic Moment	21
8.	Load Orientation - Case 1	25
9.	Load Orientation - Case 2	27
10.	Load Distribution Parameter vs Loaded Zone Parameter	32
11.	Computer Calculation Model	42
12.	Critical Speed Calculation Model	60
13.	Critical Speed vs Bearing Stiffness	63
14.	Temperature History Prior to Bearing Failure	72
15.	Photograph of Failed Bearing	74
16.	Photographic Comparison of New and Old Oil	77

III 22

I. INTRODUCTION

The SNAP-8* electrical generating system is a light weight power supply intended for space operation. It is designed to deliver 35 Kwe.

The power is generated by a three-phase, 400 cycle alternator driven by a turbine which operates on a mercury vapor Rankine cycle. The alternator operates on a conventional ball bearing lubricated and cooled with an organic lubricant, Dow ET-378, polyphenyl ether.

The design and manufacture of the alternator is being carried out by the General Electric Aerospace Motor and Generator Department under contract to Aerojet General Corporation (AGC). The bearing type and lubricant have been specified by AGC in order to attain parts conformity between the turbine and the alternator. Since the alternator operating conditions and bearing loads differ from those found in the turbine, it has been necessary to evaluate the specified bearing and lubricant for the loads and operating conditions existing in the alternator. This report summarizes the results of this evaluation.

---

*Systems for Nuclear Auxiliary Power

II. BEARING EVALUATION

Figure 1 is a cutaway drawing of the alternator. The rotor is mounted on two 208 J type angular contact type bearings. A DB type mount is used with the bearing contact angles diverging. The rotor is driven through a flexible quill - spline connection.

The lubricant oil is jetted on the bearing through a multiple jet ring. Oil is also jetted on the shaft, inboard of the bearings, to remove the heat arising from the pole face electrical losses.

A. Bearing Type and Geometry

A-1. General Information

The type of bearing defined in the specification (Reference 21) is the type normally chosen for high-speed, high-temperature operation. The low shoulder on the inner ring permits the use of the outer ring riding, one-piece separator. Pertinent operating data taken from the specification are shown in Table 1. The bearing internal dimensions as supplied by Industrial-Tectonics, the vendor, are shown in Figure 2.

Table 1

From AGC Specification 10206

Bearing Geometry

208 bearing
80 mm OD 40 mm ID
18 mm width No. of balls - 13
Ball diam. - .46875 in.
Inner race curvature - .52
Outer race curvature - .53
Contact angle, 16°
ABEC-7 Class

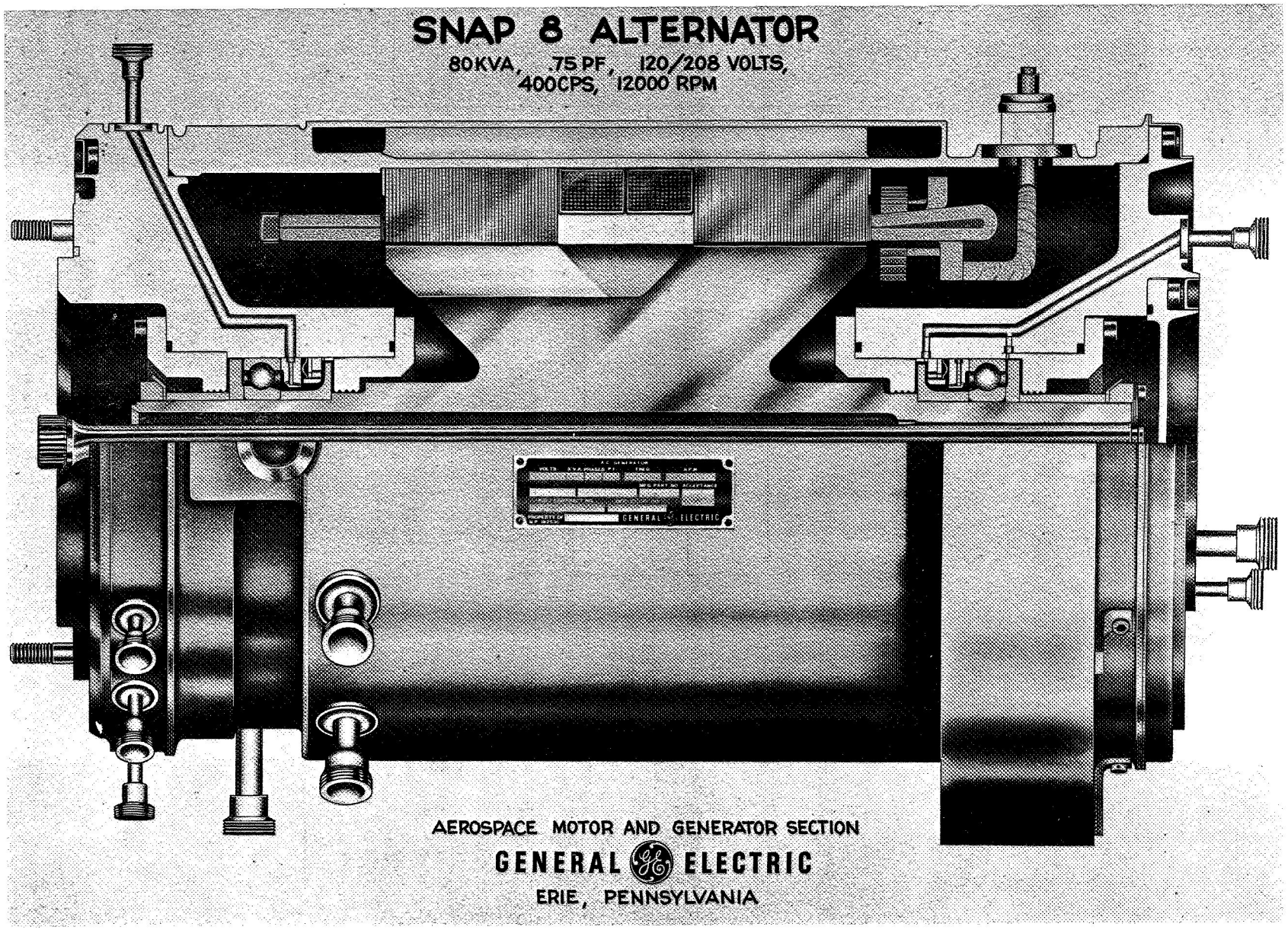

Figure 1. Cut-Away Drawing of Alternator
R&U Erie Photo DC-1197

BEARING DIMENSIONS

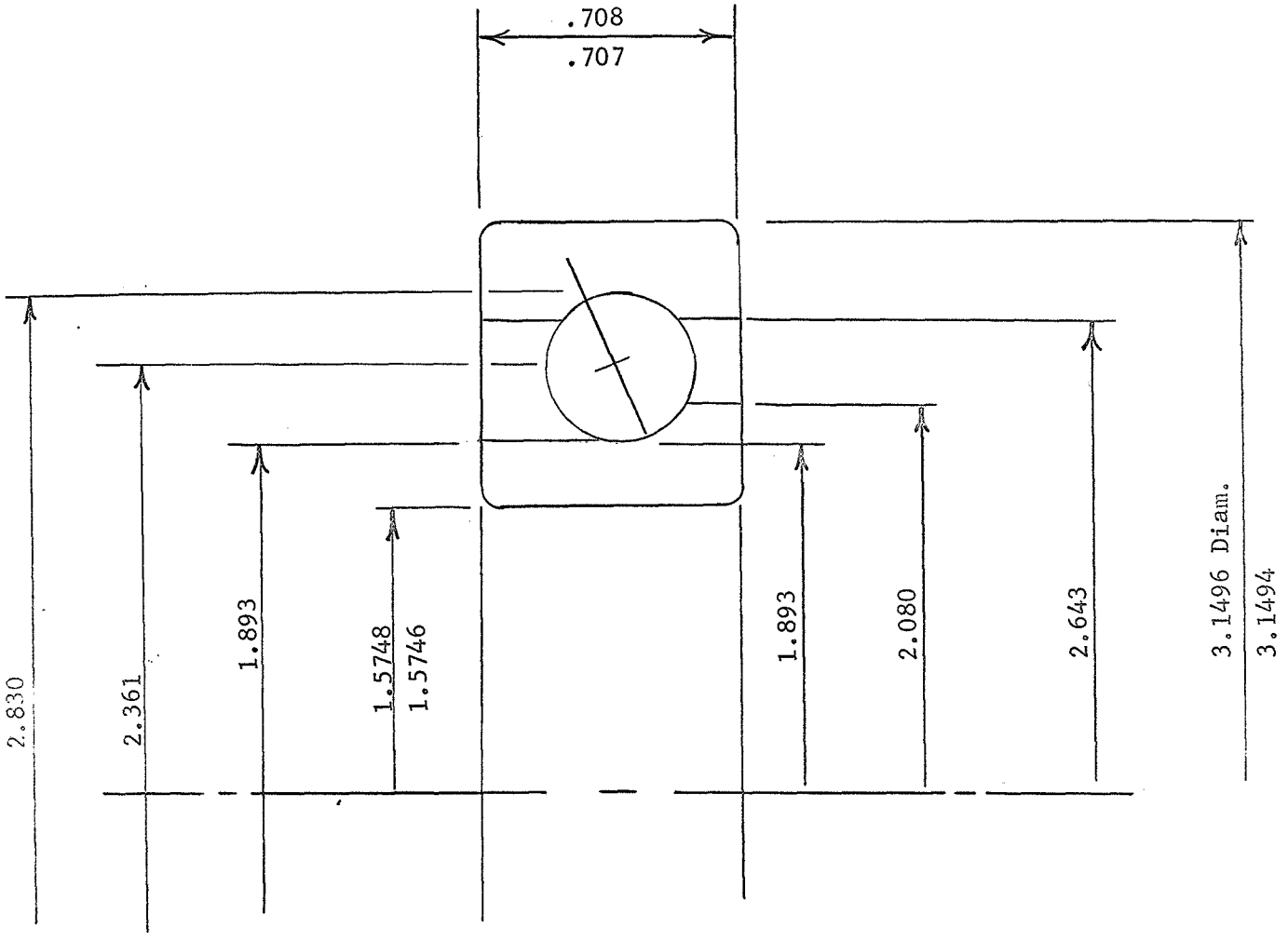

Dimensions in inches.

Reference:
Industrial Tectonics
Drawing 7007

Figure 2

Table 1 (continued)

Alternator Operation Conditions

Speed 12,000 rpm Life - 10,000 hours
Bearing Reliability - 99.5%
Lubricant - Dow ET-378 or equivalent
Temp. in - 210°F
Flow - 3.33 lb./min./brg.

A-2. Race Curvature

The race curvature is a measure of the conformity of the race to the ball in a plane passing through the bearing axis and transverse to the raceway. The curvature of the race is defined by:

$$\mathcal{F} = \frac{r}{d} \tag{1}$$

The distance between the centers of curvatures of the two races is fixed by the race radii and the ball diameter, and is given by:

$$D = r_o + r_i - d \tag{2}$$

or,

$$D = Bd \tag{3}$$

where,

$$B = (\mathcal{F}_o + \mathcal{F}_i - 1) \tag{4}$$

Using the dimensions of Figure 2, B, the total curvature is:

$$B = .05$$

And D, the distance between center of curvatures is:

$$D = .0234 \text{ in.} \tag{5}$$

A-3. Contact Angle and Diametral Clearance

The free contact angle is the angle made by a line passing through the points of contact of the ball and both raceways with a plane perpendicular to the axis of the bearing when both races are centered with respect to each other without the application of measurable force. The free contact angle is denoted by β_o and is expressed by:

$$\text{Cos } \beta_o = (2Bd - P_D) / 2Bd \qquad (6)$$

Free contact angle versus diametral clearance for this bearing is shown in Figure 3.

A-4. Reduction in Contact Angle Due to Press Fit

If a bearing is mounted with an interference fit, there is a change in diameter of the press fitted raceway and a corresponding reduction in diametral clearance and free contact angle. The initial mounted contact angle is:

$$\text{Cos } \beta_o' = \text{Cos } \beta_o + \frac{\Delta P_D}{2\ Bd} \qquad (7)$$

where ΔP_D, the reduction in diametral clearances,is:

$$\Delta P_D = \frac{\Delta \text{ x Bore}}{E - d} \qquad (8)$$

Both the initial mounted contact angle, β_o' and the reduction in diametral clearance, ΔP_D, are presented in Figure 4 as a function of the interference.

A-5. Increase in Free Contact Angle Due to Preload

Application of a preload will cause an increase in contact angle. From equation 179 of Reference 13 this increase is given by:

III 23

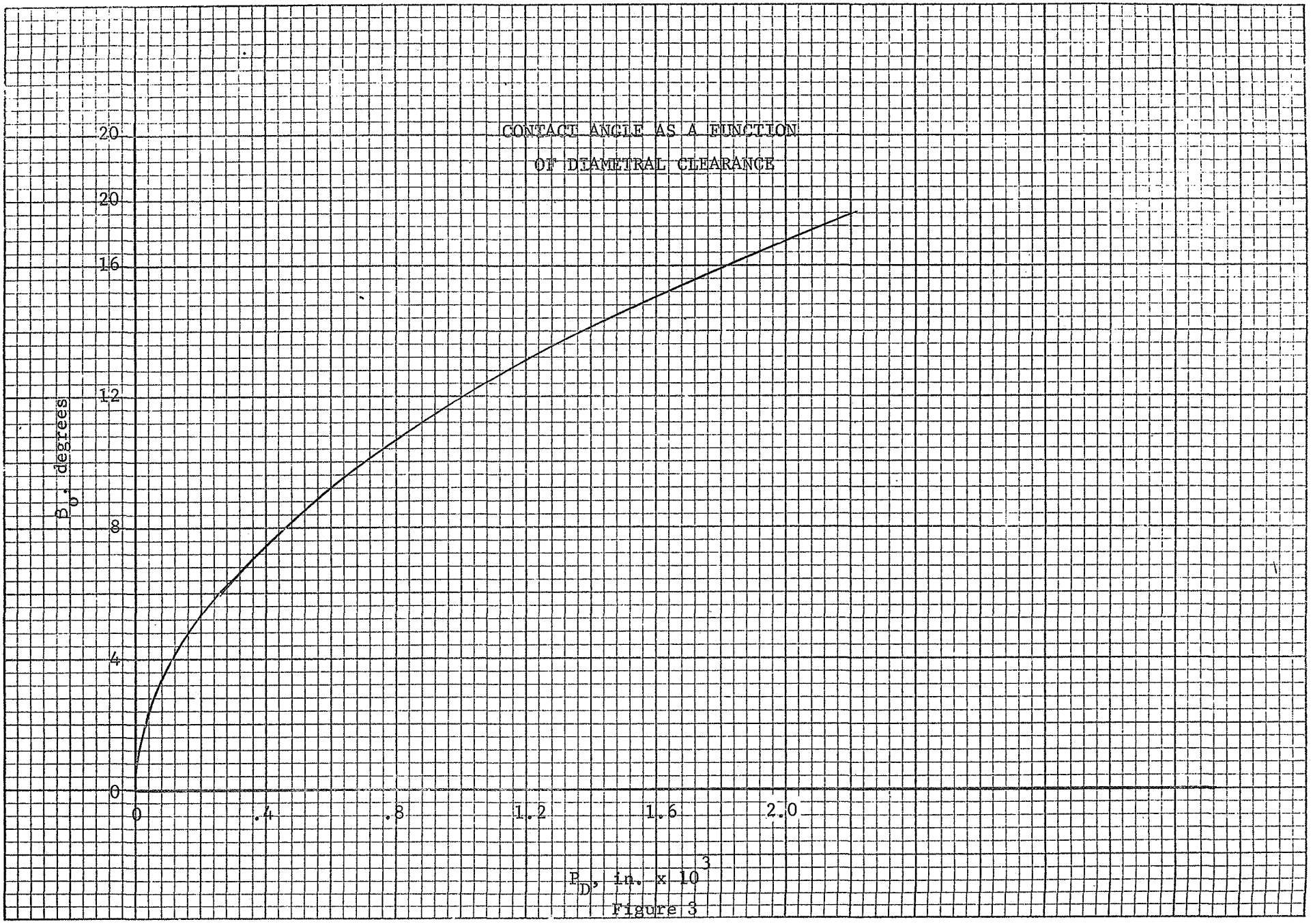
CONTACT ANGLE AS A FUNCTION
OF DIAMETRAL CLEARANCE
20
20
16
12
8
4
0
β_o, degrees
0
.4
.8
1.2
1.6
2.0
P_D, in. x 10^3

Figure 3

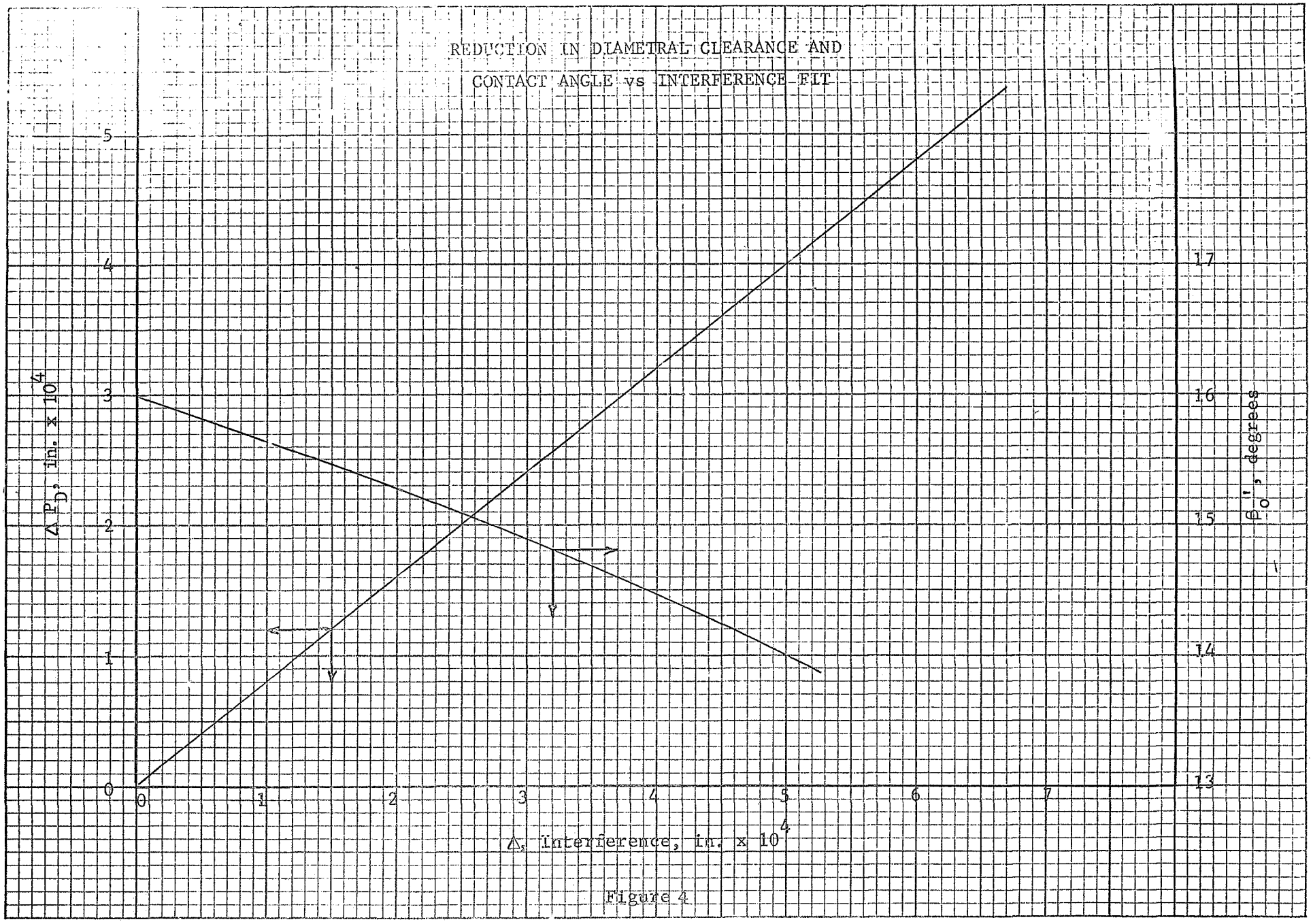

Figure 4

DOC III 8

$$\frac{T_P}{nd^2K} = \text{Sin}\,\beta_1 \left(\frac{\text{Cos}\,\beta_o}{\text{Cos}\,\beta} - 1\right)^{3/2} \tag{9}$$

From equation 186 of the same reference, the axial deflection due to the preload is:

$$\delta = BdA \tag{10}$$

The axial deflection and increase in contact angle versus spring preload appear in Figure 5.

A-6. Speed Ratio

The speed ratio is the ratio of the angular velocity of the pitch circle to the angular velocity of the rotating member. For this bearing at 12,000 rpm:

$$V_i = \pi\, EN_i \left(1 - \frac{d}{E}\,\text{Cos}\,\beta\right) \tag{11}$$

$$V_i = 1,198 \text{ in/sec}$$

and,

$$V_E = 1/2\, V_i = 599 \text{ in/sec.} \tag{12}$$

The speed ratio is:

$$\frac{\omega_E}{\omega_i} = \frac{N_E}{N_i} = \frac{1}{2}\left(1 - \frac{d}{E}\,\text{Cos}\,\beta\right) = .4045 \tag{13}$$

and the angular velocity of the ball is:

$$N_B = \frac{EN_i}{2d}\left[1 - (d/E)^2\,\text{Cos}^2\,\beta\right] = 29,175 \text{ rpm} \tag{14}$$

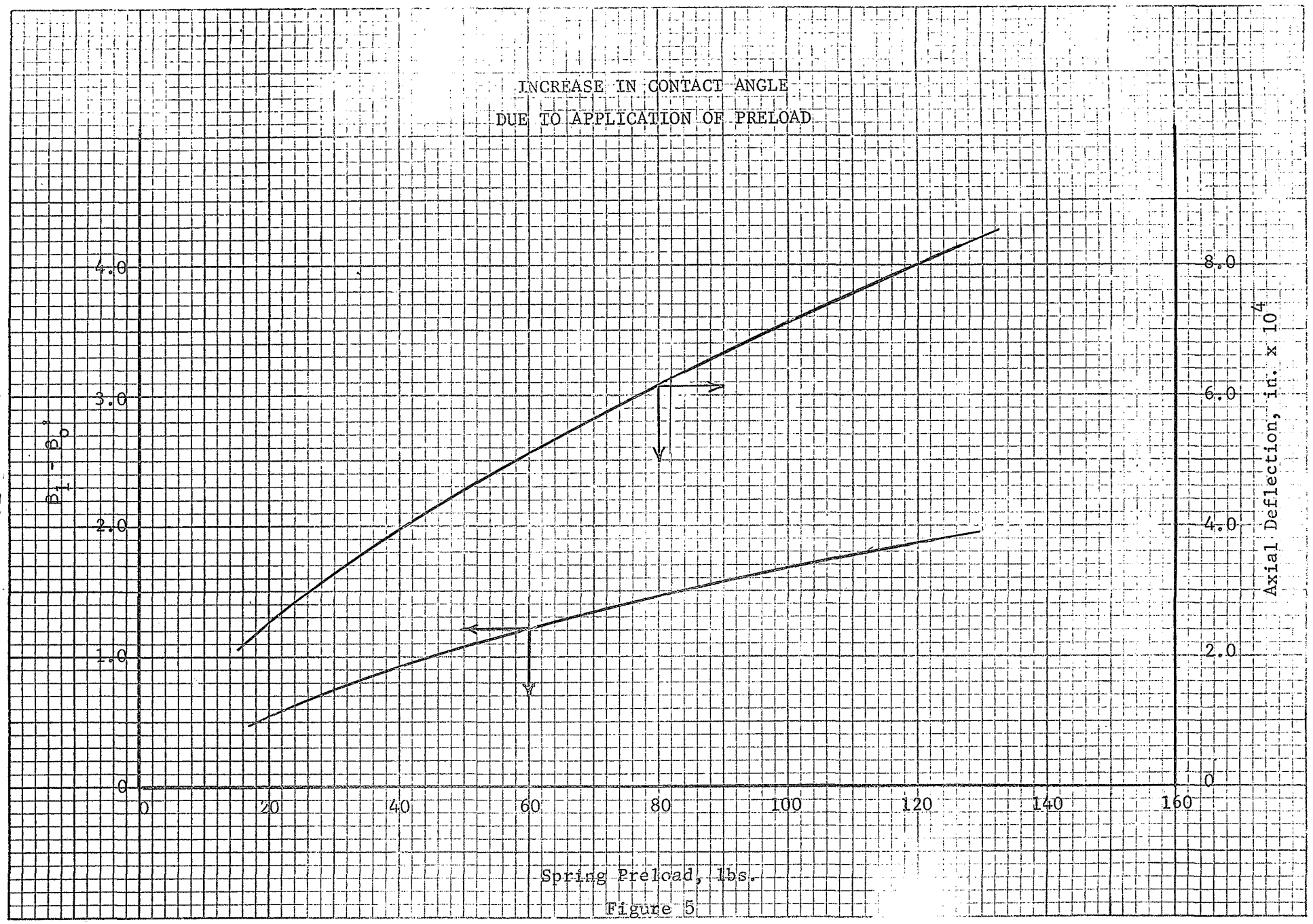
INCREASE IN CONTACT ANGLE
DUE TO APPLICATION OF PRELOAD
$\beta_1 - \beta_0'$
4.0
3.0
2.0
1.0
0
0
20
40
60
80
100
120
140
160
Spring Preload, lbs.
8.0
6.0
4.0
2.0
0
Axial Deflection, in. x 10^4

Figure 5

or,

$$\omega_B = 3,048 \text{ rad/sec.}$$

B. Materials

B-1. Lubricant Dow ET-378

The polyphenyl ether oil, Dow ET-378, is a new class of fluid developed for use at relatively high temperature and/or nuclear radiation environment. This fluid falls in the class of the polynuclear aromatics which are known to be the most radiation resistant, thermally and oxidatively stable fluids currently available.

The Dow Chemical Company, developers of ET-378, claim corrosion in ET-378 is nil based on a 48 hour corrosion-oxidation test at 500°F. (Ref. 1) Dow has also assured General Electric that the ET-378 would not react with copper alloys to 300°F, the maximum allowable bearing temperature. Oxidation-corrosion tests at 500°F and 550°F by Monsanto on its OS-124 polyphenyl ether oil showed very little attack on pure copper at even these elevated temperatures.

Although there is no information within General Electric on the use of ET-378 with rolling element bearings, there is some experience with other types of polyphenyl ethers. In Reference 2, a study was made of the effect of several lubricants on the rolling contact fatigue life of M-50 tool steel. One of the lubricants evaluated was a polyphenyl ether called GTO-929.

Using MIL-L-7808, a diester oil, and MIL-L-6082 Grade 1100 petroleum base oil, as references, and the L_{10} life as a criterion, the performance of the polyphenyl ether is compared in the following table:

Table 2

RC Rig Test Life (Stress Cycles)

	L_{10} Life	L_{50} Life	Viscosity (CS) 210°F	Viscosity (CS) 400°F
GTO-929	7.9×10^6	23×10^6	13.4	2.08
MIL-L-7808	2.8×10^6	---	4.38	1.40
MIL-L-6082	1.3×10^6	5.5×10^6	20.3	---

RC Rig tests were conducted at 425°F and 7×10^5 psi Hertzian Stress.

The test data in Table 2 indicates that the polyphenyl ether GTO-929 was superior to the other two lubricants with respect to their lubricating effect on the rolling contact fatigue life of M-50 tool steel. It is of further interest to note that the polyphenyl ether lubricant ranked second out of six lubricants tested in that investigation. Mr. C.C. Moore, the author of Reference 2, reports that recent full-scale jet-engine tests with polyphenyl ether have shown no deficiencies as far as lubrication properties are concerned.

Work was carried out at Marlin-Rockwell (Ref. 3) with 150 MM bearings made of M-50 (CEMV), silver-plated iron-silicon-bronze cages, 18,000 lb. thrust load, 8000 RPM, operating in GTO-929 (polyphenyl ether) at 400°F. The L_{10} bearing life, using GTO-929, was found to be over eleven times that of catalog rated life.

Static seals for "O" rings and gaskets may be a problem. Dow Chemical has informed ATL that Teflon (or Viton A) is the only satisfactory organic material they know for use with ET-378. Organic materials, however, are unsatisfactory because of the high radiation level. Teflon and Viton A "O" rings and gaskets were used in the bearing test rig for ease of assembly since these tests will not be performed in a radiation environment. No material problems were encountered. The actual design will have to rely on welds

and tight fits for static sealing.

B-2. Bearing Material

M-50 is a tool steel used for ball bearings that are generally required to operate at elevated temperatures. M-50 tool steel, composed of 4.25 Mo, 4.10 Cr, 1.10 V, 0.80 C, and balance Fe is an excellent bearing material that possesses good hot hardness properties. The Rockwell C 63-65 hardness of balls and races specified in the Aerojet-General Corporation Specification is satisfactory and is in a range conducive to optimum bearing life. Further, reducing the inclusion content of M-50 by consumable electrode vacuum melting reduces fatigue life scatter, and in some investigations (Ref. 4) has shown longer fatigue life over that of air-melted steels. The iron-silicon-bronze cage material called for in the specification is suitable for this application.

C. Bearing Capacity

C-1. Dynamic Capacity

From Reference 7 the basic dynamic capacity is defined as that constant stationary radial load which a group of apparently identical bearings with stationary outer ring can endure for a rating of one million revolutions of the inner ring. The magnitude of the basic load capacity for angular contact bearings with balls not larger than 25.4 millimeters or one inch in diameter is:

$$C = f_c (i \cos \beta)^{0.7} n^{2/3} d^{1.8} \qquad (15)$$

The factor f_c depends upon the units used, the geometry of the bearing components, the accuracy to which the various parts are made, and the material. Values of f_c are obtained by multiplying the value of f_c/f which varies with $\frac{d \cos \beta}{D_m}$, in Table 1 of Reference 7, by a factor of f.

The value of f recommended in Reference 7 for ball bearings of good quality hardened steel is, $f = 7450$ when pound and inch units are used.

For the bearing evaluated here $\frac{d \cos \beta}{D_m} = .189$ and $f_c/f = .611$

The basic dynamic capacity then becomes $C = 6242$ lbs.
AGC quoted General Electric a dynamic capacity of 6,788 lbs. for this bearing. This figure is nine percent higher than our calculated value, but is permissible since their specification calls for an M-50 tool steel.

C-2. Static Capacity

The dynamic capacity applies to a bearing subjected to a load while the bearing is rotating. When the bearing is not rotating the load capacity is determined by the permanent deformations which develop in the load carrying surfaces. The static capacity is defined by the static load radial load which corresponds to a total permanent deformation of ball and race at the most heavily stressed contact of 0.0001 of the ball diameter. The magnitude of the basic static load rating C_o is:

$$C_o = f_o \; i \, n \, d^2 \cos \beta \qquad (16)$$

The values of f_o for different kinds of bearings as commonly designed and manufactured are given in Table 3 of Reference 7. For this geometry of bearing

$$C_o = 4894 \text{ lbs.}$$

D. External Bearing Loads

The first step required in evaluating the suitability of the AGC bearing selection is to determine the direction and magnitude of the forces acting on the alternator bearings. These loads are of five types:

(a) Rotor weight when in ground operation

(b) Residual unbalance forces

(c) Magnetic pullover forces

(d) Possible axial loads transmitted through the spline coupling

(e) Maximum shock loading during launch (spec. no. 10175)

D-1. Rotor Weight

During ground operation the bearings must be able to support the rotor weight in addition to the residual unbalance forces and the magnetic pullover forces. As the final rotor design was not complete at the time of this evaluation the rotor weight was assumed to be 70 lbs.

D-2. Residual Unbalance Loads

The rotors for the SNAP-8 alternators are, of course, balanced. However, there is a limit to the sensitivity of balancing machines and, because of this, there is always some residual rotor unbalance which will contribute to the bearing load at operating speed. In order to estimate this residual unbalance load it is necessary to start with the limitations of the balancing machine and work backwards.

Most balancing machines consist of two supports with a means to drive the rotor to some balancing speed. The bearing supports are made flexible in either the vertical or horizontal direction in order to achieve large amplitudes of vibration for even small unbalance. The amount of vibration of the bearing supports is used as a measure of the unbalance of the rotor. Most commercially available balancing machines indicate an unbalance if the peak to peak vibration amplitude of the bearing supports exceeds 20 microinches. Since the bearing supports are not restrained in the direction of the displacement, the peak to peak displacement amplitude can be taken as twice the mass center displacement of the rotor. The residual unbalance then is:

$$U = r W = .0112 \text{ in-oz.}$$

At 12,000 rpm the force resulting from this unbalance is:

$$F = \frac{U}{g_o} \omega^2 = 2.86 \text{ lbs.} \qquad \text{or,}$$

$$F/brg = 1.43 \text{ lbs.}$$

D-2-a. Balancing Speed

The best speed for balancing a rotor is at its design operating speed. However, this is not always feasible, especially for high speed rotors. The rotor of the SNAP-8 alternator is relatively stiff in that the operating speed of 12,000 rpm is considerably below the rotor first critical (about 24,000 rpm). In this case, the rotor can be considered rigid, and when balanced at a relatively low balancing speed, it is balanced at all speeds up through the design speed.

D-2-b. Unbalance due to the Ball Bearings

The ball bearings on which the rotor is supported may also introduce apparent unbalance. Any eccentricity of the bearing bore diameter to the inner race diameter will cause unbalance. Balancing the rotor in its own bearings will compensate for this type of unbalance. Care must be taken to assure that the position of the bearing on the shaft does not change after balancing since, if this happens, the vibration will be worse because the correction unbalance would add to the eccentricity unbalance.

The ball bearings may also introduce vibrations, which are not of the unbalance type, i.e., a force rotating at rotor frequency. Out-of-roundness of the ball bearing outer ring will cause an unbalance force of rotor frequency which shows up in one direction only. Precessional motion of the balls in the race, unequal ball diameters, and bearing misalignment may also lead to unwanted bearing vibratory forces. Forces of this type are not reduced by balancing but require close bearing and machine tolerances for

their suppression.

D-2-c. Unbalance Due to Temperature and Centrifugal Loading Effects

The rotor for the SNAP-8 alternator was balanced at room temperature and at a relatively low speed, about 2000 rpm. During actual operation the rotor will be subjected to considerable temperature gradients. If the rotor distortions caused by these temperature gradients are not symmetrical about the axis of rotation, unbalance forces may result. Unbalance may also result from nonuniform distortion due to centrifugal loading at high speed.

D-3. Magnetic Pull Forces

The magnetic pull force was supplied by the Aerospace Motor and Generator Engineering Department. A curve of magnetic pull versus eccentricity is presented in Figure 6 and shows a 65 lb. force per end at a rotor eccentricity ratio of 0.1.

A description of the magnetic pull force follows. The magnetic pull on each end of the alternator varies with eccentricity from 0 to 1200 lbs. The force goes to zero twice per revolution. The forces on the two ends are out of phase with each other by one-quarter revolution. The forces at each end are in the same direction.

If the axis of the rotor is cocked with respect to the stator such that the minimum eccentricity points are 90 mechanical degrees apart, the forces lie in perpendicular planes but in phase. This represents a slightly more serious case than the one described in the previous paragraph. Both conditions were considered and are discussed more fully in Section H. This force is the largest radial force on the bearing. It can be reduced by closer manufacturing tolerances on the rotor eccentricity.

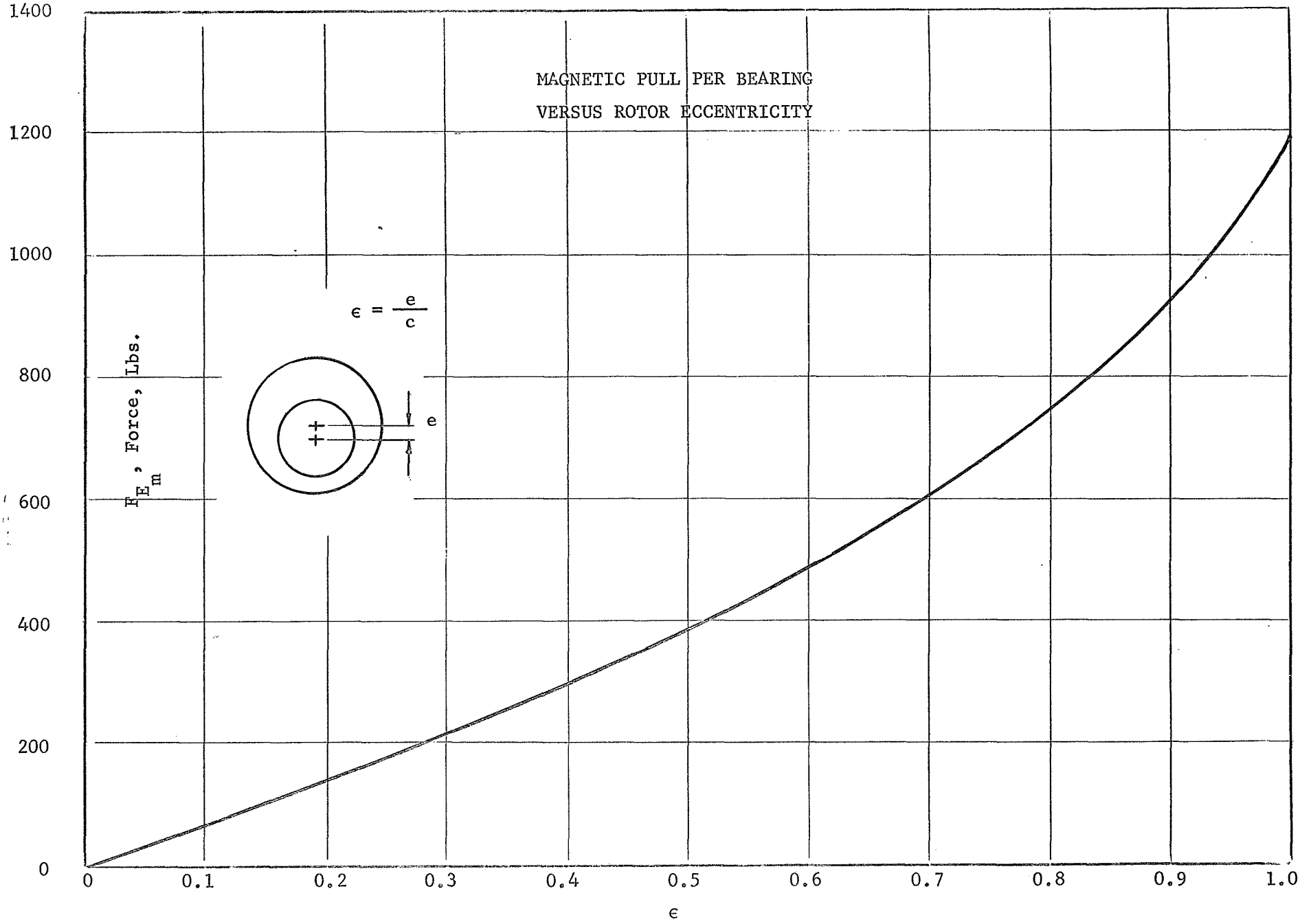
MAGNETIC PULL PER BEARING
VERSUS ROTOR ECCENTRICITY
$\epsilon = \frac{e}{c}$
e
F_{E_m}, Force, Lbs.
1400
1200
1000
800
600
400
200
0
0
0.1
0.2
0.3
0.4
0.5
0.6
0.7
0.8
0.9
1.0
ϵ

Figure 6

D-4. Spline Loads

The AGC Turbine-alternator interface drawing, No. 090916 calls for a splined shaft between the turbine and alternator packages. The spline is a "flexible" one in that the fits are chosen to permit relative movement between the internal and external spline teeth while the spline is transmitting torque. This particular design has no distance piece and with a slight amount of misalignment, the coupling begins to operate as an internal gear set with a one to one ratio.

Instead of all of the teeth contacting as in the usual spline or coupling, only one or two pairs of teeth may contact at the point of closest approach. The load may be applied (at any instant of time) to a very few teeth instead of being distributed around the circle of coupling teeth. As pointed out in Reference 11, this can cause an overload on the tooth surfaces as much as 10 to 20 times the load obtained with the load evenly distributed among all of the teeth, if the shaft is very stiff. The reaction of the internal teeth to this load causes a load to be imposed on the bearings. In the SNAP-8 alternator design the shaft is made flexible (k = 200 lbs/in). With the involute spline the internally toothed part tends to center itself on the externally toothed part. Thus the maximum force which can be transmitted to the bearings is the force required to center the quill shaft if it were misaligned to the maximum tolerance. This force is 0.416 lbs. and results in a +0.5 lb. force on the inboard bearing and a - 0.1 force on the outboard bearing. Since these forces are so small, they will be neglected.

There is also the possibility of axial loads originating in the spline. These can arise from two sources:

1. Linear expansion of quill shaft under load due to temperature fluctuations
2. Linear movement under load due to eccentric spline motion.

For an unlubricated spline this load was found to be 237 lbs. and for a lubricated spline 16 lbs. This makes lubrication of the spline absolutely necessary.

E. Shock Loading

The alternator specification 10175 calls for an extremely high shock loading of 35 g. Since the orientation of the generator on the launch vehicle is not yet known, it will be assumed that the 35 g load must be sustained in any direction. In this case high bearing loads will occur while the bearing is stationary. There is a limit to the load the bearing can carry while it is not rotating. This load, known as the basic static capacity, is defined as that which the bearing can carry without permanent deformations which would be noticeable when the bearing subsequently rotates under a lesser load. This load is defined in Section C-2 as the static load which would cause a total permanent deformation of ball and race at the most heavily stressed contact of 0.0001 of the ball diameter. The calculations of Section C-2 indicate that the basic static load rating of this bearing is larger than the force (2450 lbs.) which a 35 g acceleration could impose on it.

F. Internal Bearing Loads

100 lb rotor
100 × [illegible] = 3500
7000

F-1. Gyroscopic Moment

In an angular contact bearing, the balls change the direction of their axes of rotation as they roll on the inner ring. This causes a gyroscopic load on the ball which tends to make the ball spin in the race. The spinning of the ball is resisted by the friction moment caused by the ball load. This is illustrated in Figure 7.

The resisting torque on the ball is given by:

$$M_d = I\,\omega_m\,\omega_{n'}\,\sin\beta \qquad (17)$$

III 42

ILLUSTRATION OF GYROSCOPIC MOMENT

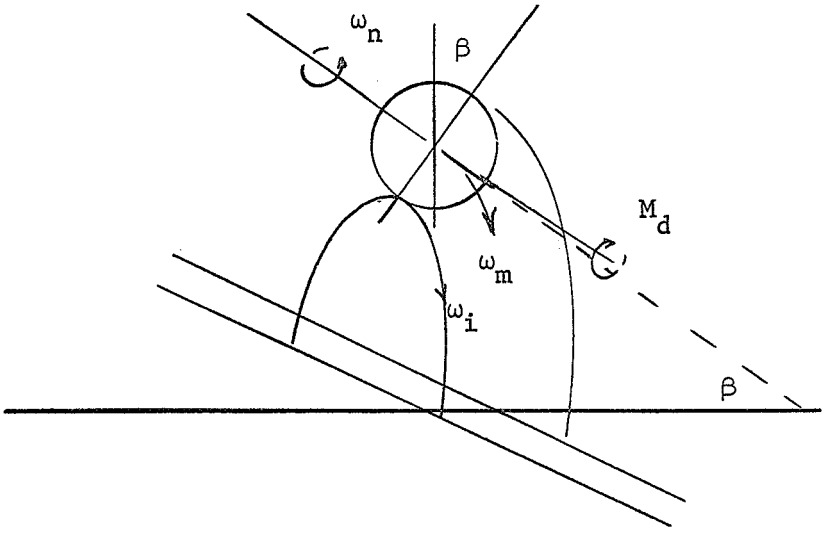

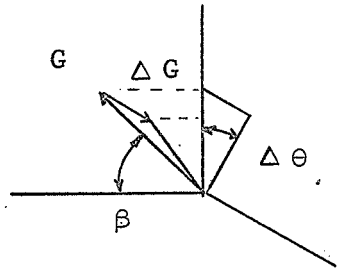

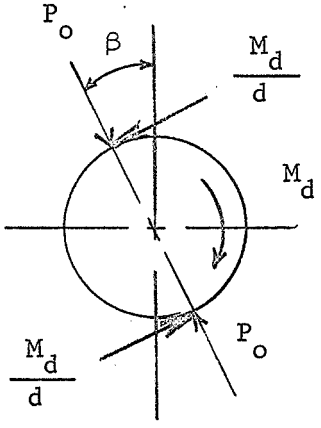

Figure 7

For the 208 ball size $I = 8.77 \times 10^{-7}$ lb-in-sec^2 and for $\beta = 16^o$ at 12,000 rpm, the gyroscopic moment becomes:

$$M_d = .392 \text{ in-lb.}$$

Referring to Figure 7 (c), force equilibrium on the ball requires:

$$F_X = \frac{P_o}{n} \operatorname{Sin} \beta \tag{18}$$

and moment equilibrium requires:

$$M_d = \mu \; P_o \; d \tag{19}$$

Taking $\beta_i = \beta_o = 16^o$, and a coefficient of friction, $\mu = .02$, we obtain:

$$P_o = 39.8 \text{ lbs. and } F_x = 142 \text{ lbs.}$$

Thus a ball load of 39.8 lbs. or a preload of 142 lbs. is required to prevent spin. This calculation assumes a $\mu = .02$ based on the work of Palmgren, Reference 8. Other sources give values of $\mu = .05$ to $.1$ so that F_x could possibly be as low as 28 lbs. to prevent spin.

As shown in Section F, the ball load does become less than 38 lbs., and spin is possible. Palmgren (Ref. 8) reports that this is not serious as long as the equivalent bearing load is less than $.0016 \; C_o = 78$ lbs. The load on the generator bearing is 154 lbs., which is slightly higher than $.0016 \; C_o$ but less than the load required to prevent sliding. However, only infrequently does this cause any damage.

F-2. Centrifugal Loads

When the ball rotates at cage speed it exerts a centrifugal force on the rings. This load is given by:

$$\frac{F_c}{\text{ball}} = \frac{M}{g} r_m \omega_m^2 = 12.3 \text{ lbs.} \tag{20}$$

for this bearing at 12,000 rpm. The effect of this load in an angular contact bearing with both radial thrust loads is to:

a. Load the outer race and unload the inner race.
b. Tend to decrease the contact angle on the outer race and increase it on the inner race.

These effects may either increase or decrease the bearing life depending on bearing geometry and the types of loads imposed. Reference 10 reports techniques for calculating the effect for deep groove bearings under radial load and angular contact bearings under pure thrust load. In general, the effect is small and in the hand calculations we have made no correction for this centrifugal load. It is included in the computer solution of Section II-N.

G. Selection of the Preload

The preload is usually selected high enough to prevent any ball from going through an unloaded zone. The calculations of Section II-F show that this condition is satisfied for a 60 lb. preload, even under extreme loading conditions.

Another factor in high speed bearings is skidding due to the gyroscopic moment. Depending upon the assumed coefficient of friction between the ball and the race, the 60 lb. preload is or is not high enough to prevent skidding. The computer output sheets (Section N) also indicate that skidding is possible as the coefficient of friction required to prevent skidding (MU-B) is larger than .02, the minimum value usually assumed.

H. Bearing Equivalent Load

The equivalent load is defined in Reference 7 as that constant stationary

radial load, which, if applied to a bearing with rotating inner ring and stationary outer ring, would give the same life as that which the bearing will attain under actual conditions of load and rotation.

Since the magnetic pull force depends upon the eccentricity and orientation of the rotor which will vary from machine to machine, it is difficult to calculate an equivalent load that would apply to all machines. Thus, worst case conditions have been assumed, and all of the machines manufactured within tolerance should fall within the boundaries of the assumptions.

H-1. Case 1. Parallel Axis Displacement

Consider an end view of the alternator in which the point of minimum rotor eccentricity lines up with the weight vector as shown in Figure 8, and that the rotor is not cocked, but that the axis of the rotor is parallel to the axis of the stator.

The unbalance load is given by:

$$F_U = F_{U_m} \cos \omega t \tag{21}$$

The magnetic pull load at each bearing can be represented by:

$$F_{E_1} = \frac{F_{E_m}}{2} \left[1 + \cos 2 \omega t \right] \tag{22}$$

and:

$$F_{E_2} = \frac{F_{E_m}}{2} \left[1 + \cos 2 (\omega t - \pi / 2) \right] \tag{23}$$

LOAD ORIENTATION - CASE 1

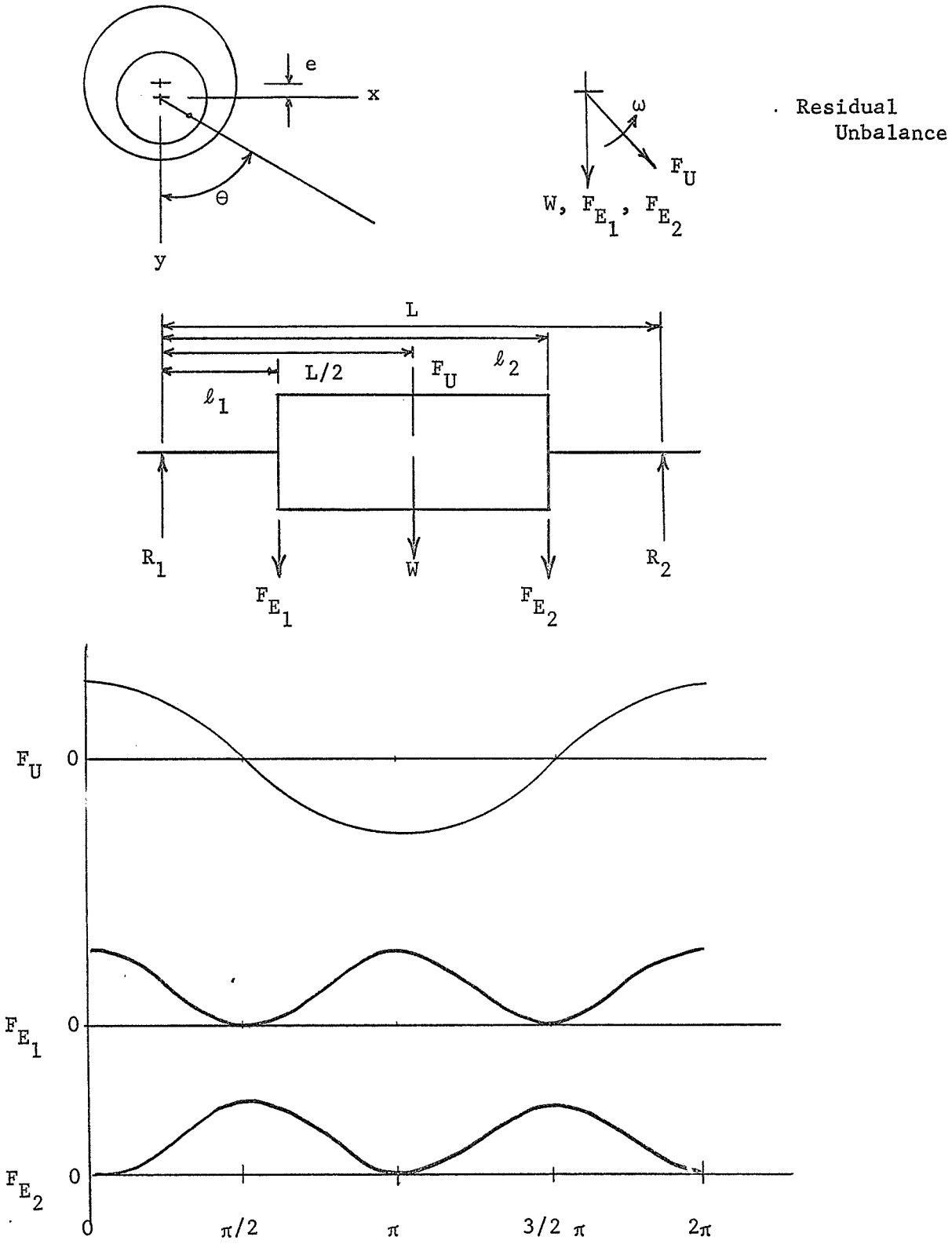

Figure 8

The rotor weight is a constant at:

$$W = 70 \text{ lbs.}$$

This load is shown schematically in Figure 8. Taking moments about R_1, the maximum bearing reaction becomes:

$$R_2 = \frac{W}{2} + \frac{\ell}{2} F_{U_m} \cos \omega t + \frac{\ell_1}{L} F_{E_m} \cos^2 \omega t \qquad (24)$$

$$+ \frac{\ell_2}{L} F_{E_m} \sin^2 \omega t$$

where it is observed that:

$$\cos 2\omega = 2 \cos^2 \omega t - 1$$

$$\cos (\omega t - \pi/2) = \sin \omega t \qquad (25)$$

H-2. Case 2. Cocked Rotor

In the previous case, it was assumed that the points of minimum eccentricity lay in one plane. Another possibility occurs when the rotor is cocked and the points of minimum eccentricity lie in planes 90° apart. For this case the magnetic pull forces are 90 mechanical degrees apart but in phase in time. This is illustrated in Figure 9. If the unbalance force is neglected, the resultant force is:

$$R_2 = \left\{ \left[\frac{\ell_2}{L} F_{E_m} \cos^2 \omega t \right]^2 + \left[\frac{W}{2} + F_{E_m} \frac{\ell_1}{L} \cos^2 \omega t \right]^2 \right\}^{1/2} \qquad (26)$$

LOAD ORIENTATION - CASE 2

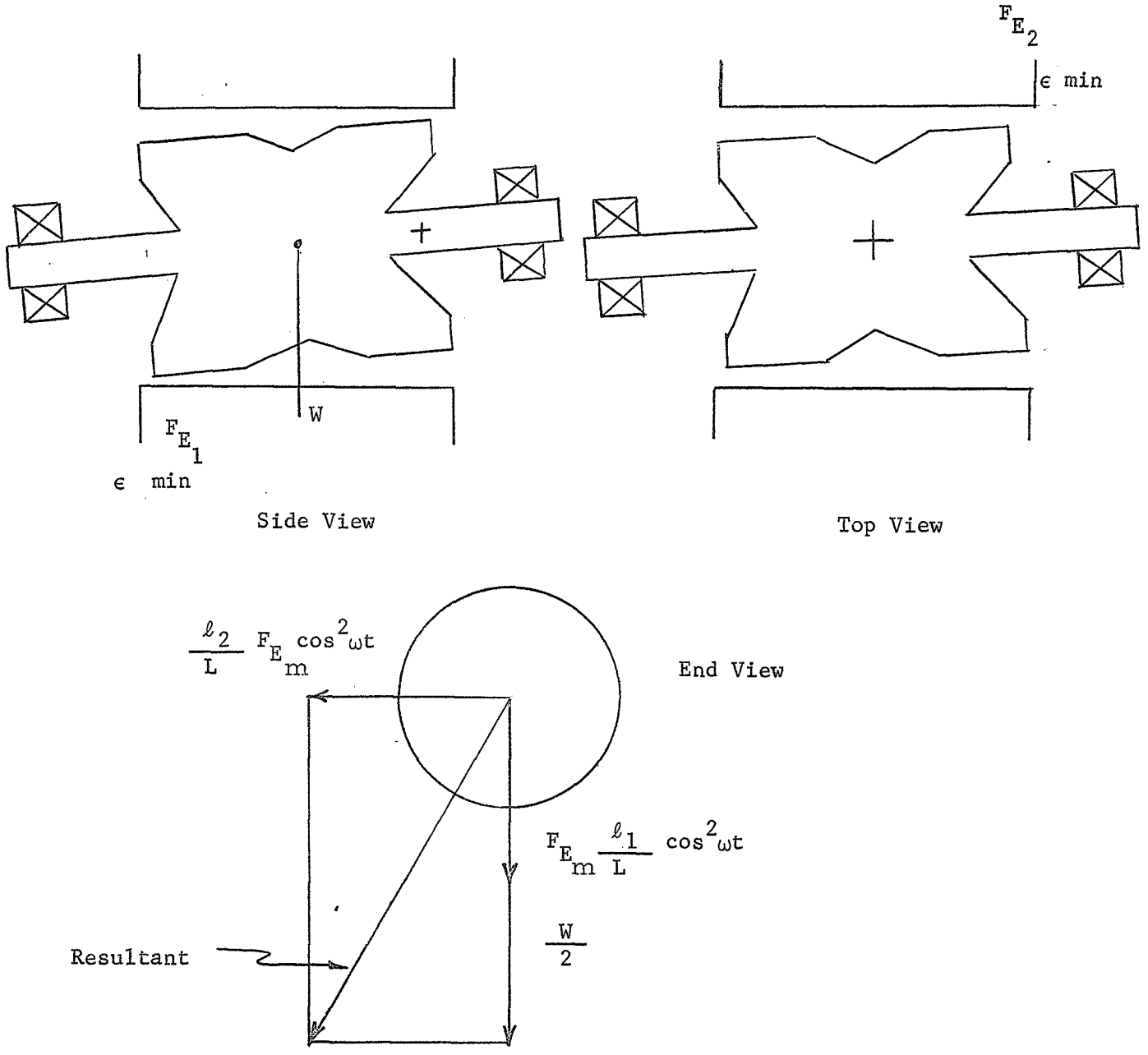

Figure 9

H-3. Calculation of Equivalent Load

The basic ball bearing life formula is:

$$L = (C/P)^3 \tag{27}$$

where L is the life in millions of revolutions, C is the basic dynamic load capacity and P is the bearing load acting under the conditions applicable to the basic dynamic load capacity. For the single row angular contact bearing considered here, P is the radial component of a load, under the influence of which half the circumference of the bearing ring is loaded. It is further assumed that the inner ring rotates in relation to the line of action of the load P, while the outer ring remains stationary in relation to this line.

Now for this application the loads are not constant nor are they purely radial. Thus, a hypothetical load, called the equivalent bearing load, must be used in the life formula. This load is given by:

$$P = X V F_r + Y F_a \text{ for } \frac{F_a}{F_r} \geqq 1.5 \tan \beta \tag{28}$$

where,

P	=	equivalent bearing load
F_r	=	the radial component of actual bearing load
F_a	=	the axial component of the actual bearing load
X	=	radial factor of the bearing
Y	=	the thrust factor of the bearing
V	=	rotation factor

If the inner ring rotates in relation to the direction of the load while the outer ring is stationary, then V = 1. If, on the other hand, the inner ring is stationary in relation to the load, then V can be considerably greater than 1. Tables of V, X, and Y are given in References 7 and 8 for various types of bearings.

Account must also be taken of the fluctuation of the bearing load with time. Since bearing life is inversely proportional to a power of the load, a heavy load may have considerable effect even though it acts for a short time. Thus an integrated mean load must be used, and if the load fluctuates periodically, this is the mean load for one period. The expression for the equivalent load then becomes:

$$P = \left[\frac{1}{2\pi}\int_0^{2\pi} (X\,V\,F_r + Y\,F_a)^3 \; d(\omega t)\right]^{1/3} \tag{29}$$

From Table 2 of Reference 7, V = 1.0 for all loads except the unbalance load for which V = 1.2. Now for Case 1, F can be expressed by:

$$F = X\left(\frac{W}{2} + V\,\frac{F_{U_m}}{2} + \frac{\ell_1}{L}\,F_{E_m}\,\cos^2\omega t + \frac{\ell_2}{L}\,F_{E_m}\,\sin^2\omega t\right) + YF_a \tag{30}$$

Substituting equation 30 into equation 29, the following integral is obtained:

$$P = \left[\frac{1}{2\pi}\int_0^{2\pi} \left(C_1 + C_2\,\cos^2\omega t + C_3\,\sin^2\omega t\right)^3 \; d\,(\omega t)\right]^{1/3} \tag{31}$$

Evaluation of this integral gives:

$$P = \left[C_1^3 + \frac{3}{2}\,C_1^2\,C_2 + \frac{3}{2}\,C_1^2\,C_3 + \frac{9}{8}\,C_3^2\,C_1 + \frac{9}{8}\,C_2^2\,C_1 + \frac{3}{4}\,C_1\,C_2\,C_3 + \frac{5}{16}\,C_2^3 + \frac{5}{16}\,C_3^3\right]^{1/3} \tag{32}$$

where:

$$C_1 = \frac{XW}{2} + X V \frac{F_{U_m}}{2} + YF_a \tag{33}$$

$$C_2 = X \frac{\ell_1}{L} F_{E_m} \tag{34}$$

$$C_3 = X \frac{\ell_2}{L} F_{E_m} \tag{35}$$

For the following assumed values:

$$\frac{\ell_1}{L} = \frac{1.7}{12.38} = .136 \qquad \frac{\ell_2}{L} = \frac{10.8}{12.38} = .864$$

$$F_{E_m} = 65 \text{ lbs. for } \epsilon = .1 \qquad W = 70 \text{ lbs.} \tag{36}$$

$$\frac{F_{U_m}}{2} = 1.43 \text{ lbs.} \qquad F_a = 60 + 16 = 76 \text{ lbs.}$$

and from Reference 7, Table 2,

$$\frac{F_a}{F_r} > e = .38 \qquad \beta = 15^o$$

$$X = .44 \qquad Y = 1.47 \tag{37}$$

$$V = 1.2 \qquad \frac{F_a}{C_o} = \frac{76}{4894} = 0.155$$

the value of the equivalent load becomes:

$$P = 142 \text{ lbs. (Case 1)}$$

For Case 2, substitution of equation 26 in equation 29 results in an equation that is not readily solved. The solution is simplified if it is assumed that both magnetic pull forces and the weight force lie in the same plane and are in phase in time. The resulting expression for the force is:

$$F = X \frac{W}{2} + V \frac{F_{Um}}{2} + \frac{\ell_1}{L} F_{E_m} + \frac{\ell_2}{L} F_{E_m} \cos^2 \omega t + Y F_a \quad (38)$$

Substitution of this in equation 29 and evaluating the resulting integral gives:

$$P = 154 \text{ lbs. (Case 2)}$$

J. Bearing Load Distribution

In order to insure that none of the balls would operate through an unloaded zone even under unusual load conditions, the load distribution within the bearing was calculated by the methods of Reference 7. Consider the single row angular contact bearing with an arbitrary but constant contact angle β. It is loaded by an external force, F, acting at an angle α. The lines of action of the rolling element loads intersect at the load center of the bearing and consequently the bearing load, F, also acts through this point.

From the equilibrium conditions for the rolling element loads and the bearing load, it is shown in Reference 7 that the following relationship exists between the maximum rolling element load $P_{o_{max}}$ and the components F_r and F_a of the bearing load:

$$F_r = \mathcal{F}_r \cdot n \cdot P_{o_{max}} \cdot \cos \beta \quad \text{and} \quad (39)$$

$$F_a = \mathcal{F}_a \cdot n \cdot P_{o_{max}} \cdot \sin \beta \quad (40)$$

The factors $\mathcal{F}_r$ and $\mathcal{F}_a$ from Table 2.3 of Reference 7 are shown plotted in Figure 10.

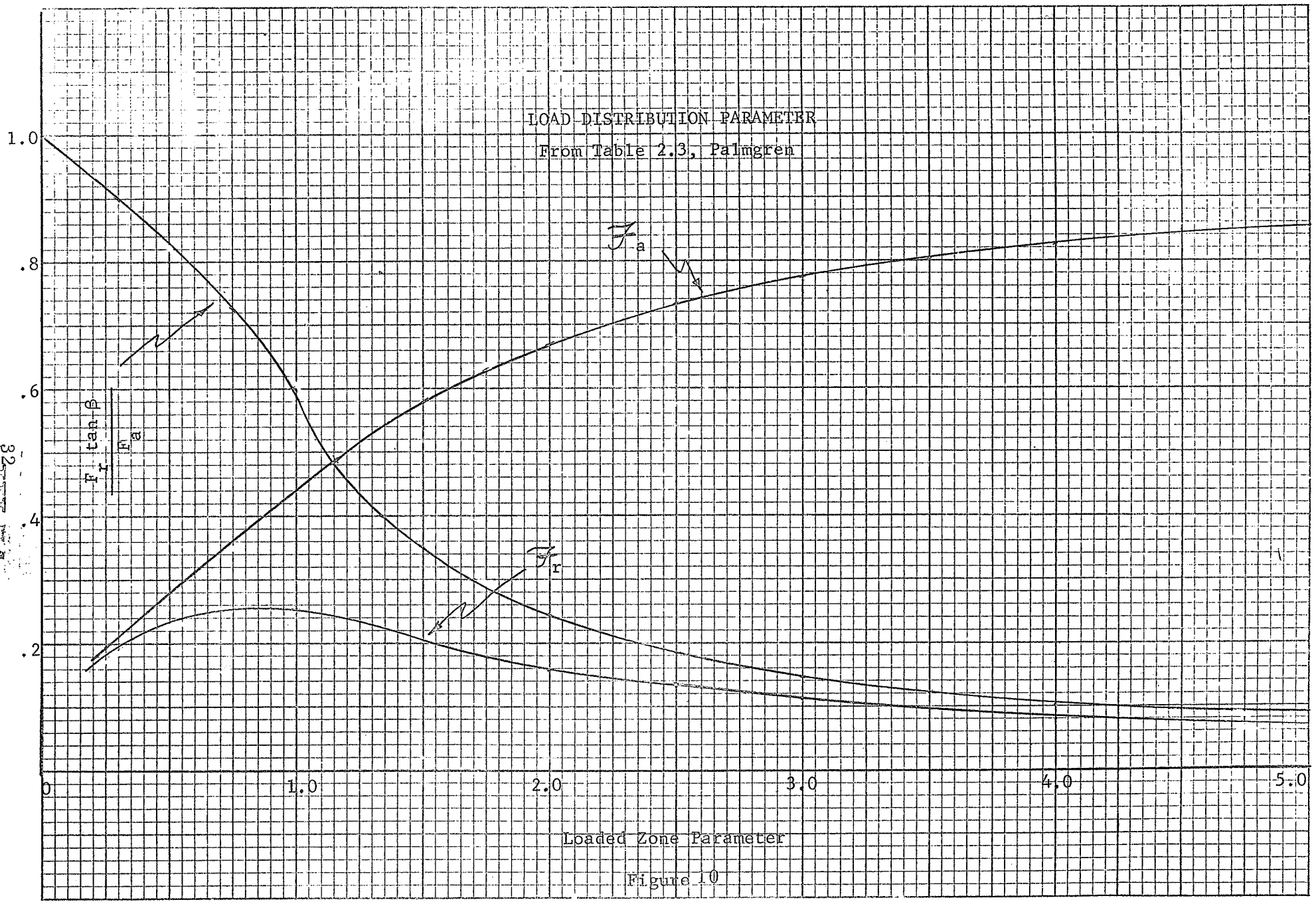
LOAD DISTRIBUTION PARAMETER
From Table 2.3, Palmgren
1.0
.8
.6
.4
.2
0
1.0
2.0
3.0
4.0
5.0
$\mathcal{F}_a$
$\mathcal{F}_r$
$\frac{F_r \tan \beta}{F_a}$
Loaded Zone Parameter

Figure 10

The external force acting on the bearing is transmitted through the rolling elements. Since more than one element carries the load, the bearing is statically indeterminate, and thus the distribution of forces is dependent upon the elastic deformation of the various bearing parts. The relation between deformation and load around the bearing is:

$$\frac{P_o}{P_{o_{max}}} = \left(\frac{\delta_\psi}{\delta_{max}}\right)^{3/2} \tag{41}$$

The extent of the loaded zone is measured by the parameter ϵ. For a bearing loaded along its entire circumference

$$\epsilon = \frac{\delta_{max}}{\delta_{max} - \delta_{min}} \geqq 1 \tag{42}$$

where δ_{max} and δ_{min} are the total elastic compressions at the contacts of the rolling elements carrying the heaviest and lightest loads respectively. If the raceway is loaded only over part of the circumference, ϵ is the ratio of the projection of the loaded zone to the diameter, and in this case, $\epsilon \leqq 1.0$.

If the bearing is under no radial load $F_r = 0$ $\epsilon = \infty$, and $\mathcal{F}_a = 1.0$. For this case:

$$P_o = P_{o_{max}} = \frac{F_a}{n \sin\beta} \tag{43}$$

All the rolling elements are equally loaded. If the preload (axial force) is kept constant and the radial is increased, the balls are no longer equally loaded. Those on the side of the bearing opposite the direction of the radial force will unload. For the alternator the worst radial load case occurs when the weight force and the magnetic pull forces are in phase in time and in the same direction. For this case $F_r = 100$ lbs. Taking a preload of 60 lbs, a

spline load of 16 lbs, and $\beta = 16^{o}$:

$$\frac{F_r}{F_a} \tan \beta = .378 \tag{44}$$

From Figure 10,

$$\mathcal{F}_a = .55 \qquad \epsilon = 1.45$$

and $$P_{o_{max}} = 38.6 \text{ lbs.}$$

Since $\epsilon > 1$, the entire race is loaded

$$\frac{\delta_{180}}{\delta_{max}} = 1 - \frac{1}{2\epsilon} = .312$$

and $$P_{o_{min}} = P_{o_{max}} \left(\delta_{180}/\delta_{max}\right)^{3/2} = 6.7 \text{ lbs.} \tag{45}$$

Even under the maximum expected radial load all balls are loaded.

K. Bearing Life

The bearing life of an individual ball bearing is defined as the number of revolutions (or hours at some given constant speed) which the bearing runs before the first evidence of fatigue develops in the material of either ring or of any of the rolling elements. Apparently identical bearings operating under the same conditions, will exhibit different lives. The dispersion of the life values is given by the Weibull distribution:

$$P_S = e^{-\left(\frac{L}{5.35L_{10}}\right)^{1.34}} \tag{46}$$

which reduces to

$$P_S = .9 \text{ for } L/L_{10} = 1.0.$$

Equation 46 assumes that a median life is 4.08 times the L_{10} life.

The bearing specification calls for a reliability of 99.5 percent. From equation 46:

$$L_{.5} = .103\ L_{10} = .103 \times 10^6 \text{ rev} \tag{47}$$

which is the number of revolutions 99.5 percent of the bearings will survive under load C.

For ball bearings the relationship between load and life is:

$$\frac{L_1}{L_2} = \left(\frac{P_2}{P_1}\right)^3 \tag{48}$$

Now $L_1 = .103 \times 10^6$ rev for a load $P_1 = C$ and .995 reliability.

The desired life, L_2, is 10,000 hours at 12,000 rpm; or 72×10^8 rev. The allowable load to attain this life is then P_2, or,

$$P_2 = 164 \text{ lbs.}$$

The maximum expected under worst case conditions is 154 lbs. Since P_2 exceeds this value, the bearing should give the required life and reliability.

It is sometimes convenient to talk about an equivalent L_{10} life for the bearing. The ratio of the operating time to the design life is from equation 47, .103.

The L_{10} life is then:

$$L_{10} = \frac{10,000}{.103} = 97,000 \text{ hours.}$$

Thus the bearing must be designed for an L_{10} life of 97,000 hours to get a life of 10,000 hours and reliability of 99.5 percent.

L. Other Factors Affecting Bearing Life

In the previous section it was concluded that the proposed alternator bearing has enough capacity to meet the 10,000 hour life requirement with 99.5 percent reliability. However, there are other factors not considered which will provide a factor of safety in these calculations.

The analysis was intentionally conservative, in that allowances were not made for an increase in life due to the following factors:

(a) Increased life due to lubricant, polyphenyl ether
(b) Increased life due to vacuum melted M-50 steel
(c) Increased life due to a lack of goodness of fit of actual bearing failures to the Weibull distribution in the high reliability range.

The excess life from these three effects represents a very substantial factor of safety in the calculation.

As pointed out in the Section II.B, the available bearing test data (Ref. 2) using polyphenyl ethers show a substantial increase in life over the catalog rated life. Ratios of actual L_{10} bearing life to catalog ratings of 8 to 11 are documented in Table 2.

In recent years the fatigue life of ball bearing materials have also shown significant improvements. Some recent data obtained from SKF demonstrate this improvement. Their test experience on a 309 size ball bearing with a dead weight load equivalent to a 10 percent fatigue life of 10,000,000 revolutions is summarized in Table 3.

From Reference 3, CEVM M-50 bearings have shown L_{10} lives 1.44 times those of comparable 52100 steel bearings.

In addition, recently published bearing life studies (Ref. 17) have shown

Table 3

Material	Life Relative to Catalog Rating
Average air melted steel (52100) from 1935 to 1955	.8
Average air melted steel in 1963	1.5
Degassed (vacuum processed)	2.2
Results with one specific heat	
Air melted	2.0
First vacuum remelt	3.8
Second vacuum remelt	6.0
Third vacuum remelt	7.7

that bearing failures in the high reliability range do not fit the commonly accepted Weibull Distribution. In fact, an excess life of about 1.45 times more than the theoretical Weibull Distribution life can be expected at reliability level of 99.5 percent.

The expected increase in life due to these effects is not part of the American Standard Method of Evaluating Load Ratings for Ball and Roller Bearings (Ref. 7) and were not used in the evaluation. These effects, however, appear to be real ones and should give a considerable improvement over calculated life in the SNAP-8 alternator bearings.

M. Bearing Mounting and Fits

M-1. Mounting

The bearings can be mounted with their contact angles diverging (DB) or converging (DF). If the contact angles diverge as they approach the axis, the resistance of the bearings to moments is greater than if the contact angles converge. This usually gives a higher system critical speed, which

is desirable.

The bearings in this application are jet lubricated. In order to attain adequate lubrication, the oil must be jetted on the bearing in the direction of the load angle; that is, for converging load angles the jets are outboard of the bearings and for diverging angles, the jets are inboard of the bearings.

Since part of the pole face heat loss must be removed through the shaft, it is desirable to jet the oil on the shaft inboard of the bearings. This reduces the heat path and lowers the temperatures in the vicinity of the bearing.

Preliminary life calculations also indicated that a slightly longer life could be reached with the DB mount. These three factors, critical speed, heat removal, and life, dictated the selection of the DB mount for the alternator.

M-2. Selection of Fits

Except as otherwise noted, the bearing called for in the specification is in accordance with the Annular Bearings Engineers Committee (ABEC) Class 7, for high precision bearing. In order to insure satisfactory operation, both the fit between the inner ring and the shaft and the fit between the outer ring and the housing must be compatible with the running conditions and the accuracy of the bearing.

The relation of the direction of the load in relation to the bearing ring is very important in determining the fits. If the ring in question rotates relative to the direction of the bearing load, the load on the ring is said to be a "rotating load"; if stationary, a "stationary load." The loads on the SNAP-8 alternator bearings are classified in this way below:

Load	Type
Rotor Weight	Rotating Inner Ring
Residual Unbalance	Stationary Inner Ring
Magnetic Pull	Rotating Inner Ring

The rotor weight and magnetic pull forces are the largest loads. In order to prevent creep between the bearing bore and shaft a tight fit is necessary here. Axial clamping alone will not prevent creep.

A loose fit between the bearing outer ring is needed to allow for axial expansion. The residual unbalance load which rotates relative to the outer ring is not large enough to cause any appreciable creep at this point.

The ranges of shaft and housing tolerances used in the SNAP-8 alternator were selected on the basis of Reference 8, which goes into considerable detail on the fits required for a variety of load conditions.

From Tables 5.1 of the same reference a rotating inner ring load less than seven percent of the basic dynamic capacity calls for a j6 shaft tolerance. For very accurate applications a j5 fit is recommended. However, because of the long life requirement and a need to limit leakage between the bearing and the shaft, a tighter tolerance, k5 , was selected for the alternator shaft.

For those applications with a fixed outer ring load in which the outer ring must be displaced axially, an H7 bearing-housing tolerance is recommended in Table 5.2 of Reference 7. The following table compares the recommended fits based on the information of Reference 7 and the actual room temperature and operating temperature fits used in the alternator.

Table 4

Shaft Fits

Bearing Bore - 1.5746/1.5748

Fit with k5 Shaft Tolerance	Actual Fit Room Temperature	Calculated Fit Operating Temp.
+.0001/-.0007	-.0001/-.0007	.0000/-.0006

Bearing-Housing Fits

Bearing OD - 3.1494/3.1496

Fit with H7 Bearing-Housing Tolerance	Actual Fit Room Temperature	Calculated Fit Operating Temp.
+.0000/+.0012	+.0001/+.0007	+.0003/+.0009

In all cases the actual fits at room temperature and at operating temperature fall in the range of recommended fits.

M-3. Finishes

A precision finish, 32 microinches rms, is called for on the bearing housing ID. This is generally an accepted value for precision bearings which must slide in the housing. A better finish is required on the shaft OD because of the interference fit. A value of 16 microinches rms was used.

N. Bearing Computer Evaluation

Since the hand computations of Section II-K indicate a bearing capacity very close to the estimated loads, it was felt wise to pursue a more comprehensive approach to the problem.

III 621

Calculations were made using the Bearing Systems Computer Program (BEST) of Reference 15. This program offers a general solution for the elastic compliances of a system of any number of ball and radial roller bearings under any steady load. Both centrifugal and gyroscopic loadings of the rolling elements are considered. The solution defines the loading and attitude of each rolling element in each bearing of the system as well as the displacement of each inner ring with respect to its outer ring. Theoretical fatigue life is also calculated.

Since the program cannot handle fluctuating loads, several different loading conditions were calculated based on the rotor-bearing model in Figure 11 with a DB mount.

The system requirement on the bearings is that they must meet a 10,000 hour life with 99.5 percent probability of survival. In order to meet this requirement, it is shown in Section II-K that the bearings must have an equivalent L_{10} life of 97,000 hours. The computer program prints out the theoretical L_{10} life, and if this number exceeds 97,000 hours, the bearing meets the system requirement.

Table 5 shows the nomenclature used on the computer output sheets. The output for the cases run is given in Tables 6 through 9.

Case 1 (Table 6) represents the worst conceivable operating condition wherein the two magnetic pull forces reach a simultaneous maximum in direction and phase. Both bearings show individual lives in excess of 97,000 hours. There is very little difference between this result and the corresponding case in Section II-J. It is noted that there is a variation in the ball velocity about the machine axis (N-E). This condition can cause fluctuating cage stresses. One way to decrease this is to increase the preload.

Case 2 (Table 7) is a repeat of Case 1 with an increased preload of 100 lbs. This does reduce the variation in ball velocity about the axis, but

III 63

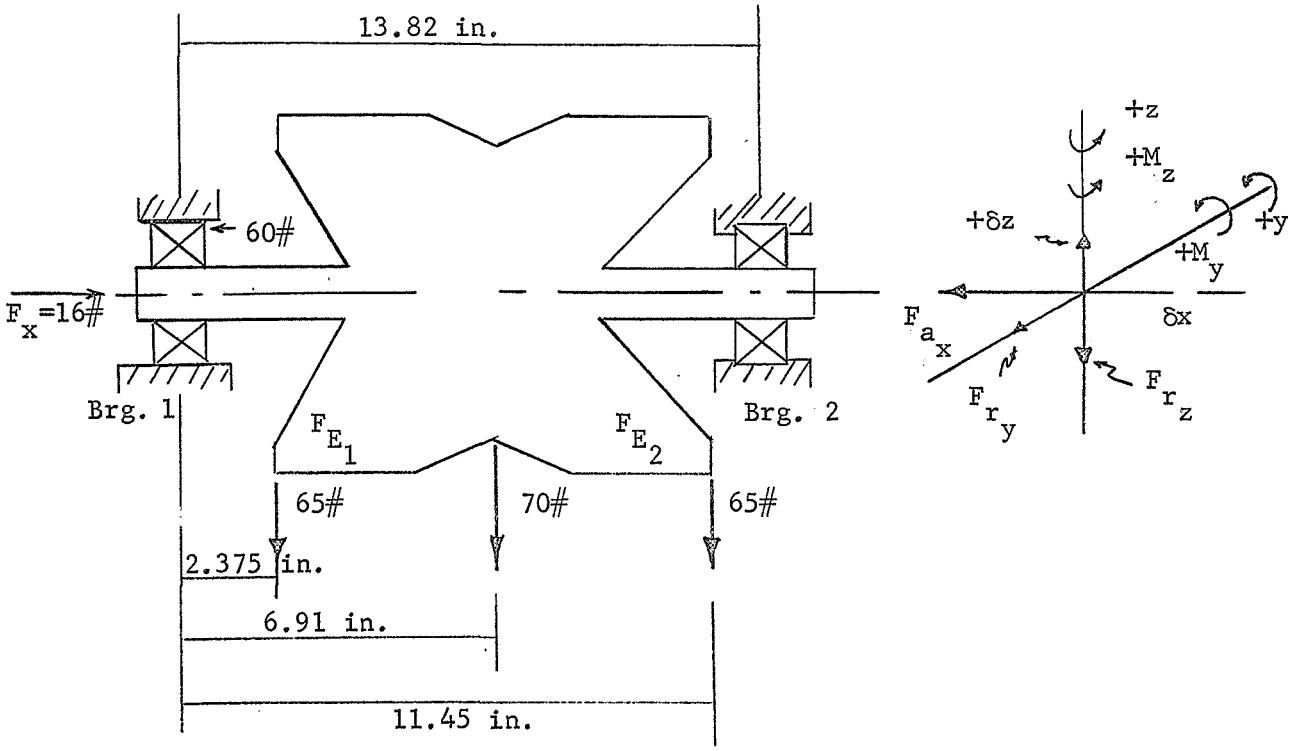

	Case	F_{E_1} lbs.	F_{E_2} lbs.	W lbs.	Preload
DB	1	65	65	70	60
	2	65	65	70	100
	3	65	0	70	60
	4	65	65	0	60

Figure 11. Computer Calculation Model

III 64

the individual bearing lives for this case drop below the required 97,000 hours. Thus a 60-lb. preload is safer. If unusual cage pocket wear is observed, the preload should be increased.

Case 3 (Table 8) represents the condition where the magnetic pull forces are out of phase by 90 degrees. Case 4 (Table 9) is a repeat of Case 1 with no weight force (Space operation). Both these cases show adequate individual bearing lives.

Table 5

BEST PROGRAM PRINT OUT

	Title	Symbol	Unit
1.	δx		in.
2.	δy		in.
3.	δz		in.
4.	αx		rad.
5.	αy		rad.
6.	F_a		lb.
7.	F_{r_z}		lb.
8.	F_{r_y}		lb.
9.	M_y		in.-lbs.
10.	M_z		in.-lbs.
11.	Spring Rates (25)		lbs./in., in-lbs./rad.
12.	Diagonal Spring Rates		lbs./in., in-lbs./rad.
13.	Outer Element Loads	Po	lb.
14.	Inner Element Loads	PI	lb.
15.	Element Contact Angle	B	deg.
16.	Centrifugal Load per Element	CF	lb.
17.	Gyro Torque	G	in.
18.	Horiz. Disp. Ball Center Rel. to Curv. Ctr.	V_1	in.
19.	Vert. Disp. Ball Center Rel. to Curv. Ctr.	V_2	in.
20.	One outer, two inner central	CTL	N
21.	Outer Major Pressure Axis	A_o	in.
22.	Inner Major Pressure Axis	A_i	in.
23.	Outer Minor Pressure Axis	B_o	in.
24.	Inner Minor Pressure Axis	B_i	in.
25.	$\measuredangle$ to outside of ellipse	θ_1(0.I)	deg.
26.	$\measuredangle$ to inside of ellipse	θ_2(0.I)	deg.

	Title	Symbol	Unit
27.	Angle of Ball Rotational Axis	α	deg.
28.	RPM of Ball About Own Axis	NB	rpm
29.	Retainer Speed	NE	rpm
30.	Spin Component Outer	NSO	rpm
31.	Spin Component Inner	NSI	rpm
32.	Rolling Component Inner	NRI	rpm
33.	Rolling Component Outer	NRO	rpm
34.	Outer Def. Const. Check	K_o	N
35.	Inner Def. Const. Check	K_i	N
36.	Ball Velocity	SU max.	
37.	Mean Comp. Stress Outer	SM O	psi
38.	Mean Comp. Stress Inner	SM I	psi
39.	Outer Torque Due to Spin	QS O	in.-lbs.
40.	Inner Torque Due to Spin	QS I	in.-lbs.
41.	Outer Rolling Torque	QR O	in.-lbs.
42.	Inner Rolling Torque	QR I	in.-lbs.
43.	Coef. Friction Necessary to Prevent Slip	MUB	N
44.	Race Depth to Contain, Outer	H/D-O	in.
45.	Race Depth to Contain, Inner	H/D-I	in.
46.	Total Friction Torque		in.-lbs.
47.	Life Inner		hrs.
48.	Life Outer		hrs.
49.	Life Bearing		hrs.
50.	Life Assembly		hrs.

Table 5

BALLS/ROLLS	DIAM.	PITCH	BETA	FO	FI	LENGTH	EQV LENGTH	SPACING
1.30000E 01	4.68750E-01	2.36100E 00	1.60000E 01	5.30000E-01	5.20000E-01	-0.	-0.	6.91050E 00
1.30000E 01	4.68750E-01	2.36100E 00	-1.60000E 01	5.30000E-01	5.20000E-01	-0.	-0.	-6.91050E 00

PD	DEFL EXP	DEFL CON°O	DEFL CON°I	LIFE CON°O	LIFE CON°I	PRELOAD	SPRING THRUST
-2.40000E-04	1.50000E 00	2.45740E 07	2.66483E 07	7.14000E 03	7.14000E 03	-0.	-0.
-2.40000E-04	1.50000E 00	2.45740E 07	2.66483E 07	7.14000E 03	7.14000E 03	-0.	6.00000E 01

ELAST.CON.	ROTAT°O	ROTAT°I	COEF FRICT°O	COEF FRICT°I	CONTROL	DENSITY
2.58600E-07	1.00000E 00	-0.	7.50000E-02	7.50000E-02	1.00000E 00	2.83000E-01

INITIAL DEFLECTIONS

X	Y	Z	ALPHA°Y	ALPHA°Z
-0.	-0.	-0.	-0.	-0.
-0.	-0.	-0.	-0.	-0.

ITERATION COUNTS AND TOLERANCES FOR DELTA AND V

1.50000E 01 1.00000E 01 1.00000E-06 1.00000E-06

APPLIED LOADS AND OPERATING RPM

THRUST	RADIAL Y	RADIAL Z	MOMENT Y	MOMENT Z	OUTER RPM	INNER RPM
-1.60000E 01	-0.	2.00000E 02	-0.	-0.	-0.	1.20000E 04

DISPLACEMENTS BASED ON DYNAMIC LOADING

INITIAL GUESSES OF SHAFT DISPLACEMENTS

2.99813E-03 0. -2.99985E-03 0. 0.

SHAFT DISPLACEMENTS

-2.51802E-04 0. -2.90629E-04 6.81045E-06 0.

BEARING LOADS

7.09188E 01 0. -9.99186E 01 -3.38773E 01 0.
-5.48738E 01 0. -1.00082E 02 3.27192E 01 0.

SPRING RATES

9.60501E 04 -1.83910E-02 -1.51006E 05 -1.09587E 06 -1.17088E-01
-8.00555E-02 7.18156E 05 -9.29130E-02 1.42852E 00 8.81953E 05
-8.70821E 03 -7.71049E-02 1.13483E 06 3.43391E 05 1.39947E 00
-2.12346E 06 1.35089E 00 3.43871E 05 5.94609E 07 -6.08045E 00
3.79656E-01 8.82703E 05 1.35235E 00 -5.11170E 00 3.78124E 07

DIAGONAL SPRING RATES FOR EACH BEARING ABOUT ITS CENTER

9.60501E 04 4.19666E 05 5.90409E 05 1.45089E 06 1.07503E 06
0. 2.98490E 05 5.44422E 05 1.25794E 06 7.43790E 05

FLOATING BEARINGS ° AXIAL DISPLACEMENTS

0. 8.77778E-04

FRICTION TORQUES = 8.92226E-02 6.93403E-02

OUTER RACE LIVES = 3.26855E 05 3.97929E 05
INNER RACE LIVES = 2.12832E 05 2.66034E 05
BEARING LIVES = 1.37807E 05 1.70508E 05
RESULTANT BALL AND ROLLER BEARING LIVES = 8.16302E 04 0.

Case 1, Table 6 a

BEARING NO. 1

P-O	P-I	BETA-O	BETA-I	CF	G	V1	V2	CTL
1.88205E 01	6.04842E 00	8.30132E 00	2.63253E 01	1.30863E 01	-1.77180E-01	4.17401E-03	8.43607E-03	1.00000E 00
1.99932E 01	7.45374E 00	9.13249E 00	2.49189E 01	1.28686E 01	-1.91519E-01	3.96804E-03	8.54102E-03	1.00000E 00
2.28968E 01	1.06701E 01	1.04446E 01	2.27313E 01	1.25813E 01	-2.13839E-01	3.64358E-03	8.69692E-03	1.00000E 00
2.96458E 01	1.76963E 01	1.19572E 01	2.02383E 01	1.23271E 01	-2.39413E-01	3.26938E-03	8.86762E-03	1.00000E 00
4.10308E 01	2.92314E 01	1.30403E 01	1.84356E 01	1.21903E 01	-2.57818E-01	2.99837E-03	8.99477E-03	1.00000E 00
5.02878E 01	3.85396E 01	1.34740E 01	1.76870E 01	1.21448E 01	-2.65231E-01	2.88714E-03	9.05369E-03	1.00000E 00
5.02878E 01	3.85396E 01	1.34740E 01	1.76870E 01	1.21448E 01	-2.65231E-01	2.88714E-03	9.05369E-03	1.00000E 00
4.10308E 01	2.92314E 01	1.30403E 01	1.84356E 01	1.21903E 01	-2.57818E-01	2.99837E-03	8.99477E-03	1.00000E 00
2.96458E 01	1.76964E 01	1.19572E 01	2.02383E 01	1.23271E 01	-2.39413E-01	3.26938E-03	8.86762E-03	1.00000E 00
2.28968E 01	1.06701E 01	1.04446E 01	2.27313E 01	1.25813E 01	-2.13839E-01	3.64358E-03	8.69692E-03	1.00000E 00
1.99932E 01	7.45374E 00	9.13249E 00	2.49189E 01	1.28686E 01	-1.91519E-01	3.96804E-03	8.54102E-03	1.00000E 00
1.88205E 01	6.04839E 00	8.30132E 00	2.63253E 01	1.30863E 01	-1.77180E-01	4.17401E-03	8.43607E-03	1.00000E 00
1.85042E 01	5.64584E 00	8.01966E 00	2.68062E 01	1.31668E 01	-1.72268E-01	4.24391E-03	8.39925E-03	1.00000E 00

A-O	A-I	B-O	B-I	THETA1°O	THETA2°O	THETA1°I	THETA2°I	ALPHA
2.18773E-02	1.81375E-02	3.80927E-03	1.97895E-03	1.33533E 01	3.24932E 00	3.05927E 01	2.20580E 01	6.92944E 00
2.23233E-02	1.94493E-02	3.88604E-03	2.11879E-03	1.42878E 01	3.97723E 00	2.94955E 01	2.03423E 01	7.62377E 00
2.33569E-02	2.19258E-02	4.06433E-03	2.38317E-03	1.58393E 01	5.05000E 00	2.78921E 01	1.75704E 01	8.72021E 00
2.54591E-02	2.59609E-02	4.42780E-03	2.81513E-03	1.78390E 01	6.07536E 00	2.63522E 01	1.41243E 01	9.98471E 00
2.83739E-02	3.06943E-02	4.93264E-03	3.32328E-03	1.95983E 01	6.48225E 00	2.56698E 01	1.12014E 01	1.08906E 01
3.03656E-02	3.36596E-02	5.27792E-03	3.64215E-03	2.04946E 01	6.45343E 00	2.56244E 01	9.74964E 00	1.12535E 01
3.03656E-02	3.36596E-02	5.27792E-03	3.64215E-03	2.04946E 01	6.45343E 00	2.56244E 01	9.74964E 00	1.12535E 01
2.83739E-02	3.06943E-02	4.93264E-03	3.32328E-03	1.95983E 01	6.48225E 00	2.56698E 01	1.12014E 01	1.08906E 01
2.54591E-02	2.59609E-02	4.42779E-03	2.81513E-03	1.78390E 01	6.07537E 00	2.63522E 01	1.41243E 01	9.98471E 00
2.33569E-02	2.19258E-02	4.06433E-03	2.38317E-03	1.58393E 01	5.05000E 00	2.78921E 01	1.75704E 01	8.72021E 00
2.23233E-02	1.94493E-02	3.88604E-03	2.11879E-03	1.42878E 01	3.97723E 00	2.94955E 01	2.03423E 01	7.62377E 00
2.18773E-02	1.81374E-02	3.80927E-03	1.97895E-03	1.33533E 01	3.24933E 00	3.05926E 01	2.20580E 01	6.92945E 00
2.17539E-02	1.77246E-02	3.78804E-03	1.93497E-03	1.30431E 01	2.99626E 00	3.09762E 01	2.26362E 01	6.69420E 00

N-B	N-E	NS-O	NS-I	NR-O	NR-I	K-O	K-I	SV MAX
-3.04957E 04	5.05691E 03	-0.	1.32065E 04	-2.54831E 04	-3.49880E 04	2.45919E 07	2.67060E 07	8.40915E 04
-3.02295E 04	5.01467E 03	-0.	1.19302E 04	-2.52679E 04	-3.51978E 04	2.45905E 07	2.66966E 07	8.74368E 04
-2.98707E 04	4.95837E 03	0.	9.95294E 03	-2.49810E 04	-3.54767E 04	2.45880E 07	2.66830E 07	9.28371E 04
-2.95429E 04	4.90804E 03	-0.	7.71206E 03	-2.47238E 04	-3.57252E 04	2.45848E 07	2.66688E 07	1.00998E 05
-2.93591E 04	4.88073E 03	-0.	6.10637E 03	-2.45836E 04	-3.58589E 04	2.45822E 07	2.66596E 07	1.11899E 05
-2.92960E 04	4.87162E 03	-0.	5.44836E 03	-2.45365E 04	-3.59030E 04	2.45811E 07	2.66560E 07	1.20109E 05
-2.92960E 04	4.87162E 03	-0.	5.44836E 03	-2.45365E 04	-3.59030E 04	2.45811E 07	2.66560E 07	1.20109E 05
-2.93591E 04	4.88073E 03	-0.	6.10637E 03	-2.45836E 04	-3.58589E 04	2.45822E 07	2.66596E 07	1.11899E 05
-2.95429E 04	4.90804E 03	-0.	7.71206E 03	-2.47238E 04	-3.57252E 04	2.45848E 07	2.66688E 07	1.00998E 05
-2.98707E 04	4.95837E 03	0.	9.95294E 03	-2.49810E 04	-3.54767E 04	2.45880E 07	2.66830E 07	9.28371E 04
-3.02295E 04	5.01467E 03	-0.	1.19302E 04	-2.52679E 04	-3.51978E 04	2.45905E 07	2.66966E 07	8.74368E 04
-3.04957E 04	5.05691E 03	-0.	1.32065E 04	-2.54831E 04	-3.49880E 04	2.45919E 07	2.67060E 07	8.40912E 04
-3.05932E 04	5.07245E 03	0.	1.36438E 04	-2.55622E 04	-3.49108E 04	2.45923E 07	2.67093E 07	8.29372E 04

SM-O	SM-I	QS-O	QS-I	QR-O	QR-I	MU-B	H/D°O	H/D°I
7.18862E 04	5.36389E 04	1.20469E-02	3.14257E-03	2.30526E-04	5.15246E-05	3.03981E-02	1.43289E-02	7.23802E-02
7.33612E 04	5.75749E 04	1.30582E-02	4.15263E-03	2.54904E-04	7.29418E-05	2.97720E-02	1.63937E-02	6.73950E-02
7.67754E 04	6.49989E 04	1.56466E-02	6.70096E-03	3.19380E-04	1.32478E-04	2.71809E-02	2.01235E-02	6.04084E-02
8.37109E 04	7.70752E 04	2.20812E-02	1.31579E-02	4.90715E-04	3.07298E-04	2.15769E-02	2.54819E-02	5.40373E-02
9.33173E 04	9.12169E 04	3.40592E-02	2.56963E-02	8.42303E-04	7.07921E-04	1.56560E-02	3.07043E-02	5.13210E-02
9.98777E 04	1.00067E 05	4.46729E-02	3.71512E-02	1.18122E-03	1.12095E-03	1.27399E-02	3.35464E-02	5.11428E-02
9.98777E 04	1.00067E 05	4.46729E-02	3.71512E-02	1.18122E-03	1.12095E-03	1.27399E-02	3.35464E-02	5.11428E-02
9.33173E 04	9.12169E 04	3.40592E-02	2.56963E-02	8.42303E-04	7.07921E-04	1.56560E-02	3.07043E-02	5.13210E-02
8.37109E 04	7.70753E 04	2.20812E-02	1.31580E-02	4.90714E-04	3.07300E-04	2.15769E-02	2.54819E-02	5.40373E-02
7.67754E 04	6.49989E 04	1.56466E-02	6.70096E-03	3.19380E-04	1.32478E-04	2.71809E-02	2.01235E-02	6.04084E-02
7.33612E 04	5.75749E 04	1.30582E-02	4.15263E-03	2.54904E-04	7.29418E-05	2.97720E-02	1.63937E-02	6.73950E-02
7.18862E 04	5.36388E 04	1.20469E-02	3.14255E-03	2.30526E-04	5.15242E-05	3.03982E-02	1.43289E-02	7.23802E-02
7.14776E 04	5.23997E 04	1.17776E-02	2.86667E-03	2.24119E-04	4.59452E-05	3.04351E-02	1.36736E-02	7.41618E-02

Case 1, Table 6 b

III 83 47

BEARING NO. 2

P-O	P-I	BETA-O	BETA-I	CF	G	V1	V2	CTL
1.67272E 01	3.37260E 00	-5.56225E 00	-2.82947E 01	1.35822E 01	1.23473E-01	-4.45576E-03	8.27708E-03	1.00000E 00
1.73810E 01	4.36962E 00	-6.55899E 00	-2.66160E 01	1.32575E 01	1.42015E-01	-4.21351E-03	8.40830E-03	1.00000E 00
1.92188E 01	6.67681E 00	-8.18360E 00	-2.39293E 01	1.28213E 01	1.71123E-01	-3.81870E-03	8.60551E-03	1.00000E 00
2.44332E 01	1.23358E 01	-1.02604E 01	-2.05626E 01	1.24101E 01	2.07224E-01	-3.31380E-03	8.83374E-03	1.00000E 00
3.68412E 01	2.50035E 01	-1.19834E 01	-1.77836E 01	1.21775E 01	2.36989E-01	-2.89261E-03	9.01829E-03	1.00000E 00
4.94013E 01	3.76395E 01	-1.26456E 01	-1.66861E 01	1.21113E 01	2.48500E-01	-2.72797E-03	9.10082E-03	1.00000E 00
4.94013E 01	3.76395E 01	-1.26456E 01	-1.66861E 01	1.21113E 01	2.48500E-01	-2.72797E-03	9.10082E-03	1.00000E 00
3.68412E 01	2.50035E 01	-1.19834E 01	-1.77836E 01	1.21775E 01	2.36989E-01	-2.89261E-03	9.01829E-03	1.00000E 00
2.44332E 01	1.23358E 01	-1.02604E 01	-2.05626E 01	1.24101E 01	2.07224E-01	-3.31380E-03	8.83374E-03	1.00000E 00
1.92188E 01	6.67681E 00	-8.18360E 00	-2.39293E 01	1.28213E 01	1.71123E-01	-3.81870E-03	8.60551E-03	1.00000E 00
1.73810E 01	4.36962E 00	-6.55899E 00	-2.66160E 01	1.32575E 01	1.42015E-01	-4.21351E-03	8.40830E-03	1.00000E 00
1.67272E 01	3.37260E 00	-5.56225E 00	-2.82947E 01	1.35822E 01	1.23473E-01	-4.45576E-03	8.27708E-03	1.00000E 00
1.65652E 01	3.08552E 00	-5.22752E 00	-2.88642E 01	1.37020E 01	1.17091E-01	-4.53711E-03	8.23111E-03	1.00000E 00

A-O	A-I	B-O	B-I	THETA1°O	THETA2°O	THETA1°I	THETA2°I	ALPHA
2.10324E-02	1.49243E-02	3.66432E-03	1.63213E-03	-1.04186E 01	-7.05861E-01	-3.18050E 01	-2.47844E 01	-4.64214E 00
2.13085E-02	1.62739E-02	3.71085E-03	1.77621E-03	-1.14781E 01	-1.63984E 00	-3.04442E 01	-2.27878E 01	-5.47427E 00
2.20305E-02	1.87510E-02	3.83605E-03	2.04058E-03	-1.32711E 01	-3.09614E 00	-2.83412E 01	-1.95173E 01	-6.83094E 00
2.38678E-02	2.30179E-02	4.15349E-03	2.49673E-03	-1.57734E 01	-4.74736E 00	-2.59812E 01	-1.51439E 01	-8.56602E 00
2.73717E-02	2.91386E-02	4.76037E-03	3.15320E-03	-1.83088E 01	-5.65800E 00	-2.46493E 01	-1.09179E 01	-1.00064E 01
3.01846E-02	3.33986E-02	5.24824E-03	3.61114E-03	-1.96241E 01	-5.66701E 00	-2.45615E 01	-8.81068E 00	-1.05602E 01
3.01846E-02	3.33986E-02	5.24824E-03	3.61114E-03	-1.96241E 01	-5.66701E 00	-2.45615E 01	-8.81068E 00	-1.05602E 01
2.73717E-02	2.91386E-02	4.76037E-03	3.15320E-03	-1.83088E 01	-5.65800E 00	-2.46493E 01	-1.09179E 01	-1.00064E 01
2.38678E-02	2.30179E-02	4.15348E-03	2.49673E-03	-1.57734E 01	-4.74736E 00	-2.59812E 01	-1.51439E 01	-8.56602E 00
2.20305E-02	1.87510E-02	3.83605E-03	2.04058E-03	-1.32711E 01	-3.09614E 00	-2.83412E 01	-1.95173E 01	-6.83094E 00
2.13035E-02	1.62739E-02	3.71085E-03	1.77621E-03	-1.14781E 01	-1.63984E 00	-3.04442E 01	-2.27878E 01	-5.47427E 00
2.10324E-02	1.49243E-02	3.66432E-03	1.63213E-03	-1.04186E 01	-7.05861E-01	-3.18050E 01	-2.47844E 01	-4.64214E 00
2.09641E-02	1.44870E-02	3.65263E-03	1.58540E-03	-1.00681E 01	-3.86934E-01	-3.22715E 01	-2.54569E 01	-4.36273E 00

N-B	N-E	NS-O	NS-I	NR-O	NR-I	K-O	K-I	SV MAX
-3.10966E 04	5.15185E 03	0.	-1.57217E 04	-2.59650E 04	-3.45143E 04	2.45955E 07	2.67199E 07	-6.76814E 04
-3.07120E 04	5.08989E 03	0.	-1.41729E 04	-2.56499E 04	-3.48226E 04	2.45943E 07	2.67080E 07	-7.26382E 04
-3.01830E 04	5.00545E 03	0.	-1.17112E 04	-2.52201E 04	-3.52423E 04	2.45921E 07	2.66903E 07	-7.98320E 04
-2.96663E 04	4.92453E 03	0.	-8.65136E 03	-2.48076E 04	-3.56431E 04	2.45884E 07	2.66706E 07	-8.90511E 04
-2.93596E 04	4.87817E 03	0.	-6.14812E 03	-2.45702E 04	-3.58710E 04	2.45847E 07	2.66564E 07	-1.01567E 05
-2.92679E 04	4.86489E 03	-0.	-5.17199E 03	-2.45016E 04	-3.59354E 04	2.45832E 07	2.66514E 07	-1.12309E 05
-2.92679E 04	4.86489E 03	-0.	-5.17199E 03	-2.45016E 04	-3.59354E 04	2.45832E 07	2.66514E 07	-1.12309E 05
-2.93596E 04	4.87817E 03	0.	-6.14813E 03	-2.45702E 04	-3.58710E 04	2.45847E 07	2.66564E 07	-1.01567E 05
-2.96663E 04	4.92453E 03	0.	-8.65136E 03	-2.48076E 04	-3.56431E 04	2.45884E 07	2.66706E 07	-8.90510E 04
-3.01830E 04	5.00545E 03	0.	-1.17112E 04	-2.52201E 04	-3.52423E 04	2.45921E 07	2.66903E 07	-7.98320E 04
-3.07120E 04	5.08989E 03	0.	-1.41729E 04	-2.56499E 04	-3.48226E 04	2.45943E 07	2.67080E 07	-7.26382E 04
-3.10966E 04	5.15185E 03	0.	-1.57217E 04	-2.59650E 04	-3.45143E 04	2.45955E 07	2.67199E 07	-6.76814E 04
-3.12367E 04	5.17450E 03	0.	-1.62493E 04	-2.60802E 04	-3.44014E 04	2.45959E 07	2.67240E 07	-6.58845E 04

SM-O	SM-I	QS-O	QS-I	QR-O	QR-I	MU-B	H/D°O	H/D°I
6.90863E 04	4.40724E 04	1.02938E-02	1.44197E-03	1.89469E-04	1.95056E-05	2.62101E-02	8.73827E-03	7.80796E-02
6.99844E 04	4.81178E 04	1.08339E-02	2.03707E-03	2.01947E-04	3.00129E-05	2.78581E-02	1.05996E-02	7.16961E-02
7.23883E 04	5.55445E 04	1.23880E-02	3.58612E-03	2.38690E-04	6.07624E-05	2.81949E-02	1.41537E-02	6.23293E-02
7.84522E 04	6.83252E 04	1.70619E-02	8.13246E-03	3.55777E-04	1.68682E-04	2.40462E-02	1.99575E-02	5.25525E-02
8.99998E 04	8.66226E 04	2.95020E-02	2.08655E-02	7.04165E-04	5.46105E-04	1.63499E-02	2.68302E-02	4.73838E-02
9.92633E 04	9.93393E 04	4.36247E-02	3.60013E-02	1.14671E-03	1.07797E-03	1.21813E-02	3.07844E-02	4.70520E-02
9.92633E 04	9.93393E 04	4.36247E-02	3.60013E-02	1.14671E-03	1.07797E-03	1.21813E-02	3.07844E-02	4.70520E-02
8.99998E 04	8.66225E 04	2.95020E-02	2.08654E-02	7.04165E-04	5.46104E-04	1.63499E-02	2.68302E-02	4.73838E-02
7.84522E 04	6.83251E 04	1.70618E-02	8.13242E-03	3.55776E-04	1.68681E-04	2.40463E-02	1.99575E-02	5.25525E-02
7.23883E 04	5.55445E 04	1.23880E-02	3.58612E-03	2.38690E-04	6.07624E-05	2.81949E-02	1.41537E-02	6.23293E-02
6.99845E 04	4.81178E 04	1.08339E-02	2.03707E-03	2.01948E-04	3.00129E-05	2.78580E-02	1.05996E-02	7.16961E-02
6.90863E 04	4.40724E 04	1.02938E-02	1.44197E-03	1.89469E-04	1.95056E-05	2.62101E-02	8.73827E-03	7.80796E-02
6.88598E 04	4.27623E 04	1.01611E-02	1.28060E-03	1.86427E-04	1.68217E-05	2.54234E-02	8.16167E-03	8.03258E-02

Table 1 Table of c

BALLS/ROLLS	DIAM.	PITCH	BETA	FC	[illegible]	LENGTH	[illegible] LENGTH	[illegible]ING
[illegible]	[illegible]	[illegible]	[illegible]	[illegible]	5.20000E-01	-0.	-0.	6.91050E 00
1.30000E 01	4.68750E-01	2.36100E 00	-1.60000E 01	5.30000E-01	5.20000E-01	-0.	-0.	-6.91050E 00

PC	DEFL EXP	DEFL CON°O	DEFL CON°I	LIFE CON°O	LIFE CON°I	PRELOAD	SPRING THRUST
-2.40000E-04	1.50000E 00	2.45740E 07	2.66483E 07	7.14000E 03	7.14000E 03	-0.	-0.
-2.40000E-04	1.50000E 00	2.45740E 07	2.66483E 07	7.14000E 03	7.14000E 03	-0.	1.00000E 02

ELAST.CON.	ROTAT°O	ROTAT°I	COEF FRICT°O	COEF FRICT°I	CONTROL	DENSITY
2.58600E-07	1.00000E 00	-0.	7.50000E-02	7.50000E-02	1.00000E 00	2.83000E-01

INITIAL DEFLECTIONS

X	Y	Z	ALPHA°Y	ALPHA°Z
-0.	-0.	-0.	-0.	-0.
-0.	-0.	-0.	-0.	-0.

ITERATION COUNTS AND TOLERANCES FOR DELTA AND V

1.50000E 01 1.00000E 01 1.00000E-06 1.00000E-06

APPLIED LOADS AND OPERATING RPM

THRUST	RADIAL Y	RADIAL Z	MOMENT Y	MOMENT Z	OUTER RPM	INNER RPM
-1.60000E 01	-0.	2.00000E 02	-0.	-0.	-0.	1.20000E 04

DISPLACEMENTS BASED ON DYNAMIC LOADING

INITIAL GUESSES OF SHAFT DISPLACEMENTS

2.99813E-03 0. -2.99985E-03 0. 0.

SHAFT DISPLACEMENTS

2.55328E-04 0. -1.39072E-04 1.71750E-06 0.

BEARING LOADS

1.16000E 02 0. -9.99708E 01 -3.56981E 01 0.
-9.99982E 01 0. -1.00578E 02 3.55059E 01 0.

SPRING RATES

1.65064E 05 2.23952E-02 -1.38045E 05 -1.00580E 06 1.08892E-01
2.67742E-02 1.45755E 06 -1.18113E-02 -3.77434E-01 9.38645E 05
1.00552E 04 3.95732E-04 1.53315E 06 6.56240E 05 -2.61223E-01
-2.10162E 06 -2.70013E-01 6.56446E 05 8.09995E 07 -1.89815E-01
1.39826E-01 9.38738E 05 -1.85052E-01 -2.75753E-01 7.70521E 07

DIAGONAL SPRING RATES FOR EACH BEARING ABOUT ITS CENTER

1.65064E 05 7.93163E 05 8.11453E 05 2.13975E 06 2.10280E 06
0. 6.64382E 05 7.21693E 05 1.87443E 06 1.74570E 06

FLOATING BEARINGS ' AXIAL DISPLACEMENTS

0. -3.79799E-04

FRICTION TORQUES = 1.58276E-01 1.31973E-01

OUTER RACE LIVES = 1.68209E 05 2.12592E 05
INNER RACE LIVES = 9.18066E 04 1.23844E 05
BEARING LIVES = 6.33464E 04 8.35467E 04
RESULTANT BALL AND ROLLER BEARING LIVES = 3.85740E 04 0.

Case 2, Table 7 a

BEARING NO. 1

P-O	P-I	BETA-O	BETA-I	CF	G	V1	V2	CTL
2.68411E 01	1.47724E 01	1.24182E 01	2.28754E 01	1.25074E 01	-2.52172E-01	3.67057E-03	8.69985E-03	1.00000E 00
2.95670E 01	1.75890E 01	1.29371E 01	2.20184E 01	1.24214E 01	-2.60712E-01	3.54314E-03	8.76150E-03	1.00000E 00
3.49193E 01	2.30560E 01	1.36356E 01	2.08615E 01	1.23194E 01	-2.72258E-01	3.37086E-03	8.84526E-03	1.00000E 00
4.29923E 01	3.12155E 01	1.42646E 01	1.98049E 01	1.22403E 01	-2.82716E-01	3.21407E-03	8.92504E-03	1.00000E 00
5.15799E 01	3.98542E 01	1.46649E 01	1.91122E 01	1.21957E 01	-2.89405E-01	3.11237E-03	8.98181E-03	1.00000E 00
5.70980E 01	4.53914E 01	1.48466E 01	1.87881E 01	1.21767E 01	-2.92448E-01	3.06534E-03	9.01049E-03	1.00000E 00
5.70980E 01	4.53914E 01	1.48466E 01	1.87881E 01	1.21767E 01	-2.92448E-01	3.06534E-03	9.01049E-03	1.00000E 00
5.15799E 01	3.98542E 01	1.46649E 01	1.91122E 01	1.21957E 01	-2.89405E-01	3.11237E-03	8.98181E-03	1.00000E 00
4.29923E 01	3.12155E 01	1.42646E 01	1.98049E 01	1.22403E 01	-2.82716E-01	3.21407E-03	8.92503E-03	1.00000E 00
3.49193E 01	2.30560E 01	1.36356E 01	2.08615E 01	1.23194E 01	-2.72258E-01	3.37086E-03	8.84526E-03	1.00000E 00
2.95670E 01	1.75890E 01	1.29371E 01	2.20184E 01	1.24214E 01	-2.60712E-01	3.54314E-03	8.76150E-03	1.00000E 00
2.68411E 01	1.47724E 01	1.24182E 01	2.28754E 01	1.25074E 01	-2.52172E-01	3.67057E-03	8.69985E-03	1.00000E 00
2.60686E 01	1.39565E 01	1.22268E 01	2.31914E 01	1.25414E 01	-2.49025E-01	3.71749E-03	8.67717E-03	1.00000E 00

A-O	A-I	B-O	B-I	THETA1'O	THETA2'O	THETA1'I	THETA2'I	ALPHA
2.46302E-02	2.44367E-02	4.28287E-03	2.65647E-03	1.81079E 01	6.72856E 00	2.86292E 01	1.71217E 01	1.03706E 01
2.54380E-02	2.59031E-02	4.42242E-03	2.81351E-03	1.88140E 01	7.06014E 00	2.81186E 01	1.59181E 01	1.08046E 01
2.68897E-02	2.83524E-02	4.67346E-03	3.07619E-03	1.98493E 01	7.42204E 00	2.75411E 01	1.41818E 01	1.13891E 01
2.88212E-02	3.13691E-02	5.00778E-03	3.40029E-03	2.09265E 01	7.60273E 00	2.71990E 01	1.24107E 01	1.19155E 01
3.06257E-02	3.40331E-02	5.32036E-03	3.68686E-03	2.17460E 01	7.58386E 00	2.71382E 01	1.10862E 01	1.22505E 01
3.16815E-02	3.55426E-02	5.50330E-03	3.84934E-03	2.21731E 01	7.52011E 00	2.71727E 01	1.04036E 01	1.24026E 01
3.16815E-02	3.55426E-02	5.50330E-03	3.84934E-03	2.21731E 01	7.52011E 00	2.71727E 01	1.04036E 01	1.24026E 01
3.06257E-02	3.40331E-02	5.32036E-03	3.68686E-03	2.17460E 01	7.58386E 00	2.71382E 01	1.10862E 01	1.22505E 01
2.88212E-02	3.13691E-02	5.00778E-03	3.40028E-03	2.09265E 01	7.60273E 00	2.71990E 01	1.24107E 01	1.19155E 01
2.68897E-02	2.83524E-02	4.67346E-03	3.07619E-03	1.98493E 01	7.42204E 00	2.75411E 01	1.41818E 01	1.13891E 01
2.54380E-02	2.59031E-02	4.42242E-03	2.81351E-03	1.88140E 01	7.06014E 00	2.81186E 01	1.59181E 01	1.08046E 01
2.46302E-02	2.44367E-02	4.28287E-03	2.65647E-03	1.81079E 01	6.72856E 00	2.86292E 01	1.71217E 01	1.03706E 01
2.43913E-02	2.39774E-02	4.24164E-03	2.60736E-03	1.78611E 01	6.59246E 00	2.88366E 01	1.75461E 01	1.02105E 01

N-B	N-E	NS-O	NS-I	NR-O	NR-I	K-O	K-I	SV MAX
-2.97547E 04	4.94380E 03	-0.	9.18550E 03	-2.49075E 04	-3.55500E 04	2.45837E 07	2.66839E 07	1.06416E 05
-2.96426E 04	4.92676E 03	0.	8.41639E 03	-2.48204E 04	-3.56340E 04	2.45825E 07	2.66788E 07	1.09617E 05
-2.95074E 04	4.90650E 03	-0.	7.38217E 03	-2.47165E 04	-3.57336E 04	2.45807E 07	2.66722E 07	1.15269E 05
-2.94001E 04	4.89073E 03	-0.	6.44424E 03	-2.46355E 04	-3.58106E 04	2.45790E 07	2.66665E 07	1.23250E 05
-2.93381E 04	4.88181E 03	-0.	5.83574E 03	-2.45893E 04	-3.58538E 04	2.45779E 07	2.66630E 07	1.31423E 05
-2.93114E 04	4.87801E 03	-0.	5.55373E 03	-2.45696E 04	-3.58721E 04	2.45774E 07	2.66613E 07	1.36437E 05
-2.93114E 04	4.87801E 03	-0.	5.55373E 03	-2.45696E 04	-3.58721E 04	2.45774E 07	2.66613E 07	1.36437E 05
-2.93381E 04	4.88181E 03	-0.	5.83574E 03	-2.45893E 04	-3.58538E 04	2.45779E 07	2.66630E 07	1.31423E 05
-2.94001E 04	4.89073E 03	-0.	6.44425E 03	-2.46355E 04	-3.58106E 04	2.45790E 07	2.66665E 07	1.23250E 05
-2.95074E 04	4.90650E 03	-0.	7.38217E 03	-2.47165E 04	-3.57336E 04	2.45807E 07	2.66722E 07	1.15269E 05
-2.96426E 04	4.92676E 03	0.	8.41639E 03	-2.48204E 04	-3.56340E 04	2.45825E 07	2.66788E 07	1.09617E 05
-2.97547E 04	4.94380E 03	-0.	9.18550E 03	-2.49075E 04	-3.55500E 04	2.45837E 07	2.66839E 07	1.06416E 05
-2.97985E 04	4.95052E 03	0.	9.46965E 03	-2.49419E 04	-3.55169E 04	2.45842E 07	2.66858E 07	1.05601E 05

SM-O	SM-I	QS-O	QS-I	QR-O	QR-I	MU-B	H/D'O	H/D'I
8.09932E 04	7.24359E 04	1.93410E-02	1.03398E-02	4.16021E-04	2.27480E-04	2.58554E-02	2.62493E-02	6.35757E-02
8.36594E 04	7.68233E 04	2.20037E-02	1.30497E-02	4.88602E-04	3.04086E-04	2.35892E-02	2.83176E-02	6.13738E-02
8.84485E 04	8.41454E 04	2.74695E-02	1.87226E-02	6.44296E-04	4.76942E-04	2.00367E-02	3.14877E-02	5.89267E-02
9.48165E 04	9.31543E 04	3.62488E-02	2.80448E-02	9.10415E-04	7.89340E-04	1.62551E-02	3.49591E-02	5.74993E-02
1.00763E 05	1.01103E 05	4.62117E-02	3.88461E-02	1.23228E-03	1.18487E-03	1.35048E-02	3.77171E-02	5.72476E-02
1.04242E 05	1.05606E 05	5.29187E-02	4.62053E-02	1.45908E-03	1.47096E-03	1.21747E-02	3.91945E-02	5.73902E-02
1.04242E 05	1.05606E 05	5.29187E-02	4.62053E-02	1.45908E-03	1.47096E-03	1.21747E-02	3.91945E-02	5.73902E-02
1.00763E 05	1.01103E 05	4.62117E-02	3.88461E-02	1.23228E-03	1.18487E-03	1.35048E-02	3.77171E-02	5.72476E-02
9.48165E 04	9.31543E 04	3.62488E-02	2.80448E-02	9.10415E-04	7.89338E-04	1.62551E-02	3.49591E-02	5.74993E-02
8.84485E 04	8.41454E 04	2.74695E-02	1.87226E-02	6.44296E-04	4.76942E-04	2.00367E-02	3.14877E-02	5.89267E-02
8.36594E 04	7.68233E 04	2.20037E-02	1.30497E-02	4.88602E-04	3.04086E-04	2.35892E-02	2.83176E-02	6.13738E-02
8.09932E 04	7.24359E 04	1.93410E-02	1.03398E-02	4.16021E-04	2.27480E-04	2.58554E-02	2.62493E-02	6.35757E-02
8.02044E 04	7.10601E 04	1.86023E-02	9.58519E-03	3.96302E-04	2.06967E-04	2.65460E-02	2.55444E-02	6.44807E-02

Case 2 Table 7 b

BEARING NO. 2

P-O	P-I	BETA-O	BETA-I	CF	G	V1	V2	CTL
2.36547E 01	1.14259E 01	-1.13153E 01	-2.37890E 01	1.26351E 01	2.32444E-01	-3.80453E-03	8.63050E-03	1.00000E 00
2.58773E 01	1.37693E 01	-1.19375E 01	-2.27699E 01	1.25183E 01	2.42766E-01	-3.65333E-03	8.70375E-03	1.00000E 00
3.05395E 01	1.85961E 01	-1.28313E 01	-2.13111E 01	1.23737E 01	2.57612E-01	-3.43576E-03	8.80724E-03	1.00000E 00
3.85499E 01	2.67296E 01	-1.36841E 01	-1.99103E 01	1.22592E 01	2.71857E-01	-3.22676E-03	8.90884E-03	1.00000E 00
4.79726E 01	3.62293E 01	-1.42320E 01	-1.89901E 01	1.21969E 01	2.81069E-01	-3.09061E-03	8.98081E-03	1.00000E 00
5.43194E 01	4.25987E 01	-1.44748E 01	-1.85713E 01	1.21718E 01	2.85166E-01	-3.02934E-03	9.01642E-03	1.00000E 00
5.43194E 01	4.25987E 01	-1.44748E 01	-1.85713E 01	1.21718E 01	2.85166E-01	-3.02934E-03	9.01642E-03	1.00000E 00
4.79726E 01	3.62293E 01	-1.42320E 01	-1.89901E 01	1.21969E 01	2.81069E-01	-3.09061E-03	8.98081E-03	1.00000E 00
3.85499E 01	2.67296E 01	-1.36841E 01	-1.99103E 01	1.22592E 01	2.71857E-01	-3.22676E-03	8.90884E-03	1.00000E 00
3.05395E 01	1.85961E 01	-1.28313E 01	-2.13111E 01	1.23737E 01	2.57612E-01	-3.43576E-03	8.80724E-03	1.00000E 00
2.58773E 01	1.37693E 01	-1.19375E 01	-2.27699E 01	1.25183E 01	2.42766E-01	-3.65333E-03	8.70375E-03	1.00000E 00
2.36547E 01	1.14259E 01	-1.13153E 01	-2.37890E 01	1.26351E 01	2.32444E-01	-3.80453E-03	8.63050E-03	1.00000E 00
2.30241E 01	1.07478E 01	-1.10954E 01	-2.41502E 01	1.26797E 01	2.28794E-01	-3.85793E-03	8.60427E-03	1.00000E 00

A-O	A-I	B-O	B-I	THETA1'O	THETA2'O	THETA1'I	THETA2'I	ALPHA
2.36128E-02	2.24288E-02	4.10764E-03	2.44046E-03	-1.67692E 01	-5.86133E 00	-2.90686E 01	-1.85095E 01	-9.44819E 00
2.43311E-02	2.38709E-02	4.23164E-03	2.59469E-03	-1.75579E 01	-6.31713E 00	-2.83899E 01	-1.71498E 01	-9.96846E 00
2.57137E-02	2.63905E-02	4.47055E-03	2.86452E-03	-1.87721E 01	-6.89040E 00	-2.75266E 01	-1.50955E 01	-1.07160E 01
2.77912E-02	2.97878E-02	4.83003E-03	3.22917E-03	-2.01068E 01	-7.26129E 00	-2.69297E 01	-1.28908E 01	-1.14295E 01
2.98936E-02	3.29688E-02	5.19419E-03	3.57119E-03	-2.11430E 01	-7.32109E 00	-2.67636E 01	-1.12167E 01	-1.18881E 01
3.11582E-02	3.47990E-02	5.41333E-03	3.76812E-03	-2.16796E 01	-7.26999E 00	-2.67792E 01	-1.03634E 01	-1.20913E 01
3.11582E-02	3.47990E-02	5.41333E-03	3.76812E-03	-2.16796E 01	-7.26999E 00	-2.67792E 01	-1.03634E 01	-1.20913E 01
2.98936E-02	3.29688E-02	5.19419E-03	3.57119E-03	-2.11430E 01	-7.32109E 00	-2.67636E 01	-1.12167E 01	-1.18881E 01
2.77912E-02	2.97878E-02	4.83003E-03	3.22917E-03	-2.01068E 01	-7.26129E 00	-2.69297E 01	-1.28908E 01	-1.14295E 01
2.57137E-02	2.63905E-02	4.47055E-03	2.86452E-03	-1.87721E 01	-6.89040E 00	-2.75266E 01	-1.50955E 01	-1.07160E 01
2.43311E-02	2.38709E-02	4.23164E-03	2.59469E-03	-1.75579E 01	-6.31713E 00	-2.83899E 01	-1.71498E 01	-9.96846E 00
2.36128E-02	2.24288E-02	4.10764E-03	2.44046E-03	-1.67692E 01	-5.86133E 00	-2.90686E 01	-1.85095E 01	-9.44819E 00
2.34008E-02	2.19750E-02	4.07108E-03	2.39198E-03	-1.65002E 01	-5.69058E 00	-2.93227E 01	-1.89777E 01	-9.26438E 00

N-B	N-E	NS-O	NS-I	NR-O	NR-I	K-O	K-I	SV MAX
-2.99241E 04	4.96898E 03	0.	-1.02480E 04	-2.50358E 04	-3.54253E 04	2.45862E 07	2.66894E 07	-9.99577E 04
-2.97749E 04	4.94596E 03	0.	-9.32741E 03	-2.49183E 04	-3.55391E 04	2.45848E 07	2.66832E 07	-1.03121E 05
-2.95864E 04	4.91729E 03	0.	-8.01404E 03	-2.47717E 04	-3.56804E 04	2.45827E 07	2.66747E 07	-1.08388E 05
-2.94331E 04	4.89450E 03	0.	-6.76048E 03	-2.46548E 04	-3.57921E 04	2.45806E 07	2.66671E 07	-1.16584E 05
-2.93473E 04	4.88204E 03	0.	-5.94461E 03	-2.45905E 04	-3.58527E 04	2.45791E 07	2.66623E 07	-1.25640E 05
-2.93121E 04	4.87702E 03	-0.	-5.57663E 03	-2.45645E 04	-3.58769E 04	2.45785E 07	2.66603E 07	-1.31341E 05
-2.93121E 04	4.87702E 03	-0.	-5.57663E 03	-2.45645E 04	-3.58769E 04	2.45785E 07	2.66603E 07	-1.31341E 05
-2.93473E 04	4.88204E 03	0.	-5.94461E 03	-2.45905E 04	-3.58527E 04	2.45791E 07	2.66623E 07	-1.25640E 05
-2.94331E 04	4.89450E 03	0.	-6.76048E 03	-2.46548E 04	-3.57921E 04	2.45806E 07	2.66671E 07	-1.16584E 05
-2.95864E 04	4.91729E 03	0.	-8.01404E 03	-2.47717E 04	-3.56804E 04	2.45827E 07	2.66747E 07	-1.08388E 05
-2.97749E 04	4.94596E 03	0.	-9.32741E 03	-2.49183E 04	-3.55391E 04	2.45848E 07	2.66832E 07	-1.03121E 05
-2.99241E 04	4.96898E 03	0.	-1.02480E 04	-2.50358E 04	-3.54253E 04	2.45862E 07	2.66894E 07	-9.99577E 04
-2.99805E 04	4.97773E 03	0.	-1.05748E 04	-2.50805E 04	-3.53820E 04	2.45867E 07	2.66917E 07	-9.89906E 04

SM-O	SM-I	QS-O	QS-I	QR-O	QR-I	MU-B	H/D'O	H/D'I
7.76296E 04	6.64451E 04	1.63413E-02	7.34050E-03	3.37170E-04	1.48399E-04	2.82709E-02	2.25383E-02	6.54999E-02
8.00015E 04	7.07635E 04	1.84204E-02	9.41451E-03	3.91470E-04	2.02395E-04	2.61258E-02	2.46912E-02	6.25394E-02
8.45641E 04	7.83021E 04	2.29738E-02	1.40562E-02	5.15595E-04	3.33624E-04	2.23696E-02	2.81928E-02	5.88658E-02
9.14147E 04	8.84531E 04	3.13420E-02	2.28040E-02	7.59420E-04	6.09918E-04	1.77686E-02	3.23018E-02	5.63873E-02
9.83438E 04	9.79478E 04	4.19530E-02	3.42084E-02	1.09233E-03	1.01123E-03	1.42423E-02	3.56779E-02	5.57064E-02
1.02510E 05	1.03408E 05	4.95125E-02	4.24550E-02	1.34292E-03	1.32369E-03	1.25540E-02	3.74901E-02	5.57703E-02
1.02510E 05	1.03408E 05	4.95125E-02	4.24550E-02	1.34292E-03	1.32369E-03	1.25540E-02	3.74901E-02	5.57703E-02
9.83438E 04	9.79478E 04	4.19530E-02	3.42084E-02	1.09233E-03	1.01123E-03	1.42423E-02	3.56779E-02	5.57064E-02
9.14147E 04	8.84531E 04	3.13420E-02	2.28040E-02	7.59420E-04	6.09918E-04	1.77686E-02	3.23018E-02	5.63873E-02
8.45641E 04	7.83021E 04	2.29738E-02	1.40562E-02	5.15595E-04	3.33624E-04	2.23696E-02	2.81928E-02	5.88658E-02
8.00015E 04	7.07635E 04	1.84204E-02	9.41451E-03	3.91470E-04	2.02395E-04	2.61258E-02	2.46912E-02	6.25394E-02
7.76296E 04	6.64451E 04	1.63413E-02	7.34050E-03	3.37170E-04	1.48399E-04	2.82709E-02	2.25383E-02	6.54999E-02
7.69294E 04	6.50853E 04	1.57630E-02	6.76527E-03	3.22356E-04	1.34039E-04	2.89053E-02	2.18261E-02	6.66246E-02

Case 2, Table 7 c

BALLS/ROLLS	DIAM.	PITCH	BETA	FO	FI	LENGTH	EQV LENGTH	SPACING
1.36000E 01	4.68750E-01	2.36100E 00	1.60000E 01	5.30000E-01	5.20000E-01	-0.	-0.	6.91050E 00
1.36000E 01	4.68750E-01	2.36100E 00	-1.60000E 01	5.30000E-01	5.20000E-01	-0.	-0.	-6.91050E 00

TC	DEFL EXP	DEFL CON°O	DEFL CON°I	LIFE CON°O	LIFE CON°I	PRELOAD	SPRING THRUST
-2.40000E-04	1.50000E 00	2.45740E 07	2.66483E 07	7.14000E 03	7.14000E 03	-0.	-0.
-2.40000E-04	1.50000E 00	2.45740E 07	2.66483E 07	7.14000E 03	7.14000E 03	-0.	6.00000E 01

ELAST.CON.	ROTAT°O	ROTAT°I	COEF FRICT°O	COEF FRICT°I	CONTROL	DENSITY
2.58600E-07	1.00000E 00	-0.	7.50000E-02	7.50000E-02	1.00000E 00	2.83000E-01

INITIAL DEFLECTIONS

X	Y	Z	ALPHA°Y	ALPHA°Z
-0.	-0.	-0.	-0.	-0.
-0.	-0.	-0.	-0.	-0.

ITERATION COUNTS AND TOLERANCES FOR DELTA AND V

1.50000E 01 1.00000E 01 1.00000E-06 1.00000E-06

APPLIED LOADS AND OPERATING RPM

THRUST	RADIAL Y	RADIAL Z	MOMENT Y	MOMENT Z	OUTER RPM	INNER RPM
-1.60000E 01	-0.	1.35000E 02	2.95750E 02	-0.	-0.	1.20000E 04

DISPLACEMENTS BASED ON DYNAMIC LOADING

INITIAL GUESSES OF SHAFT DISPLACEMENTS

2.99813E-03 0. -2.99978E-03 -2.99990E-04 0.

SHAFT DISPLACEMENTS

-1.19771E-04 0. -1.59376E-04 -3.91316E-06 0.

BEARING LOADS

7.60026E 01 0. -8.78781E 01 -3.03791E 01 0.
-5.99922E 01 0. -4.66917E 01 1.61235E 01 0.

SPRING RATES

1.04651E 05 9.50717E-05 -1.39832E 05 -1.01561E 06 -4.35044E-03
-3.26207E-02 8.38612E 05 -2.45788E-02 3.43828E-01 7.81144E 05
-5.68046E 04 -2.92175E-02 1.02657E 06 1.14528E 06 3.39922E-01
-1.61475E 06 3.41875E-01 1.14469E 06 5.40796E 07 -1.27835E 00
1.91971E-01 7.81230E 05 2.64727E-01 -1.04789E 00 4.42734E 07

DIAGONAL SPRING RATES FOR EACH BEARING ABOUT ITS CENTER

1.04651E 05 4.73173E 05 5.92319E 05 1.49614E 06 1.22831E 06
0. 3.65438E 05 4.34252E 05 1.11470E 06 9.60000E 05

FLOATING BEARINGS ° AXIAL DISPLACEMENTS

0. 3.43730E-04

FRICTION TORQUES = 9.36033E-02 6.56906E-02

OUTER RACE LIVES = 3.41942E 05 6.63717E 05
INNER RACE LIVES = 2.36911E 05 7.43497E 05
BEARING LIVES = 1.49718E 05 3.75774E 05
RESULTANT BALL AND ROLLER BEARING LIVES = 1.13547E 05 0.

Case 3, Table 8 a

74

BEARING N

P-O	P-I	BETA-O	BETA-I	CF	G	V1	V2	CTL
2.03628E 01	7.84220E 00	9.50803E 00	2.51222E 01	1.28673E 01	-1.99306E-01	3.99894E-03	8.52822E-03	1.00000E 00
2.18143E 01	9.46024E 00	1.02197E 01	2.39534E 01	1.27063E 01	-2.11378E-01	3.82654E-03	8.61340E-03	1.00000E 00
2.50667E 01	1.29464E 01	1.13043E 01	2.21872E 01	1.24966E 01	-2.29656E-01	3.56365E-03	8.73805E-03	1.00000E 00
3.15080E 01	1.95896E 01	1.24808E 01	2.02801E 01	1.23140E 01	-2.49470E-01	3.27770E-03	8.87024E-03	1.00000E 00
4.06361E 01	2.88350E 01	1.33177E 01	1.89113E 01	1.22104E 01	-2.63644E-01	3.07264E-03	8.96866E-03	1.00000E 00
4.75235E 01	3.57700E 01	1.36805E 01	1.83046E 01	1.21716E 01	-2.69821E-01	2.98261E-03	9.01615E-03	1.00000E 00
4.75235E 01	3.57700E 01	1.36805E 01	1.83046E 01	1.21716E 01	-2.69821E-01	2.98261E-03	9.01615E-03	1.00000E 00
4.06361E 01	2.88350E 01	1.33177E 01	1.89113E 01	1.22104E 01	-2.63644E-01	3.07264E-03	8.96866E-03	1.00000E 00
3.15080E 01	1.95896E 01	1.24808E 01	2.02801E 01	1.23140E 01	-2.49470E-01	3.27770E-03	8.87024E-03	1.00000E 00
2.50667E 01	1.29464E 01	1.13043E 01	2.21872E 01	1.24966E 01	-2.29656E-01	3.56365E-03	8.73805E-03	1.00000E 00
2.18143E 01	9.46024E 00	1.02197E 01	2.39534E 01	1.27063E 01	-2.11378E-01	3.82654E-03	8.61340E-03	1.00000E 00
2.03628E 01	7.84220E 00	9.50803E 00	2.51222E 01	1.28673E 01	-1.99306E-01	3.99894E-03	8.52822E-03	1.00000E 00
1.99572E 01	7.37321E 00	9.26304E 00	2.55267E 01	1.29272E 01	-1.95126E-01	4.05828E-03	8.49817E-03	1.00000E 00

A-O	A-I	B-O	B-I	THETA1°O	THETA2°O	THETA1°I	THETA2°I	ALPHA
2.24604E-02	1.97809E-02	3.90947E-03	2.15539E-03	1.46950E 01	4.32103E 00	2.97770E 01	2.04673E 01	7.93759E 00
2.29826E-02	2.10605E-02	3.99949E-03	2.29196E-03	1.55276E 01	4.91172E 00	2.89100E 01	1.89968E 01	8.53226E 00
2.40736E-02	2.33872E-02	4.18781E-03	2.54066E-03	1.68650E 01	5.74365E 00	2.76931E 01	1.66813E 01	9.43891E 00
2.59822E-02	2.68554E-02	4.51785E-03	2.91224E-03	1.84839E 01	6.47773E 00	2.66056E 01	1.39547E 01	1.04227E 01
2.82831E-02	3.05534E-02	4.91629E-03	3.30933E-03	1.98547E 01	6.78080E 00	2.61121E 01	1.17105E 01	1.11228E 01
2.97990E-02	3.28311E-02	5.17900E-03	3.55426E-03	2.05695E 01	6.79157E 00	2.60454E 01	1.05638E 01	1.14264E 01
2.97990E-02	3.28311E-02	5.17900E-03	3.55426E-03	2.05695E 01	6.79157E 00	2.60454E 01	1.05638E 01	1.14264E 01
2.82831E-02	3.05534E-02	4.91629E-03	3.30933E-03	1.98547E 01	6.78080E 00	2.61121E 01	1.17105E 01	1.11228E 01
2.59822E-02	2.68554E-02	4.51785E-03	2.91224E-03	1.84839E 01	6.47773E 00	2.66056E 01	1.39547E 01	1.04227E 01
2.40736E-02	2.33872E-02	4.18781E-03	2.54066E-03	1.68650E 01	5.74365E 00	2.76931E 01	1.66813E 01	9.43891E 00
2.29826E-02	2.10605E-02	3.99949E-03	2.29196E-03	1.55276E 01	4.91172E 00	2.89100E 01	1.89968E 01	8.53226E 00
2.24604E-02	1.97809E-02	3.90947E-03	2.15539E-03	1.46950E 01	4.32103E 00	2.97770E 01	2.04673E 01	7.93759E 00
2.23100E-02	1.93774E-02	3.88358E-03	2.11236E-03	1.44152E 01	4.11086E 00	3.00863E 01	2.09670E 01	7.73290E 00

N-B	N-E	NS-O	NS-I	NR-O	NR-I	K-O	K-I	SV MAX
-3.02239E 04	5.01442E 03	-0.	1.18954E 04	-2.52670E 04	-3.51994E 04	2.45898E 07	2.66979E 07	9.01674E 04
-3.00236E 04	4.98296E 03	-0.	1.08325E 04	-2.51066E 04	-3.53553E 04	2.45885E 07	2.66905E 07	9.31499E 04
-2.97575E 04	4.94167E 03	-0.	9.23200E 03	-2.48960E 04	-3.55597E 04	2.45863E 07	2.66798E 07	9.80074E 04
-2.95192E 04	4.90544E 03	-0.	7.51264E 03	-2.47107E 04	-3.57382E 04	2.45836E 07	2.66691E 07	1.05281E 05
-2.93793E 04	4.88474E 03	-0.	6.28747E 03	-2.46044E 04	-3.58395E 04	2.45815E 07	2.66620E 07	1.14134E 05
-2.93256E 04	4.87698E 03	-0.	5.74912E 03	-2.45643E 04	-3.58771E 04	2.45806E 07	2.66589E 07	1.20540E 05
-2.93256E 04	4.87698E 03	-0.	5.74912E 03	-2.45643E 04	-3.58771E 04	2.45806E 07	2.66589E 07	1.20540E 05
-2.93793E 04	4.88474E 03	-0.	6.28747E 03	-2.46044E 04	-3.58395E 04	2.45815E 07	2.66620E 07	1.14134E 05
-2.95192E 04	4.90544E 03	-0.	7.51264E 03	-2.47107E 04	-3.57382E 04	2.45836E 07	2.66691E 07	1.05281E 05
-2.97575E 04	4.94167E 03	-0.	9.23200E 03	-2.48960E 04	-3.55597E 04	2.45863E 07	2.66798E 07	9.80074E 04
-3.00236E 04	4.98296E 03	-0.	1.08325E 04	-2.51066E 04	-3.53553E 04	2.45885E 07	2.66905E 07	9.31499E 04
-3.02239E 04	5.01442E 03	-0.	1.18954E 04	-2.52670E 04	-3.51994E 04	2.45898E 07	2.66979E 07	9.01674E 04
-3.02977E 04	5.02608E 03	-0.	1.22640E 04	-2.53264E 04	-3.51415E 04	2.45903E 07	2.67006E 07	8.91828E 04

SM-O	SM-I	QS-O	QS-I	QR-O	QR-I	MU-B	H/D°O	H/D°I
7.38162E 04	5.85485E 04	1.33812E-02	4.44358E-03	2.62792E-04	7.93638E-05	3.01498E-02	1.73364E-02	6.86581E-02
7.55419E 04	6.23846E 04	1.46681E-02	5.70692E-03	2.94673E-04	1.08430E-04	2.88375E-02	1.93442E-02	6.48025E-02
7.91443E 04	6.93547E 04	1.76547E-02	8.67236E-03	3.71277E-04	1.82718E-04	2.57770E-02	2.27948E-02	5.95660E-02
8.54403E 04	7.97291E 04	2.39501E-02	1.50676E-02	5.43033E-04	3.63850E-04	2.08308E-02	2.73413E-02	5.50625E-02
9.30246E 04	9.07757E 04	3.36233E-02	2.52318E-02	8.28906E-04	6.91971E-04	1.61921E-02	3.15048E-02	5.30741E-02
9.80191E 04	9.75739E 04	4.14293E-02	3.36332E-02	1.07531E-03	9.90153E-04	1.38214E-02	3.37893E-02	5.28078E-02
9.80191E 04	9.75739E 04	4.14293E-02	3.36332E-02	1.07531E-03	9.90153E-04	1.38214E-02	3.37893E-02	5.28078E-02
9.30246E 04	9.07757E 04	3.36233E-02	2.52318E-02	8.28906E-04	6.91971E-04	1.61921E-02	3.15048E-02	5.30741E-02
8.54403E 04	7.97291E 04	2.39501E-02	1.50676E-02	5.43033E-04	3.63850E-04	2.08308E-02	2.73413E-02	5.50625E-02
7.91443E 04	6.93547E 04	1.76547E-02	8.67236E-03	3.71277E-04	1.82718E-04	2.57770E-02	2.27948E-02	5.95660E-02
7.55419E 04	6.23846E 04	1.46681E-02	5.70692E-03	2.94673E-04	1.08430E-04	2.88375E-02	1.93442E-02	6.48025E-02
7.38162E 04	5.85485E 04	1.33812E-02	4.44358E-03	2.62792E-04	7.93638E-05	3.01498E-02	1.73364E-02	6.86581E-02
7.33191E 04	5.73381E 04	1.30269E-02	4.09267E-03	2.54145E-04	7.16251E-05	3.04619E-02	1.66860E-02	7.00591E-02

Case 3, Table 8 b

BEARING NO. 2

P-O	P-I	BETA-O	BETA-I	CF	G	V1	V2	CTL
2.06499E 01	8.19454E 00	-9.53521E 00	-2.44288E 01	1.27923E 01	1.98699E-01	-3.89598E-03	8.57719E-03	1.00000E 00
2.17269E 01	9.38472E 00	-1.00325E 01	-2.35978E 01	1.26819E 01	2.07144E-01	-3.77290E-03	8.63674E-03	1.00000E 00
2.37976E 01	1.16247E 01	-1.07767E 01	-2.23635E 01	1.25340E 01	2.19724E-01	-3.58889E-03	8.72308E-03	1.00000E 00
2.72236E 01	1.52006E 01	-1.15953E 01	-2.10128E 01	1.23940E 01	2.33539E-01	-3.38631E-03	8.81577E-03	1.00000E 00
3.14904E 01	1.95756E 01	-1.22601E 01	-1.99162E 01	1.22967E 01	2.44776E-01	-3.22128E-03	8.89084E-03	1.00000E 00
3.46496E 01	2.27877E 01	-1.26083E 01	-1.93387E 01	1.22513E 01	2.50678E-01	-3.13439E-03	8.93104E-03	1.00000E 00
3.46496E 01	2.27877E 01	-1.26083E 01	-1.93387E 01	1.22513E 01	2.50678E-01	-3.13439E-03	8.93104E-03	1.00000E 00
3.14904E 01	1.95756E 01	-1.22601E 01	-1.99162E 01	1.22967E 01	2.44776E-01	-3.22128E-03	8.89084E-03	1.00000E 00
2.72236E 01	1.52006E 01	-1.15953E 01	-2.10128E 01	1.23940E 01	2.33539E-01	-3.38631E-03	8.81577E-03	1.00000E 00
2.37976E 01	1.16247E 01	-1.07767E 01	-2.23635E 01	1.25340E 01	2.19724E-01	-3.58889E-03	8.72308E-03	1.00000E 00
2.17269E 01	9.38472E 00	-1.00325E 01	-2.35978E 01	1.26819E 01	2.07144E-01	-3.77290E-03	8.63674E-03	1.00000E 00
2.06499E 01	8.19454E 00	-9.53521E 00	-2.44288E 01	1.27923E 01	1.98699E-01	-3.89598E-03	8.57719E-03	1.00000E 00
2.03270E 01	7.82873E 00	-9.36148E 00	-2.47203E 01	1.28332E 01	1.95737E-01	-3.93900E-03	8.55602E-03	1.00000E 00

A-O	A-I	B-O	B-I	THETA1°O	THETA2°O	THETA1°I	THETA2°I	ALPHA
2.25655E-02	2.00747E-02	3.92773E-03	2.18577E-03	-1.47466E 01	-4.32387E 00	-2.91529E 01	-1.97047E 01	-7.96025E 00
2.29517E-02	2.10052E-02	3.99434E-03	2.28511E-03	-1.53333E 01	-4.73175E 00	-2.85414E 01	-1.86542E 01	-8.37582E 00
2.36596E-02	2.25621E-02	4.11655E-03	2.45144E-03	-1.62414E 01	-5.31188E 00	-2.76745E 01	-1.70524E 01	-8.99774E 00
2.47455E-02	2.46760E-02	4.30426E-03	2.67768E-03	-1.73118E 01	-5.87895E 00	-2.68230E 01	-1.52025E 01	-9.68216E 00
2.59770E-02	2.68501E-02	4.51734E-03	2.91072E-03	-1.82620E 01	-6.25819E 00	-2.62404E 01	-1.35920E 01	-1.02380E 01
2.68187E-02	2.82467E-02	4.66308E-03	3.06059E-03	-1.88054E 01	-6.41114E 00	-2.59933E 01	-1.26841E 01	-1.05292E 01
2.68187E-02	2.82467E-02	4.66308E-03	3.06059E-03	-1.88054E 01	-6.41114E 00	-2.59933E 01	-1.26841E 01	-1.05292E 01
2.59770E-02	2.68501E-02	4.51734E-03	2.91072E-03	-1.82620E 01	-6.25819E 00	-2.62404E 01	-1.35920E 01	-1.02380E 01
2.47455E-02	2.46760E-02	4.30425E-03	2.67768E-03	-1.73117E 01	-5.87895E 00	-2.68230E 01	-1.52025E 01	-9.68216E 00
2.36596E-02	2.25621E-02	4.11655E-03	2.45144E-03	-1.62414E 01	-5.31188E 00	-2.76745E 01	-1.70524E 01	-8.99774E 00
2.29517E-02	2.10052E-02	3.99434E-03	2.28511E-03	-1.53333E 01	-4.73175E 00	-2.85414E 01	-1.86542E 01	-8.37582E 00
2.25655E-02	2.00747E-02	3.92773E-03	2.18577E-03	-1.47466E 01	-4.32387E 00	-2.91529E 01	-1.97047E 01	-7.96025E 00
2.24471E-02	1.97706E-02	3.90732E-03	2.15934E-03	-1.45454E 01	-4.17756E 00	-2.93727E 01	-2.00679E 01	-7.81509E 00

N-B	N-E	NS-O	NS-I	NR-O	NR-I	K-O	K-I	SV MAX
-3.01343E 04	4.99979E 03	0.	-1.14378E 04	-2.51922E 04	-3.52716E 04	2.45898E 07	2.66935E 07	-8.93346E 04
-2.99966E 04	4.97816E 03	0.	-1.06868E 04	-2.50820E 04	-3.53788E 04	2.45888E 07	2.66883E 07	-9.14368E 04
-2.98097E 04	4.94906E 03	-0.	-9.57374E 03	-2.49335E 04	-3.55229E 04	2.45874E 07	2.66808E 07	-9.45800E 04
-2.96293E 04	4.92133E 03	0.	-8.35950E 03	-2.47919E 04	-3.56598E 04	2.45856E 07	2.66731E 07	-9.88645E 04
-2.95014E 04	4.90198E 03	0.	-7.37749E 03	-2.46928E 04	-3.57550E 04	2.45841E 07	2.66671E 07	-1.03367E 05
-2.94406E 04	4.89292E 03	-0.	-6.86236E 03	-2.46463E 04	-3.57994E 04	2.45833E 07	2.66641E 07	-1.06445E 05
-2.94406E 04	4.89292E 03	-0.	-6.86236E 03	-2.46463E 04	-3.57994E 04	2.45833E 07	2.66641E 07	-1.06445E 05
-2.95014E 04	4.90198E 03	0.	-7.37749E 03	-2.46928E 04	-3.57550E 04	2.45841E 07	2.66671E 07	-1.03367E 05
-2.96293E 04	4.92133E 03	0.	-8.35951E 03	-2.47919E 04	-3.56598E 04	2.45856E 07	2.66731E 07	-9.88645E 04
-2.98097E 04	4.94906E 03	-0.	-9.57374E 03	-2.49335E 04	-3.55229E 04	2.45874E 07	2.66808E 07	-9.45800E 04
-2.99966E 04	4.97816E 03	0.	-1.06868E 04	-2.50820E 04	-3.53788E 04	2.45888E 07	2.66883E 07	-9.14368E 04
-3.01343E 04	4.99979E 03	0.	-1.14378E 04	-2.51922E 04	-3.52716E 04	2.45898E 07	2.66935E 07	-8.93346E 04
-3.01850E 04	5.00777E 03	0.	-1.17015E 04	-2.52329E 04	-3.52320E 04	2.45901E 07	2.66953E 07	-8.86301E 04

SM-O	SM-I	QS-O	QS-I	QR-O	QR-I	MU-B	H/D°O	H/D°I
7.41620E 04	5.94459E 04	1.36333E-02	4.71207E-03	2.68980E-04	8.53933E-05	2.93914E-02	1.74575E-02	6.58720E-02
7.54377E 04	6.22354E 04	1.45897E-02	5.64645E-03	2.92709E-04	1.07005E-04	2.84078E-02	1.88659E-02	6.31944E-02
7.77754E 04	6.69006E 04	1.64729E-02	7.51227E-03	3.40545E-04	1.52768E-04	2.64661E-02	2.11514E-02	5.94879E-02
8.13582E 04	7.32279E 04	1.97089E-02	1.07431E-02	4.25883E-04	2.38647E-04	2.34874E-02	2.40091E-02	5.59497E-02
8.54192E 04	7.97295E 04	2.39321E-02	1.50536E-02	5.42516E-04	3.63446E-04	2.04515E-02	2.66943E-02	5.35877E-02
8.81937E 04	8.39031E 04	2.71860E-02	1.84349E-02	6.35968E-04	4.67907E-04	1.86214E-02	2.82920E-02	5.26006E-02
8.81937E 04	8.39031E 04	2.71860E-02	1.84349E-02	6.35968E-04	4.67907E-04	1.86214E-02	2.82920E-02	5.26006E-02
8.54192E 04	7.97295E 04	2.39321E-02	1.50536E-02	5.42516E-04	3.63446E-04	2.04515E-02	2.66943E-02	5.35877E-02
8.13582E 04	7.32279E 04	1.97089E-02	1.07431E-02	4.25882E-04	2.38647E-04	2.34874E-02	2.40091E-02	5.59497E-02
7.77754E 04	6.69006E 04	1.64729E-02	7.51227E-03	3.40545E-04	1.52768E-04	2.64661E-02	2.11514E-02	5.94879E-02
7.54377E 04	6.22354E 04	1.45897E-02	5.64645E-03	2.92709E-04	1.07005E-04	2.84078E-02	1.88659E-02	6.31944E-02
7.41620E 04	5.94459E 04	1.36333E-02	4.71207E-03	2.68980E-04	8.53933E-05	2.93914E-02	1.74575E-02	6.58720E-02
7.37707E 04	5.85341E 04	1.33497E-02	4.43358E-03	2.62021E-04	7.91458E-05	2.96617E-02	1.69870E-02	6.68473E-02

Case 3, Table 8c

```
 BALL  LLS   DIAM      TCH      B        F        FI       TH      EQV      TH      PACI
 1.30000E 01  4.68750E-01  2.36100E 00  1.60000E 01  5.30000E-01  5.20000E-01 -0.          -0.          6.91050E 00
 1.30000E 01  4.68750E-01  2.36100E 00 -1.60000E 01  5.30000E-01  5.20000E-01 -0.          -0.         -6.91050E 00

    PD          DEFL EXP     DEFL CON'O   DEFL CON'I   LIFE CON'O   LIFE CON'I  PRELOAD    SPRING THRUST
-2.40000E-04  1.50000E 00  2.45740E 07  2.66483E 07  7.14000E 03  7.14000E 03 -0.          -0.
-2.40000E-04  1.50000E 00  2.45740E 07  2.66483E 07  7.14000E 03  7.14000E 03 -0.           6.00000E 01

 ELAST.CON.    ROTAT'O      ROTAT'I     COEF FRICT'O  COEF FRICT'I   CONTROL      DENSITY
 2.58600E-07  1.00000E 00 -0.            7.50000E-02  7.50000E-02  1.00000E 00  2.83000E-01

     INITIAL DEFLECTIONS
     X            Y            Z          ALPHA'Y      ALPHA'Z
-0.          -0.          -0.          -0.          -0.
-0.          -0.          -0.          -0.          -0.

  ITERATION COUNTS AND TOLERANCES FOR DELTA AND V
 1.50000E 01  1.00000E 01  1.00000E-06  1.00000E-06

  APPLIED LOADS AND OPERATING RPM

  THRUST       RADIAL Y     RADIAL Z     MOMENT Y     MOMENT Z     OUTER RPM    INNER RPM
-1.60000E 01 -0.           1.30000E 02 -0.          -0.          -0.           1.20000E 04

DISPLACEMENTS BASED ON DYNAMIC LOADING

 INITIAL GUESSES OF SHAFT DISPLACEMENTS
 2.99813E-03  0.          -2.99977E-03  0.           0.

 SHAFT DISPLACEMENTS
-5.18062E-05  0.          -1.59752E-04  3.69539E-06  0.

 BEARING LOADS
 7.59993E 01  0.          -6.49742E 01 -2.26137E 01  0.
-5.99998E 01  0.          -6.59011E 01  2.25716E 01  0.

SPRING RATES
 1.06382E 05 -7.55381E-02 -1.11046E 05 -8.06612E 05 -5.85239E-01
 2.34830E-02  8.49923E 05  1.38132E-01 -3.66098E-01  1.01279E 06
-4.16681E 02  1.29770E-01  1.04249E 06  6.41478E 05 -1.93247E-01
-1.60410E 06 -2.80649E-01  6.42007E 05  5.49129E 07  7.04149E 00
-1.15302E 00  1.01351E 06 -3.97837E-01  7.55712E 00  4.48722E 07

 DIAGONAL SPRING RATES FOR EACH BEARING ABOUT ITS CENTER
 1.06382E 05  4.94604E 05  5.65121E 05  1.45511E 06  1.29582E 06
 0.           3.55319E 05  4.77372E 05  1.19389E 06  9.23665E 05

 FLOATING BEARINGS ' AXIAL DISPLACEMENTS
 0.           3.48488E-04

 FRICTION TORQUES =   9.00485E-02  6.83244E-02

 OUTER RACE LIVES =   4.12235E 05  5.61119E 05
 INNER RACE LIVES =   3.32627E 05  5.15036E 05
 BEARING LIVES    =   1.97175E 05  2.87790E 05
RESULTANT BALL AND ROLLER BEARING LIVES =   1.25163E 05  0.
```

Case 4, Table 9 a

III

77

BEARING NO. 1

P-O	P-I	BETA-O	BETA-I	CF	G	V1	V2	CIL
2.22052E 01	9.87070E 00	1.04927E 01	2.40025E 01	1.26966E 01	-2.16798E-01	3.83451E-03	8.61144E-03	1.00000E 00
2.36525E 01	1.14477E 01	1.10263E 01	2.31151E 01	1.25880E 01	-2.25730E-01	3.70279E-03	8.67471E-03	1.00000E 00
2.66404E 01	1.45875E 01	1.18039E 01	2.18282E 01	1.24480E 01	-2.38727E-01	3.51074E-03	8.76496E-03	1.00000E 00
3.15930E 01	1.96742E 01	1.26204E 01	2.04784E 01	1.23231E 01	-2.52402E-01	3.30846E-03	8.85906E-03	1.00000E 00
3.76155E 01	2.57846E 01	1.32287E 01	1.94648E 01	1.22437E 01	-2.62636E-01	3.15661E-03	8.93142E-03	1.00000E 00
4.18802E 01	3.00899E 01	1.35243E 01	1.89651E 01	1.22090E 01	-2.67629E-01	3.08204E-03	8.96864E-03	1.00000E 00
4.18802E 01	3.00899E 01	1.35243E 01	1.89651E 01	1.22090E 01	-2.67629E-01	3.08204E-03	8.96864E-03	1.00000E 00
3.76155E 01	2.57846E 01	1.32287E 01	1.94648E 01	1.22437E 01	-2.62636E-01	3.15661E-03	8.93142E-03	1.00000E 00
3.15930E 01	1.96742E 01	1.26204E 01	2.04784E 01	1.23231E 01	-2.52402E-01	3.30846E-03	8.85906E-03	1.00000E 00
2.66404E 01	1.45876E 01	1.18039E 01	2.18282E 01	1.24480E 01	-2.38727E-01	3.51074E-03	8.76496E-03	1.00000E 00
2.36525E 01	1.14477E 01	1.10263E 01	2.31151E 01	1.25880E 01	-2.25730E-01	3.70279E-03	8.67471E-03	1.00000E 00
2.22052E 01	9.87070E 00	1.04927E 01	2.40025E 01	1.26966E 01	-2.16798E-01	3.83451E-03	8.61144E-03	1.00000E 00
2.17540E 01	9.37913E 00	1.03079E 01	2.43114E 01	1.27368E 01	-2.13699E-01	3.88017E-03	8.58906E-03	1.00000E 00

A-O	A-I	B-O	B-I	THETA1°O	THETA2°O	THETA1°I	THETA2°I	ALPHA
2.31194E-02	2.13606E-02	4.02293E-03	2.32474E-03	1.58323E 01	5.15311E 00	2.90300E 01	1.89751E 01	8.76052E 00
2.36117E-02	2.24450E-02	4.10787E-03	2.44054E-03	1.64800E 01	5.57263E 00	2.83985E 01	1.78318E 01	9.20652E 00
2.45678E-02	2.43374E-02	4.27301E-03	2.64297E-03	1.74791E 01	6.12866E 00	2.75585E 01	1.60980E 01	9.85662E 00
2.60057E-02	2.68934E-02	4.52170E-03	2.91688E-03	1.86290E 01	6.61188E 00	2.68128E 01	1.41439E 01	1.05395E 01
2.75641E-02	2.94339E-02	4.79148E-03	3.18958E-03	1.95987E 01	6.85862E 00	2.64004E 01	1.25291E 01	1.10483E 01
2.85692E-02	3.09902E-02	4.96559E-03	3.35679E-03	2.01277E 01	6.92093E 00	2.62694E 01	1.16608E 01	1.12957E 01
2.85692E-02	3.09902E-02	4.96559E-03	3.35679E-03	2.01277E 01	6.92093E 00	2.62694E 01	1.16608E 01	1.12957E 01
2.75641E-02	2.94339E-02	4.79148E-03	3.18958E-03	1.95987E 01	6.85862E 00	2.64004E 01	1.25291E 01	1.10483E 01
2.60057E-02	2.68934E-02	4.52170E-03	2.91688E-03	1.86290E 01	6.61187E 00	2.68128E 01	1.41439E 01	1.05395E 01
2.45678E-02	2.43374E-02	4.27301E-03	2.64297E-03	1.74791E 01	6.12867E 00	2.75585E 01	1.60979E 01	9.85662E 00
2.36117E-02	2.24450E-02	4.10787E-03	2.44054E-03	1.64800E 01	5.57263E 00	2.83985E 01	1.78317E 01	9.20652E 00
2.31194E-02	2.13606E-02	4.02293E-03	2.32474E-03	1.58323E 01	5.15311E 00	2.90300E 01	1.89751E 01	8.76052E 00
2.29615E-02	2.09991E-02	3.99570E-03	2.28614E-03	1.56110E 01	5.00486E 00	2.92536E 01	1.93692E 01	8.60606E 00

N-B	N-E	NS-O	NS-I	NR-O	NR-I	K-O	K-I	SV MAX
-3.00086E 04	4.98106E 03	-0.	1.07443E 04	-2.50971E 04	-3.53650E 04	2.45879E 07	2.66908E 07	9.50407E 04
-2.98714E 04	4.95971E 03	-0.	9.94420E 03	-2.49882E 04	-3.54707E 04	2.45868E 07	2.66853E 07	9.71767E 04
-2.96919E 04	4.93205E 03	-0.	8.78694E 03	-2.48470E 04	-3.56073E 04	2.45851E 07	2.66777E 07	1.01038E 05
-2.95281E 04	4.90723E 03	-0.	7.57790E 03	-2.47199E 04	-3.57295E 04	2.45832E 07	2.66701E 07	1.06484E 05
-2.94216E 04	4.89140E 03	-0.	6.67513E 03	-2.46387E 04	-3.58070E 04	2.45817E 07	2.66648E 07	1.12421E 05
-2.93743E 04	4.88448E 03	-0.	6.23268E 03	-2.46030E 04	-3.58408E 04	2.45810E 07	2.66622E 07	1.16394E 05
-2.93743E 04	4.88448E 03	-0.	6.23268E 03	-2.46030E 04	-3.58408E 04	2.45810E 07	2.66622E 07	1.16394E 05
-2.94216E 04	4.89140E 03	-0.	6.67513E 03	-2.46387E 04	-3.58070E 04	2.45817E 07	2.66648E 07	1.12421E 05
-2.95281E 04	4.90723E 03	-0.	7.57790E 03	-2.47199E 04	-3.57295E 04	2.45832E 07	2.66701E 07	1.06484E 05
-2.96919E 04	4.93205E 03	-0.	8.78693E 03	-2.48470E 04	-3.56073E 04	2.45851E 07	2.66777E 07	1.01039E 05
-2.98714E 04	4.95971E 03	-0.	9.94419E 03	-2.49882E 04	-3.54707E 04	2.45868E 07	2.66853E 07	9.71766E 04
-3.00086E 04	4.98106E 03	-0.	1.07443E 04	-2.50971E 04	-3.53650E 04	2.45879E 07	2.66908E 07	9.50407E 04
-3.00589E 04	4.98893E 03	-0.	1.10231E 04	-2.51372E 04	-3.53260E 04	2.45883E 07	2.66927E 07	9.42152E 04

SM-O	SM-I	QS-O	QS-I	QR-O	QR-I	MU-B	H/D°O	H/D°I
7.59953E 04	6.32717E 04	1.50197E-02	6.03941E-03	3.03508E-04	1.16359E-04	2.88380E-02	2.01060E-02	6.53297E-02
7.76216E 04	6.65219E 04	1.63391E-02	7.35968E-03	3.37107E-04	1.48895E-04	2.74390E-02	2.17729E-02	6.25764E-02
8.07774E 04	7.21882E 04	1.91480E-02	1.01686E-02	4.10835E-04	2.22824E-04	2.47058E-02	2.44719E-02	5.89999E-02
8.55204E 04	7.98329E 04	2.40363E-02	1.51541E-02	5.45478E-04	3.66448E-04	2.10060E-02	2.77684E-02	5.59079E-02
9.06577E 04	8.74237E 04	3.03328E-02	2.17362E-02	7.29036E-04	5.74556E-04	1.76747E-02	3.07056E-02	5.42317E-02
9.39703E 04	9.20708E 04	3.50031E-02	2.67063E-02	8.71531E-04	7.42729E-04	1.58661E-02	3.23680E-02	5.37040E-02
9.39703E 04	9.20708E 04	3.50031E-02	2.67063E-02	8.71531E-04	7.42729E-04	1.58661E-02	3.23680E-02	5.37040E-02
9.06577E 04	8.74237E 04	3.03328E-02	2.17362E-02	7.29036E-04	5.74556E-04	1.76747E-02	3.07056E-02	5.42317E-02
8.55205E 04	7.98330E 04	2.40364E-02	1.51541E-02	5.45479E-04	3.66450E-04	2.10059E-02	2.77684E-02	5.59079E-02
8.07774E 04	7.21883E 04	1.91480E-02	1.01686E-02	4.10834E-04	2.22825E-04	2.47058E-02	2.44719E-02	5.89999E-02
7.76216E 04	6.65219E 04	1.63391E-02	7.35968E-03	3.37107E-04	1.48895E-04	2.74390E-02	2.17730E-02	6.25764E-02
7.59953E 04	6.32717E 04	1.50197E-02	6.03941E-03	3.03508E-04	1.16359E-04	2.88380E-02	2.01060E-02	6.53297E-02
7.54738E 04	6.21882E 04	1.46141E-02	5.64158E-03	2.93324E-04	1.06879E-04	2.92865E-02	1.95511E-02	6.63180E-02

Case 4 Table 9 b

56 III 28

BEARING NO. 2

P-O	P-I	BETA-O	BETA-I	CF	G	V1	V2	CTL
1.91847E 01	6.51949E 00	-8.53014E 00	-2.55553E 01	1.29789E 01	1.80527E-01	-4.06108E-03	8.49313E-03	1.00000E 00
2.02452E 01	7.75806E 00	-9.21024E 00	-2.44341E 01	1.28121E 01	1.92283E-01	-3.89611E-03	8.57534E-03	1.00000E 00
2.25771E 01	1.03346E 01	-1.02567E 01	-2.27254E 01	1.25897E 01	2.10173E-01	-3.64225E-03	8.69624E-03	1.00000E 00
2.71462E 01	1.51252E 01	-1.14512E 01	-2.07911E 01	1.23828E 01	2.30464E-01	-3.35210E-03	8.82859E-03	1.00000E 00
3.39390E 01	2.20680E 01	-1.24056E 01	-1.92457E 01	1.22508E 01	2.46704E-01	-3.11926E-03	8.93432E-03	1.00000E 00
3.94672E 01	2.76545E 01	-1.28642E 01	-1.84955E 01	1.21972E 01	2.54541E-01	-3.00655E-03	8.98797E-03	1.00000E 00
3.94672E 01	2.76545E 01	-1.28642E 01	-1.84955E 01	1.21972E 01	2.54541E-01	-3.00655E-03	8.98797E-03	1.00000E 00
3.39391E 01	2.20680E 01	-1.24056E 01	-1.92457E 01	1.22508E 01	2.46704E-01	-3.11926E-03	8.93432E-03	1.00000E 00
2.71462E 01	1.51253E 01	-1.14512E 01	-2.07911E 01	1.23828E 01	2.30464E-01	-3.35210E-03	8.82860E-03	1.00000E 00
2.25771E 01	1.03346E 01	-1.02567E 01	-2.27254E 01	1.25897E 01	2.10173E-01	-3.64225E-03	8.69624E-03	1.00000E 00
2.02453E 01	7.75806E 00	-9.21024E 00	-2.44341E 01	1.28121E 01	1.92283E-01	-3.89611E-03	8.57534E-03	1.00000E 00
1.91847E 01	6.51949E 00	-8.53014E 00	-2.55553E 01	1.29789E 01	1.80527E-01	-4.06108E-03	8.49313E-03	1.00000E 00
1.88825E 01	6.15101E 00	-8.29653E 00	-2.59426E 01	1.30405E 01	1.76456E-01	-4.11775E-03	8.46414E-03	1.00000E 00

A-O	A-I	B-O	B-I	THETA1'O	THETA2'O	THETA1'I	THETA2'I	ALPHA
2.20177E-02	1.85986E-02	3.83348E-03	2.02752E-03	-1.36146E 01	-3.44564E 00	-2.99313E 01	-2.11793E 01	-7.12055E 00
2.24168E-02	1.97117E-02	3.90222E-03	2.14626E-03	-1.43871E 01	-4.03333E 00	-2.90726E 01	-1.97956E 01	-7.68870E 00
2.32474E-02	2.16936E-02	4.04553E-03	2.35792E-03	-1.56259E 01	-4.88737E 00	-2.78315E 01	-1.76194E 01	-8.56309E 00
2.47218E-02	2.46358E-02	4.30036E-03	2.67277E-03	-1.71621E 01	-5.74025E 00	-2.65919E 01	-1.49903E 01	-9.56158E 00
2.66338E-02	2.79464E-02	4.63130E-03	3.02781E-03	-1.85599E 01	-6.25140E 00	-2.58293E 01	-1.26622E 01	-1.03597E 01
2.80085E-02	3.01319E-02	4.86946E-03	3.26255E-03	-1.93374E 01	-6.39101E 00	-2.55965E 01	-1.13946E 01	-1.07433E 01
2.80085E-02	3.01319E-02	4.86946E-03	3.26255E-03	-1.93374E 01	-6.39101E 00	-2.55965E 01	-1.13946E 01	-1.07433E 01
2.66338E-02	2.79464E-02	4.63130E-03	3.02781E-03	-1.85599E 01	-6.25140E 00	-2.58293E 01	-1.26622E 01	-1.03597E 01
2.47219E-02	2.46358E-02	4.30036E-03	2.67277E-03	-1.71621E 01	-5.74025E 00	-2.65919E 01	-1.49903E 01	-9.56158E 00
2.32474E-02	2.16936E-02	4.04553E-03	2.35792E-03	-1.56260E 01	-4.88738E 00	-2.78315E 01	-1.76194E 01	-8.56309E 00
2.24168E-02	1.97117E-02	3.90223E-03	2.14626E-03	-1.43872E 01	-4.03333E 00	-2.90726E 01	-1.97956E 01	-7.68870E 00
2.20177E-02	1.85986E-02	3.83348E-03	2.02752E-03	-1.36146E 01	-3.44564E 00	-2.99313E 01	-2.11793E 01	-7.12055E 00
2.19013E-02	1.82404E-02	3.81345E-03	1.98933E-03	-1.33541E 01	-3.23898E 00	-3.02342E 01	-2.16510E 01	-6.92542E 00

N-B	N-E	NS-O	NS-I	NR-O	NR-I	K-O	K-I	SV MAX
-3.03667E 04	5.03613E 03	0.	-1.26068E 04	-2.53771E 04	-3.50910E 04	2.45915E 07	2.67008E 07	-8.44523E 04
-3.01615E 04	5.00365E 03	0.	-1.15841E 04	-2.52117E 04	-3.52522E 04	2.45904E 07	2.66935E 07	-8.72355E 04
-2.98832E 04	4.96003E 03	0.	-1.00312E 04	-2.49894E 04	-3.54684E 04	2.45884E 07	2.66829E 07	-9.15957E 04
-2.96178E 04	4.91912E 03	0.	-8.28119E 03	-2.47805E 04	-3.56705E 04	2.45859E 07	2.66718E 07	-9.76319E 04
-2.94432E 04	4.89283E 03	0.	-6.89074E 03	-2.46458E 04	-3.57998E 04	2.45838E 07	2.66636E 07	-1.04630E 05
-2.93703E 04	4.88210E 03	-0.	-6.21976E 03	-2.45907E 04	-3.58522E 04	2.45826E 07	2.66599E 07	-1.09835E 05
-2.93703E 04	4.88210E 03	-0.	-6.21976E 03	-2.45907E 04	-3.58522E 04	2.45826E 07	2.66599E 07	-1.09835E 05
-2.94432E 04	4.89283E 03	0.	-6.89074E 03	-2.46458E 04	-3.57998E 04	2.45838E 07	2.66636E 07	-1.04630E 05
-2.96178E 04	4.91912E 03	0.	-8.28119E 03	-2.47805E 04	-3.56705E 04	2.45859E 07	2.66718E 07	-9.76320E 04
-2.98832E 04	4.96003E 03	0.	-1.00312E 04	-2.49894E 04	-3.54684E 04	2.45884E 07	2.66829E 07	-9.15959E 04
-3.01615E 04	5.00365E 03	0.	-1.15841E 04	-2.52117E 04	-3.52522E 04	2.45904E 07	2.66935E 07	-8.72354E 04
-3.03667E 04	5.03613E 03	0.	-1.26060E 04	-2.53771E 04	-3.50910E 04	2.45915E 07	2.67008E 07	-8.44523E 04
-3.04418E 04	5.04806E 03	0.	-1.29600E 04	-2.54379E 04	-3.50318E 04	2.45919E 07	2.67034E 07	-8.34893E 04

SM-O	SM-I	QS-O	QS-I	QR-O	QR-I	MU-B	H/D'O	H/D'I
7.23501E 04	5.50325E 04	1.23588E-02	3.47334E-03	2.37992E-04	5.83767E-05	2.99658E-02	1.48925E-02	6.93555E-02
7.36693E 04	5.83708E 04	1.32781E-02	4.38043E-03	2.60269E-04	7.79678E-05	2.92968E-02	1.66214E-02	6.55177E-02
7.64130E 04	6.43107E 04	1.53559E-02	6.42154E-03	3.11996E-04	1.25628E-04	2.72468E-02	1.95884E-02	6.01512E-02
8.12780E 04	7.31180E 04	1.96341E-02	1.06723E-02	4.23865E-04	2.36696E-04	2.32619E-02	2.35989E-02	5.50067E-02
8.75817E 04	8.30153E 04	2.64450E-02	1.76629E-02	6.14425E-04	4.43613E-04	1.87941E-02	2.75645E-02	5.19500E-02
9.21118E 04	8.95429E 04	3.23394E-02	2.38647E-02	7.89613E-04	6.45581E-04	1.61802E-02	2.99001E-02	5.10332E-02
9.21118E 04	8.95429E 04	3.23394E-02	2.38647E-02	7.89613E-04	6.45581E-04	1.61802E-02	2.99001E-02	5.10332E-02
8.75818E 04	8.30153E 04	2.64451E-02	1.76629E-02	6.14428E-04	4.43613E-04	1.87941E-02	2.75645E-02	5.19500E-02
8.12781E 04	7.31181E 04	1.96341E-02	1.06724E-02	4.23866E-04	2.36697E-04	2.32619E-02	2.35989E-02	5.50067E-02
7.64130E 04	6.43108E 04	1.53559E-02	6.42157E-03	3.11996E-04	1.25629E-04	2.72468E-02	1.95885E-02	6.01512E-02
7.36694E 04	5.83708E 04	1.32782E-02	4.38043E-03	2.60270E-04	7.79678E-05	2.92968E-02	1.66214E-02	6.55176E-02
7.23501E 04	5.50325E 04	1.23588E-02	3.47334E-03	2.37992E-04	5.83767E-05	2.99658E-02	1.48925E-02	6.93555E-02
7.19650E 04	5.39580E 04	1.20998E-02	3.21397E-03	2.31790E-04	5.29907E-05	3.00747E-02	1.43305E-02	7.07334E-02

Case 4, Table 9 c

P. Selection of Preload Spring

A standard wave spring (Wallace Barnes Cat.No. 80) for a 208 bearing was chosen to apply the thrust preload on the bearing. This type was chosen because it requires a minimum of space and has a low cost. Since the shape of these springs cannot be held with any uniformity, it is necessary to calibrate each one and shim them to obtain the required preload on the bearing at operating temperature.

One drawback of this washer is that it extends below the ID of the outer race of the bearing and may impede the lubricant flow from the bearing to the slinger. Although test results to date have not indicated it, this may cause the bearing to run flooded. If this should become a problem, a special design spring could be obtained which has a larger ID but a comparable spring rate.

The standard spring is made of a SAE 1074 steel. When springs are subjected to high temperature under compression they often shorten or "set" and lose load. Use of an SAE 1074 spring steel is not recommended over 400°F. But even at 300°F, the maximum temperature in the bearing area, there is about a five percent loss of load. Should this effect become a problem, it can be corrected by going to a higher grade material such as a chrome-vanadium steel.

III. ALTERNATOR CRITICAL SPEEDS

The critical speeds of a rotating shaft are dependent on the dynamic characteristics of the rotor itself, the bearings, and the support structure. To show this, consider the shaft-bearing-support system in Figure 12 a. The shaft is considered to be a flexible distributed mass and the bearing-support structure as springs.

If the bearings are much more stiff than the shaft, the shaft deflects in its lowest frequency mode as shown in Figure 12 b.

If the bearings are much less stiff than the shaft, the rotor vibrates in its first mode as shown in Figure 12 c, that is, as a rigid body on springs.

From these figures we see that as the stiffness of the bearing-support structure changes, we can expect that the mode and natural frequencies of the system will also change. For the case of a very flexible bearing and support, the system has two natural frequencies which are proportional to the square root of the spring rate. At large values of bearing-support stiffness, the system vibrates as a flexible rotor on rigid supports.

The critical speed of the rotor-bearing-support structure lies somewhere between these two extremes. For instance, if the system critical speed is plotted against the bearing-support stiffness, a curve similar to Figure 12 d is obtained.

The system critical approaches the stiff shaft-flexible spring at low bearing-support stiffnesses and the flexible shaft-rigid support at high bearing-support stiffnesses.

The ball bearing stiffness has been previously calculated in Section II-N and is included in Table 10 for the various types of anticipated alternator loads. It can be seen that the stiffness varies from a low of 7.95×10^5 lb./in. to 1.36×10^6 lb./in. and is a function of both angular position and load. Since

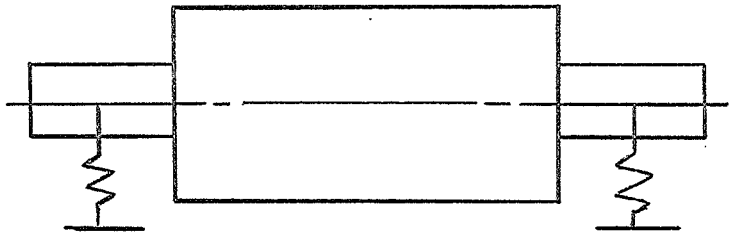

Rotor, Bearing-Support Model

Figure 12a

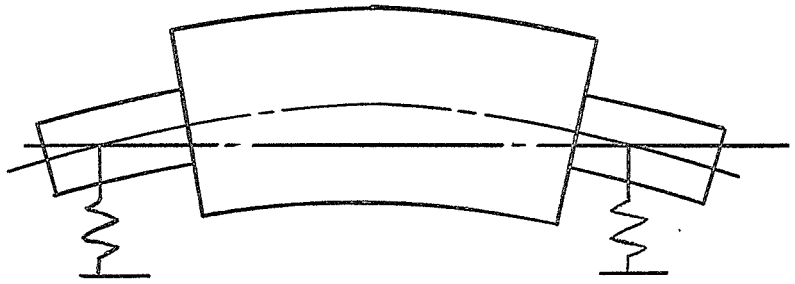

First Mode Deflection for Very Stiff Springs

Figure 12b

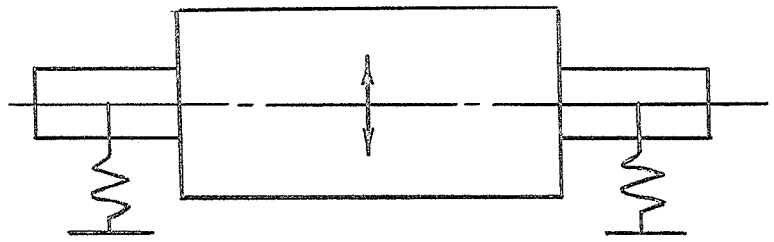

First Mode of Deflection for Very Soft Springs

Figure 12c

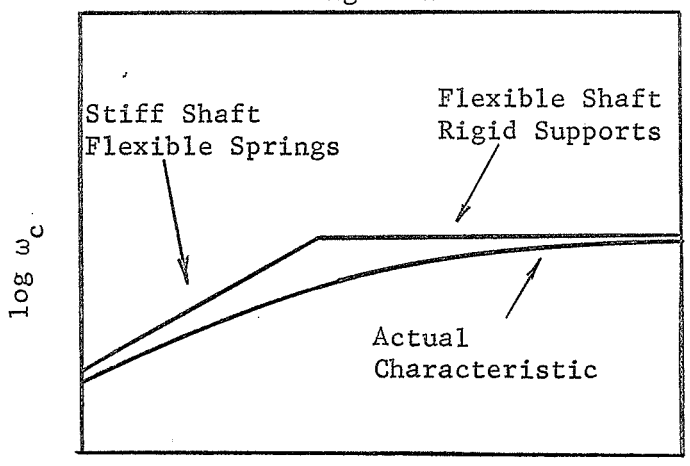

Log K, Bearing-Support Stiffness

Figure 12d

the magnetic pullover forces are a function of eccentricity and it is not possible to predict ahead of time where the point of minimum eccentricity will be, the variation of bearing stiffness with angular position will also be indeterminate. The stiffnesses presented in Table 10 are for a magnetic pull force in the y direction.

Using the computer program described in References 18 and 19, the rotor critical speed was calculated as function of bearing stiffness, and the results are plotted in Figure 13. The mode shapes are given in Tables 11 through 17. The calculation assumes that the bearings are rigidly mounted and there is no damping. The latter assumption is quite reasonable for ball bearings.

In Tables 11 through 17, the excess moment is tabulated against rotational speed. Whenever the excess moment undergoes a change in sign, a critical speed occurs, and its magnitude and the corresponding mode shapes are listed.

For a variation in stiffness from 7.95×10^5 lb./in. to 1.36×10^6 lb./in., the critical speed will vary from 22,000 rpm to 25,000 rpm. Thus, there is an adequate margin of safety between the operating speed of 12,000 rpm and the first critical speed.

Mount	Case	F_{E_1} lb.	F_{E_2} lb.	W lb.	Preload lb.	$\frac{\partial F_r}{\partial y}$ $\frac{lb}{in}$	$\frac{\partial F_r}{\partial Z}$ $\frac{lb}{in}$
	1	65	65	70	60	7.18×10^5	1.13×10^6
	2	65	65	70	100	1.45×10^6	1.53×10^6
	3	65	0	70	60	8.38×10^5	1.02×10^6
	4	65	65	0	60	8.50×10^5	1.04×10^6

CALCULATED BEARING STIFFNESS

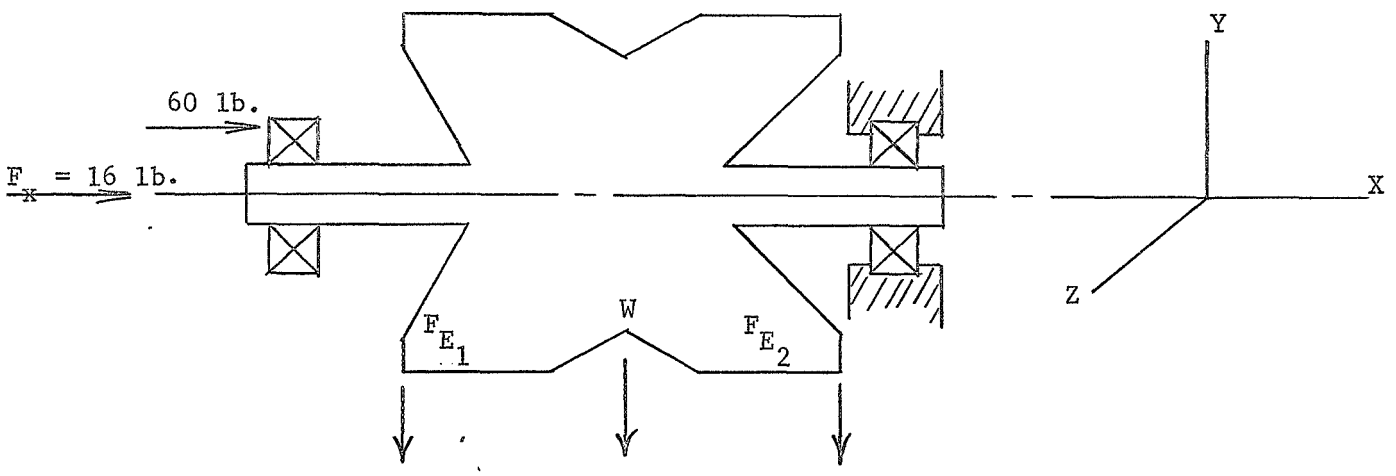

TABLE 10

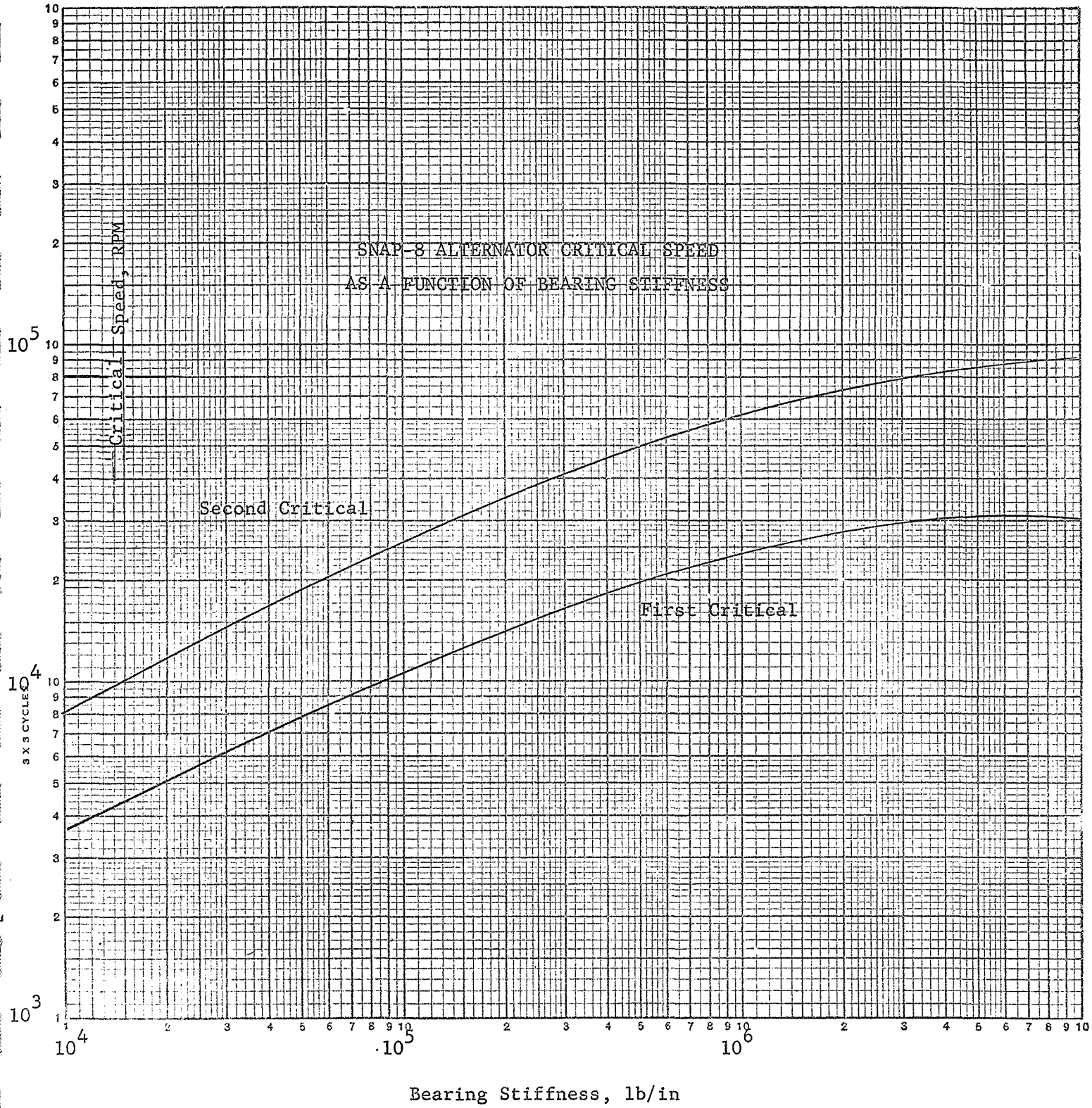
SNAP-8 ALTERNATOR CRITICAL SPEED
AS A FUNCTION OF BEARING STIFFNESS
Critical Speed, RPM
Second Critical
First Critical
3 X 3 CYCLES
Bearing Stiffness, lb/in

Figure 13

TMMD009

$K = 0.01 \times 10^6 \frac{LB}{IN}$

T

RPM	DELTA
0.00	0.22644785,-4
5000.00	-0.16045557,-4
2500.00	0.93883151,-5

CRITICAL SPEED	DELTA
3569.31	-0.18470658,-5

STA NO	NET DEFLECTION - V
1	-0.53665
2	-0.53161
3	-0.50137
4	-0.44284
5	-0.27865
6	-0.09959
7	0.44635
8	0.62957
9	0.87696
10	0.91962
11	0.95535
12	1.00000

RPM	DELTA
10000.00	0.96236355,-4
7500.00	-0.10777232,-4

CRITICAL SPEED	DELTA
7916.92	-0.23267676,-5

STA NO	NET DEFLECTION - V
1	-0.93644
2	-0.92986
3	-0.89037
4	-0.81391
5	-0.59917
6	-0.36450
7	0.35144
8	0.58646
9	0.87223
10	0.91700
11	0.95389
12	1.00000

RPM	DELTA
15000.00	0.10364438,-2
20000.00	0.39059417,-2
25000.00	0.10190623,-1
30000.00	0.21705968,-1
35000.00	0.40527936,-1

TABLE 11

TMMD009
T

$K = 0.1 \times 10^6 \frac{LB}{IN}$

RPM	DELTA
0.00	0.22644786,-2
5000.00	0.16493811,-2
10000.00	0.83473455,-4
15000.00	-0.16040131,-2
12500.00	-0.81776907,-3

CRITICAL SPEED	DELTA
10218.81	0.41341100,-5

STA NO	NET DEFLECTION - V
1	0.88077
2	0.88271
3	0.89431
4	0.91565
5	0.96354
6	0.98729
7	1.00000
8	0.98432
9	0.90210
10	0.88469
11	0.87023
12	0.85214

RPM	DELTA
20000.00	-0.20606408,-2
25000.00	0.54527237,-3
22500.00	-0.12721540,-2

CRITICAL SPEED	DELTA
24381.68	-0.15597790,-4

STA NO	NET DEFLECTION - V
1	-0.96899
2	-0.96321
3	-0.92848
4	-0.86018
5	-0.65719
6	-0.40997
7	0.39334
8	0.64264
9	0.89648
10	0.93280
11	0.96267
12	1.00000

RPM	DELTA
30000.00	0.84640272,-2
35000.00	0.24288142,-1

TABLE 12

TMMD009
T

$K = 1.0 \times 10^6 \frac{LB}{IN}$

RPM	DELTA
0.00	0.22644787
5000.00	0.21411130
10000.00	0.17813214
15000.00	0.12158435
20000.00	0.49532630,-1
25000.00	-0.31054992,-1
22500.00	0.97990520,-2

CRITICAL SPEED	DELTA
23105.93	-0.41907653,-4

STA NO	NET DEFLECTION - V
1	0.41764
2	0.42711
3	0.48363
4	0.58768
5	0.82141
6	0.93752
7	1.00000
8	0.92276
9	0.52414
10	0.44101
11	0.37219
12	0.28616

RPM	DELTA
30000.00	-0.11142831
35000.00	-0.18120892
40000.00	-0.22857534
45000.00	-0.24047790
50000.00	-0.20288106
55000.00	-0.10103109
60000.00	0.80253676,-1
57500.00	-0.21275327,-1

CRITICAL SPEED	DELTA
58071.12	-0.69156289,-4

STA NO	NET DEFLECTION - V
1	0.92240
2	0.92721
3	0.95548
4	0.99887
5	1.00000
6	0.72238
7	-0.66964
8	-0.97981
9	-0.85627
10	-0.80212

TABLE 13

TMMD009
T

$K = 10 \times 10^6 \frac{LB}{IN}$

RPM	DELTA
0.00	0.22644787,2
5000.00	0.21919496,2
10000.00	0.19776249,2
15000.00	0.16312761,2
20000.00	0.11691376,2
25000.00	0.61382675,1
30000.00	-0.57640076,-1
27500.00	0.31001892,1

CRITICAL SPEED	DELTA
29955.20	-0.26321411,-3

STA NO	NET DEFLECTION - V
1	0.05364
2	0.06903
3	0.16090
4	0.33004
5	0.71020
6	0.89908
7	1.00000
8	0.87122
9	0.21001
10	0.07218
11	-0.04194
12	-0.18459

RPM	DELTA
35000.00	-0.65460930,1
40000.00	-0.12917187,2
45000.00	-0.18703384,2
50000.00	-0.23381798,2
55000.00	-0.26376778,2
60000.00	-0.27062691,2
65000.00	-0.24767181,2
70000.00	-0.18774429,2

TABLE 14

III 89

TMMD009
T

$K = 100 \times 10^6 \ \frac{LB}{IN}$

RPM	DELTA
0.00	0.22644766,4
5000.00	0.21970508,4
10000.00	0.19975234,4
15000.00	0.16741523,4
20000.00	0.12406992,4
25000.00	0.71636328,3
30000.00	0.12575000,3
35000.00	-0.50117969,3
32500.00	-0.18526563,3

CRITICAL SPEED	DELTA
31015.55	0.28906250

STA NO	NET DEFLECTION - V
1	-0.00906
2	0.00735
3	0.10526
4	0.28554
5	0.69080
6	0.89222
7	1.00000
8	0.86225
9	0.15511
10	0.00770
11	-0.11435
12	-0.26692

RPM	DELTA
40000.00	-0.11292266,4
45000.00	-0.17179688,4
50000.00	-0.22219297,4
55000.00	-0.25906563,4
60000.00	-0.27688594,4
65000.00	-0.26965469,4
60000.00	-0.23092031,4

TABLE 15

TMMD009
T

RPM	DELTA
0.00	0.22646400,6
5000.00	0.22003200,6
10000.00	0.20096000,6
15000.00	0.17017600,6
20000.00	0.12870400,6
25000.00	0.78464000,5
30000.00	0.21568000,5
35000.00	-0.39040000,5
32500.00	-0.82560000,4

CRITICAL SPEED	DELTA
31815.94	-0.12800000,3

$K = 1000 \times 10^6 \frac{LB}{IN}$

STA NO	NET DEFLECTION - V
1	-0.01588
2	0.00081
3	0.10047
4	0.28469
5	0.70055
6	0.90516
7	1.00000
8	0.85112
9	0.14574
10	0.00085
11	-0.11905
12	-0.26893

RPM	DELTA
40000.00	-0.10009600,6
45000.00	-0.15820800,6
50000.00	-0.20902400,6
55000.00	-0.24780800,6
60000.00	-0.27008000,6
65000.00	-0.26931200,6
70000.00	-0.24064000,6

TABLE 16

III 91

TMMD009
T

RPM	DELTA
0.00	0.22544384,8
5000.00	0.22020096,8
10000.00	0.20447232,8
15000.00	0.16252928,8
20000.00	0.13107200,8
25000.00	0.73400320,7
30000.00	0.20971520,7
35000.00	-0.41943040,7
32500.00	-0.10485760,7

CRITICAL SPEED	DELTA
32500.00	-0.10485760,7

$K = 10000 \times 10^6 \frac{LB}{IN}$

STA NO	NET DEFLECTION - V
1	-0.01712
2	0.00008
3	0.10282
4	0.29261
5	0.71958
6	0.92520
7	1.00000
8	0.84219
9	0.13982
10	0.00008
11	-0.11463
12	-0.25804

RPM	DELTA
40000.00	-0.94371840,7
45000.00	-0.16777216,8
50000.00	-0.20971520,8
55000.00	-0.25165824,8
60000.00	-0.27262976,8
65000.00	-0.20971520,8
70000.00	-0.20971520,8

TABLE 17

IV. OPERATING EXPERIENCE

A. Introduction

The main purpose of this evaluation has been to ascertain the suitability of the bearing specified in AGC specification for the loads and operating conditions existing in the SNAP-8 alternator. It has been primarily a paper study and no bearing life tests were carried on.

However, in conducting the seal tests described in Reference 23, a test rig very similar to the alternator in design was used. The bearing span differed slightly, the bearings were mounted DF rather than DB, and there was no magnetic pull force. However, heat removal from the shaft was simulated and in all other respects, rotational speed, rotor weight, etc., the test rig closely approximated the actual alternator.

B. Bearing Failure

During the first part of the seal test program it was not possible to obtain delivery of the ITT bearing of Figure 2. For an interim period then, substitute bearings, Barden 208BX1 type, were used.

During startup of Test No. 5 of Reference 23, a bearing failure occurred on the test rig anti-drive end. Test No. 5 had been scheduled as a usual test but with heat input to the rotor for simulation of pole face losses. The startup for Test No. 5 varied from the previous startup procedures on two counts:

1. A more rapid acceleration to operating speed was employed. (See Figure 14)

2. The oil was introduced to the bearing cavity cold. (See Figure 14) The reason for the change in procedure was to more closely approximate what were thought to be the final operational requirements.

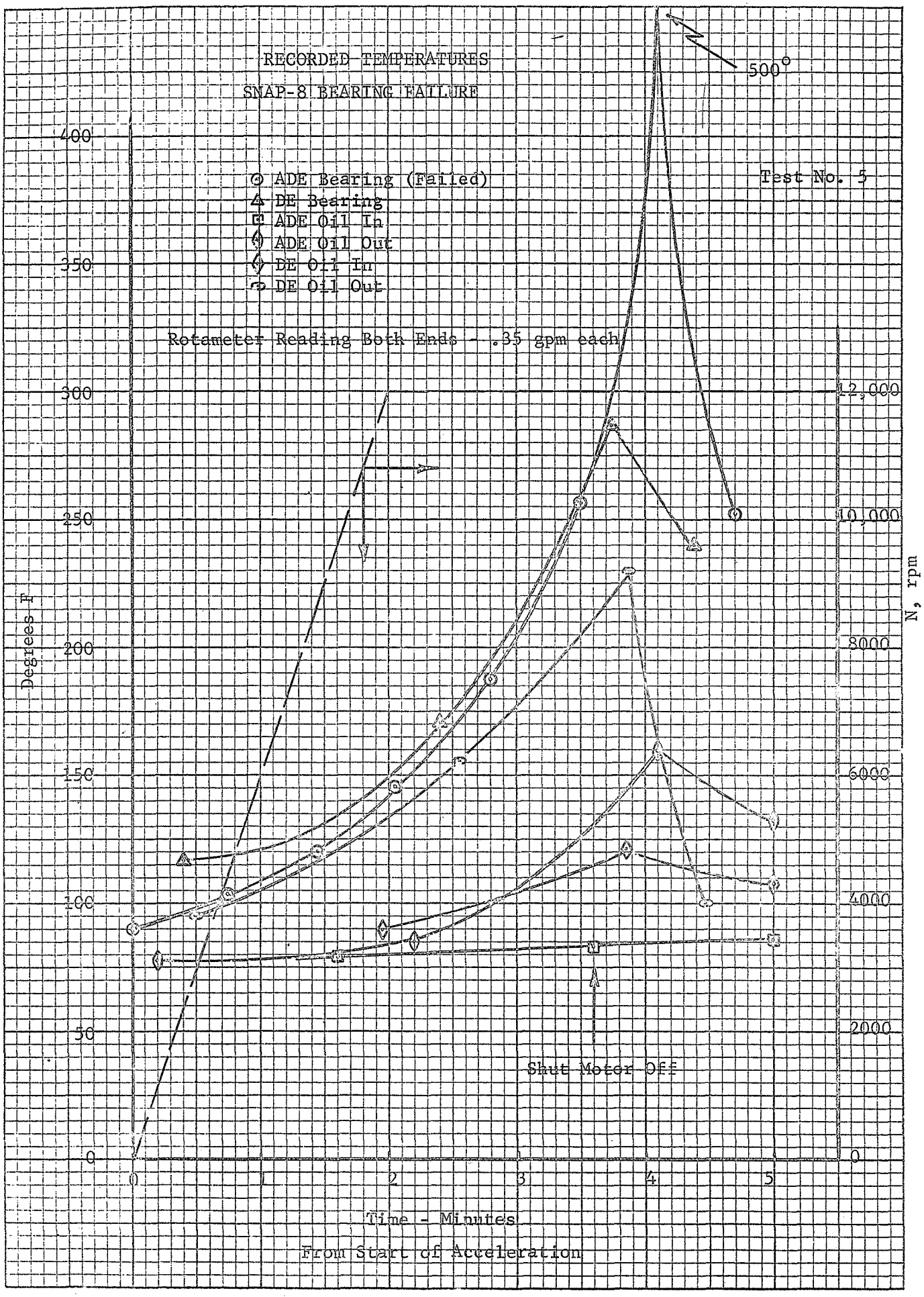
RECORDED TEMPERATURES
SNAP-8 BEARING FAILURE
500°
ADE Bearing (Failed)
DE Bearing
ADE Oil In
ADE Oil Out
DE Oil In
DE Oil Out
Test No. 5
Rotameter Reading Both Ends - .35 gpm each
Shut Motor Off
Degrees F
N, rpm
400
350
300
250
200
150
100
50
0
12,000
10,000
8000
6000
4000
2000
0
0
1
2
3
4
5
Time - Minutes
From Start of Acceleration

Figure 14

Prior to Test No. 5, approximately forty (40) hours at 12,000 rpm had been accumulated on the Barden 208BX1 bearings. It is significant to note that prior to Test No. 5, the entire unit was disassembled and inspected visually. No evidence of any malfunction was detected during this inspection. The subsequent assembly of the unit in preparation for Test No. 5 was straightforward and uneventful.

During the acceleration to full speed the bearing temperatures as well as the oil temperatures were monitored constantly. Figure 14 is a plot of the various temperatures as recorded during the period of acceleration to rated speed and power shutoff. During this time, although the rate of temperature increase was of some concern, the bearing temperature was not considered excessive. Therefore, the rotor speed was increased to rated speed at which time a somewhat unfamiliar sound was heard coincident with the start of rotor deceleration. At this point power was turned off and the unit came to a fairly quick stop. The unit was subsequently disassembled and inspected.

Bearing Disassembly and Inspection

A photograph of the failed bearing is shown in Figure 15. Careful examination of the failed bearing was made both by General Electric Bearing Laboratory personnel and the Barden Co. The bronze retainer was broken into a number of pieces of various sizes. Actual bearing seizure was caused by the retainer pieces which became lodged under the balls, causing skidding and smearing of the retainer material on the inner and outer ring races. In addition, the inner ring race material showed a combination of wear and plastic flow with some of the race metal swaged over the race edges. Because of the advanced state of the failure, it was impossible to detect other characteristics which might have contributed to the bearing failure.

During the disassembly before Test No. 5 no evidence of plastic flow or wear on any of the bearing parts was noted. The thirty-five (35) hour test

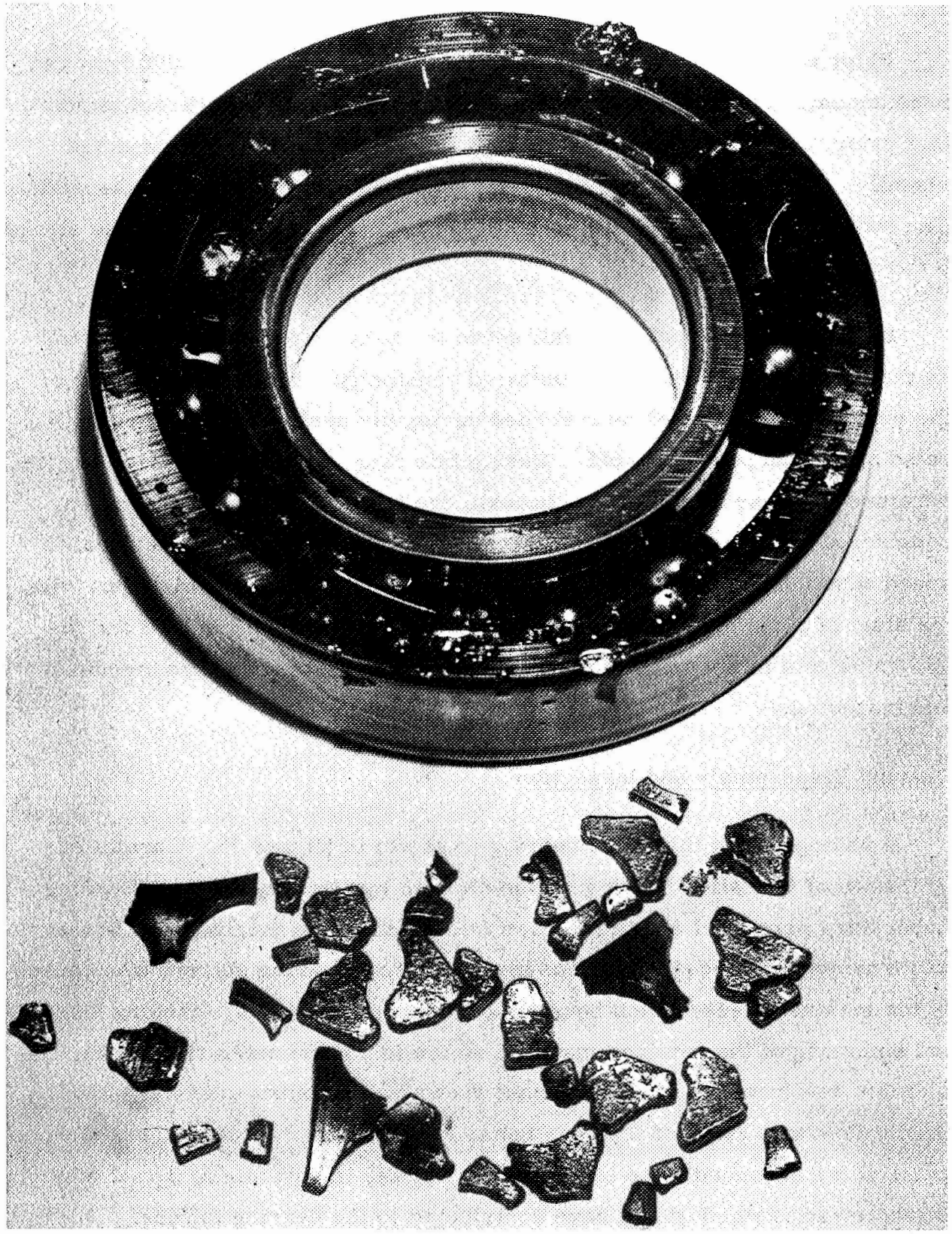

Figure 15. Photograph of Failed Bearing
A&SP Photo 1184599

(Test No. 4) just prior to Test No. 5 was very smooth and without any vibration. It should be noted, however, that prior to Test No. 4 and during initial checkout of the system, some vibrations did occur as a result of quill whipping. The vibration problem was corrected by adding additional dampers on the quill. However, it is judged that the bearings were subjected to approximately four hours of fairly heavy vibration at 9000 rpm prior to Test No. 4. No high bearing temperatures were noted during the runs in which vibration occurred. Also, no evidence of bearing deterioration was ever noticed during unit disassembly following operation with vibration.

Actually, it appears that the main problem involves the cause of retainer failure. Since the ET-378 oil has a very steep viscosity-temperature curve, there is approximately an 18 to 1 increase in viscosity with temperature change from 210°F to 70°F. This increase in viscosity could then result in a significant increase in retainer drag. This in turn could lead to retainer loads of sufficient magnitude to cause failure.

After failure of the retainer, the action of the balls on the race rings would cause the observed swaging, smearing, and plastic flow. Once failure occurred, it became impossible to tell whether the race damage occurred before or after the cage failure.

During startup, the rotameter flow indicator to the bearings was maintained at .35 gpm. The rotameters are calibrated for oil at 210° F. A decrease in oil temperature means that for the same scale reading actual flow decreases with temperature. At 150° F, actual rotameter flow is ten percent below indicated flow. At 70° F, there is a 30 percent decrease. This means that actual flow to the bearings during this startup was 140 lbs./hr., and increased as the inlet oil temperature rose. Based on previous test results, this rate of oil flow to the bearings should have been adequate.

Conclusions

1. The primary cause of failure was the introduction of cold oil during startup. The high oil viscosity led to high retainer drag which in turn led to the retainer failure.

2. A contributing factor may have been the four hours of running with vibration due to quill whip. Since the bearing was carefully inspected prior to Run No. 5, and no signs of race damage were noted it appears unlikely that the vibration was a cause. If it had been, some race damage would have been noticed prior to assembly. However, there is the possibility that the race damage may have been slight and escaped detection. For this reason, running with vibration must be retained as a possible contributing factor to failure.

3. As a result of this failure investigation, it is recommended that startup be made with hot oil. Failure to maintain sufficiently high lubricant temperatures with adequate flow may result in high retainer drag and subsequent bearing failure.

C. Lubricant Deterioration

The lubricant chosen for this application, Dow ET-378 polyphenyl ether, was selected on the basis of its radiation resistance and thermal and oxidative stability. However, during the course of the seal tests described in Reference 23, a period of approximately 6 months, the oil darkened and then precipitated a sugar-like substance which clung to the bearing and flow passages of the seal test rig. Figure 16 shows a photograph comparing a sample of clear ET-378 and a sample containing the precipitate.

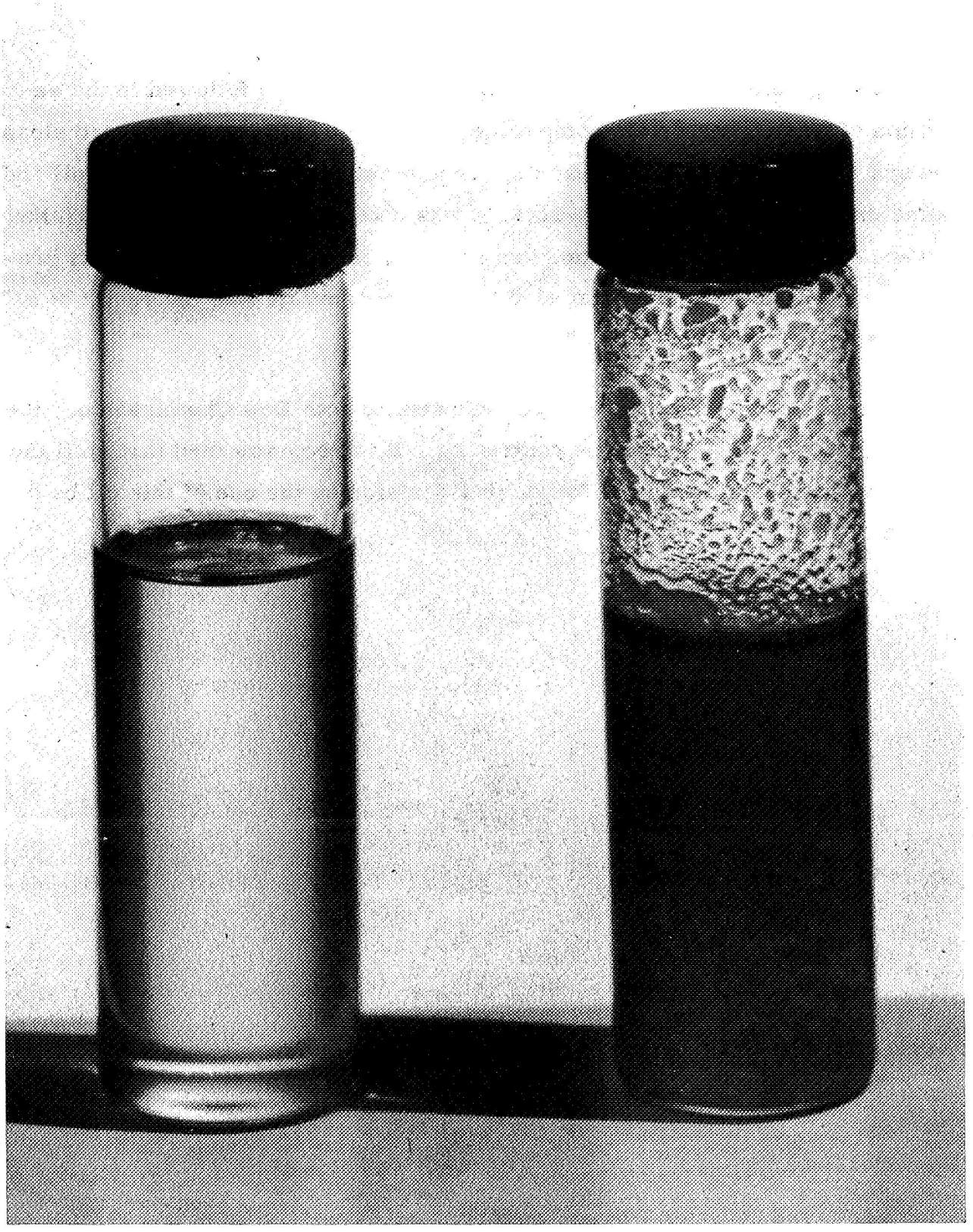

Figure 16. Photographic Comparison of New and Old Oil
A&SP Photo 1186723.

Although the manufacturer's recommendations were followed in the selection of test rig materials compatible with the ET-378, it was nevertheless thought the precipitate was caused by a chemical reaction between the oil and some material in the test rig. Later it was noted that even the oil which had never been removed from its original shipping containers contained this precipitate. It was therefore concluded that the precipitate was the result of a time dependent deterioration of the oil.

Samples of the deteriorated oil were sent to both Dow Chemical Co., the vendor, and to AGC, the prime contractor. It is recommended that until the cause of this deterioration is found, that decision on the use of this oil be delayed.

V. CONCLUSIONS AND RECOMMENDATIONS

Conclusions

1. Both the hand and computer calculations indicate that the specified bearing has adequate load carrying capacity and is of high enough quality to meet the 10,000 hour life requirement with 99.5 percent probability of survival under the operating conditions expected for the SNAP-8 alternator.

2. Computations using calculated bearing stiffness show that the first alternator critical speed is almost twice running speed.

3. Initial tests with specified lubricant, Dow ET-378, a polyphenyl ether, indicate a time dependent deterioration of this oil. Decision on the use of this oil should be delayed until the cause of the observed deterioration is determined and corrected.

Recommendations

1. Appropriate chemical analyses and material tests should be conducted on the specified lubricant, Dow ET-378, to determine and correct the cause of observed deterioration of this oil in initial testing.

2. Since the available analytical methods for calculating magnetic pull forces have not been verified experimentally, it is suggested that these forces be measured in the SNAP-8 alternator. Actual measurement of these forces would permit more accurate bearing life calculations and in addition provide information for improving the analytical magnetic pull calculation techniques.

REFERENCES

1. "Polyphenyl Ethers, Property and Data Performance Sheet," The Dow Chemical Company, Technical Service and Development, Midland, Michigan.

2. Bamberger, E. N., and C. C. Moore, "Evaluation of the Effect of Six Lubricants on Rolling Contact Fatigue Life of M-50," General Electric Report No. R61FPD553.

3. Irwin, A., "Lubricants -- Calculated Bearing Life," Marlin Rockwell Corp., Informal paper presented at 1963 ASME Spring Symposium.

4. "Discussion on Chemical Analysis Variation and Melting Practices," ASME Spring Lubrication Symposium, SKF Industries, Inc.

5. "Evaluation of Rolling Contacts in the Range of 550 F to 1000 F," General Electric Co. Report No. 58GL30, Class III.

6. "Nuclear Radiation Resistant High Temperature Lubricants," Shell Development Company, WADC TR 59-173, December 1958.

7. "American Standard Method for Evaluating Load Ratings for Ball and Roller Bearings," ASA B3.11-1959.

8. Palmgren, A., "Ball and Roller Bearing Engineering," SKF Industries, 1959.

9. Shaw and Macks, "Analysis and Lubrication of Bearings," McGraw-Hill Book Company, 1949.

10. Jones, A. B., "The Life of High Speed Ball Bearings," ASME Paper No. 51-A-69.

11. Dudley, Darle W., "The Design of Splines and Gear Tooth Couplings," General Electric Report No. DF59MSD200, 1959.

12. Dorsey, R. S., and Botje, "A Method for Predicting Operating Temperatures of Deep Groove Ball Bearings," G. E. Report R56AGT231, 1956.

13. Jones, A. B., "Analysis of Stress and Deflections," Vols. I and II, New Departure Division, General Motors Corporation.

14. Tallian, T., "Weibull Distribution of Rolling Contact Fatigue Life and Deviations Therefrom," ASLE Trans. 5, 183-196, 1962.

15. Jones, A. B., "A General Theory for Elastically Constrained Ball and Radial Roller Bearing Under Arbitrary Load and Speed Conditions," Fafnir Bearing Company, Nov. 1958.

16. Morrison, T. W., Walp, H. O, and Remerenko, R. P., "Materials in Rolling Element Bearings for Normal and Elevated Temperatures," ASLE Trans. Vol. 2, No. 1, April 1959.

17. Tallian, T., "Weibull Distribution of Rolling Contact Fatigue Life and Deviations Therefrom," ASLE Trans. 5, 183-196, 1962.

18. Prohl, M. A., and Bedford, C. E., "Calculation of Critical Speeds on IBM 701 Computer," TIS Report No. 53TG421.

19. Prohl, M. A., "A General Method for Calculating Critical Speeds of Flexible Rotors (Revised Procedure)," DF74176.

20. "Handbook of Mechanical Spring Design," Associated Spring Corporation, Bristol, Connecticut, 1958.

21. "Development Component Specification Bearing, Ball, Angular Contact, 40 mm Bore," AGC Specification 10206, 28 June 1963.

22. "Development Component Specification Alternator, Brushless, Liquid-Cooled," AGC Specification 10175, 6 August 1963.

23. McGrew, J. M., Orsino, A. J., and Ketola, H. N., "Design and Test of Three Seal Systems for SNAP-8 Alternator," G. E. Report No. 64GL126, 1964.

DISTRIBUTION LIST

H. O. Slone Lewis Research Center	5	Herman Ernst Evendale Bldg. 701, N-13	1
P. H. Hudson Aerojet-General Corp.	5 + 1 repro.	E. Schnetger Evandale	1
G. Oiye Aerojet-General Corp.	1	A. Schnake Evandale	1
C. T. Luddy Erie	3 + 1 repro.	J. F. Davis Erie	1
R. H. Guedet Erie	1	C. S. Renner Erie	1
P. M. Tabor Waynesboro Room 242	1	ICM&G Technical Library 1-9, Erie	1
D. A. Fisk Waynesboro Room 250	1	T. Salmon 3-64B, Erie	1
T. F. Bruce Los Angeles Office	1		
J. M. McGrew Schenectady	10		
E. Ray Valley Forge	1		
L. Lady Valley Forge	1		

DISTRIBUTION LIST (Continued)

Title Page Only

Space Power and Propulsion Engineering
Attn: W. R. Becraft
Valley Forge

A. E. Truran
Fitchburg

M. E. Petersen
Schenectady

E. P. Smith
Schenectady

I. E. Andreason
Erie

ATL

S. Neal

W. E. Gray

W. L. Zabriskie

H. Stern

G. R. Fox

J. P. Hanna

III 135

1-7-11-63

GENERAL ELECTRIC

REV NO.	TITLE	CONT ON SHEET	SH NO. 1
	BEARING FORCES DUE TO ECCENTRICITY (72 SLOTS)		
CONT ON SHEET	SH NO.	FIRST MADE FOR SNAP 8	

Base calculations on DF 57M140, by V.J. Picozzi (10/1/57). This gives the bearing load as

$$F = K F_o$$

For a 2 circuit design the folder shows F_o as varying linearly from 0 to 1.414 for eccentricities varying from 0 to a full gap.

$$K = \frac{34.7 \times \text{total airgap cross section}}{2} \times \left(\frac{\text{gap density}}{50}\right)^2$$

Determine force for each end of rotor. Then:

gap area $= 7.5\pi(3.3) = 77.8 \text{ in}^2$

$\phi_{ac} = 170 \times \frac{120}{132} = 700$ Klines/pole at 120 volts

Over $\frac{1}{2}$ rotor pitch, $B_{gap} = \frac{K_u \phi_{ac}}{\frac{1}{2}\text{gap area}} = \frac{2.21 \times 700}{.5(77.8)} = 39.8 \text{ Klines/in}^2$

Then

$$K = \frac{34.7 \times 77.8}{2}\left(\frac{39.8}{50}\right)^2 = 854$$

Then at full eccentricity, the total force becomes

$F_{net} = 1.414 \times 854 = 1210$ pounds (for .060" eccentricity) (This does not allow for saturation and is felt to be pessimistic)

MADE BY G.A. Osborn	APPROVALS	DIV. OR DEPT.	III	106
ISSUED 6/26/63		LOCATION	CONT ON SHEET	SH NO.

GENERAL ELECTRIC

REV NO.	TITLE	CONT ON SHEET	SH NO. 2
	BEARING FORCES (ROTOR ECCENTRICITY		
CONT ON SHEET SH NO.	FIRST MADE FOR SNAP 8		

From W R Kruest's Book:

$$F_{net} = \frac{4 B_o^2 A}{72 \times 10^6} \left(\frac{e}{g}\right)$$

$B_o = 9.8 \times 10^3$ lines/in^2

$A = \frac{778}{4} = 19.45$ in^2/pole

$$F_{net} = \frac{4 (39.8)^2 \times 10^6 \times 19.45}{72 \times 10^6} \left(\frac{e}{g}\right) = 172 \left(\frac{e}{g}\right) \text{ pounds}$$

For $\frac{e}{g} = 1$ (max. displacement)

$F_{net} = 172$ pounds

MADE BY G A Osborn	APPROVALS	DIV. OR DEPT.	CONT ON SHEET III 107 SH NO.
ISSUED 6/26/63		LOCATION	

BEARING FORCES (ROTOR ECCENTRICITY)

In the October 1962 issue of the Ansaldo - San Giorgio bulletin (Italian), L. Centurioni writes the article "Transverse Magnetic Attractions in Rotating Machines", discussing several cases of magnetic pull. For the case of a round rotor eccentrically located within a round stator he derives the net unbalanced pull (considering a single electrical circuit design). His equation for this force is Eq. (23):

$$F_1 = \frac{T_b' B_M^2 b D L}{\mu_0 K_d} \qquad (23)$$

where B_M = maximum induction at pole center
K_d = Carter's coefficient (>1)
b = square of ratio between average and maximum values of induction B_M
D = diameter, L = length of stack

$$T_b' = \int_{-\pi/2}^{\pi/2} \frac{t' \cos^2\theta \, d\theta}{(1 - t'^2 \cos^2\theta)^2}$$

where $t' = \frac{\delta_0}{d}$

δ_0 = magnitude of eccentricity
d = nominal air gap
$d' = \frac{d}{G}$

$G = \frac{\tan\beta}{\tan\alpha}$

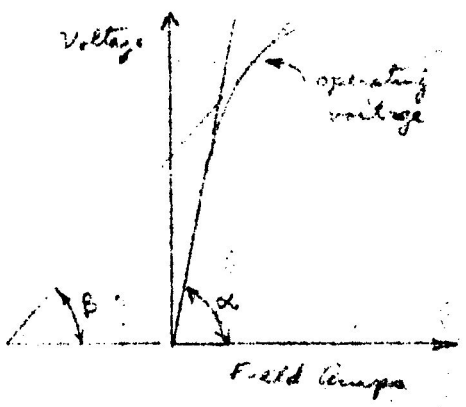

where these angles are defined on the saturation curve at the left. The saturation in question should include only stator and rotor tooth AT, for the case of the SNAP 8 salient pole case.

Eq. 23 is in MKS units. To convert to English system, multiply by

$$\left[10^{-5} \frac{\text{weber}}{\text{Kilolinc}} (39.37)^2 \frac{\text{in}^2}{\text{m}^2}\right]^2 \left[\frac{\text{in}}{39.37\,\text{in}}\right]^2 \left[.224 \frac{\text{pound}}{\text{newton}}\right] = .349 \times 10^{-7}$$

$\mu_0 = 4\pi \times 10^{-7}$

Then Eq (23) becomes

$$F_t = \frac{T_b' B_M^2 b D L}{4\pi \times 10^{-7} K_d} \times .349 \times 10^{-7} = 0.0278\ T_b' B_M^2 b, ID, \frac{HI}{2} a_1 a_2 \text{ (pounds force per end)}$$

where DCM & G nomenclature has been adopted
dimensions are in inches.
B_M = peak density in kilolines/in^2

The above expression is valid for a round rotor as represented by the dashed line in the sketch. For that case the limits of integration are $\pm \pi/2$ radians. For the SNAP 8 inductor generator the limits of integration must be reduced to $.35 \frac{\pi}{2}$, where .35 is the "Per unit Pole Arc".

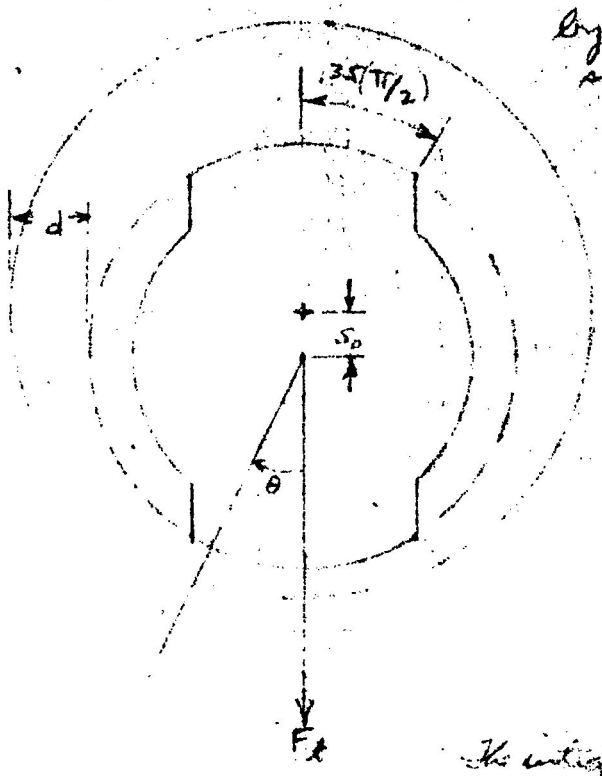

T_b' is evaluated numerically on pages 5, 6 and 7 for the following values of t'. The integration is quite approximate and T_b' is expected to be on the low side of the true value.

Results are.

t'	0.1	0.3	0.5	0.7
T_b'	0.101	0.3525	0.833	2.295

(Continue on page 9)

Evaluation of

$$T_b' = \int_{-a}^{a} \frac{c\cos^2\theta}{(1-c^2\cos^2\theta)^2}\,d\theta = \int_{-a}^{a} f(c,\theta)\,d\theta \quad \text{where } c = \frac{e}{g}, \text{ and}$$

$$a = .35\frac{\pi}{2} = .175\pi = .55 \text{ rad.}$$

I In $\underline{c = 0.1}$ $\quad f = \dfrac{0.1\cos^2\theta}{(1-.01\cos^2\theta)^2}$

a) $\theta = 0 \quad f = \dfrac{0.1}{(1-.01)^2} = \dfrac{0.1}{.981} = .102$

b) $\theta = .55 \quad f = \dfrac{0.1(.8526)^2}{[1-.01(.8526)^2]^2} = \dfrac{.0728}{[1-.00723]^2} = \dfrac{.0728}{(.993)^2} = .0738$

c) $\theta = \pi/2 \quad f = 0$

d) $\theta = \frac{2}{3}a = .3667 \quad f = \dfrac{.1(.9336)^2}{[1-.01(.9336)^2]^2} = \dfrac{.0871}{(1-.00871)^2} = .0888$

e) $\theta = \frac{a}{3} = .1833 \quad f = \dfrac{.1(.983)^2}{[1-.01(.983)^2]^2} = \dfrac{.0967}{(1-.00967)^2} = .0987$

$$\int_{-a}^{a} f(c,\theta)\,d\theta = 2\int_{0}^{a} f(c,\theta)\,d\theta$$

$$\simeq 2\left[.102 + .0738 + 2(.0987 + .0888)\right]\frac{(.1833)}{2}$$

$$= (.1502)(.1833) = .101$$

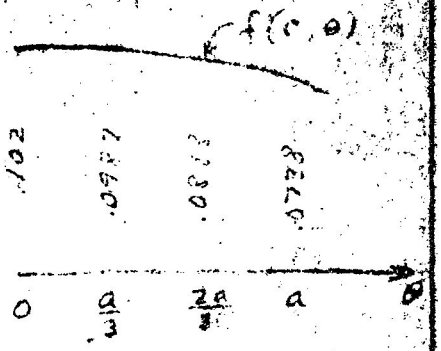

II $\underline{c = 0.5}$ $\quad f = \dfrac{0.5 \cos^2\theta}{(1 - .25\cos^2\theta)^2}$

a) $\theta = 0$ $\quad f = \dfrac{0.5}{(1-.25)^2} = .889$

b) $\theta = \frac{a}{3} = .1833$ $\quad f = \dfrac{.5(.983)^2}{[1-.25(.983)^2]^2} = \dfrac{.4835}{(1-.242)^2} = .842$

c) $\theta = \frac{2a}{3} = .3667$ $\quad f = \dfrac{.5(.934)^2}{[1-.25(.871)]^2} = \dfrac{.4355}{[1-.2177]^2} = .712$

d) $\theta = a = .55$ $\quad f = \dfrac{.5(.728)}{(1-.182)^2} = \dfrac{.364}{(.818)^2} = .545$

$$\int_0^a f(c,\theta)\,d\theta \simeq 2\left[.888 + .545 + 2(.842 + .712)\right]\left(\frac{.1833}{2}\right)$$

$$= (4.541)(.1833) = .833$$

III $\underline{c = 0.3}$ $\quad f = \dfrac{0.3\cos^2\theta}{[1 - .09\cos^2\theta]^2}$

a) $\theta = 0$ $\quad f = \dfrac{.3}{(1-.09)^2} = \dfrac{.3}{(.91)^2} = .3625$

b) $\theta = .1833$ $\quad f = \dfrac{.3(.967)}{[1-.09(.967)]^2} = \dfrac{.2901}{(1-.087)^2} = .348$

c) $\theta = .3667$ $\quad f = \dfrac{.3(.871)}{[1-.09(.871)]^2} = \dfrac{.2613}{(1-.0783)^2} = .3075$

d) $\theta = .55$ $\quad f = \dfrac{.3(.728)}{[1-.09(.728)]^2} = \dfrac{.2184}{(1-.0655)^2} = .250$

$$\int_{-a}^{a} f(c,\theta)\,d\theta \simeq 2\left[.3625 + .850 + 2(.348 + .3075)\right]\left(\frac{.1833}{2}\right)$$

$$= (1.923)(.1833) = .3525$$

IV $c = 0.7$ $\quad f = \dfrac{0.7\cos^2\theta}{(1-.49\cos^2\theta)^2}$

a) $\theta = 0$ $\quad f = \dfrac{0.7}{(.51)^2} = 2.69$

b) $\theta = .1833$ $\quad f = \dfrac{0.7(.967)}{[1-.49(.967)]^2} = 2.445$

$(.526)^2$

c) $\theta = .3667$ $\quad f = \dfrac{0.7(.871)}{[1-.49(.871)]^2} = 1.85$

$(.570)^2$

d) $\theta = .52$ $\quad f = \dfrac{0.7(.728)}{[1-.49(.728)]^2} = 1.232$

$(.6435)^2$

$$\int_{-a}^{a} f(c,\theta)\,d\theta \simeq 2\left[2.69 + 1.232 + 2(2.445 + 1.85)\right]\left[\frac{.1833}{2}\right]$$

$$= (12.51)(.1833) = 2.295$$

Evaluate "b"

For the air gap flux density, Bewley in "Two Dimensional Fields in Electrical Engineering", p. 134, gives a chart showing the variation in density along the pole arc. At the corner of the rotor the density is 84% of that at the pole centerline, and within two airgaps towards the centerline (6% of the distance) the local density is within 1% of the maximum. This would estimate the following ratio for SNAP 8:

$$\sqrt{b} = \frac{B_{ave}}{B_{max}} \approx .995, \quad \text{or} \quad b \approx .99$$

Evaluate F_t

From page 4

$$F_t = .0278\, T_b'\, B_M^2\, b\, ID_1\, \frac{HI}{2}\, a_1 a_2$$

$ID_1 = 7.50$ $\quad \frac{HI}{2} = 3.3''$ $\quad a_1 a_2 = .960''$,

$$B_M = \frac{K_v K_m \Phi_{ac}}{2 A_g} = \frac{2.21 \times 2.63 \times 700}{2 \times 37.3} = 54.5 \text{ kilolines/in.}^2 \text{ at } 120 \text{ volts}$$

Then

$$F_t = .0278\, T_b' (54.5)^2 (.99)(7.50)(3.3)(.96) = 1935\, T_b' \text{ pounds}$$

Now, referring to the table of T_b' vs. d' on page 4:

d'	0.1	0.3	0.5	0.7
F_t (lbs.)	195	681	1610	4440

Note $d' = \frac{\delta_0}{d'} = \frac{\delta_0}{d'} \frac{\tan\beta}{\tan\alpha}$ to account for variation in rotor and stator B.H.

To account for saturation, construct saturation curve on sheet 10.

a) Air gap AT at 120 volts 1025 AT per end

b) Saturation in stator and rotor teeth only:

1) at 132 volts we have for stator teeth $AT_{st} = \frac{192}{2} = 96$ AT

$AT_{Rot} = 1.65'' \times 67$ AT/in $= 110$ AT

$AT_{tot} = 96 + 110 = 206$ AT

2) at 120 volts

$B_{st} = \frac{120}{132} \times 110.8 = 100.7$ $\qquad AT_{st} = .525 \times 65 = 34$

$B_{Rot} = \frac{120}{132} \times 94 = 85.5$ $\qquad AT_{Rot} = 1.65 \times 50.5 = 83$

$AT_{tot} = 117$

From sheet 10, $\frac{\tan\alpha}{\tan\beta} = \frac{120/1140}{120/2235} = 1.96$

Then

$S_0 = d\,t' \frac{\tan\alpha}{\tan\beta} = .063(1.96)\,t' = .118\,t'$

Now the force can be expressed as a function of eccentricity S_0

t'	0.1	0.3	0.5	0.7
S_0	.0118"	.0353"	.0588"	*
F_t (lbs)	195	681	1610	

(These forces may be reduced by approx. 30% due to 2 circuit connection of stator winding.)

* $S_0 = .088''$, which has no meaning, as this exceeds the nominal gap of .063"

Saturation of water and carbon tetra

SNAP-8

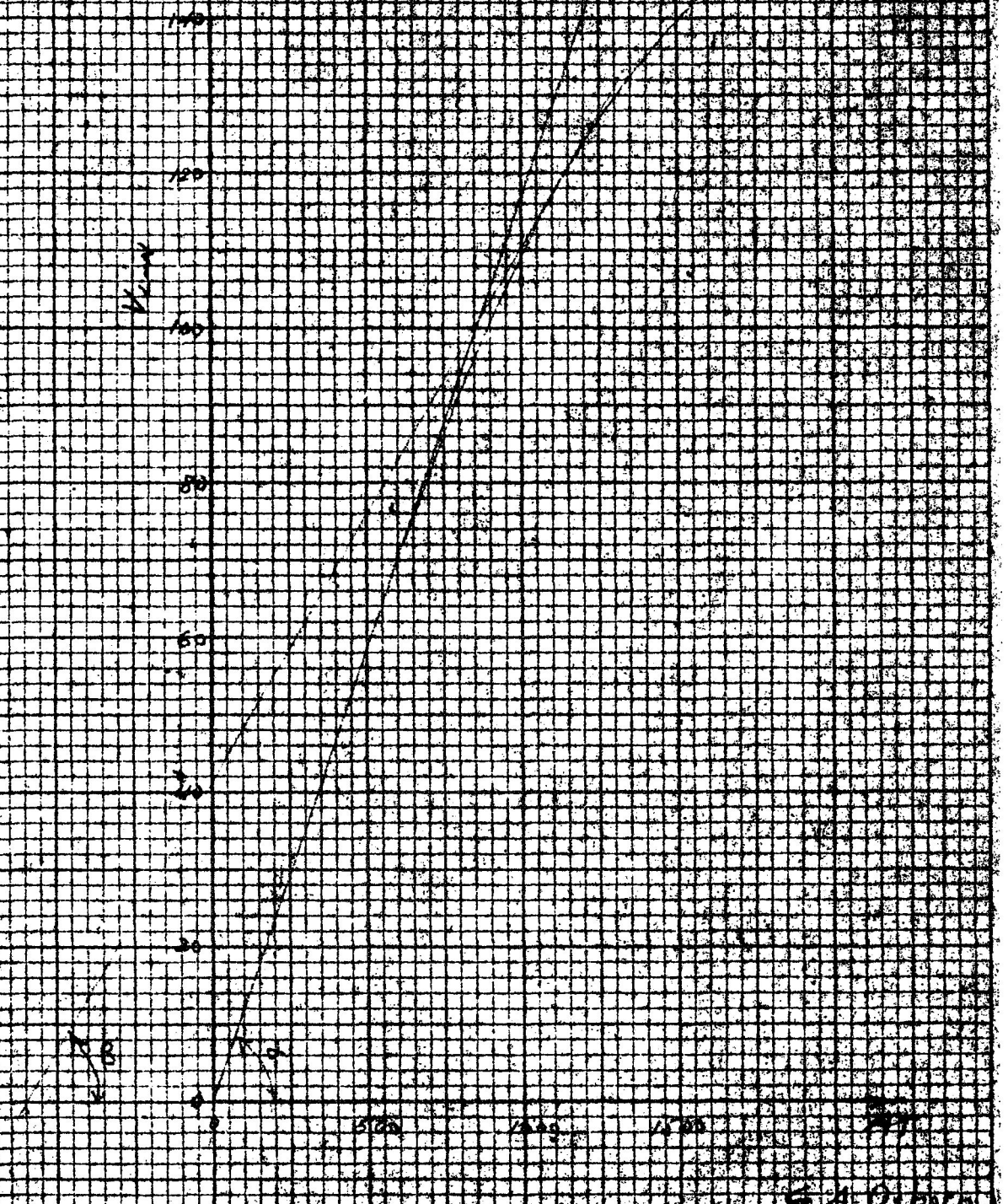

Sheet 11

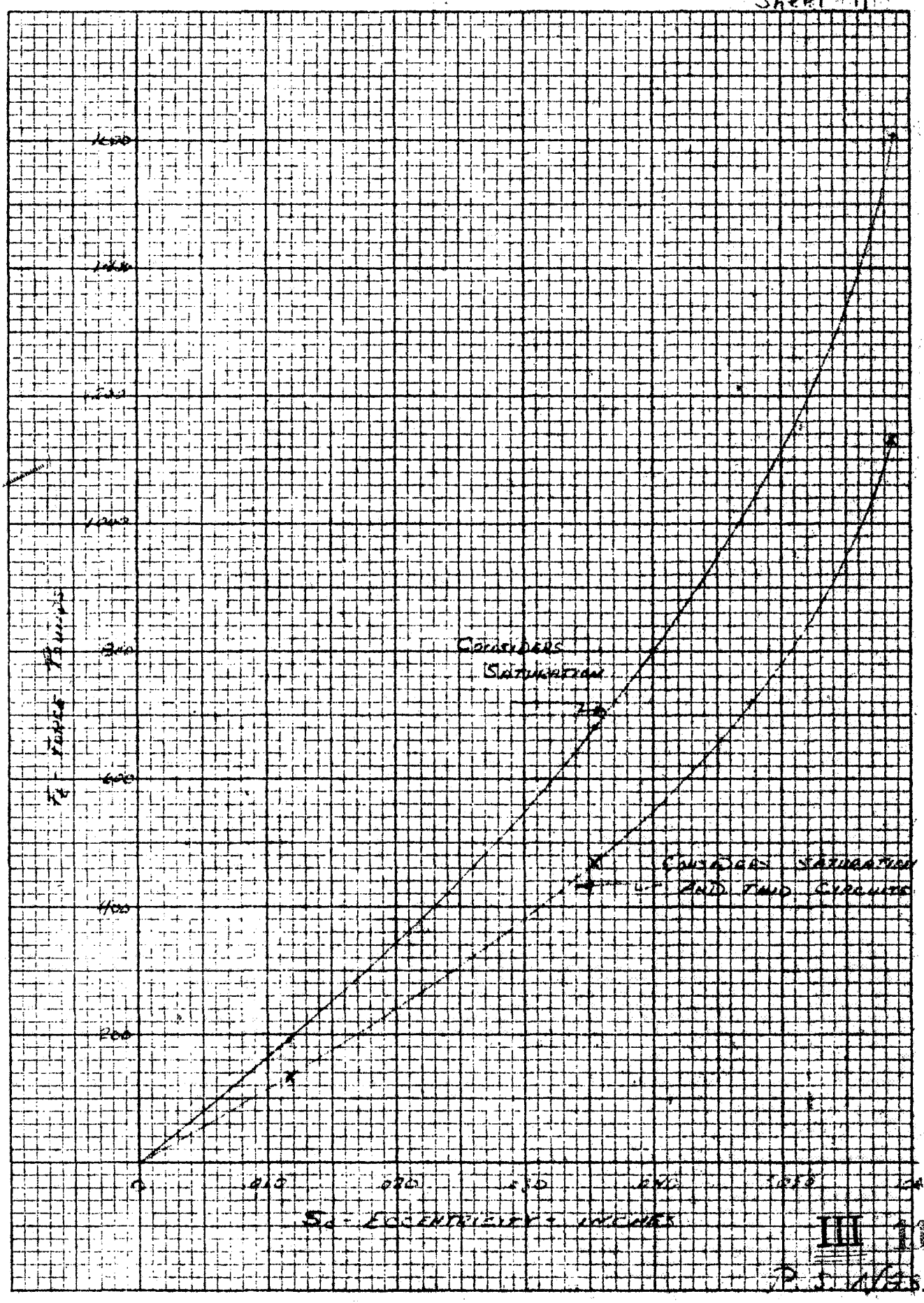

III 116

P. S. Naska

IV. SEAL DESIGN

The design and test of the dynamic seals used in the preprototype alternator are described in the following report:

> "Design and Test of Three Seal Systems for the SNAP-8 Alternator," by J. M. McGrew, A. J. Orsino, and H. N. Ketola, General Electric Report No. 64GL126, dated 8 October 1964

TECHNICAL INFORMATION SERIES

GENERAL ELECTRIC

ADVANCED TECHNOLOGY LABORATORIES

AUTHOR	SUBJECT	NO.
J.M. McGrew A.J. Orsino H.N. Ketola	Non-Contacting Dynamic Seals	64GL126
		DATE 10/8/64
TITLE DESIGN AND TEST OF THREE SEAL SYSTEMS FOR THE SNAP-8 ALTERNATOR		G.E. CLASS II
		GOVT. CLASS None
REPRODUCIBLE COPY FILED AT G.E. TECHNICAL DATA CENTER BLDG. 5, SCHENECTADY, N. Y.		NO. PAGES 144

SUMMARY Over 200 hours of test experience on three types of non-contacting dynamic seals have shown leakage rates comparable to mechanical face seals, and demonstrated the possibility of extremely long seal life because of the absence of rubbing parts.

The plane slinger with screw return produced leakage rates ranging from .025 cc/hr, the minimum detectable rate, to 4 cc/hr sealing a 7.5 psia polyphenyl ether to vacuum. Nominal axial clearance was 23 mils, and maximum seal temperature did not exceed 290°F. Variations in seal axial clearance account for the differences in measured leakage rates. The results indicate that by maintaining axial clearances lower than 23 mils leakage rates approaching .025 cc/hr are possible.

The housing-disk seal, a more complicated slinger seal, operating under the same conditions, exhibited leakage rates less than .025 cc/hr, but at a higher power loss. The screw seal with flooded bearing cavity gave higher leakage rates, 12 cc/hr, but has the advantage of consuming less power than the other two designs tested.

Simulation of electrical pole face losses during test by electric heaters showed that all three seal designs could remove a heat load of 150 watts per brg. end with only an average 6°F rise in bearing temperature.

KEY WORDS

Non-Contacting Seals, Screw Seals, Slinger Seals, Seals

INFORMATION PREPARED FOR Aerospace Motor and Generator Department

TESTS MADE BY H. E. Marx, R. E. Otten

AUTHOR J. M. McGrew, A. J. Orsino, H. N. Ketola

COMPONENT Bearing Laboratory

APPROVED H. Stern, Mgr., Fluids Engineering; G.R. Fox, Mgr., Bearing Lab.

IV.

TABLE OF CONTENTS

		Page
I.	Introduction and Summary	1
II.	Seal Selection and Design	3
	A. Operating Conditions	3
	B. Seal Selection	4
	1. Plane Slinger with Screw Return	4
	2. Housing-Disk Seal	5
	3. Screw Seal	6
	C. Design of Plane Slinger with Screw Return	9
	1. Selection of Dimensions	9
	2. Head Rise	10
	3. Power Loss	11
	4. Design of Screw Return	12
	5. Design of Inlet Oil Jets	13
	6. Design of Discharge Passage	13
	D. Design of Housing-Disk Seal	14
	E. Design of Screw Seal	14
	1. Selection of Dimensions	14
	2. Sealing Capability	15
	3. Power Loss	15
III.	Description of Test Rig	17
	A. Introduction	17
	B. Description	17
	1. Rotor and Casing Assembly	18
	2. Thymatrol Drive Assembly	21
	3. Lube System Assembly	21
	C. Instrumentation	21
	1. Flow Measurements	23
	2. Pressure Measurement	23
	3. Temperature Measurement	23

IV.

TABLE OF CONTENTS (continued)

Page

4. Torque Measurement 26
5. Speed Measurement 26
6. Leakage Measurement 26

IV. Test Procedure 28

V. Test Results 32

A. Plane Slinger with Screw Return 32
1. Test No. 4 Long Term Leakage Test 32
2. Test No. 5, Bearing Failure 44
3. Evaluation of Shaft Heat Removal. 44

B. Slinger Seal without Screw Return. 48

C. Housing-Disk Seal 53
1. Preliminary Component Testing 53
2. Housing-Disk Seal Tests on SNAP-8 Alternator Test Rig 53

D. Screw Seal Tests 60

E. Comparison of Measured and Calculated Power Loss 68

F. Summary of Leakage Data 69

VI. Conclusions and Recommendations 72

Appendix A - Theory of Slinger Seal 74

A. Introduction 74
B. Analysis of Partially Wetted Disk 78
1. Regime I 78
2. Regime II 81
3. Regime III 108
4. Regime IV 111
5. Pressure Characteristics of Partially Wetted Disks 123
6. Flow Characteristics of Rotating Disks 126

TABLE OF CONTENTS (continued)

Page

Appendix B - Theory of Screw Seal 130

A. Screw Seal Geometry 130

B. Screw Seal Sealing Capability 130

C. Screw Seal Power Loss 131

Appendix C - Bearing Power Loss 132

Figures 135

Tables 138

Nomenclature 139

References 143

I. Introduction and Summary

The alternator for the SNAP-8* power system, a light weight 35 kwe power supply, has a 10,000 hour reliability requirement. Because of this high reliability requirement, conventional rubbing contact seals, whose reliability is uncertain because of friction and wear, were abandoned in the design of the alternator in favor of non-contacting type seals.

Most non-contacting seals require a small but finite leakage flow. In contrast, two particular types of non-contacting seals, the slinger seal and the screw seal, offer the possibility of contact free surfaces and "zero" leakage. These types of seals are unique in that for certain operating conditions it is possible to maintain a stable liquid-to-vapor interface on the rotating parts and thus the only leakage is the evaporative loss from liquid-to-vapor interface.

Leakage in these two types of seals is minimized primarily by the introduction of external forces on the leakage fluid; centrifugal forces in the case of the slinger seal and viscous shear forces in the case of the screw seal. Although the principles of operation of these types of seals has been known for many years, commercial applications have been few. Slinger seals have been used in commercial mercury turbines and screw seals have found limited application in seals for gas cooled reactor blowers, both applications requiring high reliability components.

This report covers the design and testing of three non-contacting seal systems for the SNAP-8 alternator. Pressure capability, power loss factors and seal leakage data are given for all three systems. Over 200 hours of test experience on three types of non-contacting dynamic seals have shown leakage rates comparable to mechanical face seals, and demonstrated the possibility of extremely long seal life because of the absence of rubbing parts.

*Systems for Nuclear Auxiliary Power

The plane slinger with screw return produced leakage rates ranging from .025 cc/hr, the minimum detectable rate, to 4cc/hr sealing a 7.5 psia polyphenyl ether to vacuum. Nominal axial clearance was 23 mils, and maximum seal temperature did not exceed 290°F. Variations in seal axial clearance account for the differences in measured leakage rates. The results indicate that by maintaining axial clearances lower than 23 mils leakage rates approaching .025 cc/hr are possible.

The housing-disk seal, a more complicated slinger seal, operating under the same conditions, exhibited leakage rates less than .025 cc/hr, but at a higher power loss. The screw seal with flooded bearing cavity gave higher leakage rates, 12 cc/hr, but has the advantage of consuming less power than the other two designs tested.

Simulation of electrical pole face losses during test by electric heaters showed that all three seal designs could remove a heat load of 150 watts per bearing end with only an average 6°F rise in bearing temperature.

II. Seal Selection and Design

A. Operating Conditions

The operating conditions which the bearing-seal system must meet are given in the Aerojet-General Corporation specifications AGC-10206 and AGC 10175 respectively[15, 16]. Those conditions pertinent to the bearing-seal design are tabulated below.

Table 1

Summary of SNAP-8 Alternator
Bearing-Seal Operating Conditions

Speed	12,000 rpm
Lubricant	Dow ET-378 polyphenyl ether or equivalent
Lubricant Flow Rate	400 lb/hr. max (200 lb/hr. per brg.)
Lubricant Inlet Pressure	$33.0 \begin{smallmatrix} +0.0 \\ -1.0 \end{smallmatrix}$ psia
Lubricant Outlet Pressure	$5.0 \begin{smallmatrix} +0.0 \\ -0.25 \end{smallmatrix}$ psia
Lubricant Inlet Temperature	$210^{\circ}F \begin{smallmatrix} +0 \\ -10 \end{smallmatrix}$ $^{\circ}F$
Lubricant Hot Spot Temp.	500°F max.
Maximum Bearing Temp.	300°F
Overspeed/Underspeed	11,800 to 13,200 rpm

The specification further states that the rotor will be supported by rolling contact type bearings, and, unless deemed impractical by the manufacturer, the bearing type, size, lubrication and scavenging system shall be consistent with that used on the turbine assembly of the SNAP-8 Power Conversion System. The first two seal systems, the plane slinger with screw return and the housing disk seal are consistent with the turbine assembly. The third seal type, the screw seal is not and was considered as back up alternative system.

The specification does not dictate a leakage rate for the seals. Liquid

lubricant accumulations in the alternator cavity as high as 2500 cc could probably be tolerated without adversely affecting alternator performance. However, as a design goal, a liquid lubricant accumulation of 500 cc was assumed. Over a 10,000 hour period this limit represents a maximum leakage rate of .025 cc/hour from each of the inboard seals. Leakage from the outboard seals is not critical as the cavity outboard of the alternator drive end is scavenged and the anti-drive end outboard cavity is dead ended.

B. Seal Selection

In the SNAP-8 alternator application, the differential thermal expansion between the stator and the rotor make it very difficult to maintain close axial clearances. Because of this, only those types of non-contacting dynamic seals which do not depend upon close axial clearances for their operation were selected for this study. The theory of operation of the slinger and screw seal is given in appendices A and B.

The plane disk rotating in a housing is the simplest slinger seal configuration. However, experiments have shown that except at very close axial clearances, this seal configuration does not establish a stable interface between the liquid and the vapor in the seal. Visual observations reported in Reference 9 show that the leakage occurs on the stationary wall. Although in the study of Reference 9, it was occasionally possible to maintain a stable interface to speeds as high as 10,000 rpm, the onset of instability usually occurred at lower speeds and once started, it was impossible to stop the leakage even by decelerating to speeds as low as 1,000 rpm. Because of this many schemes have been devised to suppress the leakage which results from this instability. As reported in References 9 and 12, these schemes employing tangs, paddles, lips, on either the stationary or rotating part, have been partially successful. They are, however, dependent upon very close axial clearances in almost every case.

B-1. Plane Slinger with Screw Return

In the first configuration tested, the plane slinger with the screw return shown in Figure 1, the axial clearance between the rotating disk and stationary wall was maintained at the relatively large value of .020 to .025 inches and the screw return at the base of the stationary wall was

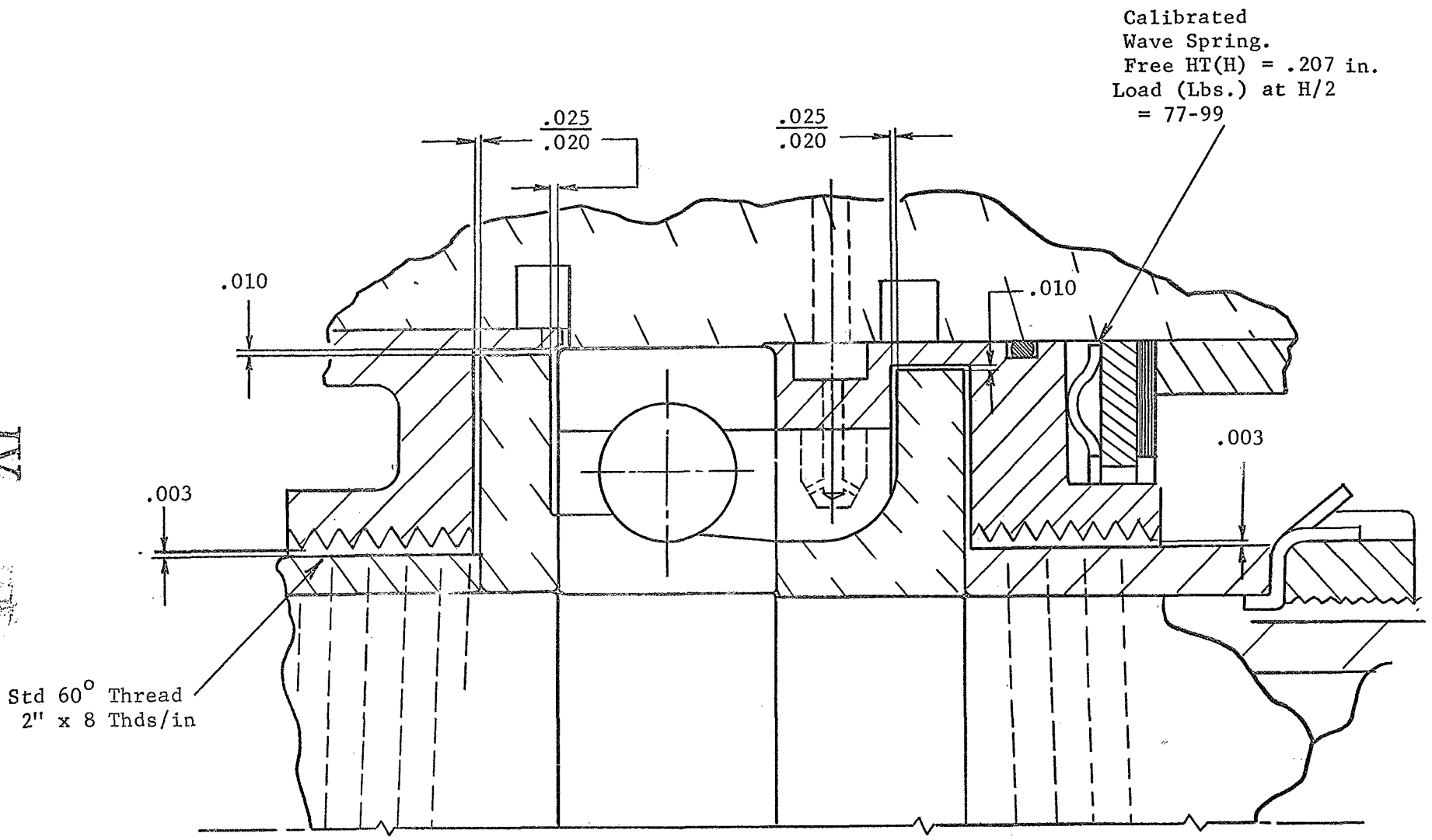

PLANE SLINGER WITH SCREW RETURN

Figure 1

relied upon to return any leakage down the stationary wall to the seal interface.

Both the plane slinger and housing disk seal configurations utilize a jet lubrication system. The slinger seal also acts as a centrifugal separator. Since the pressure on both sides of the slinger is that of the vapor pressure of the saturated liquid, the slinger seals against little if any pressure difference. Its main function is to form a stable interface between the vapor and the liquid and to pump the liquid up to the return line pressure.

B-2. Housing-Disk Seal

The second type of seal tested was the housing-disk configuration shown in Figure 2. The housing-disk seal is a variation of the slinger seal which not only restricts the leakage from the interface but provides a method for the return of any leakage to the interface. It consists of a hollow slinger, the outer portion of which operates as an ordinary slinger and serves to scavenge the bearing cavity. Any leakage from the outboard side of this slinger is admitted to the hollow cavity inside the slinger. The hollowed out portion of this disk, called the housing part, is connected to the space between the disk and the stationary enclosure. The leakage from the outboard interface which accumulates in the rotating housing is thrown to the outside by the centrifugal field, and returned to the seal through the two holes in the housing

Since both walls of the housing rotate at shaft speed, there is no relative motion between the fluid in the housing and the housing itself. Thus there is no shearing action in this space and it is much easier to establish a stable interface. This is in contrast to the fluid between the rotating disk and the stationary wall which has zero velocity at the wall and shaft velocity on the disk.

The lip which projects into the housing is designed so that its outermost radius is below the minimum radius of the fluid interface in the housing. Tests have shown that if the interface touches the lip, the seal will leak.

B-3. Screw Seal

In the previous two seal configurations, the bearing cavity was scavenged in contrast to the screw seal configuration depicted in Figure 3

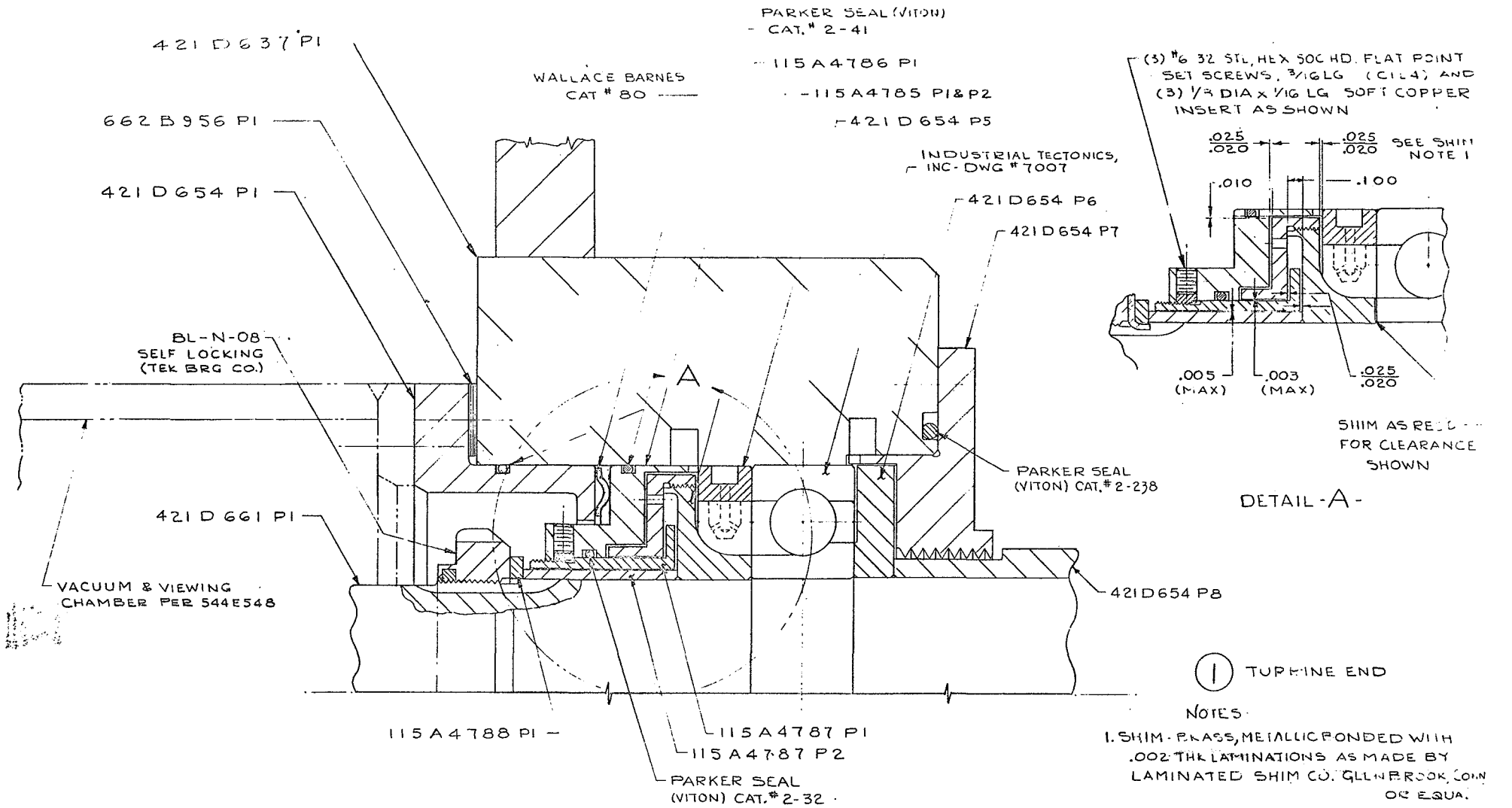

Figure 2. Drawing of Housing-Disk Seal

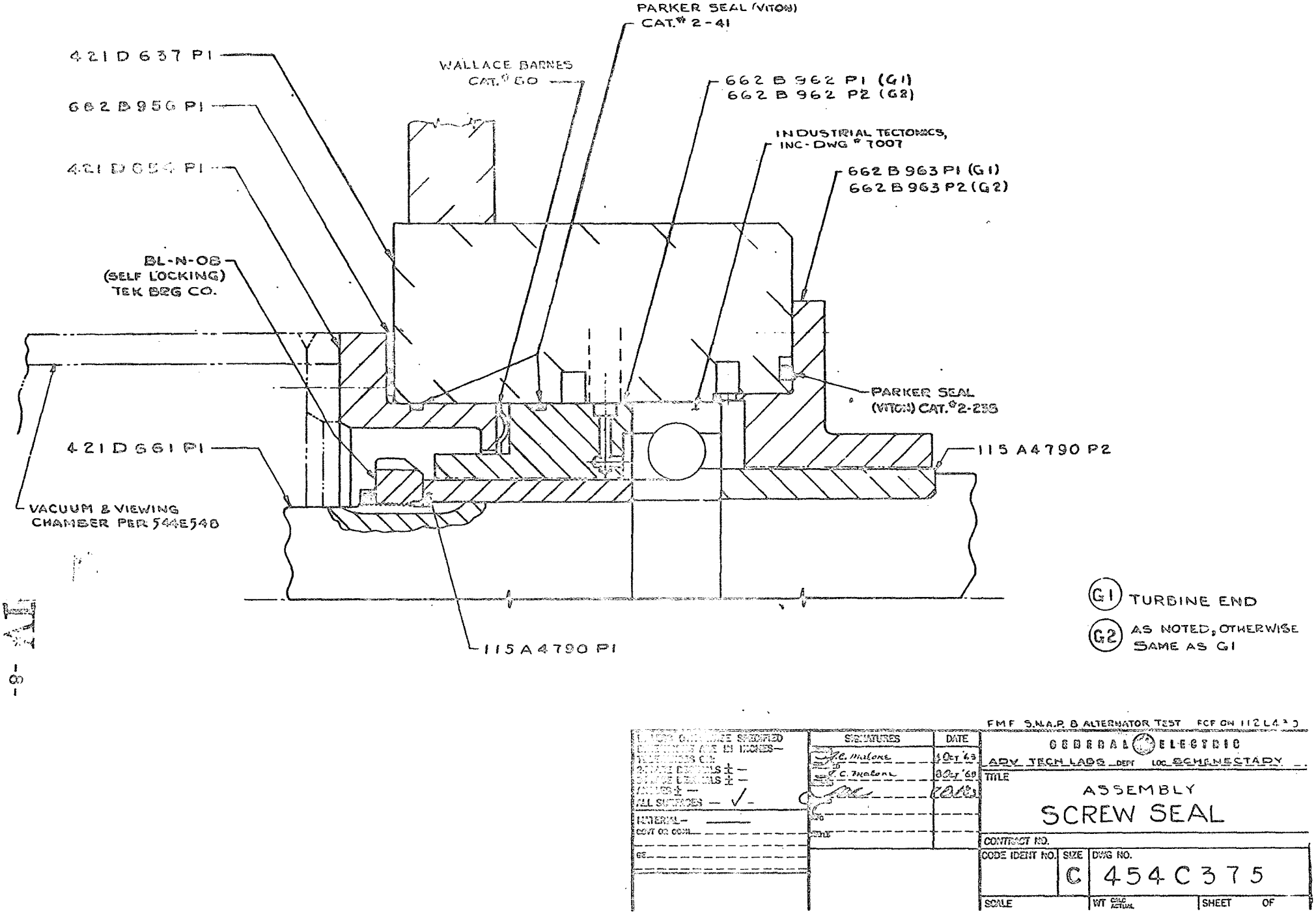

Figure 3. Drawing of Screw Seal

where the bearing cavity runs flooded. Unfortunately, there is little information available for predicting bearing life or power loss in flooded operation. References 13 and 14 give some information concerning the effect of oil flow rate on bearing performance. In Reference 13 a comparison is given of bearing outer ring temperature for a jet lubricated system and a flooded system for a 75 mm bore bearing operating at 16,000 rpm with a 2000 lb. thrust load. There was little difference in outer ring temperature and at high oil flow the outer ring temperature was essentially the same for both modes of operation.

In Reference 14, power loss of 202, 203, and 204 bearings is given as a function of oil flow rate for several different speeds. A 500-fold increase in oil flow rate, representing operation from jet to effectively flooded operation, resulted in only a twofold increase in friction loss at 30,000 rpm. The conclusion of this study was that bearings of the size range tested could best be operated with cross feed and paddling techniques rather than jet or mist lubrication schemes. The General Electric Company currently operates fuel pumps, jet engine gear boxes, and some alternators with flooded bearings.

Although there is no confirming data it would appear that jet lubricated bearing would have a longer life than the flooded bearing. This is the result primarily of the lower drag on the balls and retainer of the jet lubricated bearing. As will be pointed out later, the advantage of the screw seal system with a flooded bearing cavity is an overall lower system power loss compared to the slinger system with a jet lubricated bearing.

C. Design of the Plane Slinger with Screw Return

C-1. Selection of Dimensions

To ease assembly problems, the slinger diameter was dictated by the outer diameter of the bearing. A slinger diameter of 3 inches was chosen. The axial clearance was taken as .025 inches to allow for differential expansion between the rotor and stator. The slinger Reynolds number for ET-378 at 210°F is then:

$$R = \frac{\omega a^2}{\nu} = 3.21 \times 1 \times 10^5$$

where

$$\nu = .0088 \text{ in}^2/\text{sec}$$

$$\omega = 1255 \text{ rad/sec}$$

$$a = 1.5 \text{ in.}$$

The spacing ratio s/a becomes

$$s/a = \frac{.025}{1.5} = .017$$

which, from Figure A2, puts the operation in Regime III, that is the turbulent mode with merged boundary layers. If we were to choose a larger clearance, such that $s/a > .042$, operation would move to Regime IV. for this same Reynolds number.

The maximum engagement ratio is given by

$$X = (a - r)/a = .12$$

where $r = 1.3215$ inches is the inner radius of the bearing outer race.

The ratio of radial clearance to slinger radius was chosen as $c/a = .00637$ which was the value used in Reference 8. The slinger width was made 0.23 inches.

C-2. Head Rise

The pressure generating capability of the slinger is given by:

$$\Delta p = \frac{\rho}{2} (K\omega a)^2 \left[1 - (1 - X)^2\right] \qquad \text{(A75)}$$

Now in Regime III the effect of cylindrical wall is minor, and for this reason the value of K is close to 0.5. Therefore

$$\Delta p' = 10.3 \text{ psi}$$

where the following conditions were assumed:

$$\rho = .0406 \text{ lb/in}^3$$

$$\omega = 1255 \text{ rad/sec}$$

$$X = .12$$

$$a = 1.5 \text{ in.}$$

C-3. Power Loss

In Regime III the moment coefficient for one side of the disk is given by:

$$C_m = \frac{.0311\ C_4}{(s/a)^{1/4}\ (Re)^{1/4}} \qquad \text{(A60)}$$

where C_4 is a function of X in Figure A2.0. For X = .12, s/a = .017, R = 3.21×10^5 and C_4 = .46

$$C_m = 1.66 \times 10^{-3}$$

The moment on one side of the disk is given by equation

$$M = C_m \frac{\rho}{2} \frac{\omega^2 a^5}{g_o}$$

which gives $M = 1.04$ in-lb.

Multiplying the moment by the angular velocity, the power lost on one side of the disk is:

$$P = M\omega = .19 \text{ hp}$$

The power loss in the annulus between the slinger tip and the cylindrical wall was obtained by treating this flow as flow in a two dimensional duct with no side wall friction. The mean velocity in the flow was taken as one-half the slinger peripheral velocity and the shear stress on the slinger tip as

$$\tau_o = \frac{f}{4} \frac{\rho}{2} \left(\frac{\omega a}{2}\right)^2 \qquad (1)$$

A Reynolds number based on a hydraulic diameter was used to determine f, that is

$$R_p = \frac{4VR}{v} = \frac{\omega ac}{v} \qquad (2)$$

where $V = \frac{\omega a}{2}$ $\quad R = \frac{c}{2}$

For this design, $c = .010$ inches and $R_p = 2140$.

From a smooth-pipe Moody diagram for $R_p = 2140$

$$f = .035$$

The moment coefficient is then

$$C_m' = \frac{f\Pi b}{8a} = 2.1 \times 10^{-3} \qquad (3)$$

and the moment is

$$M' = C_m' \rho \omega^2 a^5 = 1.32 \text{ in-lb.}$$

and the power consumed

$$p' = .24 \text{ hp}$$

The power lost in the bearing is from Appendix C.

$$P_{Brg} = .12 \text{ hp}$$

The total power loss is tabulated below.

Table 2

Power Loss Tabulation per Bearing
End, Plane Slinger with Screw Return

Source	Power Loss
Sides of 4 slingers	.76 hp
Tip of 2 slingers	.48 hp
One bearing	.12 hp
	1.36 hp = 1.01 kw

C-4. Design of Screw Return

The purpose of the screw return is to stop the drops of fluid coming from the interface due to interfacial instability and return them to the interface. As the screw will not normally run flooded, a simple 2 inch - 8 threads/inch std 60° thread form was used. The threads were finished on the inside diameter to attain the required running clearance.

More recent experience has shown that even though the screw return does not normally run flooded, a rectangular thread-form patterned

after the screw threads described in Appendix B is more efficient. On the seals for the prototype alternator, a rectangular thread form will be used.

C-5. Design of Inlet Oil Jets

Oil jet lubrication was selected as the means of lubricating the SNAP-8 alternator bearings. The recommended method of applying the oil is to play three or more jets of oil on the inner ring of the bearing opposite the load angle direction. To simplify assembly a DF mount was used on the test rig which meant the jet ring must be located outboard of the bearings.

In order to use film cooling to remove the pole face losses in the alternator, it is also necessary to spray directly on the slinger. Since the power loss in the slingers are the largest, it is best to have equal distribution of oil between the inboard and outboard slingers. Assuming that not all the oil sprayed on the bearing passes through the bearing, the following division of oil was made.

Table 3

Oil Jet Ring Design

Location	Number of Holes	Hole Diameter	Oil Flow	Pressure Drop	Approx. Jet Veloc.
Outboard	2	0.025	0.020	33 psi	800 in/sec.
Inboard	4	0.020	0.030	33 psi	800 in/sec.

Figures 8 and 9 are calibration curves for the jet rings used in the test rig.

C-6. Design of Discharge Passage

The flow in the chamber enclosing a slinger moves radially outward over the rotating slinger. For this reason the discharge path was designed to be opposite the periphery of the slinger at operating temperature. Although the slinger axial clearance was only 0.025 in., two 0.070 mil slots, 0.62 inches long, at 180° were used. This was done to permit axial growth of the rotor with respect to the casing and still have the slinger tip beneath the discharge opening. The maximum flow per slinger is 0.030 lb/sec or 0.75 in^3/sec. The slot discharge velocity is

$$V_{dis} = \frac{Q}{A} = 8.65 \text{ in/sec}$$

a low value.

D. Design of Housing-Disk Seal

The housing-disk seal design, Figure 2, is similar to that of the plane slinger. The same disk diameter, and (s/a) ratio were used so the K value remains the same. Because Re and s/a are the same, the power loss on the sides of the slinger will remain the same. The loss over the tip will increase, however, because of the larger slinger width, b = .33 inches. The larger tip moment coefficient will be

$$C_m' = \frac{f\Pi b}{8a} = 3.02 \times 10^{-3} \qquad (3)$$

and the power lost is

$$P = .344 \text{ hp.}$$

The total power loss per bearing end is tabulated below.

Table 4

Housing-Disk Seal Power Loss Tabulation
Per Bearing End

Source	Power Loss
Sides of 4 slingers	.76 hp
Tip of 2 slingers	.70 hp
One bearing.	.12 hp
	1.58 hp = 1.18 kw

E. Design of the Screw Seal

E-1. Selection of Dimensions

The seal geometry used in the design was based on that of Reference 18, which has been optimized for maximum sealing capability in laminar flow. This was chosen because both pressure and drag data were available for this design. The geometry is presented in Table 5 on the following page:

Table 5

Screw Seal Geometry

Parameter	Value
δ/h	0.32
h/w	0.082
$w/(w + w')$	.62
ϕ, helix angle	14.5°
h, clearance	.0032 inches
Inboard diameter	2.08 inches
Outboard diameter	1.89 inches

The final seal configuration is shown in Figure 3.

E-2. Sealing Capability

The screw seal Reynolds number for a mean diameter of 2 inches, and a shaft speed of 12,000 rpm is

$$Re = \frac{U\delta}{\nu} = 457$$

From Reference 17, it shows that for the chosen geometry the sealing coefficient can be expressed by

$$\frac{\Delta p \delta^2}{\mu UL} = .313 \times 4.3 \times 10^{-4} Re^{1.044} \qquad \text{(B3)}$$

which for this Reynolds number is

$$\frac{\Delta p \delta^2}{\mu UL} = .57$$

For ET-378 oil at 210°F, the absolute viscosity is 98.7×10^{-8} lb sec/in^2 and the sealed pressure from Table 1 is 33 psia. The length of seal required is

$$L = .47 \text{ inches}$$

E-3. Power Loss

The power consumption is obtained from the moment coefficient. Since Re_δ is less than the critical value of 1000, the power loss is given by the laminar flow moment coefficient

$$\lambda = \frac{4\,\Pi}{Re_\delta} = .0274 \qquad \text{(B4)}$$

The moment on the shaft for wetted length of .47 inches is

$$M = \lambda \frac{\rho\omega^2\gamma^4 L}{2g_o} = 1.07 \text{ in-lb.} \qquad \text{(B6)}$$

and the power is

$$P = M\,\omega = .22 \text{ hp.}$$

The power loss in the bearing is .12 hp for jet lubricated operation. For this case the bearing operates flooded and based on the work of Reference 14, the bearing power is increased by a factor of three. A tabulation of power loss for the screw seal system is given in Table 6.

Table 6

Screw Seal System Power Loss Tabulation
Per Bearing End

Source	Power Loss
2 Screw seals	.44 hp
Flooded bearing	.36 hp
	.80 hp = .60 kw

It is noted that system power loss for this design is lower than either the plane slinger with screw return or the housing-disk.

III. Description of Test Rig

A. Introduction

A test rig was designed and built for the purpose of conducting performance tests on the dynamic sealing elements for the SNAP-8 Alternator. The facility was designed to simulate as closely as possible the operating conditions which will exist in a production alternator.

Two important conditions, namely the weightlessness associated with a zero-gravity environment and the rotor magnetic pull forces arising from rotor eccentricity in the magnetic field between rotor and stator, were not duplicated.

A vapor-liquid interface exists in all three types of dynamic seals tested. It is known that surface tension phenomena can affect these types of seals in which such an interface exists even in a gravity environment. Therefore, it is suspected that such effects may be amplified in a zero-gravity environment, and the question remains as to whether leakage rates measured in the laboratory on earth can be extrapolated to predict leakage rates in space operation. The answer to this question lies in a better understanding of zero-gravity hydrodynamics, and our lack of understanding of this field should temper the use of seal leakage data obtained in the laboratory for predicting seal leakage in space operation.

The fact that the magnetic pull forces were not duplicated had little effect on seal operation. Since this force constitutes a major part of the total bearing load, it did have some effect on bearing operation. However, as the object of the program was to test seals and not bearings, the lack of simulation of this force had little influence on the test program.

B. Description

The test rig consists of the following major assemblies mounted on a slotted base plate

i. Rotor and Casing Assembly

ii. Thymotrol Drive Assembly

iii. Lube System Assembly

Figure 4 is a drawing of the Rotor and Casing Assembly and Figure 5 is a photograph of the entire test rig with drive and lube system.

1. Rotor and Casing Assembly

This assembly is intended to simulate the actual alternator environmental conditions as closely as possible with reasonable expenditure of time and effort. The rotor is mounted on two 208 type bearings with approximately the same bearing span as the alternator. The rotor and end shields were designed such that by the use of suitable shaft sleeves a variety of seal designs could be tested.

To reduce cost, the test rig rotor was made cylindrical without the slots which are machined in the actual alternator rotor. As a result the test rig rotor weighed 90 lbs. versus 70 lbs. in the actual alternator.

The outer casing is equipped with an outer shroud through which heated oil flows. This shroud simulates the stator cooling passages used to cool the actual alternator.

Two 250 watt calrod heating elements are provided to supply heat input to the rotor. This heat source is designed to give a temperature distribution in the rotor representative of that existing in the actual alternator. The outer diameter of the rotor was coated with a black oxide finish to increase the radiant heat transfer from the heating elements to the rotor.

A plastic viewing port was placed on the ADE end shield to provide observation of the ADE OB seal. A conventional face seal (Sealol Dwg. 8 33064) was used to seal around the DE shaft. Two face seals were mounted back to back with oil a few psi above ambient introduced between them. The oil leakage path was either through the ADE face seal to the evacuated chamber outboard of DE seal or through the DE face seal to ambient.

Four holes were drilled and tapped in the bottom of the casing to provide connections for the four traps which were used to collect leakage from each of the seals. Trap Number 4 on the ADE OB seal also collected leakage from the Sealol face seal. Except in the initial tests the face seal leakage was small and this additional leakage was negligible.

Figure 4. Drawing of Rotor and Casing Assembly

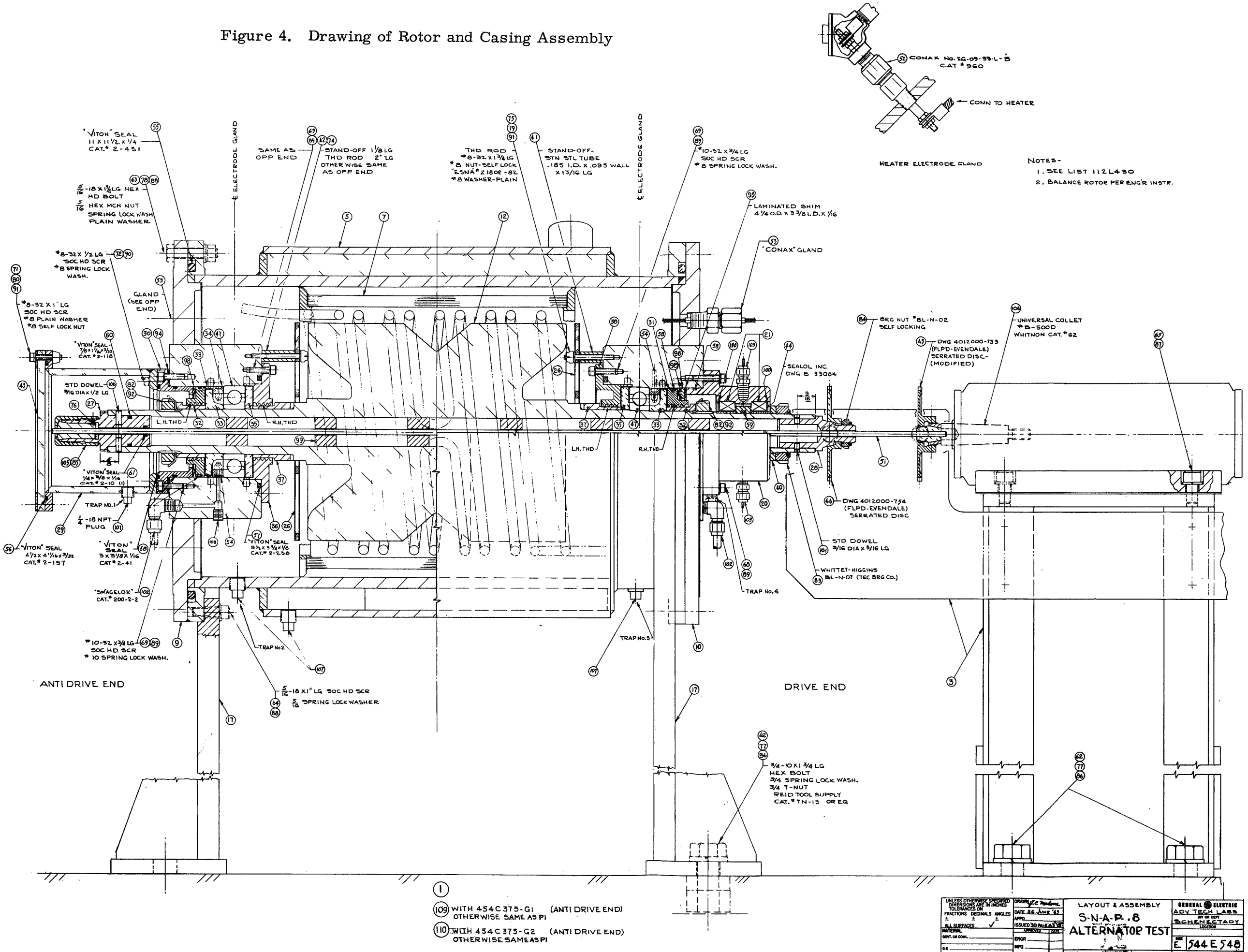

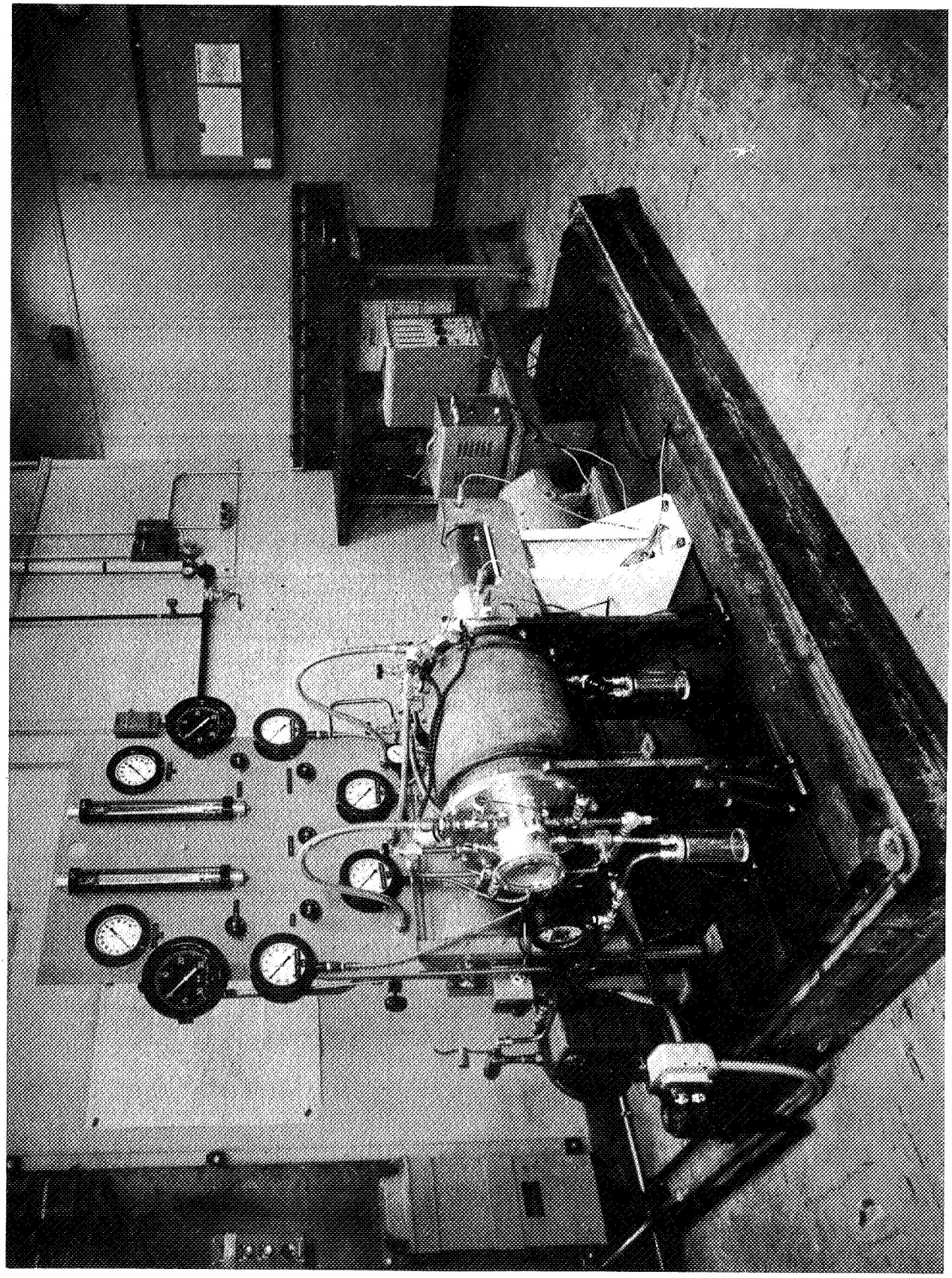

Figure 5. Photograph of Test Rig

Vacuum conditions were maintained in the system with mechanical oil-sealed rotary pumps. The sump pressure was maintained at approximately 5 psia with a Welch Model 1405 Pump (33.4 liters/min. at 10^{-3} mm Hg) and the stator cavity at about 29 inches Hg vacuum with a Welch Model 1402B (76 liters/min. at 1 mm Hg). Although the quoted catalog capacity is lower, the practical pressure limit on this type of pump is 10^{-2} mm Hg. Although careful leak checks were made on the system, the lowest vacuum that could be maintained in the system was about 29 inches Hg.

Wave springs were used to preload the bearings and also to center the rotor. As no dynamic axial clearance measurements were made, it cannot be certain that the rotor actually centered itself. However, there was only one rub during the test program indicating a relatively well centered rotor. The rotor was not perfectly centered, however. Unsymmetrical leakage rate data indicated slight shifting of the rotor.

2. Thymatrol Drive Assembly

The test rig was driven with a 3500 rpm 7-1/2 HP DC motor with "High Performance Thymatrol" speed control. The motor drove the test rig through a pulley, belt, and spindle to give a maximum shaft speed of 13,200 rpm. The unit is equipped with dynamic breaking as a standard feature and provides constant torque throughout the speed range. Speed control was excellent from 1000 rpm up to 13,200 rpm.

The rotor was driven through a flexible quill shaft. This particular method was chosen because it is similar to the alternator drive mechanism and the twist in the quill shaft is a measure of torque input. The quill was connected to the rotor and spindle with universal collets.

3. Lube System Assembly

A schematic drawing of the lubrication system is shown in Figure 6. The oil sump is a 7 gallon tank. A 2 KW oil heater with automatic temperature control is mounted directly in the tank.

The oil is circulated with a 3 GPM gear pump. (Sundstrand Model BPD-052-200). Suction pressures as low as 3 psia were attainable without pump cavitation.

A heat exchanger (Heat - X Model W10-316) was connected to the discharge of the pump and served to remove heat from the oil and as further regulation of bearing oil inlet temperature. A 10 micron glass element filter was used in the line.

An adjustment was provided to vary the oil sump elevation with respect to the bearing centerline. In addition, the entire system was constructed as a single unit and could be moved as required to any location on the base plate.

C. Instrumentation

Sufficient instrumentation was supplied in the test system, to adequately evaluate seal operation. Instrumentation on the Lube System Assembly is indicated in Figure 6, and on the Rotor and Casing Assembly in Figure 7.

1. Flow Measurement

The flow to each bearing was measured with a rotameter and regulated with a needle valve. The amount of oil in the sump was indicated by a glass face oil level gauge.

2. Pressure Measurement

The bearing inlet oil pressure was measured with a 0 to 60 psig Bourden tube gauge with an accuracy of 1/2% of full scale. All other pressures, bearing cavity, oil sump, bearing oil discharge pressure, and casing cavity were indicated with -30 to + 30 psi compound pressure gauges of 1/2% of full scale accuracy.

The pressure tap in the bearing cavity was a .0625 inch hole in the outer diameter at the top of the cavity. In later production units, pressure taps were placed at the top and bottom of the bearing cavities, and little difference was noted between the pressures indicated from either location.

3. Temperature Measurements

Bearing temperatures were taken with spring loaded temperature probes held directly against the outer race. Three probes were spaced equally around the outer race of each bearing. Oil inlet temperature at both oil jet rings and oil discharge temperature from each slinger were also

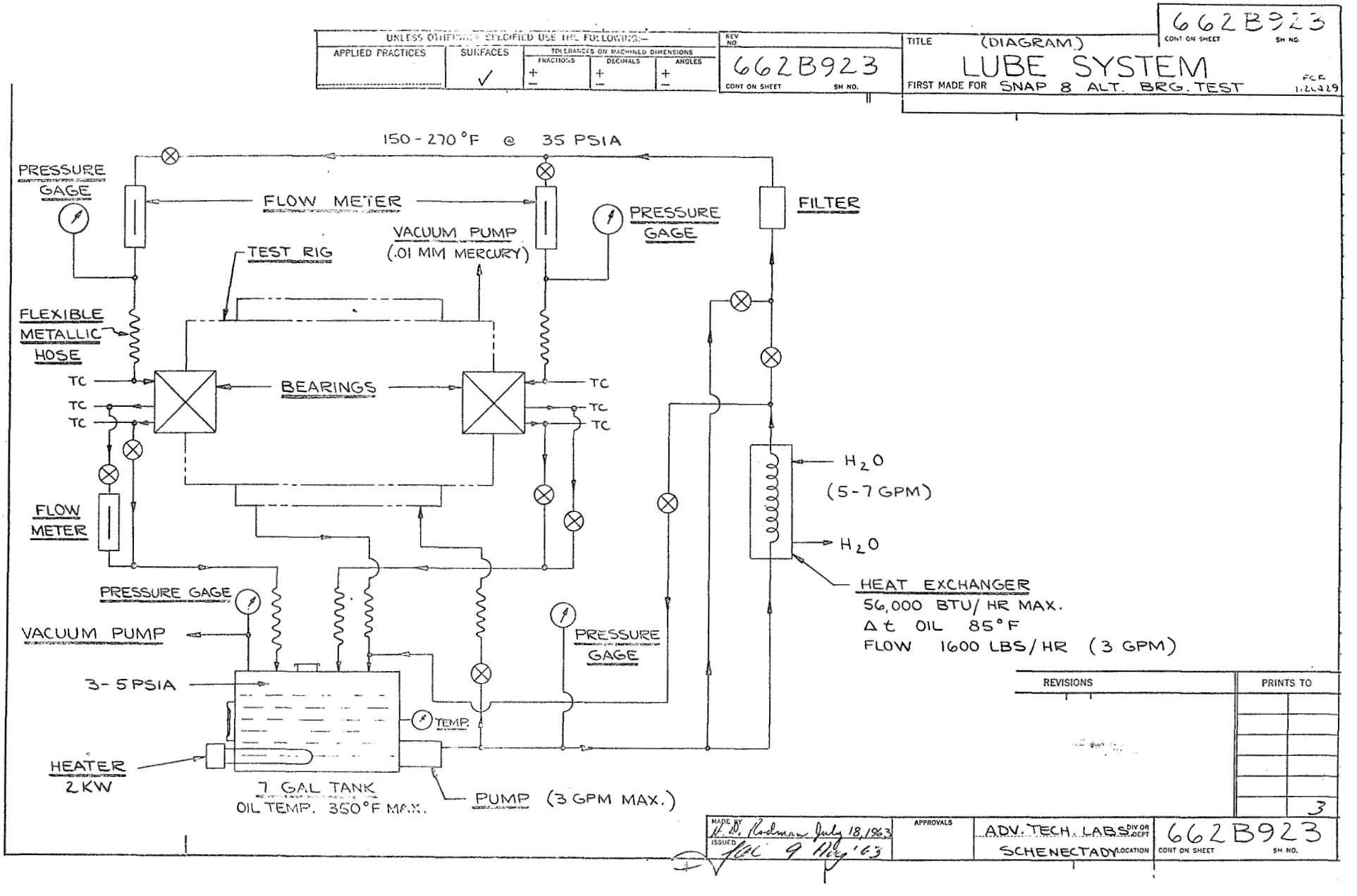

Figure 6. Lubrication System Schematic

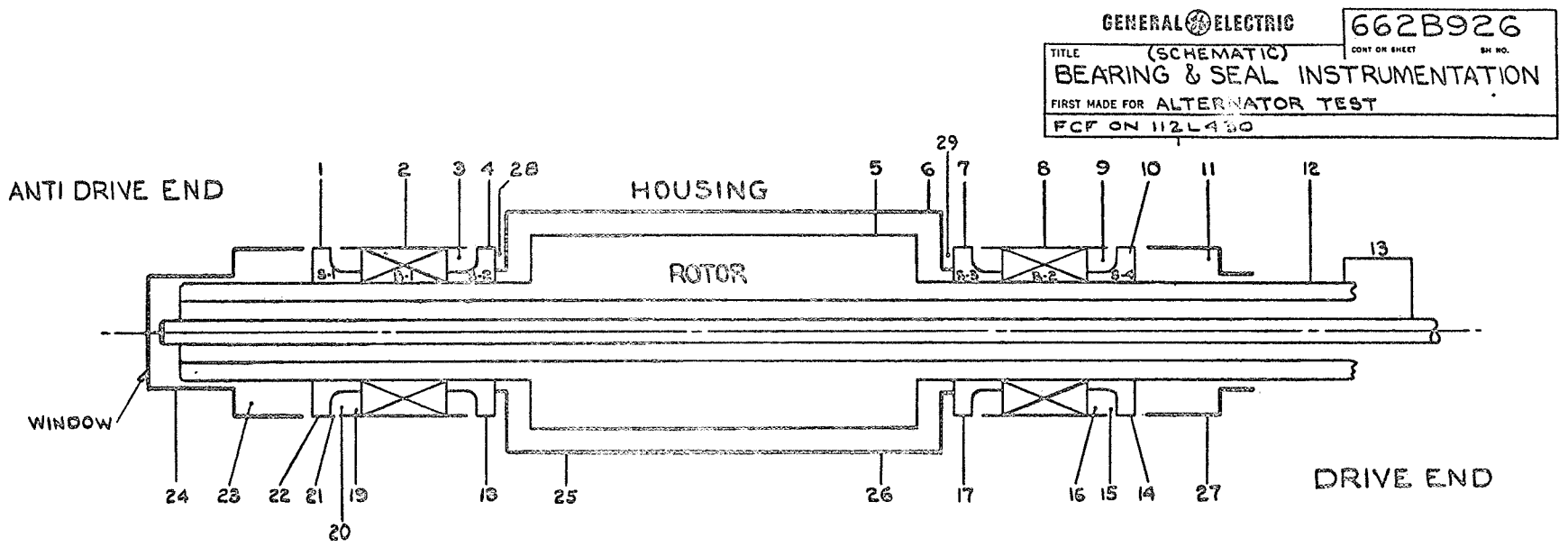

1. OUTLET PRESSURE SLINGER S-1
2. BEARING OUTER RACE TEMP B-1 BRG (3)
3. CAVITY PRESSURE B-1 BRG.
4. OUTLET PRESSURE SLINGER S-2.
5. ROTOR TEMPERATURE (TEMP. SEN. PAPER)
6. CASING PRESSURE
7. OUTLET PRESSURE SLINGER S-3.
8. BEARING OUTER RACE TEMP B-2 BRG (3)
9. CAVITY PRESSURE B-2 BRG.
10. OUTLET PRESSURE SLINGER S-4.
11. END PRESSURE B-2.
12. SHAFT SPEED
13. TORQUE
14. OUTLET LUBE TEMP SLINGER S-4.
15. INLET FLOW BRG. B-2.
16. INLET LUBE TEMP. BRG. B-2.
17. OUTLET TEMPERATURE SLINGER S-3.
18. OUTLET TEMPERATURE SLINGER S-2.
19. CAVITY PRESSURE B-1 BRG.
20. INLET FLOW BRG. B-1.
21. INLET LUBE TEMP. BRG. B-1.
22. OUTLET TEMPERATURE SLINGER S-1.
23. END PRESSURE B-1.
24. TRAP NO. 1
25. TRAP NO. 2
26. TRAP NO. 3
27. TRAP NO. 4
28. INBOARD SEAL TEMP (2)
29. INBOARD SEAL TEMP (2)

Figure 7. Instrumentation Schematic

indicated with thermocouples placed directly in the oil lines. The wall temperature on the inboard side of the inboard slingers were read out from thermocouples embedded in the stationary slinger wall to within .030 inches of the surface. A thermocouple was also clamped to both casing heating elements. All thermocouples used were copper-constantan and their output was recorded on a Leeds and Northrup temperature recorder. A mercury in glass thermometer showed oil sump temperature.

4. Torque Measurement

The torque sensing system used measured the angular deflection of the drive quill shaft. This was done by sensing the phase shift between two gears, one attached to the rotor and the other attached to the spindle as shown in Figure 4. Eighteen teeth were machined in each gear allowing a total deflection of 20° between teeth. The quill shaft was sized at 1/4 inch which gave a reasonable deflection without exceeding the allowable shear stress for the quill material.

A magnetic pickup placed in close proximity to each gear generated 18 pulses per shaft revolution. Special electronic circuitry was built to give the phase shift between the signals from each gear. The phase shift in turn was calibrated in terms of quill twist.

5. Speed Measurement

The signals generated by a magnetic pickup which sensed three pins on the spindle pulley were counted on a Berkeley counter to indicate shaft speed.

6. Leakage Measurement

The leakage from each seal was collected in the traps shown in Figure 5. Since the temperature of these containers was at essentially room temperature, a lower temperature than the 210° F minimum temperature in the test rig, these containers acted as cold traps.

Although a cold trap at lower temperature would have had a greater pumping efficiency, calculations showed that any additional lubricant vapor loss from the system would be negligible compared to measured leakage rates.

The traps are made of 6.25 cm diameter plastic tube with a capacity of 3.07 cc per mm of tube height. The smallest unit of height measurement discernible was 0.25 mm. This gave a system sensitivity of 0.766 cc, and to detect the desired leak rate of 0.025 cc/hr required a test run of 30 hours. The system sensitivity could have been improved by using a smaller diameter tube, but since it took approximately 6 hours just to reach a stable operating condition, and longer running times were desirable from a systems standpoint, it was found that the traps were adequate.

IV. Test Procedure

A. Calibration Tests

Prior to the actual test runs the necessary calibrations were completed on the instrumentation system. The oil jet orifices were first calibrated using ET 378 oil at 210°F. These curves are shown in Figures 8 and 9. A slightly higher pressure than design was required to attain the required 3 lb/min flow.

The torque measurement system was also calibrated. The shaft was run with a preset displacement between the gear teeth. Meter reading versus angular displacement is given in Figure 10. The amount of torque required to produce a given twist in the quill shaft is shown in Figure 11. The curves are almost linear and reproducibility was good.

The rotameters were also calibrated using hot oil. Some variation in oil flow with temperature was noted and this was accounted for in the data.

B. Normal test procedure was as follows:

1. The oil heaters were turned on and the oil preheated.
2. The vacuum system was turned on and the system evacuated.
3. Once the desired oil sump temperature and vacuum were attained, the drive was turned over slowly.
4. Hot oil was admitted to the bearings and the speed was increased to design.
5. The necessary adjustments were made to attain the nominal operating conditions of Table 7.
6. Once nominal test conditions were reached, data were recorded every half hour.

METERING ORIFICES DRIVE END

PRESSURE DROP versus OIL FLOW

ALL HOLES

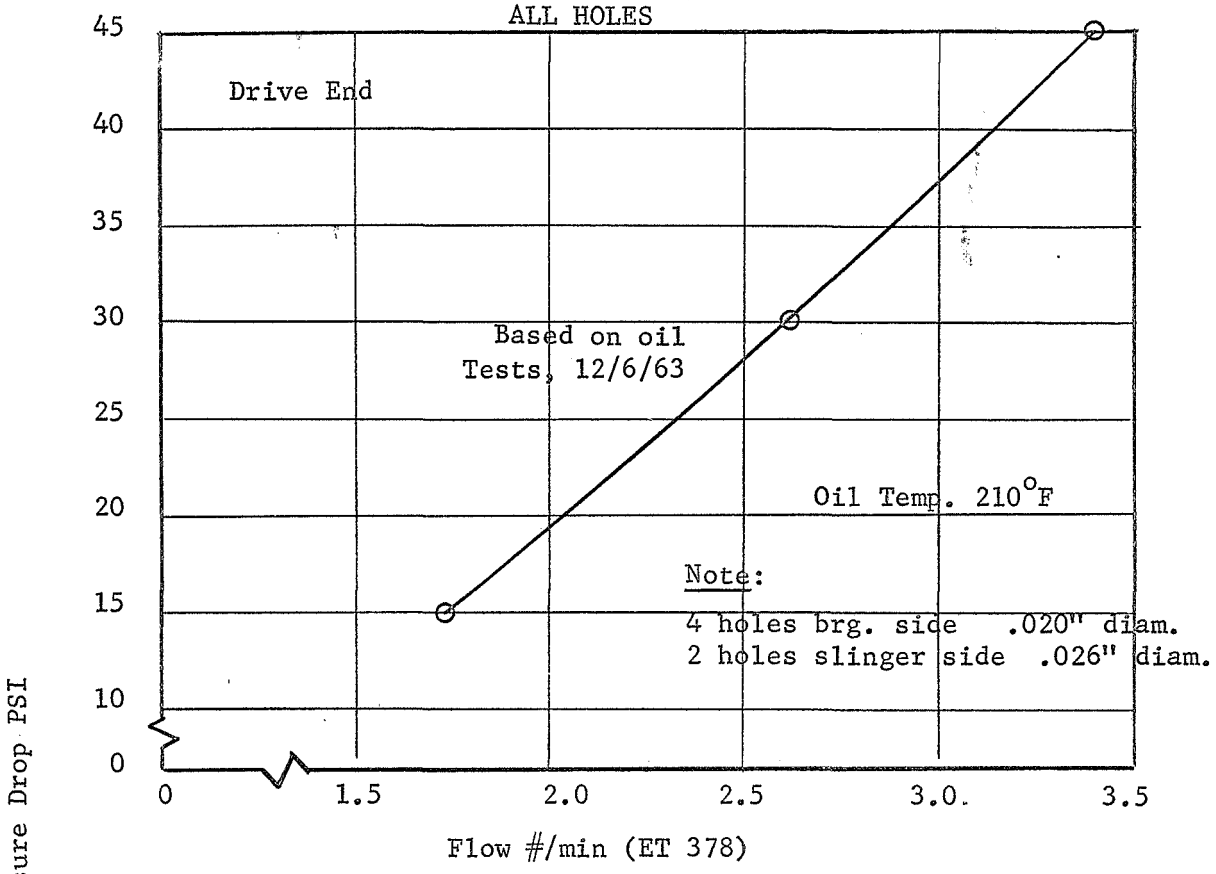

Figure 8

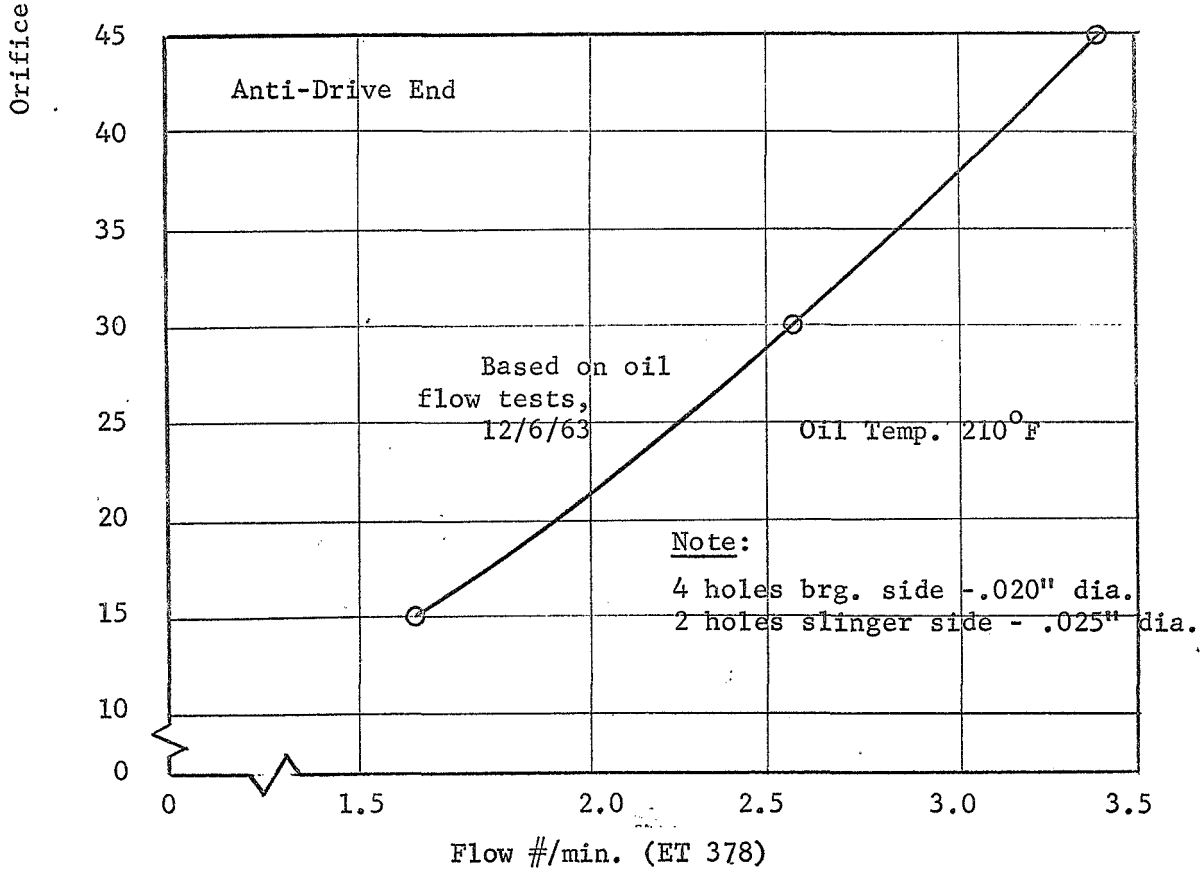

Figure 9

TORQUE DEFLECTION CURVE

Quill No. 5

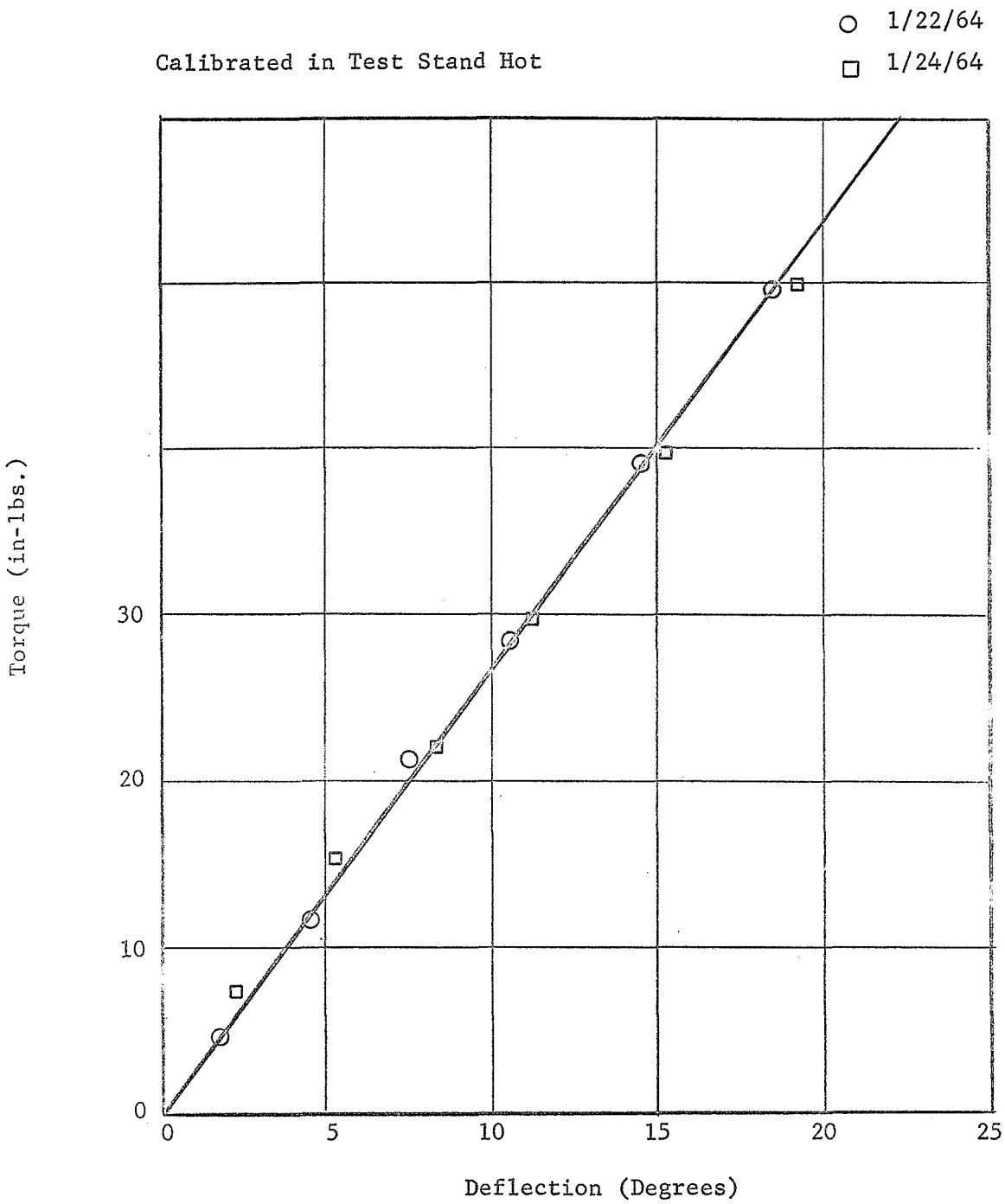

Figure 10

TORQUE METER

CALIBRATION

SNAP-8 1/8/64

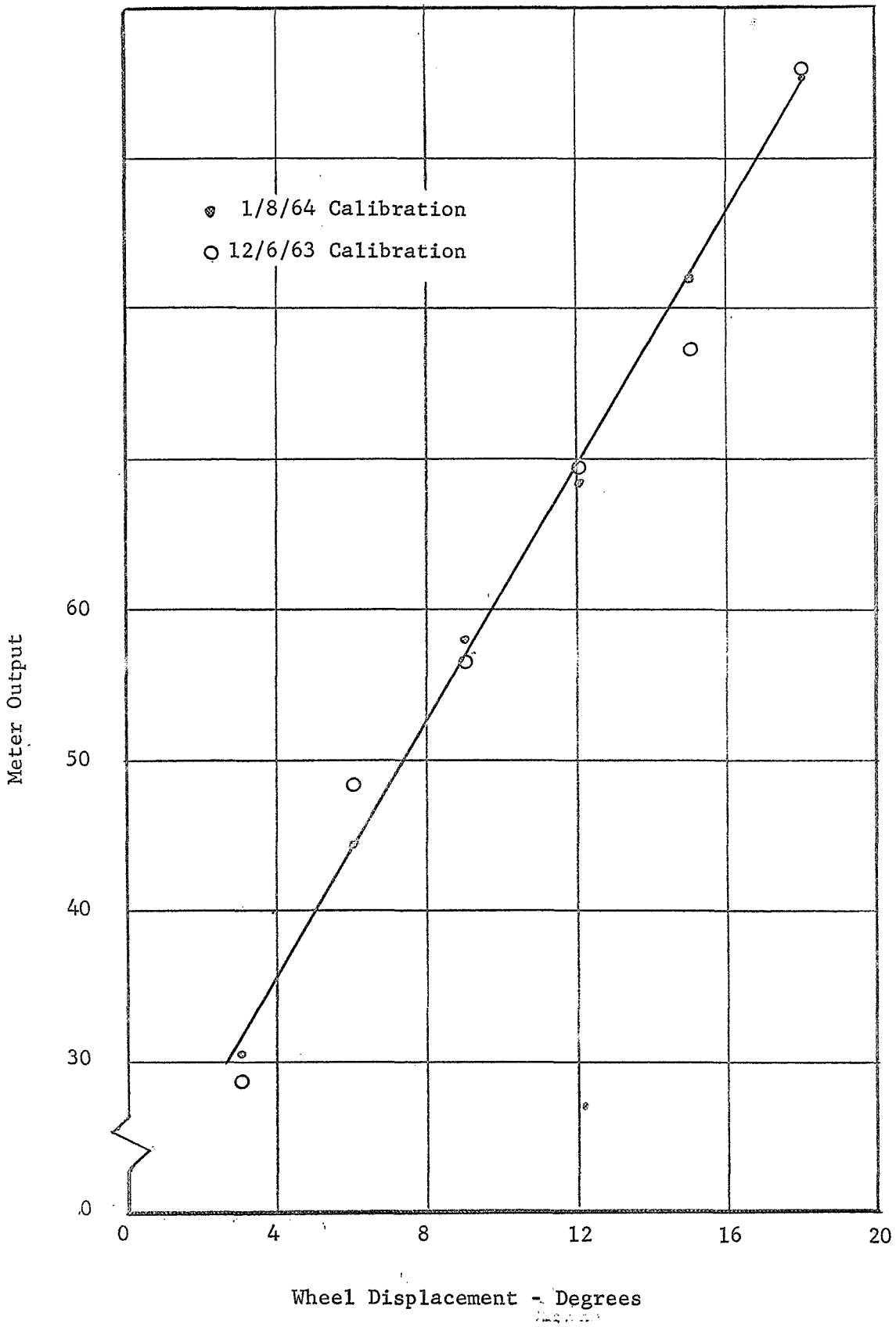

Figure 11

IV.

V. Test Results

The object of the test program was to determine the sealing, drag, flow and pumping characteristics of each of the proposed seal systems. With this information it is possible to select the seal configuration most appropriate for application in the preprototype alternators. Only a summary of the test results is presented here. More detailed information is included in the SNAP-8 Monthly Progress Reports, Reference 19. Unless otherwise stated, all of the tests were conducted under the following nominal operating conditions.

Table 7

Nominal Test Operating Conditions

Sump Pressure	5 psia
Oil Inlet Temperature	210°F
Slinger Pressure Rise	7.5 psi
Oil Flow	180 lbs./hr (per brg.)
Speed	12,000 rpm
Overspeed/Underspeed	13,200/11,800
Rotor Heat Input	300 watts max.

A. Plane Slinger With Screw Return

A series of tests (each of which was assigned a test number) were run on this seal configuration. Many of these were designed to check out the test system or calibrate instrumentation and as such are not described here.

A-1. Test No.4 - Long Term Leakage Test

Test No. 4 was a 35-hour continuous test run to determine seal leakage rates. The "as built" dimensions appear in Figure 12. The dimensions for this test run are given in the column labeled ASM#2.

Figure 13 is a summary of the flow and pressure measurements

IV

VI

NOTES -

1. THESE CLEARANCES ARE ACTUAL AND INCLUDE THE .005 AXIAL OFFSET IN THE BARDEN #208 BX1 BEARINGS AS RECEIVED.
2. INCREASE CLEARANCE DUE TO MACHINING REQUIRED TO RELIEVE RUBBING BETWEEN P36 & 35 ON ANTI DRIVE END DURING INITIAL TEST.
3. P No's IN TABLES REFER TO ASM DWG 544E548.
4. WITH BARDEN #208 BX5 BRGS + SUITABLE SHIMS TO MATCH THICKNESS OF #208 BX1 BRG.

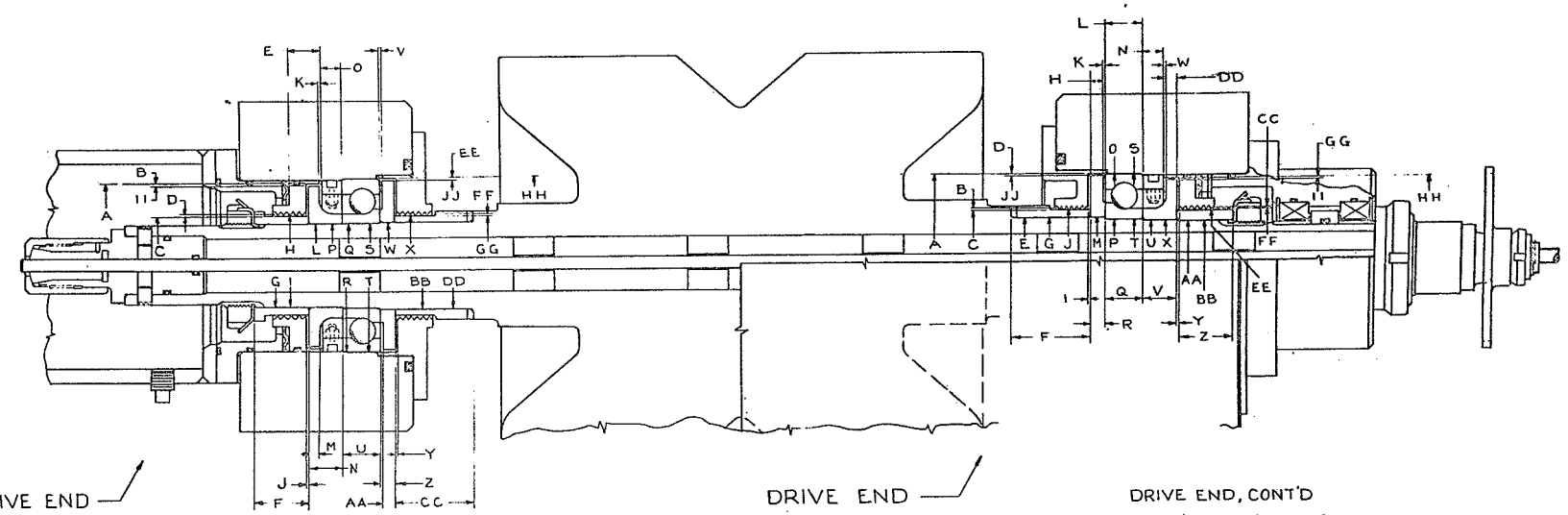

ANTI DRIVE END

DIM	ASM#1	ASM#2	ASM#3
A (P39)	3.0020	SAME AS ASM#1	
B	0.0105		
C (P32)	1.8460		
D	0.0030		
E —			
F —			
G —			
H (P39)	1.8520		
I —			
J	*0.0170		0.022Δ
K	*0.0265		0.0215
L —			
M (P33)	0.2275		
N (P33)	0.6250		
O (P34)	0.3760		
P —			
Q (P12)	1.5743		
R (P9)	3.1500		
S (P47)	1.5745		
T (P47)	3.1497		
U —			
V	*0.0170		0.022
W —			
X (P36)	1.844		
Y	*0.0230	0.0245	
Z —	0.2730		

ANTI DRIVE END, CONT'D

DIM	ASM#1	ASM#2	ASM#3
AA (P35)	0.2435	0.2405	
BB —			
CC —			
DD —			
EE	0.0095		
FF	0.0040		
GG (P37)	1.8360		
HH (P36)	3.1500		
II (P35)	2.9810		
JJ (P35)	3.1310		

*- SEE NOTE 1
☆- SEE NOTE 2
Δ- SEE NOTE 4

DRIVE END

DIM	ASM#1	ASM#2	ASM#3
A (P38)	3.1500	SAME AS ASM#1	
B	0.0040		
C (P38)	1.8430		
D	0.0095		
E —			
F —			
G —			
H	0.2435		
I	*0.0230	0.00245	
J (P37)	1.8350		
K	*0.0170		0.022
L —			
M —			
N (P34)	0.3767		
O (P10)	3.1502		
P (P12)	1.5744		
Q —			
R	0.2730		
S (P47)	3.1497		
T (P47)	1.5746		
U —			
V (P33)	0.6245		
W	*0.0265		0.0215
X —			
Y	*0.0170		0.022
Z —			

DRIVE END, CONT'D

DIM	ASM#1	ASM#2	ASM#3
AA	—		
BB	—		
CC	0.0030		
DD (P33)	0.2275		
EE (P31)	1.8420		
FF (P32)	1.8360		
GG	0.0105		
HH (P31)	3.0020		
II (P34)	2.9810		
JJ (P35)	3.1310		

NOTE 3

UNLESS OTHERWISE SPECIFIED DIMENSIONS ARE IN INCHES
TOLERANCES ON
2-PLACE DECIMALS ±
3-PLACE DECIMALS ±
ANGLES ±
ALL SURFACES ✓
MATERIAL -
GOVT OR COML

SIGNATURES | DATE
C. Malone 12 Nov 63
J. Malone 14 Nov 63
15 Nov 63

FCF ON 112L430
GENERAL ELECTRIC
ADV. TECH. LABS. DEPT LOC SCHENECTADY
TITLE
ROTOR ASSEMBLY
AS BUILT DIMENSIONS
F. F. ON: PL-112L430
CODE IDENT NO. | SIZE D | DWG NO. 421D692

Figure 12. "As Built" Drawing Plane Slinger with Screw Return

during the test. The anti-drive end cavity pressure could be scavenged to 25.9 inches of Hg Vac. and the drive end to 26.2 inches of Hg Vac. with a 7.5 psi slinger pressure rise. By reducing the slinger pressure rise to about 5 psi, lower cavity pressures were reached, 26.9 inches Hg Vac. on the ADE and 27.8 inches Hg Vac. on the DE.

Although the generator cavity line pressure shows a 30+ in Hg Vac. in Figure 13, the actual bearing cavity pressure prior to startup was 28 in Hg Vac. Thus, the slingers were adequately scavenging the bearing cavities.

The oil inlet pressure required to give a flow of 180 lb./hr. (3 lb./min) was much lower than the orifice calibration curves in Figures 8 and 9 would indicate. The calibration curves show about a 1.7 lb./min. flow at a 15 psi pressure drop while during test #4, 3 lb./min. were passed for this same pressure drop. Measurement of the jet ring and end shield housing showed an excessive clearance between these parts. Calculation and actual flow tests in the end shield verified that this excessive clearance plus a differential expansion at temperature accounts for the larger than expected flow per unit pressure drop observed. This means that although the total flow to each end shield was 3 lb. per min., only 1.7 lb. per min. actually passed through oil inlet jets to the bearing and slingers. The remaining flow leaked from the oil inlet ring to the discharge ring and bypassed the bearing cavity.

Thus all of the data taken on this test run are extremely conservative, in that actual flow to the bearings was below design. To gain some appreciation of what effect this has on bearing-seal temperature levels, reference can be made to Figures 17 and 18, which are plots of bearing-seal temperature versus total flow to the end shields. Reference to Figure 5 shows that a total flow of 472 lbs./hr. (.85 gpm) the oil inlet pressure was 25.3 psig or an approximate pressure drop across the oil jet of 38 psi. From Figures 8 and 9 this is the approximate pressure drop required to give an oil flow of 180 lb./hr through the jet ring. The test condition with a total

SNAP 8 Seal Test
Plain Slinger with Screw Return

Test No. 4
Barometer 1:00 PM - 29.51 In. Hg. 11/11/63
Amb. Temp. - 77°F

	Time	Sump Press in Hg Vac	Sump Temp °F	ADE Inlet Pressure Psig.	ADE Cavity Press. " Hg. Vac.	ADE Otbd. Slinger Press. "Hg. Vac.	ADE Inbd. Slinger Press. "Hg. Vac.	ADE Flow GPM	DE Inlet Press Psig	DE Cavity Press in Hg Vac.	DE Otbd. Slinger Press. " Hg. Vac.	DE Inbd. Slinger Press. "Hg. Vac.	DE Flow GPM	Gen. Cavity Line "Hg. Vac.	Pump Dischg. Psig.	Seal Press. Psig.	N rpm
	9:45	20	185	0	28.4	28.4	27.8	0	0	28.5	28.0	27.9	0	30+	18	2.5	0
	10:00	20.1	185	11.1	24.9	13.0	10.6	.29	9.0	26.0	10.0	11.0	.33	30+	35	1.6	12,220
A.M.	10:30	20.1	212	6.4	25.0	10.0	9.0	0	5.3	26.5	9.0	11.0		30+	30	2.05	12,160
	11:00	20.1	220	2.9	26.0	11.0	9.9	.31	2.0	26.0	10.0	10.2	.31	30+	24.5	1.7	12,020
	11:30	20.2	223	2.6	26.0	11.0	10.0	.31	1.9	26.5	10.0	10.2	.31	30+	24.5	2.15	12,020
	12:00	20.3	225	2.5	26.0	10.9	10.1	.31	1.8	26.5	9.9	10.1	.31	30+	24.3	2.1	12,040
	12:30	20.2	225	2.4	25.8	10.9	10.1	.31	1.6	26.4	9.9	10.1	.31	30+	24.3	2.1	12,020
	1:00	20.2	225	2.5	25.8	10.8	9.9	.31	1.6	26.3	9.9	10.1	.31	30+	24.3	2.1	12,000
	1:30	20.2	203	2.9	25.3	10.5	10.0	.30	2.0	26	10.0	10.2	.30	30+	25.9	2.0	11,960
	2:00	20.2	220	2.5	26.5	10.5	9.9	.31	1.9	26.5	9.9	10.0	.31	30+	24.5	2.1	11,980
	2:30	20.2	225	2.2	25.8	10.5	9.9	.31	1.7	26.5	9.9	10.0	.31	30+	24.2	2.12	11,980
	3:00	20.2	227	2.2	26.5	10.5	9.9	.31	1.6	26.5	9.9	10.0	.32	30+	24.2	2.15	11,960
	3:30	20.2	228	2.1	25.9	10.5	9.9	.32	1.6	26.5	9.9	10.0	.32	30+	24.1	2.18	12,000
	4:00	20.2	228	2.1	25.8	10.5	9.9	.32	1.6	26.5	9.9	10.0	.32	30+	24.1	2.18	11,980
	4:30	20.2	228	2.1	26.0	10.5	9.9	.32	1.6	26.5	9.9	10.0	.32	30+	24.1	2.18	11,980
P.M.	5:00	20.2	228	2.1	26.0	10.5	9.9	.32	1.6	26.3	9.8	10.0	.32	30+	24.1	2.15	12,000
	5:30	20.1	228	2.1	26.0	10.5	9.8	.32	1.5	26.3	9.7	10.0	.32	30+	24.2	2.15	12,020
	6:00	20.1	228	2.1	26.0	10.5	9.8	.32	1.5	26.3	9.7	10.0	.32	30+	24.1	2.15	12,000
	6:30	20.1	228	2.1	26.0	10.5	9.8	.32	1.6	26.3	9.7	10.0	.32	30+	24.1	2.15	12,000
	7:00	20.1	228	2.1	26.0	10.6	9.8	.32	1.6	26.3	9.7	10.0	.32	30+	24.1	2.15	12,020
	7:30	20.1	228	2.1	25.9	10.5	9.8	.32	1.5	26.3	9.5	10.0	.32	30+	24.1	2.15	12,000
	8:00	20.1	228	2.1	25.8	10.5	9.8	.32	1.5	26.2	9.5	10.0	.32	30+	24.1	2.15	12,000
	8:30	20.1	228	2.1	25.9	10.5	9.9	.32	1.5	26.2	9.5	10.0	.32	30+	24.1	2.15	12,020
	9:00	20.1	228	2.1	25.9	10.5	9.8	.32	1.5	26.2	9.5	10.0	.32	30+	24.1	2.15	12,040
	9:30	20.1	225.4	2.1	25.8	10.5	9.8	.32	1.5	26.2	9.5	10.0	.32	30+	24.1	2.15	12,000

Figure 13a
Typical Flow and Pressure Measurements, Plane Slinger with Screw Return

SNAP 8 SEAL TEST (Con't.)
Plain Slinger with Screw Return

Test No. 4 Contd.

	Time	Sump Press in Hg Vac	Sump Temp °F	Inlet Press. Psig.	ADE Cavity Press. " Hi. Vac.	ADE Otbd. Slinger Press. "Hi. Vac.	ADE Inbd. Slinger Press. "Hi. Vac.	ADE Flow GPM	DE Inlet Press Psig.	DE Cavity Press in Hg Vac.	DE Otbd Slinger Press " Hg. Vac.	DE Inbd. Slinger Pres. "Hg. Vac.	DE Flow GPM	Gen. Cavity "Hg Vac.	Pump Dischge "Hg. Vac	Seal Press Psig	N rpm
	10:00	20.1	225	2.1	25.8	10.5	9.8	.32	1.5	26.2	9.5	10.0	.32	30+	24.2	2.15	12,000
P.M.	10:30	20.1	225.2	2.1	25.9	10.5	9.8	.32	1.5	26.2	9.5	10.0	.32	30+	24.2	2.15	12,020
	11:00	20.1	225.2	2.1	25.8	10.5	9.8	.32	1.5	26.2	9.5	10.0	.32	30+	24.2	2.15	12,020
	11:30	20.1	225.2	2.1	25.9	10.5	9.5	.32	1.5	26.3	9.5	10.0	.32	30+	24.2	2.15	12,020
	12:00	20.0	225	2.1	26.0	10.5	9.8	.31	1.5	26.3	9.5	10.0	.32	30+	24.0	2.15	12,060
	1:00	20.0	225	2.1	26.0	10.5	9.8	.31	1.5	26.5	9.5	10.0	.32	30+	24.1	2.25	12,040
	2:00	20.1	225	2.1	25.9	10.5	9.9	.31	1.5	26.4	9.5	10.0	.32	30+	24.1	2.25	12,060
	3:00	20.1	225	2.1	25.8	10.6	9.8	.32	1.5	26.2	9.6	10.0	.32	30+	24.1	2.25	12,060
	4:00	20.1	225	2.1	25.8	10.7	9.8	.32	1.5	26.4	9.5	10.0	.32	30+	24.1	2.25	12,020
	5:00	20.1	225	2.1	25.8	10.8	10	.32	1.5	26.4	9.5	10.0	.32	30+	24.1	2.25	12,020
															Barometer 8:00 A.M. - 29.48 in. Hg. Amb. Temp. - 75 °F 11/12/63		
	6:00	20	225	1.8	26.0	9.0	9.8	.31	1.4	26.8	9.8	10.1	.31	30+	24.2	2.2	12,020
	7:00	20.1	223	2.0	25.8	10.8	9.8	.32	1.4	26.5	9.8	10.0	.32	30+	24.2	2.2	12,000
	7:10			Lowered Slinger Discharge Press to 15 in., Torque Increased to 20.5 and pressures fluctuated													
	8:00	20.1	218	1.1	27.0	14.5	15.2	.32	1.2	27.6	14.0	14.6	.32	30+	24.2	2.15	12,000
	9:00	20.1	215	1.1	26.9	14.5	15.2	.32	1.2	27.5	14.0	14.5	.32	30+	24.2	2.15	12,000
	10:00	20.1	215	1.1	26.9	14.5	15.2	.32	1.2	27.2	14.2	14.5	.32	30+	24.2	2.15	11,960
	11:00	20.1	215	1.1	27.1	14.6	15.2	.32	1.2	27.5	14.1 ± 1.0	14.7 ±0.7	.32	30+	24.2	2.10	11,960
	12:00	20.1	218	1.1	27.0	14.5	15.2	.32	1.2	27.9	14.2	14.8	.33	30+	24.2	2.10	12,000
	1:00	20.1	220	1.1	27.1	14.6	15.2	.32	1.2	27.9	14.2	14.7	.33	30+	24.2	2.05	12,000
P.M.	2:00	20.1	218	1.1	27.1	14.6	15.2	.32	1.2	27.8	14.1	14.7	.33	30+	24.2	2.10	12,000
	3:00	20.1	218	1.1	26.9	14.5	15.2	.32	1.2	27.8	14.1 ± 1.0	14.7 ±1.0	.35	30+	24.2	2.10	12,000
	3:10			Increased Flow				.46					.47				
	3:30	20.1	210	6.8	27.1	15.2	15.8	.46	5.5	27.8	14.9	15.5	.47	30+	20.8	1.60	12,020

Figure 13b
Typical Flow and Pressure Measurements, Plane Slinger with Screw Return

SNAP 8 SEAL TEST (Con't.)
Plain Slinger with Screw Return

Time	Sump Press in Hg Vac	Sump Temp °F	ADE Inlet Pressure PSIG	ADE Cavity Press In Hg Vac	ADE Otbd Slinger Press In Hg Vac	ADE Inbd Slinger Press In Hg Vac	ADE Flow GPM	DE Inlet Press Psig	DE Cavity Press in Hg Vac	DE Otbd Slinger Press In Hg Vac	DE Inbd Slinger Press	DE Flow gpm In Hg Vac	Gen Cavity	Pump Dischge PSIG	Seal Press	N rpm
3:35			Increased Flow													
3:55	20.1	218	11.1	27.2	14.0	14.1	.56	9.5	28.0	13.3	13.6	.96	30+	25.8	1.90	12,000
4:10			Increased flow to .65 gpm													
5:00	20.2	207	15.9	27.5	15.0	15.0	.65	13.6	28.1	15.0	15.2	.65	30+	32.4	2.2	12,000
5:10			Increased Flow to .75 gpm													
5:30	20.2	198	20.8	27.5	15.0	15.0	.75	18.4	28.2	14.8	15.0	.75	30+	38.8	2.2	12,000
5:35			Increased flow to .85 gpm													
5:50	20.2	190	25.3	27.7	14.9	14.9	.85	23.9	28.5	13.8 (max)	14.9	.85	30+	46.0	2.1	12,000
5:55			Increased flow to 1.00 gpm													
6:15	20.2	188	34.5	27.7	13.8 (max)	15.1	1.00	32.2	28.5	12.0 (max)	15.0	1.00	30+	56.0	2.0	12,000
6:20			Reduced flow to .25 gpm							pulsing						
6:40	20.2	220	---	26.9	14.8	15.1	.25	----	27.5	15 ±1	15 ±1.5	.24	30+	24.0	2.1	12,040
6:50			Reduced flow to .20 gpm													
7:05	20.2	220	---	26.9	15.0	15.0	.20	----	27.7	15 ±1	15 ± 1.5	.20	30+	25.2	2.15	12,060
7:10			Reduced flow to .15 gpm - Increase because of over temp. (7:15)													
7:20			Set flow at .31 gpm Set slinger discharge to min. setting.													
7:30	20.2	215	---	27.4	18.7 ± .2 (min.)	19.9 (min.)	31.5	----	28.0	18.2 ± .2 (min)	20.0 (min.)	.31	30+	22.8	2.10	12,080
7:50	20.2	215	---	27.1	16.0	15.9	.31	----	27.7	16.0 ± 1	16.0 ± 1	.32	30+	22.8	2.10	12,040
8:05	20.2	220	1.7	26.3	11.9 max. 9.0	12.0	.32	----	26.9	11.9	11.9	.32	30+	22.4	2.00	12,000
8:20	20.2	223	2.5	25.1	10.0	8.1	.32	2.4	25.5	8.0 max 4.5	7.9	.32	30+	22.0	1.90	12,020
8:30	20.2	226	2.4	24.9	10.0	3.9	.32	2.9	25.1	6.2	3.9	.32	30+	22.0	1.90	12,000
8:45	20.2	228	2.4	24.2	10.0	0	.32	3.4	24.1	5.3	0	.32	30+	21.8	1.9	12,000

Figure 13c
Typical Flow and Pressure Measurements, Plane Slinger with Screw Return

flow of 472 lb. /hr. actually provides the closest approximation to the bearing oil flow design condition.

The bypass leakage path was eliminated by the addition of an "O" ring at this point, and this problem did not exist in future tests.

Figures 14 and 15 give the temperature history during the leakage tests. Although some oil was being bypassed around the jet ring, the oil still picked up heat and cooled the bearing seal area. The temperatures for this run are typical of this seal design. Later tests with the bypass leakage reduced indicated little temperature difference between the two conditions. The fluctuations in temperatures towards the end of the test were due to changes in oil flow rate to the bearings. The temperature levels were well within specification, the bearings at approximately 260°F and the seal face at 295°F.

By closing the discharge valves on the slingers, the shutoff pressure head could be measured. The maximum value obtained was 19.5 inches Hg or 9.5 psi giving an experimental velocity ratio of 0.48. For a K value of 0.5 in Section II-C-2, a head rise of 10.3 psi was calculated. Thus at shutoff condition the experiment confirms the theoretical predictions. As slinger flow is increased, the delivered head and K values drop off as would be expected. The design, however, has more than adequate capacity to scavenge the bearing cavity and return the lubricant to the sump.

The total leakage for each trap is presented in Figure 16. During startup leakage rates are high, but after about 4 hours operation they reach a steady rate and remain constant from then on.

The leakage rates for the inboard slingers are very low, and for the anti-drive end slinger (Trap 2) there was no measurable increase in oil accumulation after the first 2 hours of operation. The other inboard slinger leaked at a rate of about 0.4 cc/hour. The DE and ADE outboard seals had leakage rates of 4.3 cc/hr and 3.8 cc/hr respectively.

The data indicates that the clearance was lower on the inboard seals since they had the lowest leakage rates. This is entirely possible since the rotor was not heated for this test while the casing was hot. The

IV

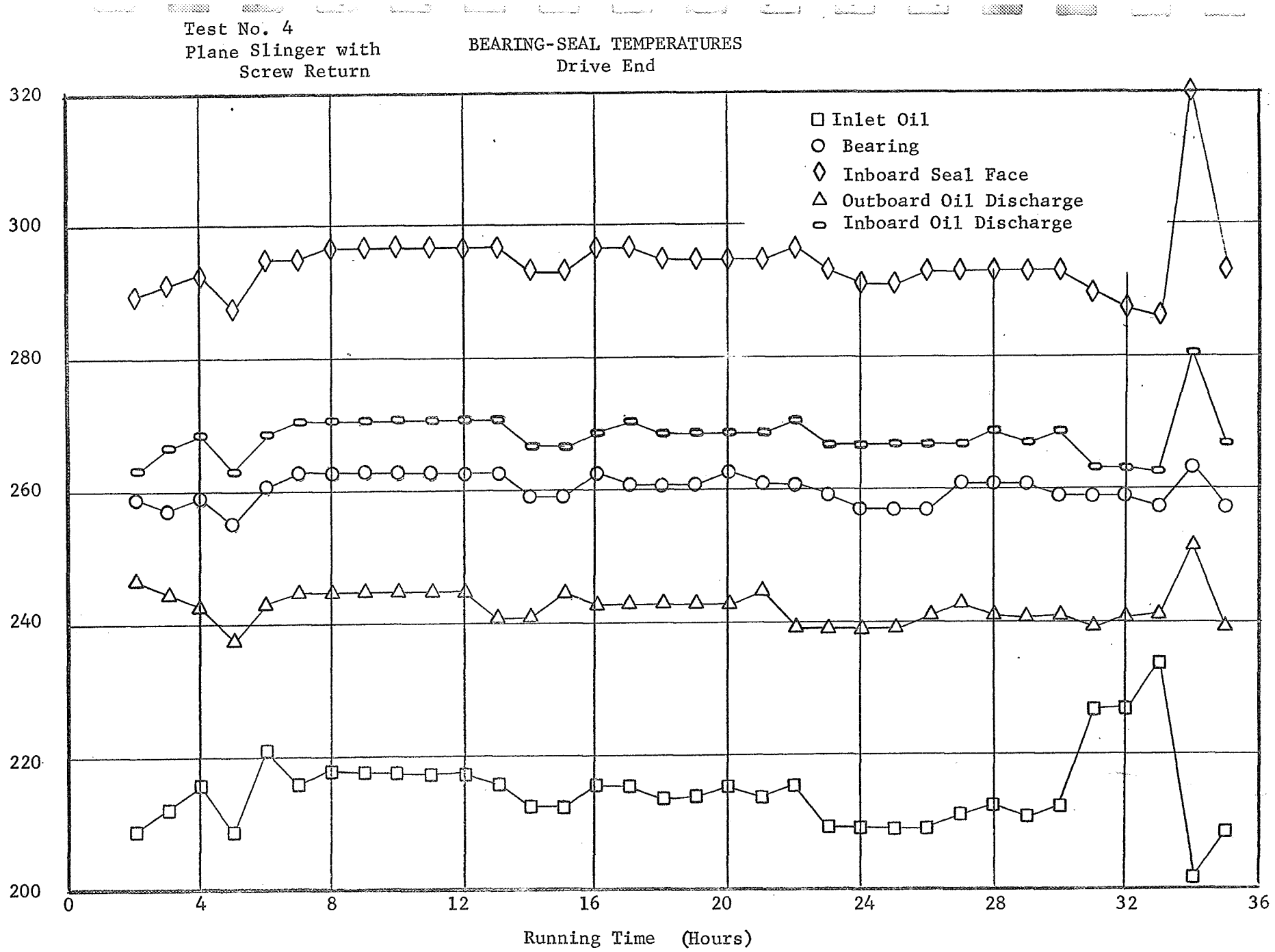
Test No. 4
Plane Slinger with
Screw Return
BEARING-SEAL TEMPERATURES
Drive End
Inlet Oil
Bearing
Inboard Seal Face
Outboard Oil Discharge
Inboard Oil Discharge
320
300
280
260
240
220
200
Temperature, °F
0
4
8
12
16
20
24
28
32
36
Running Time (Hours)

Figure 14

BEARING-SEAL TEMPERATURES

Anti-Drive End

Test No. 4
Plane Slinger with
Screw Return

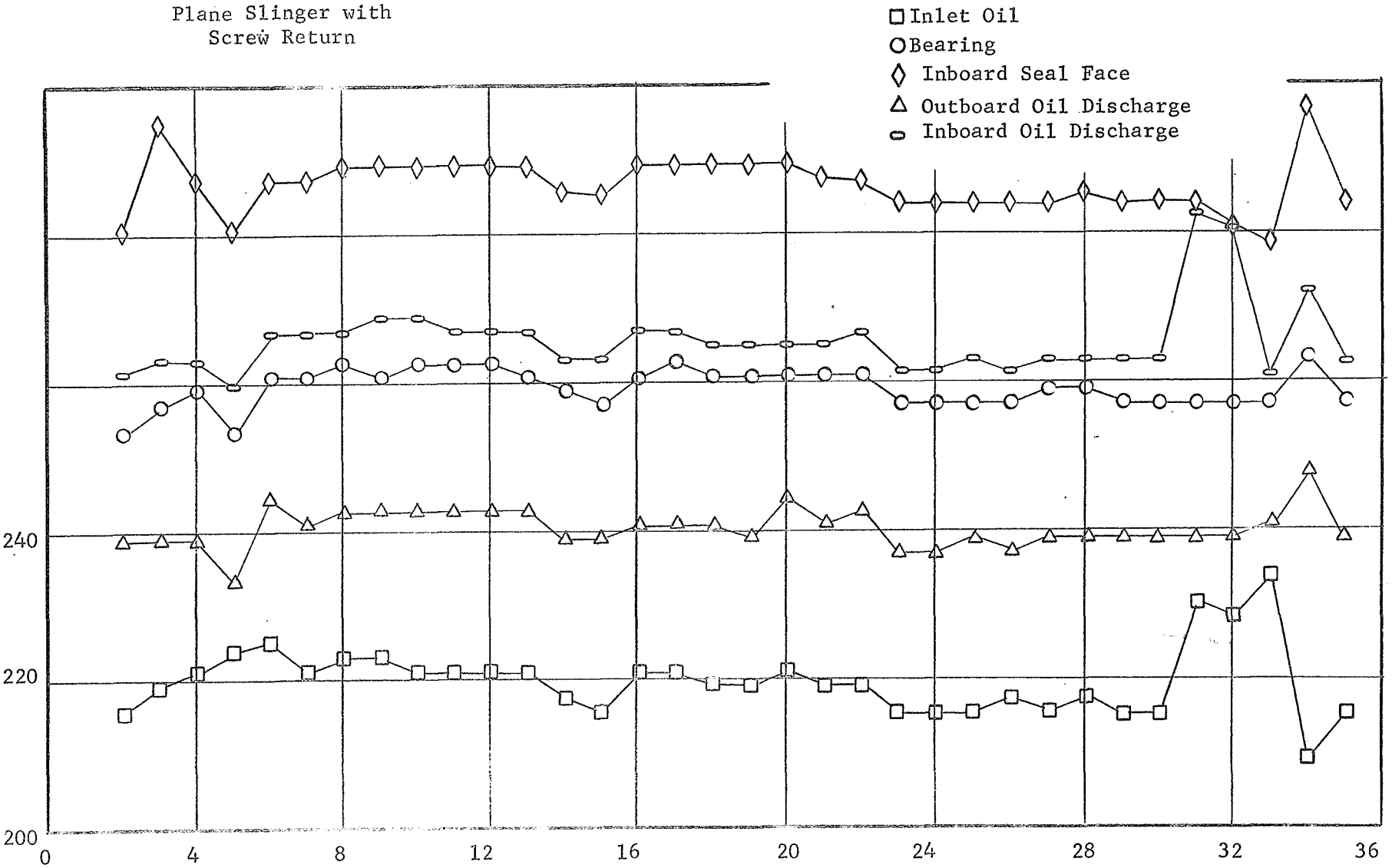

Figure 15

SNAP-8 SEAL TEST

Test of Nov. 11-12, 1965

Test No. 4

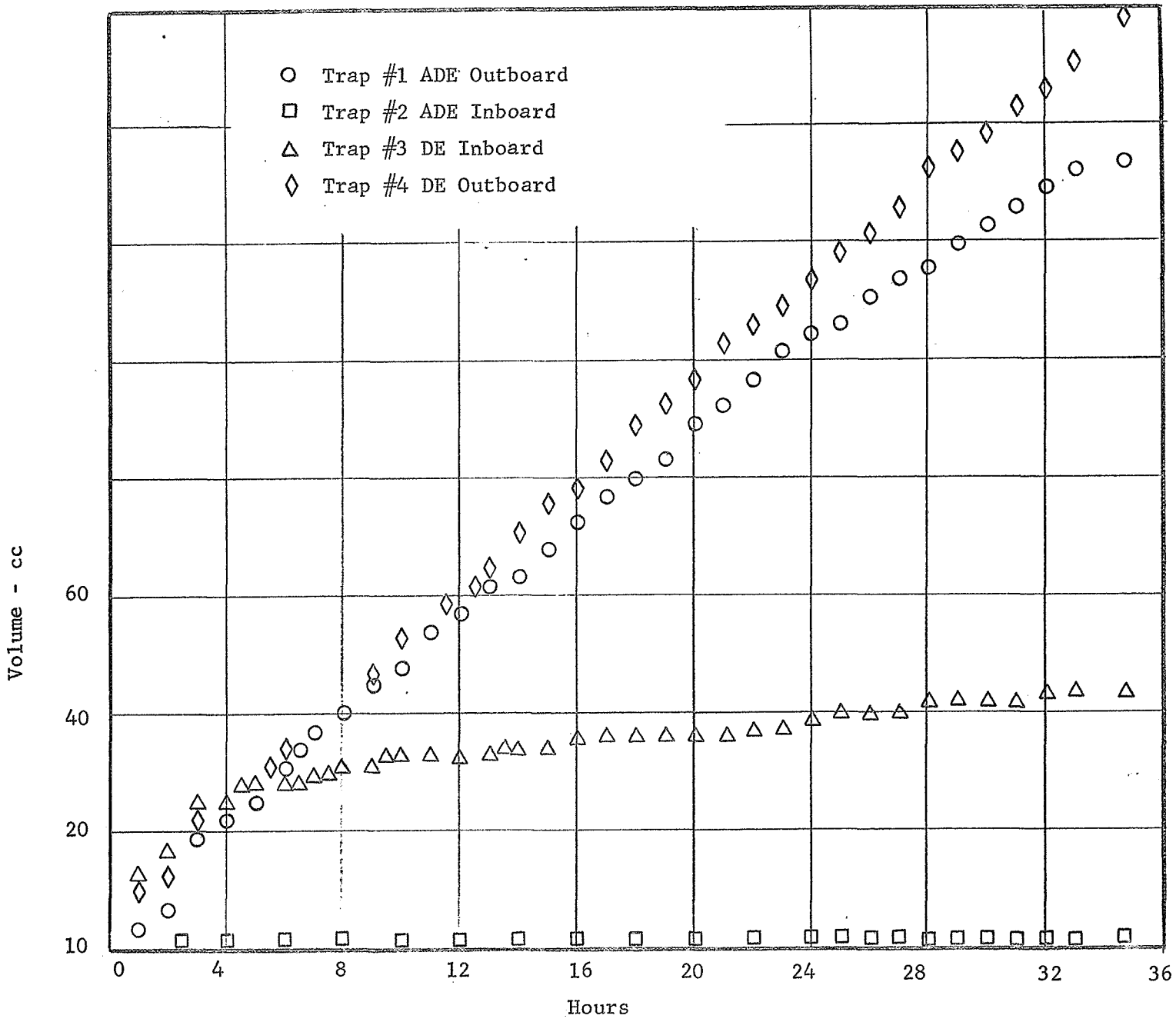

Figure 16

BEARING - SEAL TEMPERATURES

vs

FLOW RATE

DRIVE END

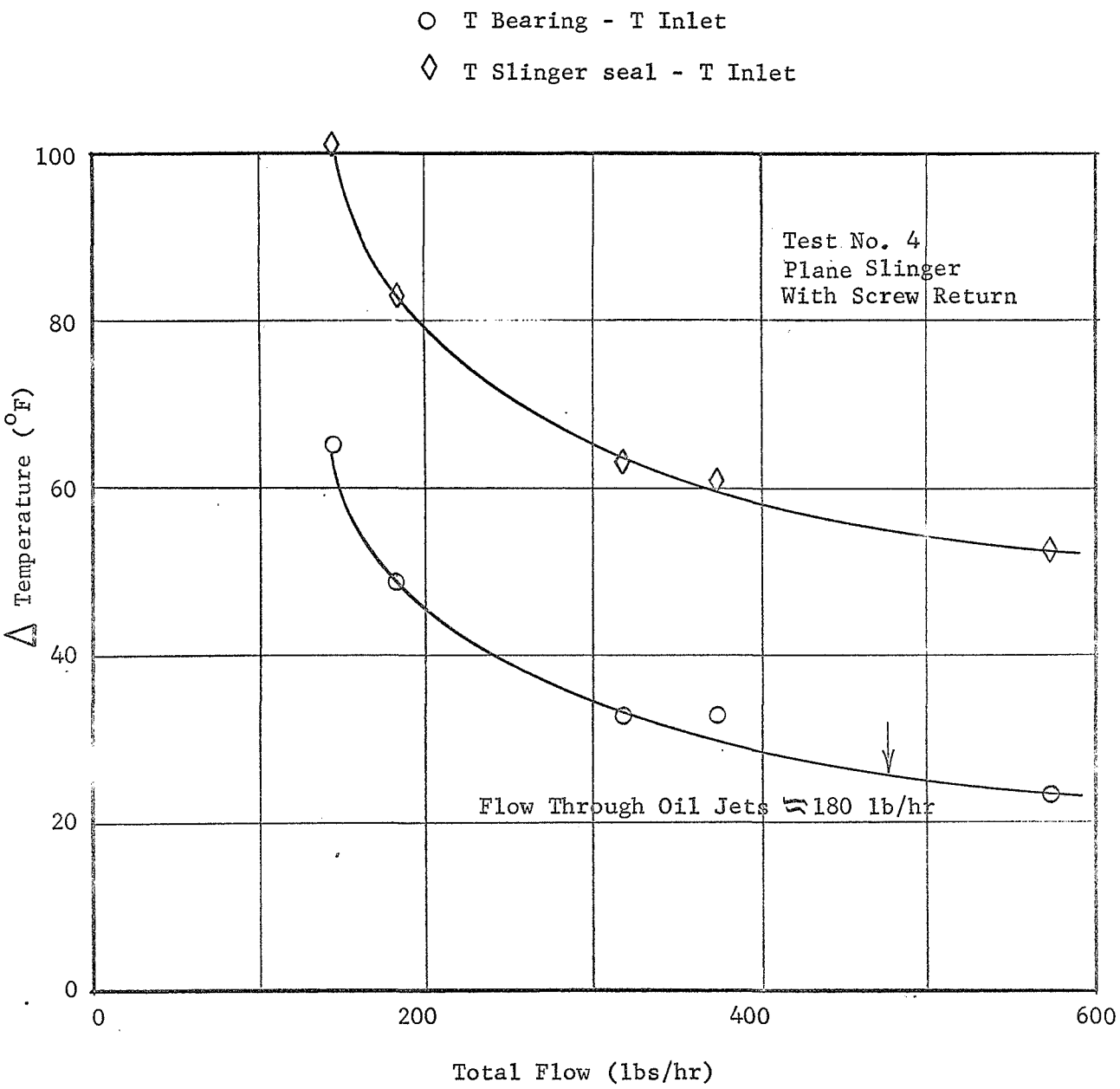

Figure 17

BEARING - SEAL TEMPERATURE RISE

vs

FLOW RATE

ANTI-DRIVE END

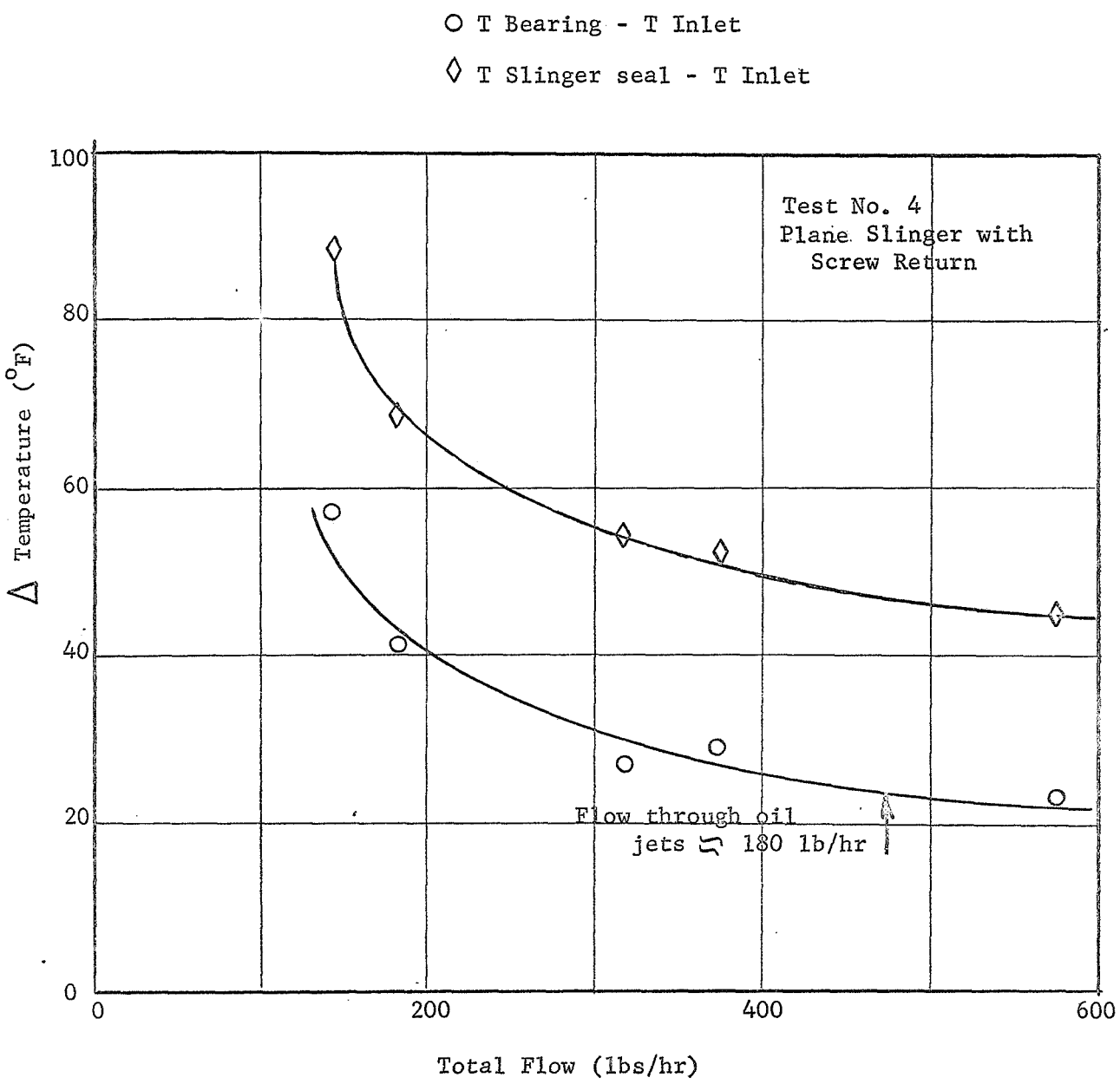

Figure 18

data also indicates that the entire rotor was shifted slightly toward the DE as both DE seals exhibit a lower leakage rate than the ADE seals. The data points out the extreme sensitivity of this type of seal to axial clearance.

A-2. Test No. 5 - Bearing Failure

Test No. 5 was to have been a repeat of Test No. 4, but with heat input to the rotor. However, during startup the ADE bearing failed. After disassembly it was found that the cage had failed. An evaluation of this bearing failure is presented in Reference 20.

A-3. Tests Nos 6 - 8. Evaluation of Shaft Heat Removal

Test No. 5 was designed to obtain long term leakage data on the plane slinger with screw return seal configuration. No heat addition to the rotor was attempted. Tests 6 through 8 were repeats of Test No. 5 except with heat addition to the rotor in an effort to evaluate the effect of this heat addition on leakage rate and bearing-seal temperature levels. The results of Test No. 7 are presented here as typical of these tests with heat input to the rotor.

During this test the system was run at several different heat inputs up to a maximum of approximately 300 watts. The maximum heat input was determined by the maximum allowable heater wire temperature of 500°F, the temperature at which the lubricant begins to breakdown.

The summary data sheet for Test No. 7 is shown in Figure 19 and represents approximately 10 hours of continuous operation at rated speed and with various rotor heater electrical power inputs. A 2" thick blanket of fiberglass insulation was placed around the cylindrical portion of the housing to reduce heat radiation to the surroundings. (The variation of measured bearing-seal temperatures with heat input is shown in Figures 20 and 21).

In general, the data indicates a rise of only a few degrees in the machine temperature levels with the heat addition of 300 watts. The results indicate that the design can easily handle a heat load of 300 watts with bearing temperatures considerably below the 300°F specification limit.

The temperature sensitive paper and pellets used to record rotor

SNAP-8 ALTERNATORS TEST #7 12/23/63
Plain Slinger With Screw Return

	10:15A	3:30P
BAROMETER	30.33	74°F
AMBIENT	30.07	77°F

Time	Sump Press " Hg VAC	Sump Temp Of	Inlet Press PSIG	Cavity Press " Hg VAC	ADE OTB Slinger Press "Hg VAC	INBD Slinger Press "Hg VAC	Flow % Full Scale GPM	Inlet Press PSIG	Cavity Press " Hg VAC	DE OTBD Slinger Press "Hg VAC	INBD Slinger Press "Hg VAC	Flow % Full Scale GPM	Gen. Cavity Press "Hg	Pump Discharge PSIG	Seal P. PSIG	N RPM	Torque Meter	E	I	W
10:15	20	225	7.0	26.1	15	15.2	31.3	12.3	26.5	15	15	31.2	30+	30.8	2.0	12,000	64.0	0	0	0
11:00	20	230	7.0	26.1	15	15.1	31.3	12.3	26.5	14.9	14.9	31.6	30+	31.0	2.0	12,000	64.6	0	0	0
12:00	20	230	7.0	26.2	15	15.2	31.3	12.2	26.5	15.0	14.9	31.5	30+	30.6	2.0	12,000	64.8	99	.84	82.4
12:45	20.1	230	7.0	26.2	15	15.2	31.3	12.3	26.5	15.0	14.9	31.5	30+	30.6	2.0	12,000	64.8	99	.84	82.4
1:15	20.1	230	7.0	26.2	15.1	15.1	31.4	12.3	26.5	15.1	14.9	31.4	30+	30.6	2.0	12,040	65.0	118.5	1.01	119.8
1:45	20.1	230	7.0	26.2	15.1	15.1	31.3	12.3	26.5	15.0	14.9	31.4	30+	30.6	2.0	12,040	65.0	119	1.015	121.0
2:15	20.1	230	7.0	26.2	15.1	15.1	31.3	12.3	26.5	15.0	14.9	31.4	30+	30.8	2.0	12,040	65.4	119	1.015	121.0
2:45	20.1	235	7.0	26.2	15.1	15.1	31.3	12.3	26.5	15.0	14.9	31.5	30+	30.8	2.0	12,040	65.4	137	1.16	159
3:30	20.1	235	7.0	26.2	15.1	15.1	31.2	12.3	26.5	15.0	14.8	31.5	30+	30.8	2.0	12,060	65.6	137	1.17	160
4:00	20.1	233	7.1	26.2	15.1	15.1	31.3	12.3	26.6	15.0	14.8	31.4	30+	30.8	2.0	12,080	65.6	133	1.13	150
4:30	20.0	235	7.0	26.2	15.2	15.1	31.3	12.3	26.5	15.0	14.8	31.5	30+	30.8	2.0	12,060	65.6	150	1.28	192
5:00	20.0	230	7.0	26.2	15.2	15.1	31.3	12.2	26.5	15.0	14.8	31.5	30+	30.8	2.0	12,080	65.8	150	1.28	192
5:30	20.0	230	7.0	26.2	15.2	15.1	31.2	12.2	26.5	15.0	14.8	31.4	30+	30.8	2.0	12,060	65.8	170	1.45	246
6:00	20.1	230	7.0	26.2	15.2	15.1	31.2	12.2	26.5	15.0	14.8	31.4	30+	31.0	2.0	12,080	65.8	170	1.45	246
6:30	20.0	228	7.0	26.2	15.2	15.1	31.2	12.2	26.5	15.0	14.8	31.4	30+	31.0	2.0	12,080	66.0	190	1.62	305
7:00	19.9	230	7.0	26.2	15.2	15.1	31.2	12.3	26.5	14.9	14.9	31.5	30+	31.0	2.0	12,100	66.0	189	1.61	304
7:20	20.0	227	20.0	26.1	15.1	14.9	40.3	26.5	26.5	15.0	14.9	40.1	30+	49.6	2.1	12,080	67.0	186	1.58	294
7:35	20.0	230	38.3	26.1	15.0	15.1	50.2	46.5	26.5	15.0	14.8	49.8	30+	60+	2.1	12,060	67.8	182	1.55	282
7:50	20.0	227	59.1	25.9	15.1	14.0	60.1	63.5	26.5	15.1	14.9	60.2	30+	60+	2.1	12,040	68.4	182	1.55	282
8:15	20.0	232	-	26.3	16.3	15.2	26.0	4.1	26.9	14.5	14.8	27.7	30+	56.0	1.9	12,100	66.0	177	1.51	267
8:35	20.0	235	-	26.3	16.8	16.9	20.0	-	27.0	15.2	16.9	20.0	30+	59	2.0	12,000	64.0	173	1.47	254

Figure 19

Typical Flow and Pressure Measurements, Plane Slinger with Screw Return, Heat Input

BEARING-SEAL TEMPERATURES vs HEAT INPUT

Drive End

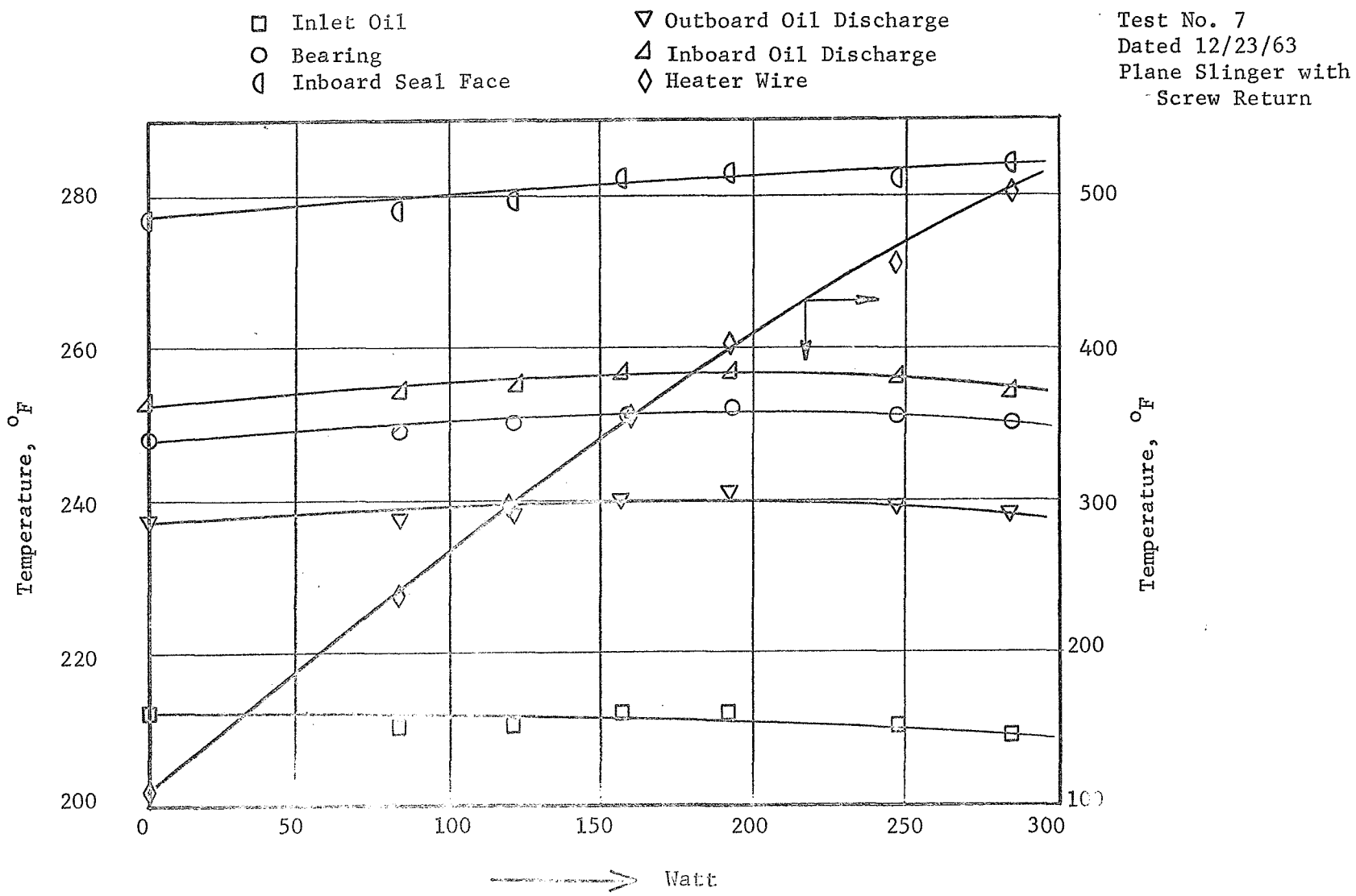

Figure 20

BEARING-SEAL TEMPERATURES vs HEAT INPUT

Anti-Drive End

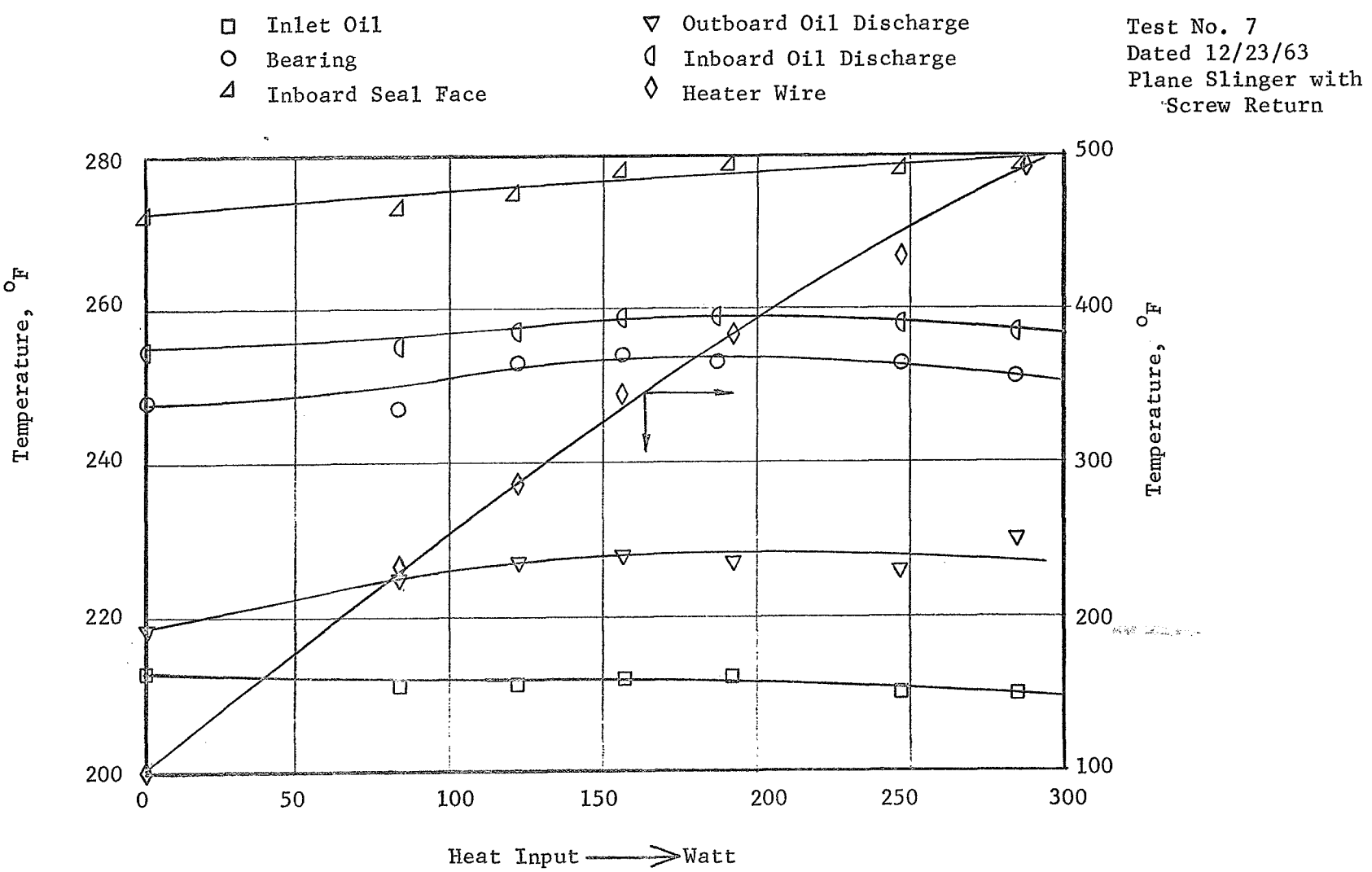

Figure 21

temperature were removed after the completion of Test No. 7. The highest paper indication was 490°F and the rotor heater wire temperature was 500°F. From this information it is concluded that the rotor temperature was only slightly above 490°F and somewhat below the heater wire temperature of 500°F. These results show that the heater wire temperature is a good approximation to rotor temperature.

Discussion of Heat Balance - Tests Nos. 6, 7, and 8

In order to correlate the data from Tests Nos. 6, 7 and 8, and check the various power measurements, overall heat balance calculations were performed.

Table 8 is a summary of this heat balance. These calculations are based on the average temperature rises and on the assumption that the flow to each end divides equally between the two slingers. It can be noted that some discrepancy does exist in this heat balance. This was felt to be caused by our inability to accurately estimate heat losses to the surroundings.

Table 8 presents the data for simulation of pole face losses. The change in temperature for the oil passing the inboard and the outboard slingers for the case of a 300 watt input are shown. The correlation between increase in heat input and change in oil output temperature is considered very good.

B. Slinger Seal Without Screw Return

Plane Slinger Without Screw Return

The previously discussed tests on the plane slinger seal always included a screw return, the purpose of which is to scavenge any oil drops coming from the interface and return them to the seal.

The object of this test was to assay the value of the screw return in reducing the seal leakage rate. To do this, the screw returns on the ADE were machined away. The "As Built" drawing of the ADE is shown in Figure 22. The DE was not changed. The radial clearance between the screw return was about .1 inch as compared to the normal .003 to .004 inch radial clearance. Nominal operating conditions were the same as Table 7.

The temperature sensitive paper installed on both the DE and ADE of the rotor were removed after the test and showed that the maximum rotor

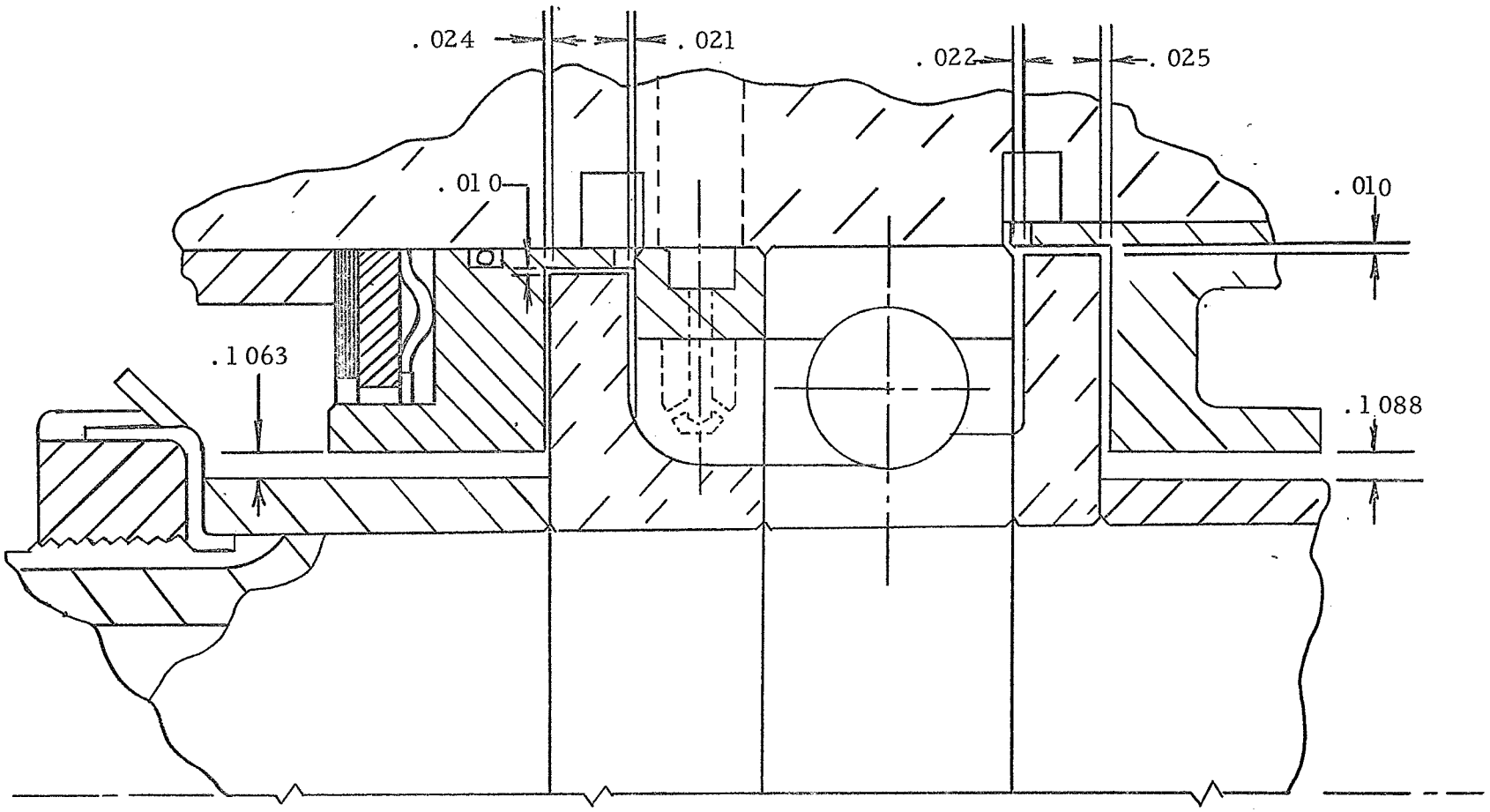

Dimensions in inches

"AS BUILT" DRAWING OF PLANE
SLINGER WITHOUT SCREW RETURN

Figure 22

Table 8

Overall Heat Balance - Tests 6, 7, and 8

	Test No. 6	Test No. 7	Test No. 8.
Power Input (KW)	2.62	2.32	2.46
Heat Removed by Oil (KW)	1.49	1.49	1.76
Estimated Heat Loss - Other Modes (KW)	0.60	0.44	0.44
Discrepancy (KW)	0.53	0.39	0.26

Simulated Pole Face Loss Heat Balance
(For 300 Watt Input)

	Test No. 7	Test No. 8
ΔT_i - DE(^oF)	5	2
ΔT_o - DE(^oF)	4	2
ΔT_i - ADE(^oF)	6	3
ΔT_o - ADE(^oF)	13	16
ΔT_{avg} - (^oF)	7	5.7
W#/Hr	180	180
ΔH BTU/Min (Increase in heat removed by oil)	16.4	13.4
Input (heaters) BTU/Min	16.2	16.2

temperature was in excess of 49[illegible]F. Since the l[illegible]ater wire temperature was limited to 500°F, actual rotor t[illegible]perature was be[illegible]en 490°F and 500°F.

The operating data, press[illegible]es, flows, and temperatures did not vary appreciably from that obtained in previous tests with the screw return in place. In addition, there was no appreciable difference in power input which was measured as 2.6 kw.

The accumulated leakage versus running time is shown in Figure 23. The leakage rate on the ADE was about twice as high as the worst leakage rate on the DE, indicating the decided advantage of including the screw return.

In addition, with the screw return in place, it is much easier to run the unit at low speed without gross leakage. For instance at 2000 rpm, the leakage rate on the DE (with screw returns) was not more than 10 cc/hr, but on the ADE, (without screw returns), the rate was about 300 cc/min, i.e., the trap would fill in less than ten minutes.

Another advantage of operating with the screw returns is that if there is a sudden loss of speed, the unit decelerates to part speed, and is subsequently brought back to speed, the seal recovers its sealing capability. Without screw returns, the seal on the ADE would continue to leak at high rate when brought back to speed after a slowdown. It was then necessary to temporarily decrease the oil flow to ADE, and then bring the unit up to design speed in order to restore stable seal operation.

This experimental comparison between the plane slinger seal with a screw return and without a screw return, shows that the screw return reduces the leakage rate below that obtained without the screw return. In addition, the screw return allows for easier startup procedures and in case of sudden loss of speed permits a restart without loss of seal stability. Without the screw return, a reduction in speed caused seal breakdown, (i.e., gross leakage), and a return to design speed in some cases did not restore seal stability. There was no measurable difference in power loss with or without the screw return.

LEAKAGE RATE

SNAP-8 SEAL TEST

Test No. 20

Date: 2-14-64

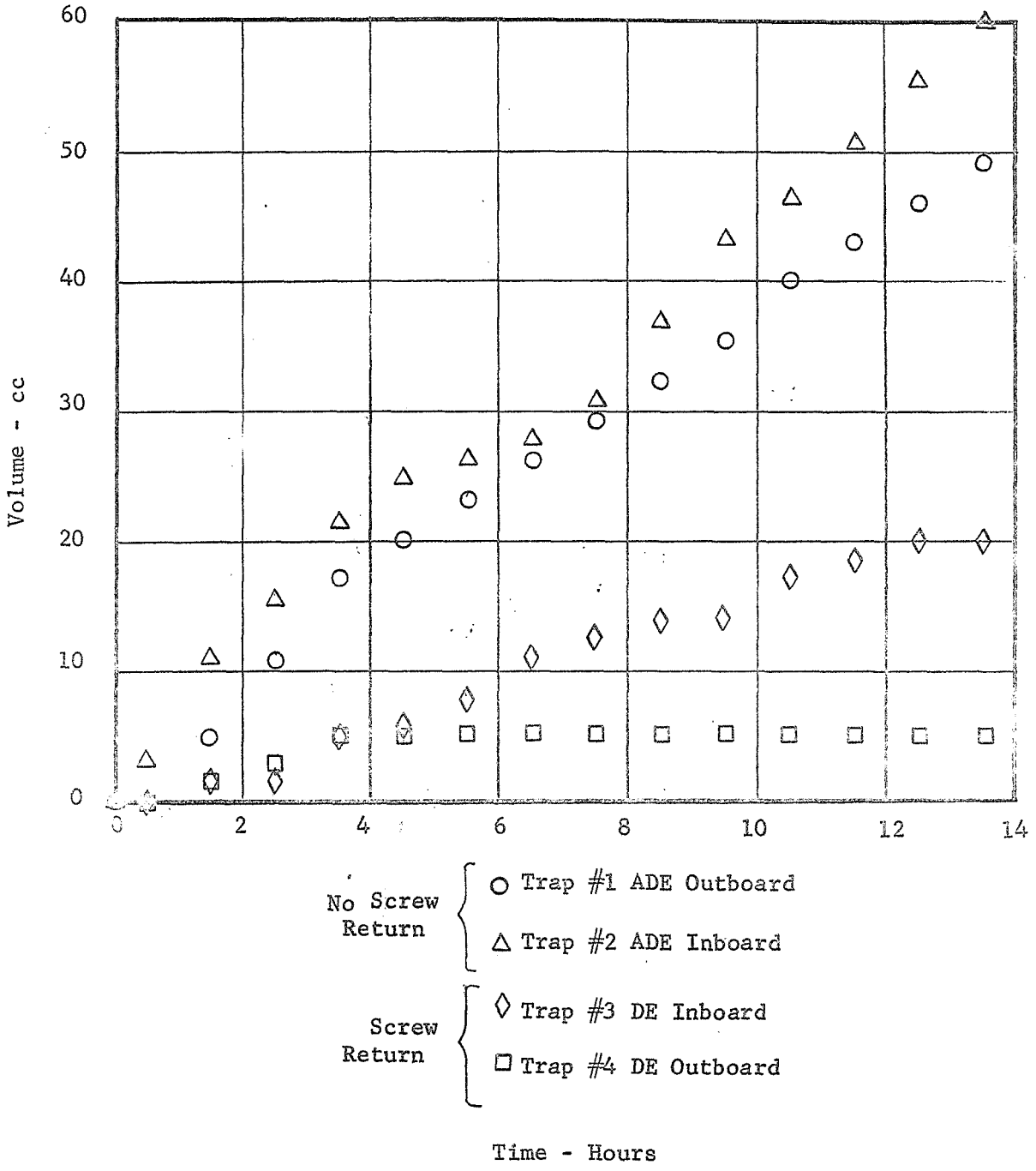

Figure 23

C. Housing Disk Seal

The housing-disk seal of Figure 2 is a more complicated mechanical design but because there is no shearing action within the housing, promises a more stable interface and consequently a lower leakage rate. Two tests were run; a preliminary test at the General Electric Evendale Plant and a long time leakage test on the SNAP-8 test rig.

C-1. Preliminary Component Testing

Preliminary tests of a 3.5 inch housing-disk seal with ET-378 were performed at the G. E. Evendale plant. The configuration tested is shown in Figure 24. It will be noted that clearance between the rotating disk and stationary wall is 0.080 inch more than enough to satisfy the SNAP-8 requirement. The minimum radial clearance was about 0.010 inches.

Although the Evendale test rig is not equipped to measure leakage rate, the results indicated that this configuration could effectively suppress interface leakage even in vacuum operation. A picture of the interface at 12,000 rpm is shown in Figure 25. The drops of oil at the bottom of the picture are from a leaky flange and not from the interface.

Measured K values, the ratio of fluid core velocity to disk velocity, are plotted in Figure 26. The Reynolds Number for this test disk at 12,000 rpm is

$$Re = \frac{\omega a^2}{\nu} = 4.37 \times 10^5$$

a spacing ratio s/a, of 0.23 and an engagement ratio of about 0.15. Reference to Figure A-2 shows that the disk was operating in Regime IV. Reference to Figure A23 gives a K value of 0.35 compared to a measured value of 0.36.

C-2. Housing Disk Seal Tests on SNAP-8 Alternator Test Rig

Based on the preliminary housing-disk seal tests at Evendale, a seal of this type was designed for checkout on the SNAP-8 alternator test rig.

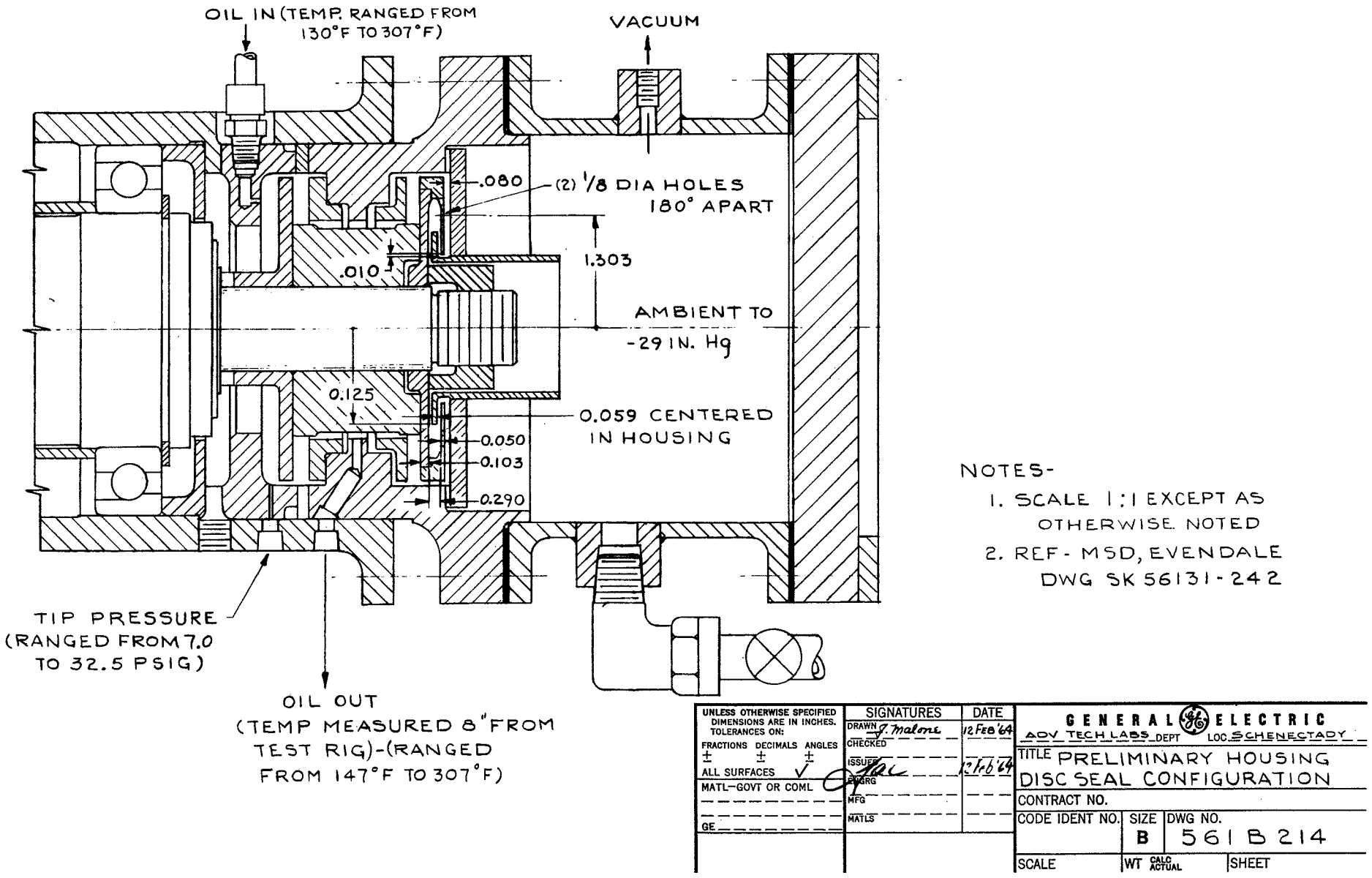

Figure 24. Preliminary Housing-Disk Seal Configuration

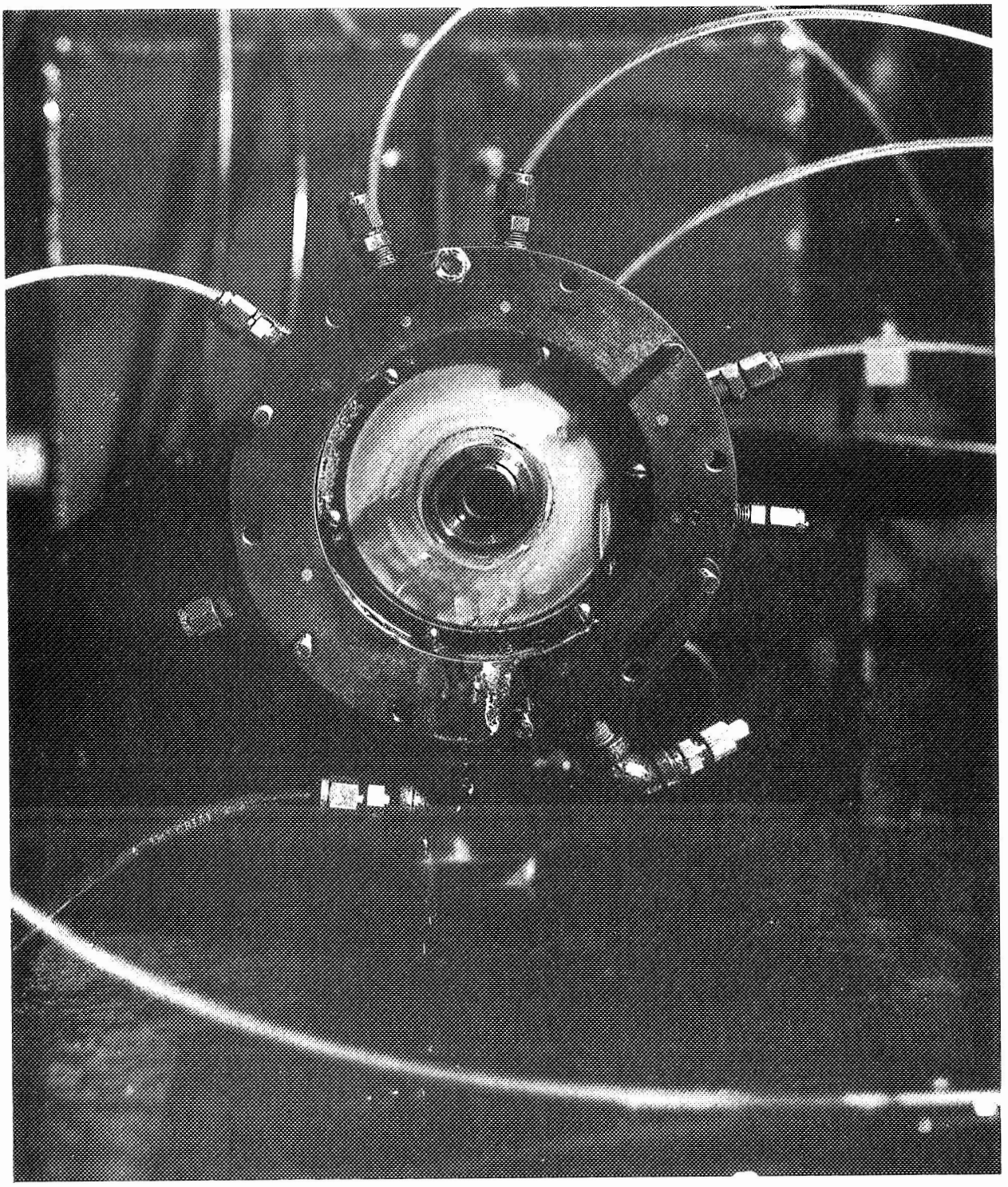

Figure 25. Picture of Interface Preliminary Housing-Disk Seal

K vs RPM FOR HOUSING DISK SEAL

with

DOW ET 378

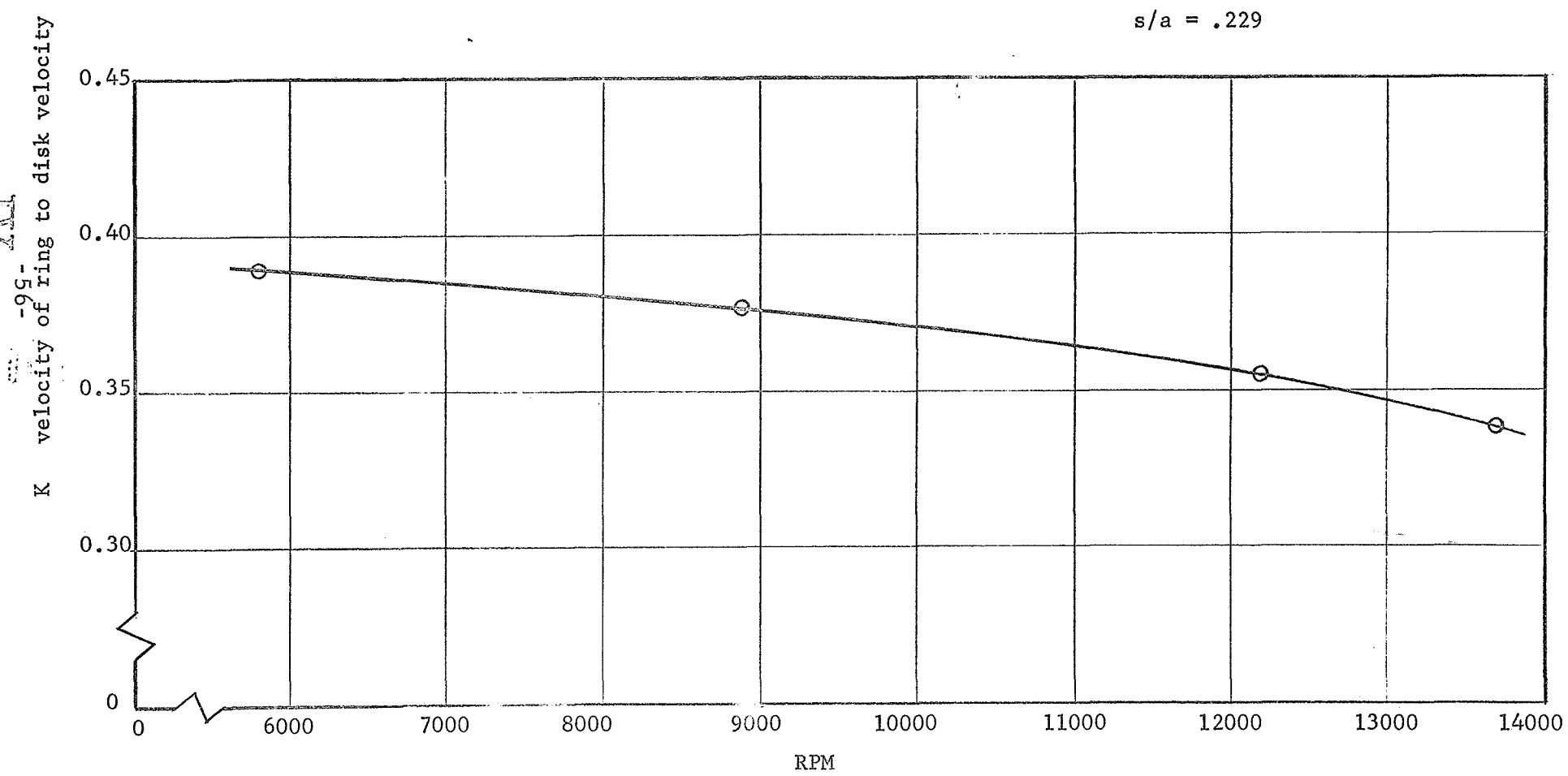

Figure 26

A drawing of this seal is shown in Figure 2. One seal of this type was installed on the outboard side of the antidrive end.

When the set screws which hold the lip in place were tightened down, the lip deformed. Because of this it was necessary to increase the clearance between the lip and the shaft above that called for on the print. The actual seal dimensions at time of assembly are given in Figure 27.

The pressure and temperature data did not differ materially from that of the plane slinger with screw return. The test run was cut short after 33 hours of running when the plexiglass cover on the anti-drive end failed. The object of the test was to determine the leakage rate of the housing-disk seal as compared to the plane slinger with screw return. Nominal operating conditions were the same as Table 7.

The temperature sensitive paper and pellets used to record maximum rotor temperature indicated that the maximum rotor temperature during this test was 400 to 450°F. The heater wire temperature was not allowed to exceed 500°F. This limitation had allowed higher rotor temperatures in previous tests. Maximum heat input was 205 watts.

In general, temperature levels at both the drive and anti-drive ends were comparable to the plane slinger tests. Also, as experienced in previous tests, there was a slight increase in temperature level with heat input. The minimum oil flow at which the seal face temperature reached 300°F was about 140 lb/hr.

Total measured leakage for this test is shown in Figure 28. A comparison between leakage rates for this test and previous tests appears in Section V-F. Leakage from the housing-disk seal was collected in trap No. 1, and over a 33 hour period there was no measurable accumulation of fluid in this trap.

The accumulation in the remaining traps, in which the leakage from the plane slinger with screw return was collected, showed a similar variation with time as observed in previous tests. There was an increase in leakage rate collected in Traps Nos. 3 and 4 after 15 hours of running which

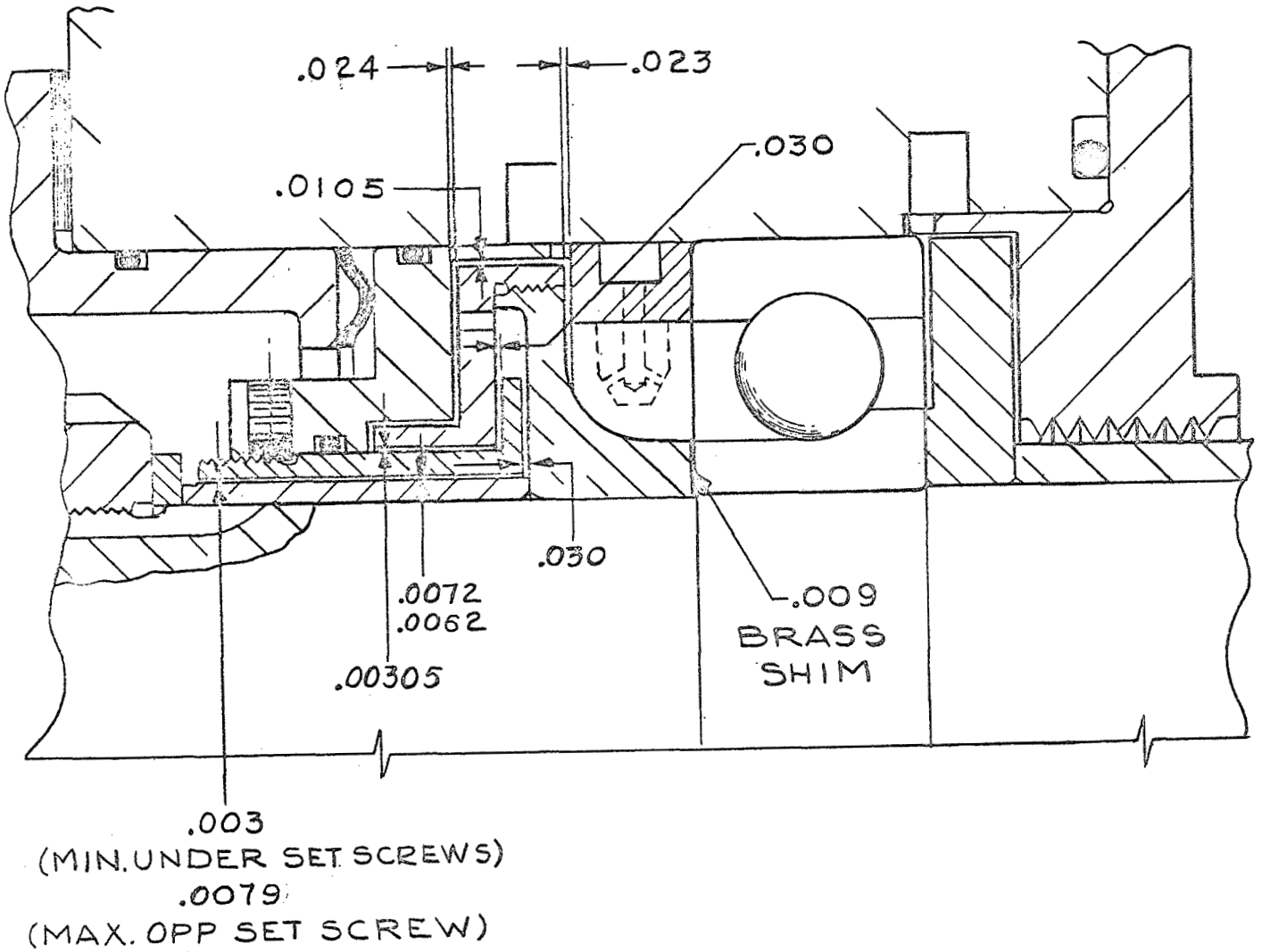

UNLESS OTHERWISE SPECIFIED DIMENSIONS ARE IN INCHES. TOLERANCES ON: FRACTIONS ± DECIMALS ± ANGLES ± ALL SURFACES ✓	SIGNATURES	DATE	GENERAL ELECTRIC ADV TECH LABS DEPT. LOC SCHENECTADY
MATL GOVT OR COML	DRAWN J. Malone	10 FEB '64	TITLE HOUSING DISC SEAL AS BUILT DIMENSIONS
	CHECKED		
	ISSUED R.J. W	10 FEB 64	
	ENGRG		CONTRACT NO.
	MFG		CODE IDENT NO. / SIZE A / DWG NO. 115A4880
GE	MATLS		SCALE / WT CALC ACTUAL / SHEET

Figure 27. "As Built" Dimensions of Screw Seal

SNAP-8 ALTERNATOR

LEAKAGE RATE

Housing-Disk Seal (Trap #1)

Test No. 11
Date: 1-15-64

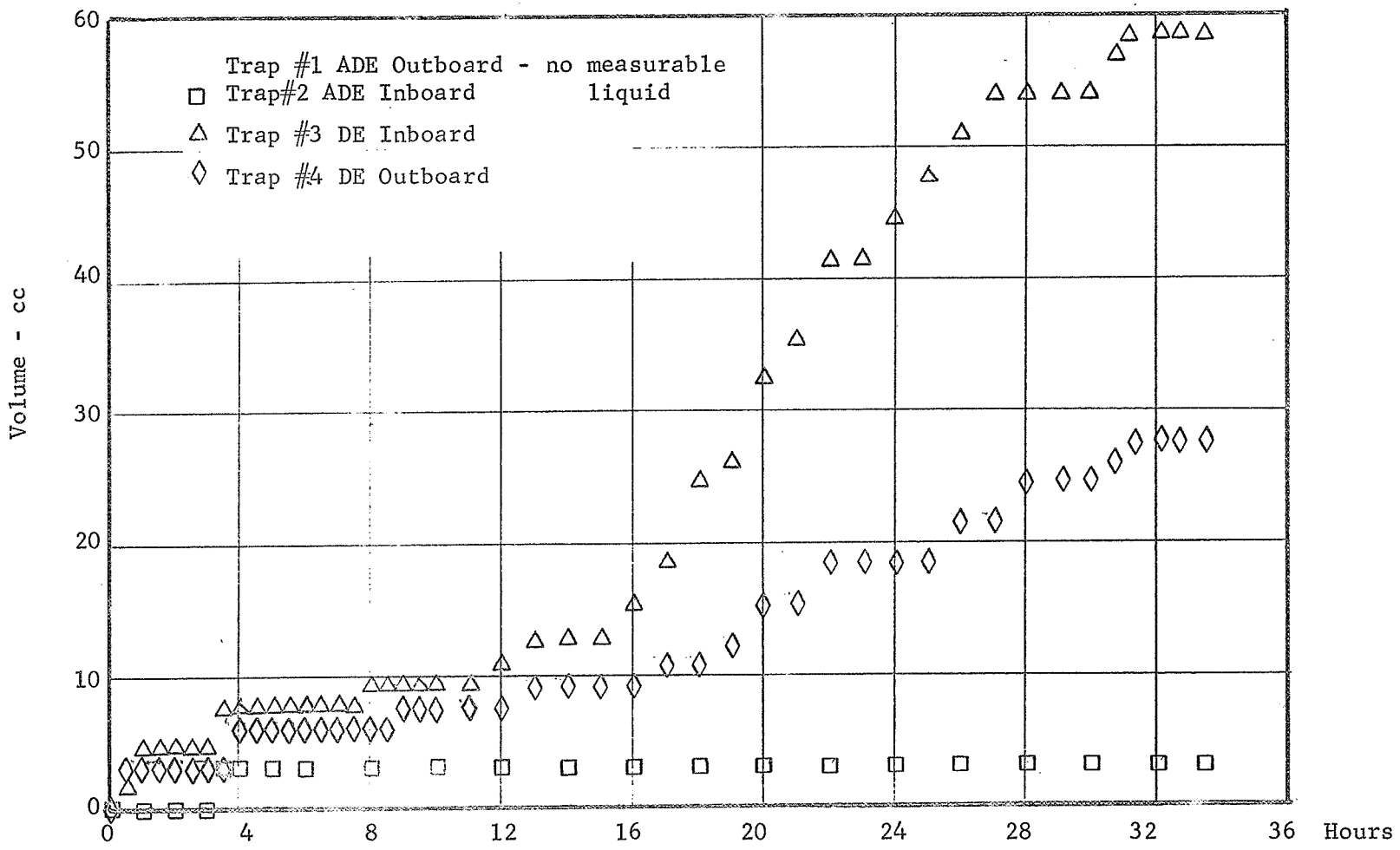

Figure 28

occurred shortly after the heat input to the rotor was turned on.

The test results indicate that the housing-disk seal has a lower leakage rate than the plane slinger with screw return. A total yearly leakage into the generator cavity of 500 cc has been assumed as a design goal. This is an allowable leakage rate of 0.025 cc/hr from each of the inboard seals. Since the minimum increment that could be reliably measured is 0.77 cc, and no leakage was detected in 33 hours, the measured leakage rate was less than .025 cc/hr, the desired rate.

D. Screw Seal Tests

Tests 16 through 18, which are covered in this section were for flooded bearing operation employing the screw seal.

Figure 3 is an assembly drawing of the screw seal tested for the SNAP-8 application. The screw seal is a threaded shaft rotating in a close clearance sleeve. By means of the grooves on the rotating shaft, pressure is generated in the fluid contained in the bearing cavity. The pressure thus generated prevents flow outward and away from the bearing. A flow through the bearing is continuously maintained to provide cooling and lubrication.

Preliminary tests on the ATL screw seal test rig using ET-378 showed that the stability of the interface in the screw seal did not seem to be improved by reducing the helix angle. Therefore, a sealing thread was chosen which gave maximum sealing pressure generation. The thread geometry is summarized in Table 5. The significant "as built" dimensions are shown in Figure 29.

Test No. 16 was a five and one-half hour test with all seals exposed to atmospheric pressure. There was no measurable leakage from the ADE, which contained the screw seal.

Test No. 17 and Test No. 18 were conducted under vacuum conditions and resulted in a total test time of seven hours at rated speed. The object of the test was to determine the leakage rate of the screw seal under simulated operating conditions. Nominal operating conditions for these tests were as in Table 7.

Screw Seal Test Configuration - SNAP-8

Significant "As Built" Dimensions

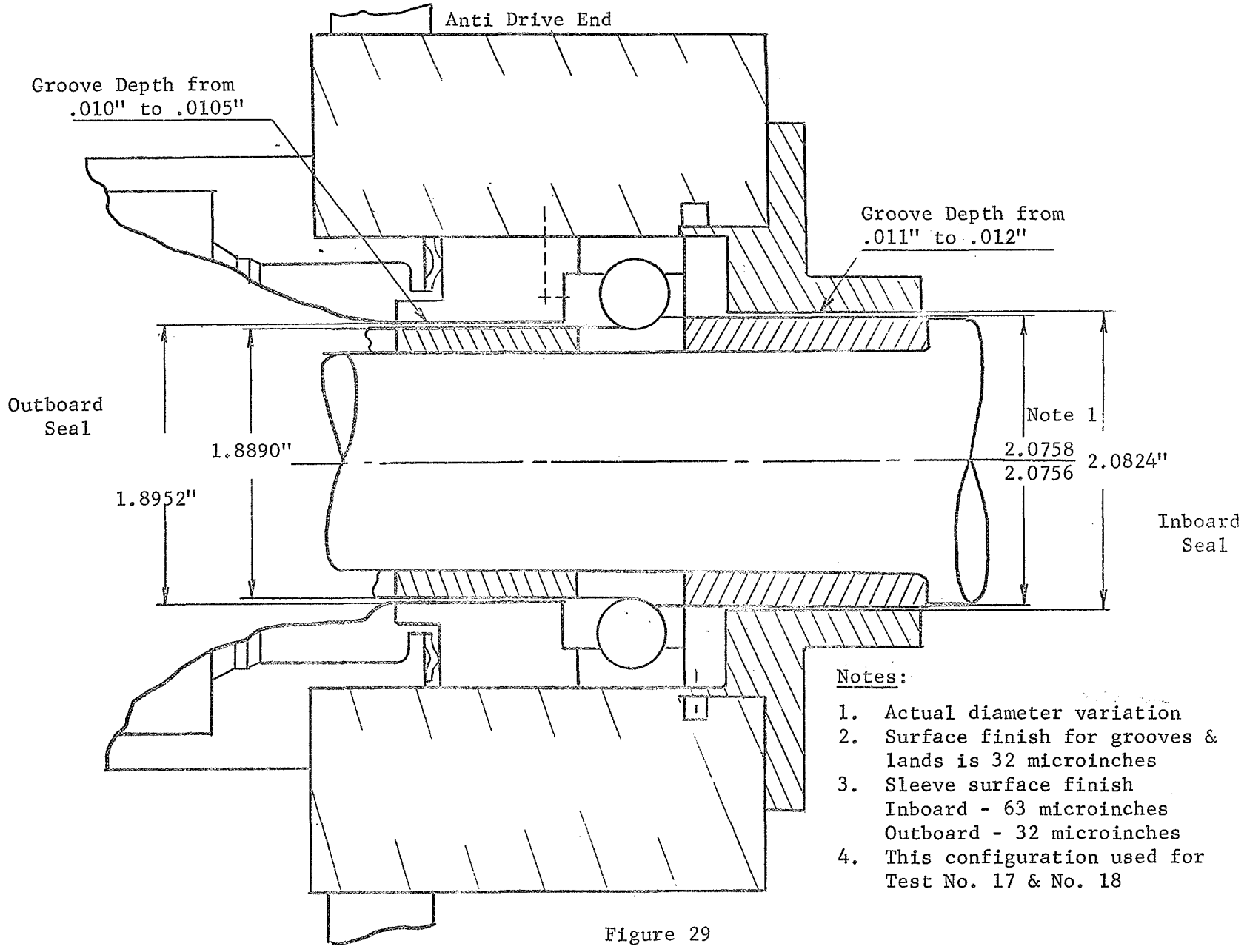

Notes:

1. Actual diameter variation
2. Surface finish for grooves & lands is 32 microinches
3. Sleeve surface finish
   Inboard - 63 microinches
   Outboard - 32 microinches
4. This configuration used for Test No. 17 & No. 18

Figure 29

The oil was fed to the bearing through four 0.0980 inch holes spaced equally about the circumference. The oil was removed from the bearing cavity through four holes at the OD of the bearing. The direction of oil flow was made the same as the outer ring thrust load in order to take advantage of the natural pumping action of the bearing. Pressure was measured, in the inlet line, bearing cavity, and in the discharge line.

The pressure, flow and heat input data are tabulated in Figure 30. The temperature data for Test No. 18 is plotted in Figures 31 and 32. The temperature data is plotted versus time and covers both the DE and ADE. Temperatures at the drive end are approximately the same as on previous tests with heat input to the rotor. At the anti-drive end the temperatures are considerably lower. For example, the bearing temperature was at least twenty-four degrees lower at the anti-drive end on both tests. It will be recalled that the screw seal is on the anti-drive end. The lower temperature level observed at the ADE is consistent with the lower torque readings obtained during Tests 17 and 18. Total measured power loss was 2.22 kw. From Section II-D-3, the average power loss for four slingers with screw return plus two bearings is 2.46 kw. Based on this value, the indicated loss for two screw seals and one bearing would be 1.00 kw. Using an estimated bearing power loss of 0.12 kw, a direct comparison can be made between the plane slinger with screw return and the screw seal. This comparison shows that each slinger seal with screw return has a loss of 0.56 kw while each screw seal has a loss of 0.32 kw. Since the bearing runs flooded, power loss has been increased by a factor of three for the screw seal calculation. At any rate, there is considerable overall power saving by substituting a screw seal for a slinger seal despite the increase in bearing power loss.

The pressure measurements on the anti-drive end demonstrate the pumping ability of the bearing. The oil flow was set at 180 lb/hr. The inlet pressure required to attain this flow was -21.0 inches Hg. The 3.5 inches Hg pressure drop from the inlet line to the cavity gives a cavity pressure on the outboard side of the bearing of -24.5 inches. The bearing

SNAP-8 ALTERNATOR TEST #17 & #18
SCREW SEAL CONFIGURATION ON ANTI DRIVE END

Quill 5
Barometer 29.40 in Hg
Amb. Temp. - 73.5°F

Test #17 (2/6/64)

Time	Sump Press in Hg	Sump Temp °F	ADE Inlet Press.	ADE Cavity Press.	ADE Discharge Pressure	ADE Flow GPM	DE Inlet Press. Psig.	DE Cavity Press.	DE Otbd. Slinger Press.	DE Inbd. Slinger Press.	DE Flow GPM	Gen. Cavity Press.	Pump Discharge Psig.	Seal Press. Psig.	N rpm	Heat Watts
11:45	0	210	1.6 psig	.1 psig	.5 psig	20.2	11.8	.5 psig	.7 psig	.5 psig	20.5	0	32.0	2.0	2,100	-
12:15	0	210	1.4	.1	.7	21.0	11.2	- .5 " Hg	.6	.5	21.0	0	31.0	2.0	4,020	-
12:30	0	217	1.1	- .5 " Hg	.5	21.7	11.0	- 1.5	.5	1.0	21.5	0	30.0	2.0	6,020	-
13:40	-20.0	235	-19.2 " Hg	-21.0 " Hg	-18.2 " Hg	21.8	.4 psig	-22.7 " Hg	-15.0 " Hg	-15.0 " Hg	21.8	-30.0	35.5	2.0	6,000	-
14:05	-20.0	230	-19.9	-22.7	-18.2	25.0	4.9	-23.8	-15.5	-15.0	25.0	30.0	38.0	2.0	8,000	-
14:35	-20.0	229	-21.0	-24.0	-18.0	28.0	8.5	-26.0	-15.5	-15.0	28.2	30.0	38.0	2.0	10,020	-
14:55	-20.0	227	-21.2	-24.6	-17.5	31.0	11.1	-27.5	-16.0	-15.0	31.0	30.0	36.0	2.0	11,980	-
15:55	-20.0	230	-21.0	-24.5	-17.5	31.0	11.2	-27.3	-16.0	-15.0	31.0	30.0	36.0	2.0	12,000	-
16:55	-20.0	230	-21.0	-24.5	-17.5	31.0	11.2	-27.3	-16.0	-15.0	31.0	30.0	36.0	2.0	12,000	-

Quill 5
Barometer 28.97 in Hg
Amb. Temp. - 73.5°F

Test #18 (2/7/64)

Time	Sump Press in Hg	Sump Temp °F	ADE Inlet Press.	ADE Cavity Press.	ADE Discharge Pressure	ADE Flow GPM	DE Inlet Press. Psig.	DE Cavity Press.	DE Otbd. Slinger Press.	DE Inbd. Slinger Press.	DE Flow GPM	Gen. Cavity Press.	Pump Discharge Psig.	Seal Press. Psig.	N rpm	Heat Watts
10:15	0	202	1.1 psig	- 1.0 " Hg	.5 psig	20.4	11.2	- .2 " Hg	.5 psig	0	20.0	0	30.0	2.0	2,100	-
10:45	0	214	1.0	- 1.5	.7	21.0	9.9	- 3.5	.5	0	21.0	0	30.0	2.0	6,020	-
11:20	-20.0	230	-20.0 "Hg	-17.0 " Hg	-17.5 " Hg	25.0	5.9	-18.0 " Hg	-15.0 " Hg	-15.0 " Hg	25.5	-30.0	37.0	2.0	8,000	-
11:45	-20.0	225	-21.5	-24.5	-17.5	31.0	11.5	-27.2	-16.5	-15.0	31.0	30.0	37.0	2.0	12.020	-
12:45	-20.0	227	-21.5	-24.8	-17.5	31.2	11.5	-27.5	-16.2	-15.0	31.4	30.0	37.0	2.0	11,980	-287
13:45	-20.0	230	-21.4	-24.5	-17.5	31.0	10.9	-27.5	-16.2	-15.0	31.0	30.0	37.0	2.0	12,000	-287
14:45	-19.8	230	-21.0	-24.5	-17.5	31.0	10.8	-27.5	-16.2	-15.0	31.0	30.0	37.5	2.0	11,980	-287
15:45	-20.0	227	-21.2	-24.8	-17.8	31.0	10.6	-27.5	-16.2	-15.0	31.0	30.0	37.5	2.0	12,020	-275
16:45	-20.0	227	-21.5	-24.9	-17.9	31.0	10.6	-27.5	-16.2	-15.0	31.0	30.0	37.5	2.0	12,020	-246

Figure 30
Pressure and Flow Data Screw Seal

BEARING-SEAL TEMPERATURE vs TIME IN HOURS

Test No. 18
Date: 2-6-64

Drive End

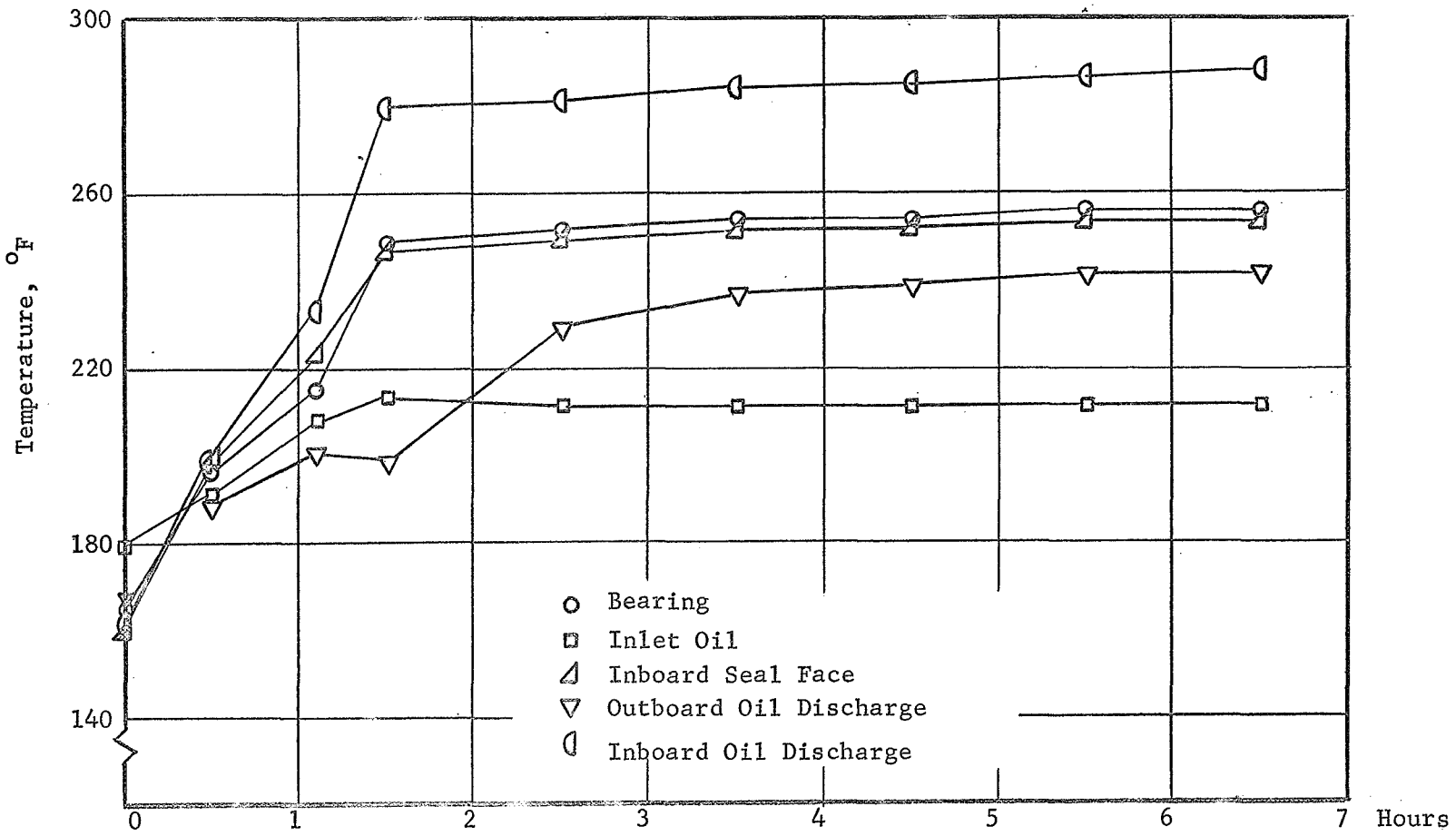

Running Time

Figure 31

BEARING-SEAL TEMPERATURE vs TIME IN HOURS

Anti-Drive End

Test No. 18
Date: 2-6-64

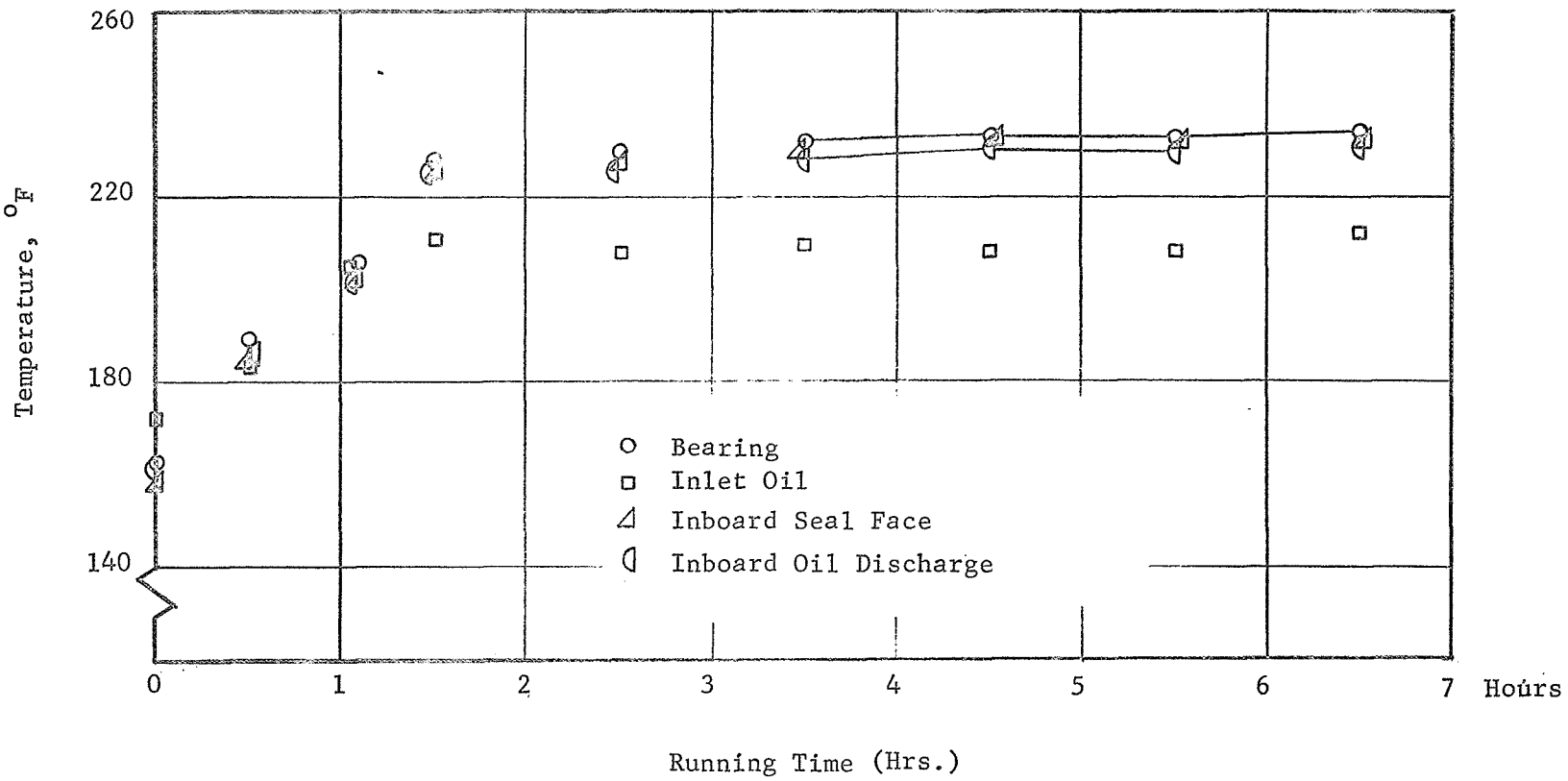

Figure 32

then pumped the fluid up to -17.5 inches Hg, a pressure rise of 7.0 inches Hg.

The leakage rates for Test No. 18 are given in Figure 33. Leakage rates on the drive end were in the range of leakage rates measured previously. On the anti-drive end, the leakage rate of the inboard screw seal was very low. On the outboard side, however, the leakage rate was excessive.

Since, under atmospheric conditions, neither side showed any measurable leakage, the addition of vacuum appears to destroy the sealing capability. It was thought at first that entrained air in the oil was contributing to the seal breakdown. Therefore, the oil was degassed at 300°F for a period of 48 hours prior to running Tests Nos. 17 and 18. This made no great improvement over previous checkout runs.

The side which leaked is on the low pressure side of the bearing. By throttling the discharge line, it is possible to raise the pressure level of the anti-drive end. This was done until the pressure drop across the screw seal exceeded the design value (i.e., the oil filled the entire length of the seal) and gross leakage occurred. Up to that point there was no discernable change in leakage rate.

Before further work could be done to pinpoint the cause of this leakage, the funds devoted to this portion of the development project were used up. The leakage is dependent upon the existence of vacuum, and occurs in the low pressure side of the bearing. Three possible causes have been suggested.

1. Perhaps the pumping action of the bearing prevents the formation of a continuous body fluid within the seal. This would break down sealing action.

2. Another possibility is that the oil is cavitating. Since the breakdown occurs on the lower pressure side of the bearing, this is consistent with the cavitation hypothesis.

3. Entrained gas in the oil may cause the seal to break down.

LEAKAGE RATE

Date: 2-7-64

SNAP-8 SEAL TEST

Test #18

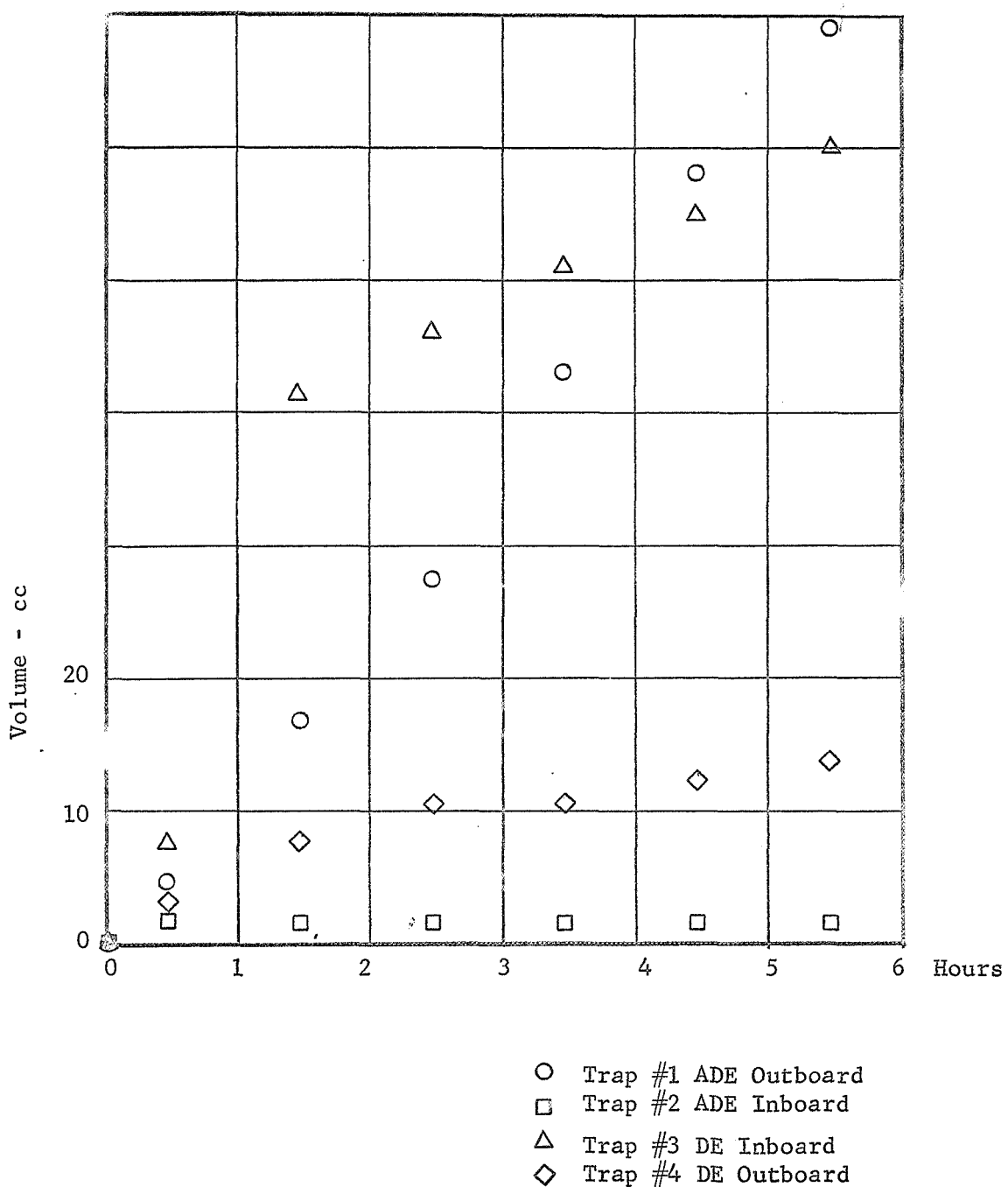

Figure 33

This cause appears unlikely since the oil was degassed prior to running.

The screw seal with flooded bearing cavity was tested under both atmospheric and vacuum conditions. Under atmospheric conditions, there was no measurable leakage. Under vacuum conditions, leakage rates were worse than either the plane slinger with screw return or the housing-disk seal described in previous reports.

Power loss for the screw seal system was lower than either the plane slinger with screw return or the housing-disk seal. The bearing also ran cooler with this type lubrication system.

E. Comparison of Measured and Calculated Power Losses

Table 9 shows a comparison between measured and calculated powers. The measured values have been corrected for the losses from the Sealol seal on the drive end of the test machine.

Table 9

Comparison of Calculated and Measured Power

Configuration	Measured Power kw	Calculated Power kw
Average Plane Slinger with Screw Return	2.46	2.02
Average Plane Slinger without Screw Return	2.46	2.02
Average Housing-Disk seal on Outbd ADE	2.62	2.45
Average Screw Seal on Inbd and Otbd ADE	2.22	1.69

The calculated values are based on the calculations of Section II. The entry for the housing-disk seal, for instance, is made up of the calculated loss for 1 housing disk, 3 slingers and 2 bearings. The measured power values are consistently higher than the calculated values. The results, however, are considered accurate enough for design purposes.

F. Summary of Leakage Data

Table 10 is a summary of the leakage rates for the three seal systems. Tests 4 through 8 were the plane slinger with screw return. Leakage rates varied from values below the sensitivity of the measurement system to 4 cc/hr. It is felt that part of this large scatter is a result of the sensitivity of this type of seal to the axial clearance. The rotor appeared to be displaced toward the drive end as the ADE Inbd and DE Otbd seals have consistently lower leakage rates except for Test No. 4, where a leaky "O" ring complicates the picture. This indicates closer clearances on the two seals with the lower rates. At any rate, a leakage rate of 4 cc/hr is entirely feasible for this configuration, and by reducing the axial clearance lower rates appear possible.

The addition of a non-wetting coating on the seal parts appears to improve seal performance. Prior to Test No. 6, the seal parts of the anti-drive end outboard seal were coated with a teflon coating, Molykote Experimental Product 519X. The leakage rate decreased for this seal. However, with further testing the leakage rate gradually increased. Examination of the seal parts showed that the coating did not hold up and had begun to fall off. If a reliable creep free coating could be obtained, the use of a thin coating on the seal parts appears to reduce leakage.

The housing-disk seal, Test No. 11, demonstrated the lowest leakages, less than .025 cc/hr. This was the only seal configuration which met the desired rate of .025 cc/hr. However, its complicated mechanical design and higher power loss are strong arguments against its use.

As pointed out in Section V-D, the screw seal worked well when sealing against atmospheric pressure. Under vacuum conditions it broke down, however, and gave 12.35 cc/hr leakage rate, ruling out its use in this environment. As the high-leakage occurred only on the low pressure side of

LEAKAGE DATA SUMMARY

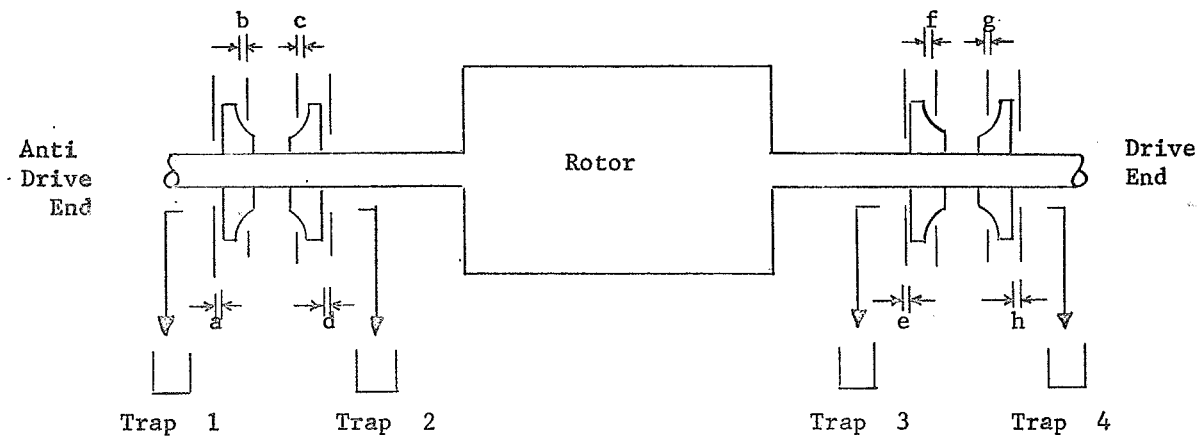

Duration / Trap No.	Test 4 36 Hrs. Gap Inches	Leak CC/HR	Test 6 6 Hrs. Gap Inches	Leak CC/HR	Test 7 10 Hrs. Gap Inches	Leak CC/HR	Test 8 5 Hrs. Gap Inches	Leak CC/HR	Test 11*** 32 Hrs. Gap Inches	Leak CC/HR	Test 18+ 5.5 Hrs. Gap Inches	Leak CC/HR	Test 20++ 14 Hrs. Gap Inches	Leak CC/HR
1	.017	3.92	0.022*	0	0.022*	0.244	0.022*	0.375	Not Applicable	0	Not App.	12.35	.024	3.17
2	.0245	0	0.0245	0	0.0245	0	0.0245	0	.0245	0	Not App.	.273	.025	4.44
3	.0245	.416	0.0245	1.33	0.0245	3.5	0.0245	0.61	.0245	1.8	.0245	4.66	.024	1.56
4	.017	4.34	.022	0**	0.022	0	0.022	0	.022	.87	.022	1.5	.022	0

* Teflon Coated on ADE - Outboard Seal
** 0" Ringe installed on OD of sealol seal DE for this and subsequent tests
***Housing-Disk Seal on Outboard Side Antidrive End
\+ Screw Seals on ADE
++ Screw Returns Removed on ADE

Note: Dimensions are given for Gap a, d, e, and h. For other gaps see drawing 421D692, Figure 12

Table 10

the bearing, it is thought that the oil may have been cavitating. This, however, is conjecture and further work is needed on this system.

VI. Conclusions and Recommendations

A. Conclusions

Tests of three types of non-contacting dynamic seals have shown leakage rates comparable to those of precision mechanical face seals. Power loss of these seals is higher than comparable rubbing face seals but the absence of rubbing parts offers the possibility of extremely long life and high reliability. Over 200 hours of test experience was accumulated on these seals.

The plane slinger with screw return produced leakage rates varying from .025 cc per hour, the minimum detectable rate, to 4 cc per hour sealing a 7.5 psia polyphenyl ether to vacuum. Nominal axial clearance was 23 mils; and maximum seal temperature did not exceed 290°F. The difference in leakage rates was due to variations in the axial clearances during and between tests. The results indicate that this type of seal is extremely sensitive to running clearance but that by maintaining axial clearances lower than 23 mils leakage rates approaching .025 cc per hour appear possible.

The housing-disk seal, a more complicated slinger seal, operating under the same conditions, exhibited leakage rates less than .025 cc per hour. The higher power loss of this seal design compared to the plane slinger with screw return and its greater mechanical complexity make it a less desirable design than the plane slinger with screw return.

The screw seal with flooded bearing cavity gave higher leakage rates, 12 cc per hour but has the advantage of consuming less power than the other designs tested. Until the leakage of this design sealing to vacuum is improved, it does not appear to have application in the SNAP-8 alternator.

Simulation of electrical pole face losses during test by electric heaters showed that all three seal designs could remove a heat load of 150 watts per bearing end with only an average 6°F rise in bearing temperature. Maximum seal temperature did not exceed 290°F and maximum bearing temperature did not exceed 260°F even with a 300 watt total heat input.

B. Recommendations

1. The test results demonstrated that the slinger seal is extremely sensitive to clearance and engagement effects (amount of surface wetted). The

test program should be extended to study the effect of clearance ratio and engagement on the leakage, drag, flow, and pressure characteristics of slinger seals.

2. The failure of the screw seal to seal adequately against a vacuum warrants additional study of screw seal operation under vacuum conditions. Visual studies of the fluid interface under vacuum conditions would be particularly helpful.

3. Initial tests indicated that the wetting characteristics of the sealed fluid on the seal parts may play a role in determining seal leakage rates. The advantage of using non-wetting coatings on seal parts should be further investigated for both slinger and screw seals.

APPENDIX A

SLINGER SEAL THEORY

A. INTRODUCTION

The slinger seal, shown in Figure A1, is simply a partially wetted disk rotating within an enclosed chamber. The totally wetted disk rotating within an enclosed chamber, a limiting situation of the partially wetted case, has been both analytically and experimentally investigated previously.

The most comprehensive analysis of the totally wetted disk is that of Daily and Nece in Reference 8. Their essential contribution was the experimental verification of the four basic modes of flow which exist for the totally wetted disk rotating within an enclosed chamber. These flow regimes are classified as follows:

TABLE A1

Regime	Description
I	Laminar Flow, Merged Boundary Layers
II	Laminar Flow, Separate Boundary Layers
III	Turbulent Flow, Merged Boundary Layers
IV	Turbulent Flow, Separate Boundary Layers

Daily and Nece showed that the possible existence of these modes of flow was dependent upon the Reynolds Number - spacing ratio combinations of the system. Figure A2, based on the work of Daily and Nece, shows the extent of the modes of flow as a function of the Reynolds Number, R, and the spacing ratio, s/a. Within each flow regime there is a different functional relation-

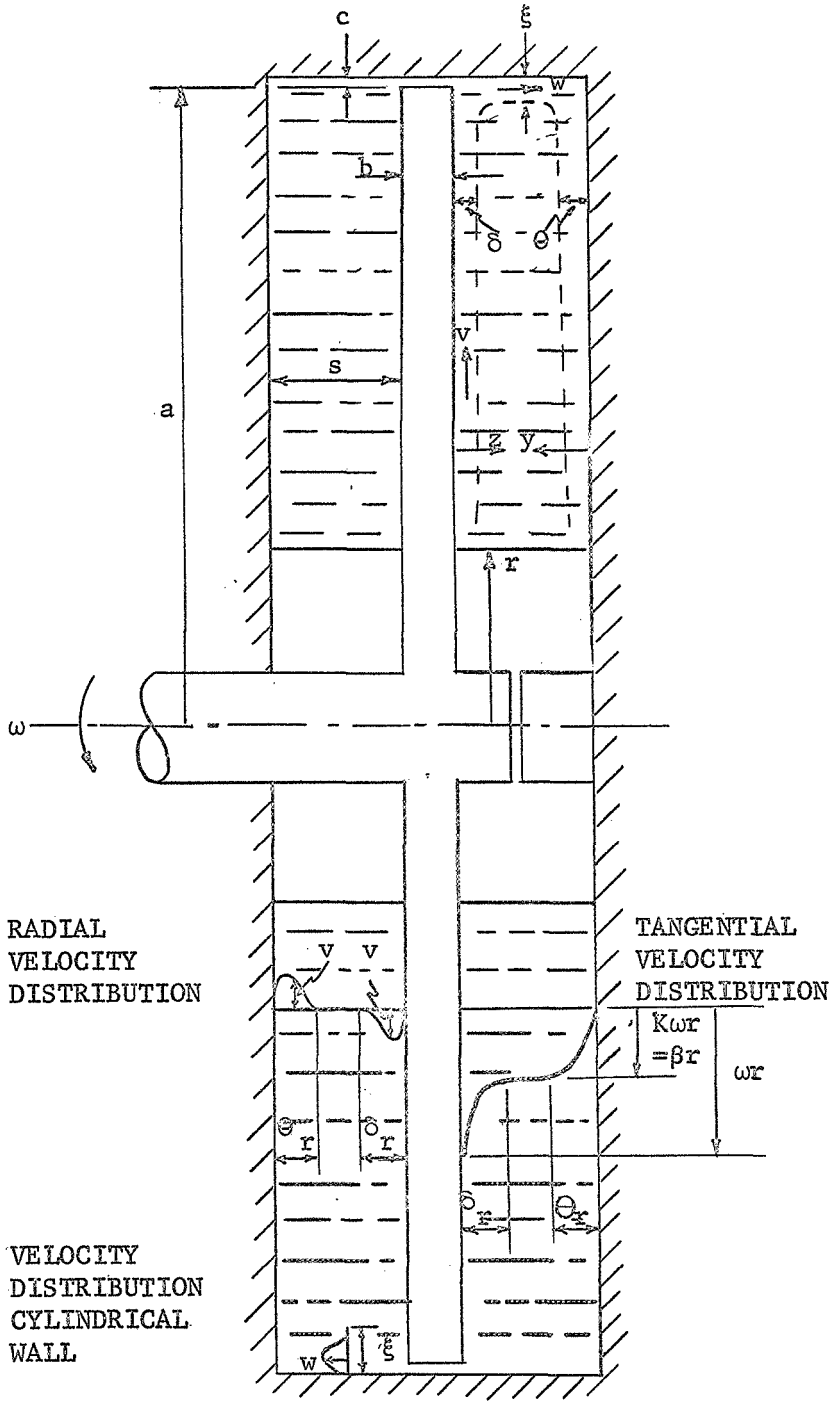

Fig. A1 - Schematic of Partially Wetted Disk

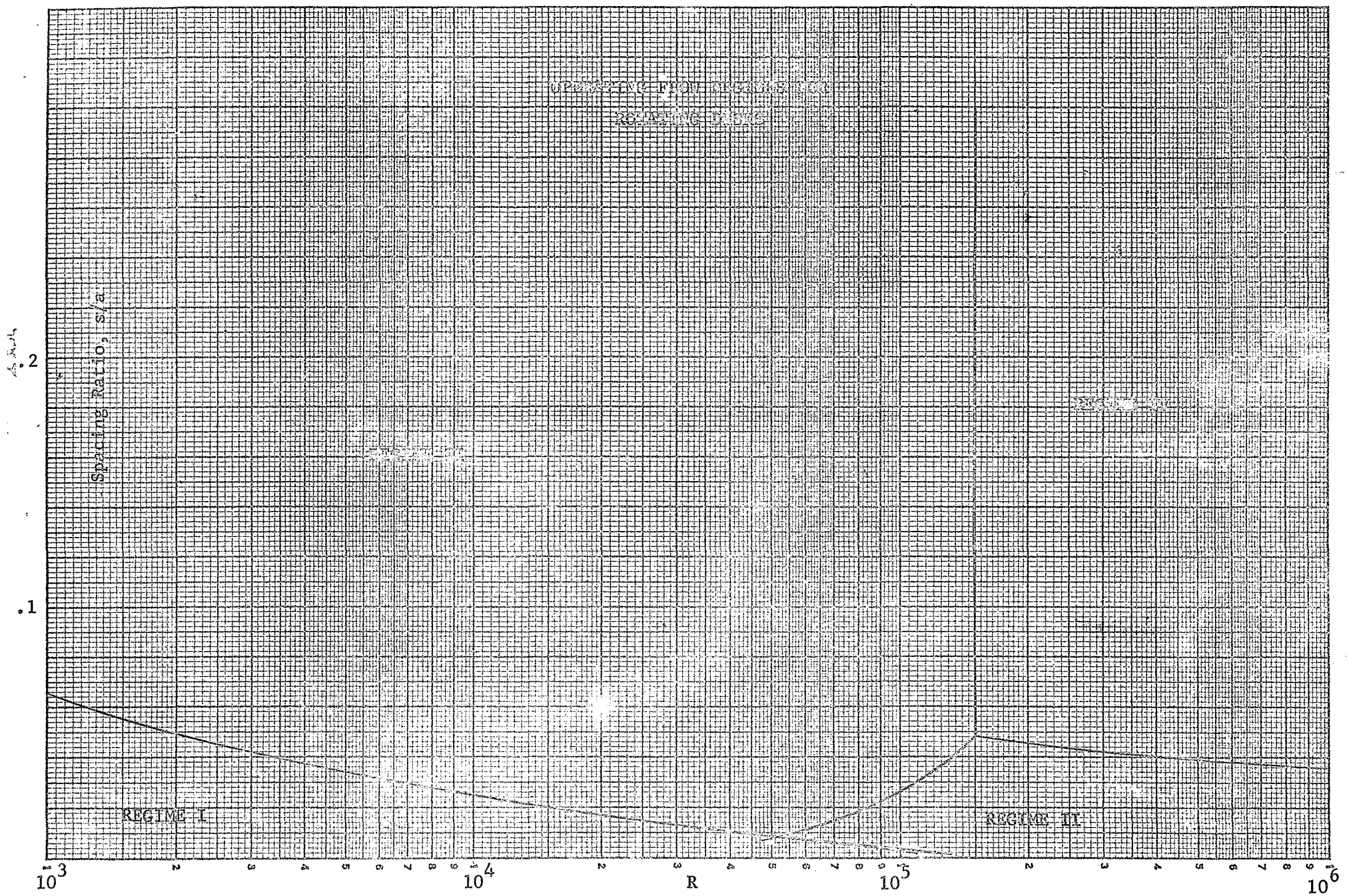

Figure A2

ship between the torque coefficient, pressure coefficient, and the Reynolds Number - spacing ratio combination. As an example, the empirical and analytical expression for frictional torque coefficients for each regime are shown in Table A2.

TABLE A2

Summary of Torque Coefficients for a Totally Wetted Rotating Disk

Regime	Empirical Equation	Theoretical Equation
I	$C_m = \frac{2\Pi}{(s/a)\,Re}$	$C_m = \frac{2\Pi}{(s/a)\,Re}$
II	$C_m = \frac{3.70\,(s/a)^{1/10}}{Re^{1/2}}$	$C_m = \frac{C}{Re^{1/2}}$, $C = \phi\,(s/a)$
III	$C_m = \frac{.080}{(s/a)^{1/6}\,Re^{1/4}}$	$C_m = \frac{.0622}{(s/a)^{1/4}\,Re^{1/4}}$
IV	$C_m = \frac{0.102\,(s/a)^{1/10}}{Re^{1/5}}$	$C_m = \frac{C}{Re^{1/5}}$, $C = \phi\,(s/a)$

It is important to note that the spacing ratio plays a crucial role in the problem. First, its absolute value determines in part the mode of flow within the chamber and, secondly, within any particular flow regime, its value affects the drag and pumping characteristics of the disk.

For the analysis of the partially wetted disk, it is assumed that all four possible modes of flow will still exist and that their existence will depend upon the Reynolds number - s/a combination of the system. Within any particular flow regime, the operational characteristics of the disk, flow,

pressure, and drag, will be a function of not only an s/a but also of another parameter, the engagement ratio, (a-r)/a. The engagement ratio is a measure of the submergence of the disk in the fluid. An engagement ratio of zero means the disk is not wetted at all, while an engagement ratio 1.0 is the limiting case of the totally wetted disk.

B. ANALYSIS OF THE PARTIALLY WETTED DISK

A theoretical analysis of the partially wetted disk has not been considered previously in the literature with the exception of the analysis by McCann [10] for Regime IV. Since all four regimes are of interest, the analysis has been extended here to cover the four possible modes of flow. An analysis of each mode of flow is presented, followed by a discussion of the pressure and flow characteristics of the partially wetted disk.

B-1. Regime I Laminar Flow, Merged Boundary Layers

For this case, a Couette laminar tangential velocity profile is assumed, with no radial components. The fluid is contained in an annular ring of arbitrary inner radius R and outer radius equal to a. Note that the radius of the disk and the stationary wall are approximately the same since the radial clearance is considered very small, therefore, $a \approx b$ (refer to Figure A1 for nomenclature).

It will be found useful to define a new variable which is denoted as x, where $x = (a-r)/a$ on the rotor or equivalently $(b-r)/b$ on the stator. For the case where $r = R$, then $x = X$ and X is denoted as the submersion ratio or engagement ratio.

Proceeding with Regime I, the effect of the cylindrical wall will be ignored since the spacing ratios for this flow regime are so small. Therefore it is possible to equate the moments on the rotating and stationary portions; which will be equivalent due to the symmetry of the linear velocity distribution. The tangential shear stress on the rotating disk is given as

$$\tau_t = \mu \frac{du}{dz} \quad \text{or} \quad \tau_t = \frac{\mu\omega r}{s}$$ for the linear velocity

distribution. Substituting this value into the moment equation for one side of the disk:

$$M = \int_R^a 2\pi\, r^2\, dr \,.\, \tau_t = \frac{2\,\pi\,\mu\,\omega}{s} \int_R^a r^3\, dr \qquad \text{(A1)}$$

Changing to the new variable x,

$$M = \frac{2\,\pi\,\mu\,\omega}{s} \int_X^0 a^3\,(1 - x)^3\,(-a\,dx) \qquad \text{(A2)}$$

Evaluating this equation:

$$M = \frac{\pi\,\mu\,\omega\,a^4}{2\,s} \left[1 - (1 - X)^4 \right] \qquad \text{(A3)}$$

The expression in brackets in Equation A3 is denoted as C_3, which is then a function of X, the submersion ratio. Casting Equation A3 in terms of the moment coefficient C_m where $C_m = \dfrac{2\,M}{\rho\,\omega^2\,a^5}$

or

$$C_m = \frac{\pi\,C_3}{\frac{s}{a}\,\frac{\omega a^2}{\nu}}$$

$$C_m = \frac{\pi\,C_3}{\left(\frac{s}{a}\right) Re} \qquad \text{(A4)}$$

This equation now is the general equation for an arbitrarily wetted disk in terms of the important parameters. For the special case where $R = 0$, and $X = 1.0$, i.e., totally wetted disk, this reduces to the totally wetted case of Table A2. The equation for C_3 is plotted in Figure A3 which shows that as the disk becomes increasingly wetted $(X > 0)$, holding other variables constant, the moment coefficient can be expected to increase rapidly at first then taper off at about $x = 0.5$ and approach the final value relatively slowly.

REGIME I ROTATING DISK

$$C_M = \frac{\pi C_3}{(s/a)Re}$$

where: $C_3 = \left[1 - (1 - X)^4\right]$

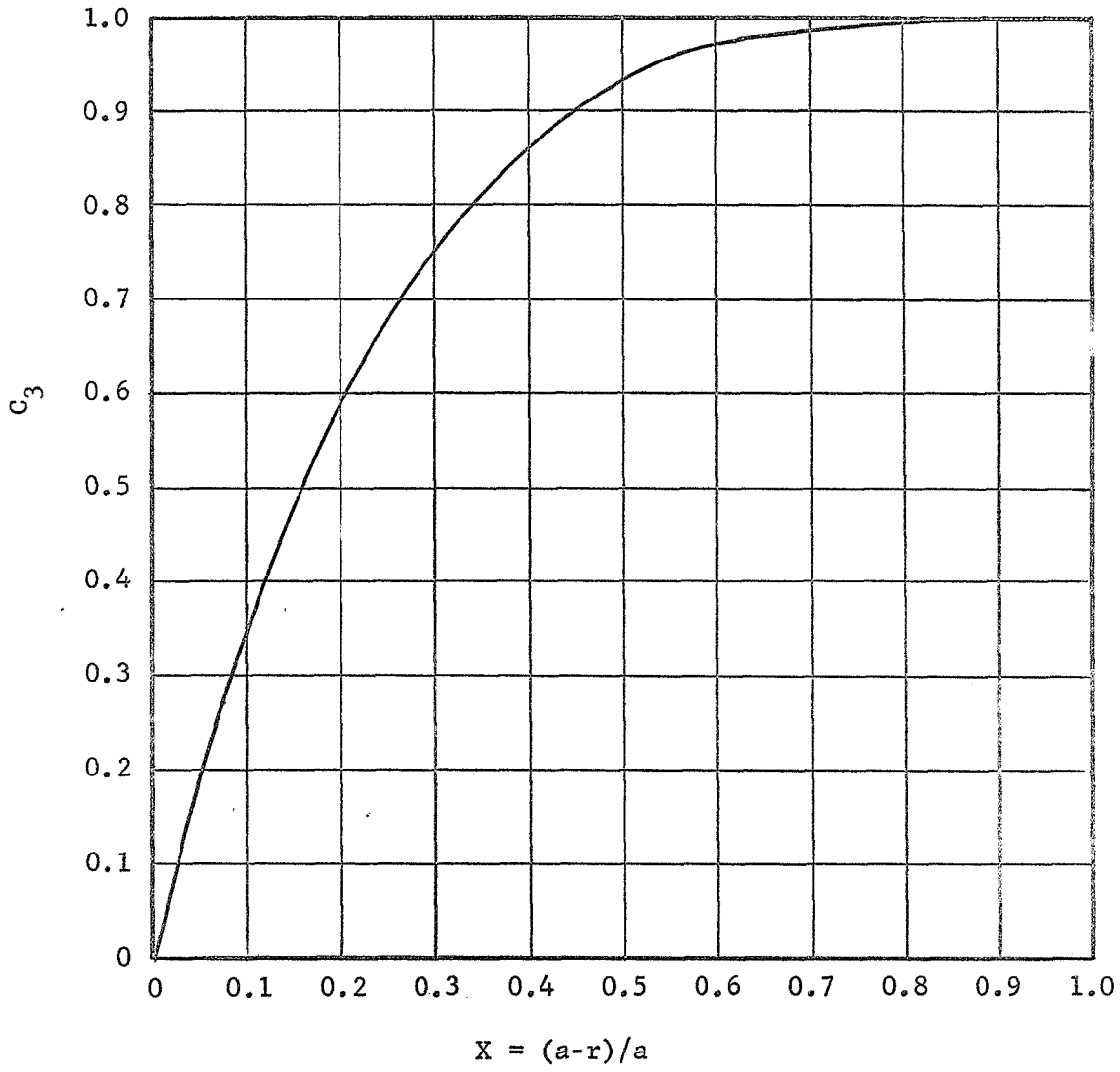

Figure A3

B-2. Regime II Laminar Flow, Separate Boundary Layers

For this regime, it is necessary to make certain assumptions regarding the secondary or radial flows. The basic assumption has been to regard all radial flow as taking place only within the boundary layers. The pattern of flow is radially outward on the rotating disk, axially away from this disk along the cylindrical wall and then radially inward along the stationary end wall.

The fluid outside of the boundary layers is assumed to rotate as a solid body with an angular velocity, β , which is less than the rotational speed of the disk, ω . The ratio of β/ω is defined as K, the velocity coefficient.

The boundary conditions that are implied in this model are:

1. Radial velocity v is zero at the surface of the disk and end wall and also at the edge of the boundary layer since no radial flow is assumed in the core. The same is true for the axial components along the cylindrical wall.
2. Tangential velocity u is equal to ωr at the disk surface at radius r, zero at the surfaces of the end and cylindrical walls, and everywhere in the core is equal to βr or $K\omega r$.
3. There is no axial pressure gradient, therefore the pressure gradient within the core is imposed on the entire body of fluid in the casing.

The method of solution for this case is based again on equating the moments for the rotating and the stationary parts. Schultz-Grunow [5] did not consider the effect of the cylindrical wall so there is no (s/a) term in his equation, while Daily and Nece did consider this effect in their analysis of the totally wetted disk. It is possible to write boundary layer momentum equations in a general form for both the rotating disk and the stationary wall as follows:

Rotating Disk

Radial Momentum Equation:

$$\rho\, r\, d\, r \int_0^{\delta} \frac{u^2}{r}\, dz - r\, d\, r\, \tau_r - \delta\, r\, \frac{dp}{dr}\, dr$$

$$= \frac{d}{dr}\left[\rho\, r \int_0^{\delta} v^2\, dz\right] dr \qquad \text{(A5)}$$

Tangential Momentum Equation:

$$r^2\, d\, r\, \tau_t = \frac{d}{dr}\left[\rho \int_0^{\delta} r^2 u v\, dz\right] dr \qquad \text{(A6)}$$

Stationary Disk

Radial Momentum Equation:

$$\rho\, r\, dr \int_0^{\Theta} \frac{u^2}{r}\, dy + r\, dr\, \tau_r - \Theta\, r\, \frac{dp}{dr}\, dr$$

$$= -\frac{d}{dr}\left[\rho\, r \int_0^{\Theta} v^2\, dy\right] dr \qquad \text{(A7)}$$

Tangential Momentum Equation:

$$r^2\, dr\, \tau_t = \frac{d}{dr}\left[\rho \int_0^{\Theta} r^2\, u\, v\, dy\right] dr \qquad \text{(A8)}$$

The analysis for this flow regime will retain the flow model as presented in the Schultz-Grunow paper [5] . Because the problem of the partially wetted disk is essentially one of utilizing the variable parameter of submersion ratio, the development is similar in many respects to the totally

wetted disk case. However, Schultz-Grunow did not allow for the consideration of the frictional moment of the cylindrical wall which shall be brought into this study.

Starting with the stationary disk, the assumed velocity profiles in the radial and tangential directions respectively are:

$$v = v_o^* \left[1 - (2\eta - 1)^2 \right] \tag{A9}$$

$$u = \beta r \left[1 - (1 - \eta)^2 \right] \tag{A10}$$

where:

$$\eta = y/\Theta$$

With these velocity distributions it is possible to calculate these typical integral expressions which appear in the momentum equation.

$$\begin{aligned}
\int_0^\Theta v^2\, dy &= (v_o^*)^2 \; (8/15) \\
\int_0^\Theta u^2\, dy &= \beta^2 r^2 \Theta \; (8/15) \\
\int_0^\Theta v\, u\, dy &= \beta r v_o^* \Theta \; (7/15) \\
\int_0^\Theta v\, dy &= v_o^* \Theta \; (2/3) \\
\left.\frac{dv}{dy}\right|_{y=0} &= 4 v_o^* / \Theta \\
\left.\frac{du}{dy}\right|_{y=0} &= 2 \beta r / \Theta
\end{aligned} \tag{A11}$$

Substituting these expressions into the radial and tangential momentum equations for the stationary wall, Equations A7 and A8, along with the assumption that there is no axial pressure gradient and the pressure imposed on the boundary layer is due to the solid body rotation of the core, i.e., $\frac{dp}{dr} = \rho \beta^2 r$ it is possible to derive the momentum equations in terms of v_o^* the maximum radial velocity at the center of the parabolic profile, Θ the boundary layer thickness, β the angular velocity of the fluid core and also containing r and v. Now, it becomes necessary to make some assumption regarding the growth of the boundary layer thickness, Θ, therefore the substitution $v_o^* \Theta = \Phi$ is made. Making the substitution and eliminating v_o^* the momentum equations reduce to,

$$\Phi^2 \Theta + 2 r \Phi \Phi' \Theta - r \Phi^2 \Theta' + \frac{7}{8} \beta^2 r^2 \Theta^3 = \frac{15}{2} \nu r \Phi \tag{A12}$$

$$\frac{11}{15} \Phi \Theta - \frac{1}{5} r \Phi' \Theta = 2 \nu r \tag{A13}$$

where the prime refers to the first derivative with respect to y or r. Rewriting these equations in terms of the variable $x = (b-r)/b$ Equations A12 and A13 become:

$$\Phi^2 \Theta - 2(1-x) \Phi \Phi' \Theta + (1-x) \Phi^2 \Theta' + \frac{7}{8} \beta^2 b^2 (1-x)^2 \Theta^3 - \frac{15}{2} \nu b \Phi (1-x) = 0 \tag{A14}$$

$$11 \Phi \Theta + 3(1-x) \Phi' \Theta - 30 \nu b (1-x) = 0 \tag{A15}$$

Solutions are introduced in the form of the following series

$$\Phi = x^n (C_o + C_1 x + C_2 x^2 + \ldots); \quad \Theta = x^p (d_o + d_1 x + d_2 x^2 + \ldots) \tag{A16}$$

By this method of solution the values of n and p have to be selected such that the exponents of x in Equations A14and A15 are different only by integers. This occurs when

$$n = 3/4, \quad p = 1/4$$

The coefficients c and d in the series solutions are then determined such that the left hand sides of Equations A14and A15are equal to zero. The results for Φ and Θ are:

$$\Phi = x^{3/4} b (\beta \nu)^{1/2} \left[3.04 - 4.64 x + 2.839 x^2 - 2.855 x^3 - 1.814 x^4\right] \quad \text{(A17)}$$

$$\Theta = x^{1/4} \left(\frac{\nu}{\beta}\right)^{1/2} \left[4.385 - 5.845 x + 4.015 x^2 - 4.46 x^3 - 1.29 x^4\right] \quad \text{(A18)}$$

It is seen that the boundary layer thickness, Θ, is a rather complicated function of x and that it starts at zero at the outer radius i.e., $r = b$; $x = 0$, and grows radially inward. It becomes possible with the information available to evaluate the moment on the stationary end wall since $\tau_t = \mu \left.\frac{du}{dy}\right|_{y=0} = \mu \frac{2 \beta r}{\Theta}$. Substituting this into the moment equation,

$$M = \int_R^b 2 \pi r^2 \left(\mu \frac{2 \beta r}{\Theta} \right) dr \quad \text{(A19)}$$

Changing to $x = (b-r)/b$ and switching the integration limits,

$$M = 4 \pi \mu \beta b^4 \int_0^X \frac{(1 - x)^3}{\Theta} dx \quad \text{(A20)}$$

Since Θ is such a complicated function of x, this integral must be evaluated graphically. It should be noted that the value of X, the submersion ratio can be varied yielding various values for the integral quantity and

therefore the variation of the moment with X. Values of Θ have been tabulated as a function of x and the function $2(1-x)^3/\Theta$ is shown plotted in Figure A4. The integral is asymptotic to the ordinate so that an approximation for the value of the integral is carried out in the range $0 \leq x \leq .02$ by assuming that $\Theta = x^{1/4}\left(\frac{\nu}{\beta}\right)^{1/2} 4.385$ and $(1-x)^3$ is equal to $(1-3x)$. On this basis,

$$M\Big/_{o}^{0.02} = 2\pi\mu\beta b^4 (\beta/\nu)^{1/2} (.0316) \tag{A21}$$

Combining this result into Equation A20

$$M = 2\pi\mu\beta b^4 (\beta/\nu)^{1/2} \left[.0316 + \int_{.02}^{X} \frac{2(1-x)^3}{\Theta}\right] \tag{A22}$$

The term in brackets in Equation A22 is denoted as C_1. Values of C_1 for a given submersion ratio, X, are tabulated in Table A3, Where the moment on the stationary disk is established.

The second part of this problem now is to find the moment on the rotating disk in terms of β/ω or K. Beginning with the radial and tangential velocity profiles,

$$v = v_o \left[1 - (2\eta - 1)^2\right] \tag{A23}$$

$$u = \omega r - (\omega - \beta) r \left[1 - (1-\eta)^2\right] \tag{A24}$$

where

$$\eta = \frac{z}{\delta}$$

FUNCTION OF BOUNDARY LAYER

GROWTH ON STATIONARY WALL, ROTATING DISK,

REGIME II

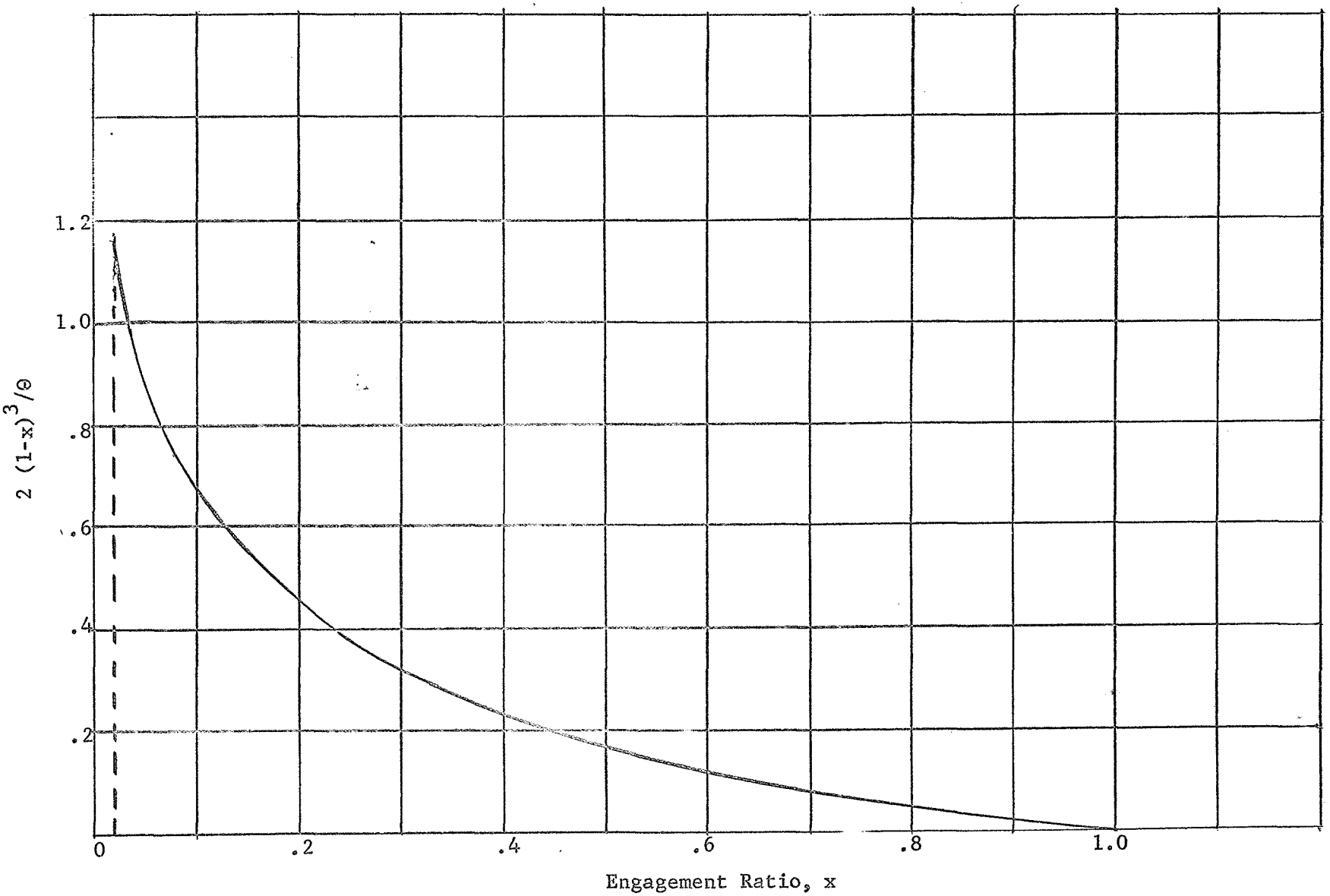

Figure A4

TABLE A3

X	$C_1 = \dfrac{.0316 + \int_{.02}^{X} \frac{2(1-x)^3}{\Theta}\, dx}{}$
.1	.1016
.2	.1566
.4	.2232
.6	.2560
1.0	.2746

Substituting these values into the momentum equations for the rotating disk (Equations A5 and A6), they become,

$$\frac{8}{15}\frac{d}{dr}\left(r\, v_o^{\,2}\delta\right) - \beta^2 r^2 \delta\left[1 + \frac{2}{3}\left(\frac{\omega}{\beta} - 1\right) + \frac{1}{5}\left(\frac{\omega}{\beta} - 1\right)^2\right]$$

$$= -8\,\nu\, r\,\frac{v_o}{\delta} - \beta^2 r^2 \delta \tag{A25}$$

$$\beta\left(\frac{7}{15} + \frac{1}{5}\frac{\omega}{\beta}\right)\frac{d}{dr}\left(r^3 \delta\, v_o\right) - \frac{2}{3}\beta r^2 \frac{d}{dr}\left(r\, v_o\, \delta\right)$$

$$= \nu\,(\omega - \beta)\, 2\left(\frac{r}{\delta}\right)^3 \tag{A26}$$

The solutions of these equations for δ, the boundary layer thickness on the rotating disk and v_o, the maximum velocity at the center of the parabolic radial velocity profile are,

$$\delta = (\nu/\beta)^{\frac{1}{2}} \frac{(150)^{\frac{1}{4}}}{\left(2 + 3\frac{\omega}{\beta}\right)^{\frac{1}{2}}} \left[\frac{6\frac{\omega}{\beta} - 1}{\frac{\omega}{\beta} + \frac{7}{3}}\right]^{\frac{1}{4}} \tag{A27}$$

$$v_o = \frac{r}{\delta^2} \; 2.5 \; \nu \left[\frac{\frac{\omega}{\beta} - 1}{\frac{\omega}{\beta} + \frac{2}{3}} \right] \tag{A28}$$

The thickness δ , is a constant value over the entire radius varying only with the value of ν , β , and ω . The moment on the rotating disk is given by

$$M = \int_R^a 2 \pi r^2 \, dr \, . \, \tau_t \tag{A29}$$

where

$$\tau_t = \mu \left(\frac{du}{dz} \right)_{z=0} = 2 \mu (\omega - \beta) \frac{r}{\delta} \tag{A30}$$

Then,

$$M_{RD} = \int_R^a 4 \pi \mu (\omega - \beta) \frac{r^3}{\delta} dr \tag{A31}$$

Switching to the new variable $x = (a-r)/a$ and changing the integration limits,

$$M_{RD} = 4 \pi \mu \frac{(\omega - \beta) a^4}{\delta} \int_0^X (1 - x)^3 dx \tag{A32}$$

Evaluating the integral,

$$M_{RD} = - \pi \mu \frac{(\omega - \beta)}{\delta} a^4 \left[1 - (1 - X)^4 \right] \tag{A33}$$

The term in brackets has been denoted as C_3 previously. Also the equation for δ can be modified and included in the equation. Rewriting Equation A27,

$$\frac{1}{\delta} = \left(\frac{\beta}{\nu} \right)^{1/2} \left[\frac{(2 + 3 \frac{\omega}{\beta})^{1/2}}{(150)^{1/4}} \left(\frac{\frac{\omega}{\beta} + \frac{7}{3}}{6 \frac{\omega}{\beta} - 1} \right)^{1/4} \right] \tag{A34}$$

Calling the term in brackets in Equation A34, C_2, then Equation A33 becomes

$$M_{RD} = -\pi \mu (\omega - \beta) a^4 \left(\frac{\beta}{\nu}\right)^{\frac{1}{2}} C_2 C_3 \tag{A35}$$

This completes the moment equation for the rotating disk, where C_2 is a function which is dependent on ω/β or $\frac{1}{K}$ and C_3 is dependent on the submersion ratio, X.

Consideration must now be given to the effect of the cylindrical wall in the problem. This will introduce the effect of spacing ratio $\frac{s}{a}$ into the equations, because obviously as the ratio $\frac{s}{a}$ grows larger it will have an increasing effect. In this case, the assumption is made that the boundary layer thickness on the cylindrical wall, ξ, is equal to the rotating disk thickness, δ, which is only a function of K. This is an approximate assumption, since no attempt is made to solve the exact equations for the cylindrical wall and match the boundary conditions at both the disk surface and the end wall.

The velocity distribution in the tangential direction corresponds to the velocity on the stationary end wall at the outside radius, a. Therefore, the tangential shear stress, τ_t, at the cylindrical wall is equal to τ_t at the end wall except that Θ must be replaced by δ. Therefore,

$$\tau_t = \mu \frac{2 \beta r}{\delta} \tag{A36}$$

or

$$\tau_t\Big/_{r=a} = \frac{2 \mu \beta a}{\delta} \tag{A37}$$

Using this value of shear stress in the moment equation for the cylindrical wall yields

$$M_{cw} = 2\pi a^2 s \cdot \tau_t = 4 \pi a^3 s \frac{\mu \beta}{\delta} \tag{A38}$$

which can be rewritten, using Equation A34 for $\frac{1}{\delta}$, as

$$M_{cw} = 4\pi a^4 \left(\frac{s}{a}\right) \mu \beta \left(\frac{\beta}{\nu}\right)^{1/2} C_2 \tag{A39}$$

Therefore, three equations are now available for the moments on all three surfaces. For a steady state condition, the moments on the stationary parts (end wall and cylindrical wall) must be equal to the moment on the rotating disk. Combining the moment equations for the stationary parts, Equations A22 and A39,

$$M_{st} = 2\pi \mu \beta b^4 \left(\frac{\beta}{\nu}\right)^{1/2} C_1 + 4\pi a^4 \left(\frac{s}{a}\right) \mu \beta \left(\frac{\beta}{\nu}\right)^{1/2} C_2 \tag{A40}$$

since $a \approx b$

$$M_{st} = 4\pi \mu \beta a^4 \left(\frac{\beta}{\nu}\right)^{1/2} \left[\frac{C_1}{2} + \left(\frac{s}{a}\right) C_2\right] \tag{A41}$$

Equating moments on the stationary and rotating parts

$$4\pi \mu \beta a^4 \left(\frac{\beta}{\nu}\right)^{1/2} \left[\frac{C_1}{2} + \left(\frac{s}{a}\right) C_2\right] = \pi \mu (\omega - \beta) a^4 (\beta/\nu)^{1/2} C_2 C_3 \tag{A42}$$

or,

$$4\beta \left[\frac{C_1}{2} + \left(\frac{s}{a}\right) C_2\right] = (\omega - \beta) C_2 C_3 \tag{A43}$$

then,

$$\frac{C_1}{2} + \left(\frac{s}{a}\right) C_2 = \left(\frac{\omega}{\beta} - 1\right) \frac{C_2 C_3}{4} \tag{A44}$$

By plotting both left and right hand sides of Equation A44 on the same graph, as a function $\frac{\omega}{\beta}$ and with $\frac{s}{a}$ as a parameter, the intersection of the curves gives the value of $\frac{\omega}{\beta}$ which satisfies the moment equilibrium

condition. Since this will also vary as the submersion ratio, this plotting was repeated for five values of X, 0.1, 0.2, 0.4, 0.6, and 1.0. Typical plots of this type are shown in Figures A5 and A6 where the extremes of X = 0.1 and 1.0 are compared. The velocity ratio, K, is plotted as a function of X with s/a as a parameter in Figure A7. Note that the values for X = 1.0 are for the special case of the totally wetted disk of Table and is plotted in Figure A8 for comparison to the theory and experimental data of Daily and Nece [8]. The agreement between the data, and the theory of this report is seen to be good.

Knowing the value of K for all conditions of X and s/a it is possible to evaluate the moment coefficient for the rotating disk. Since,

$$M_{RD} = \pi \mu \quad (\omega - \beta)\ a^4 \ \left(\frac{\beta}{\nu}\right)^{\frac{1}{2}} \quad C_2\ C_3 \tag{A45}$$

and $$C_m = \frac{2\ M}{\rho\, \omega^2\, a^5}$$

$$C_m = \frac{2\ \pi\ \mu\ (\omega - \beta)\ a^4\ (\beta/\nu)^{\frac{1}{2}}\ C_2\ C_3}{\rho\ \omega^2\ a^5} \tag{A46}$$

Simplifying Equation A46 and using $Re^{\frac{1}{2}} = (\omega)^{1/2} a \Big/ (\nu)^{1/2}$

$$C_m = \frac{2\ \pi\ (1 - K)\ K^{\frac{1}{2}}\ C_2 C_3}{Re^{\frac{1}{2}}} \tag{A47}$$

The value of $C_m (Re)^{\frac{1}{2}}$ can now be found as a function of s/a and X. These are shown plotted in Figures A9 and A10 respectively. Since the (s/a) variation is on a logarithmic scale in Figure A9, it is seen that to a very close approximation, $C_m (Re)^{\frac{1}{2}}$ varies as $(s/a)^{\frac{1}{10}}$. Therefore,

TYPICAL MOMENT EQUILIBRIUM PLOTS

ROTATING DISK, REGIME II

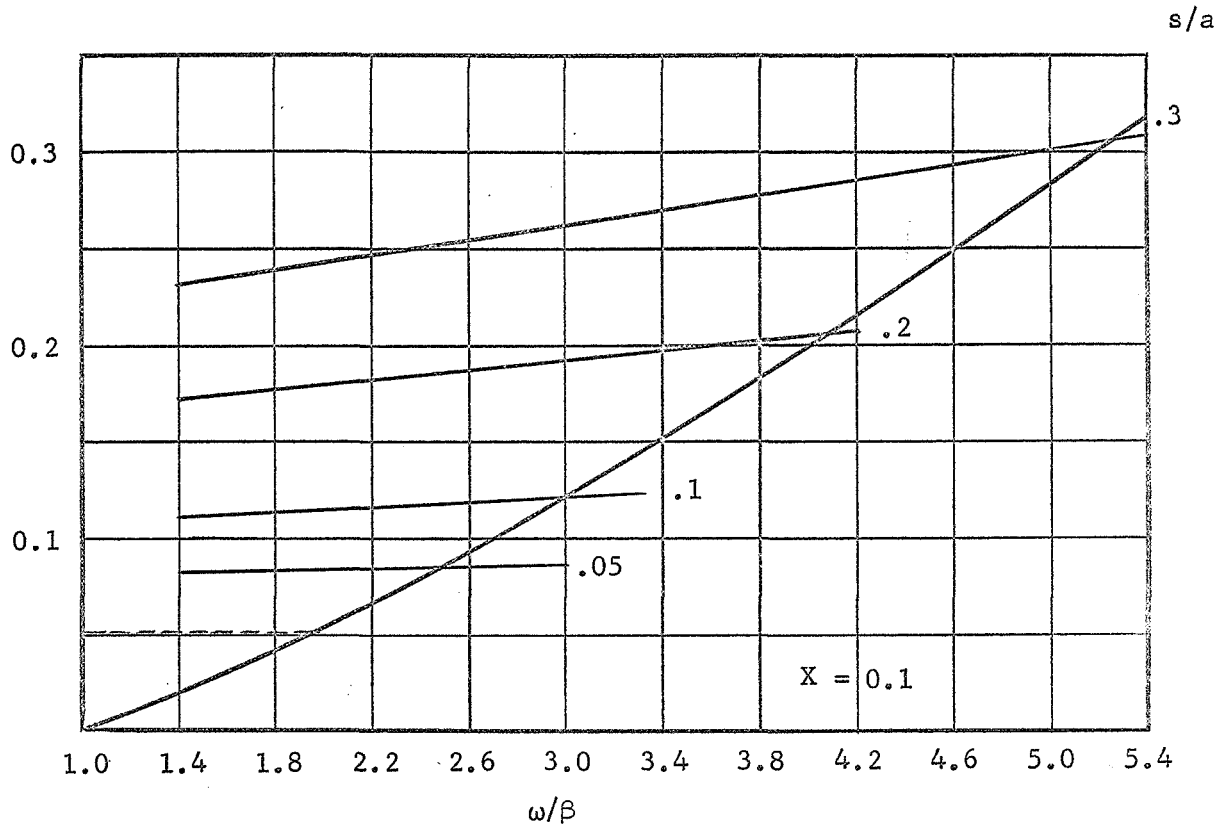

Figure A5

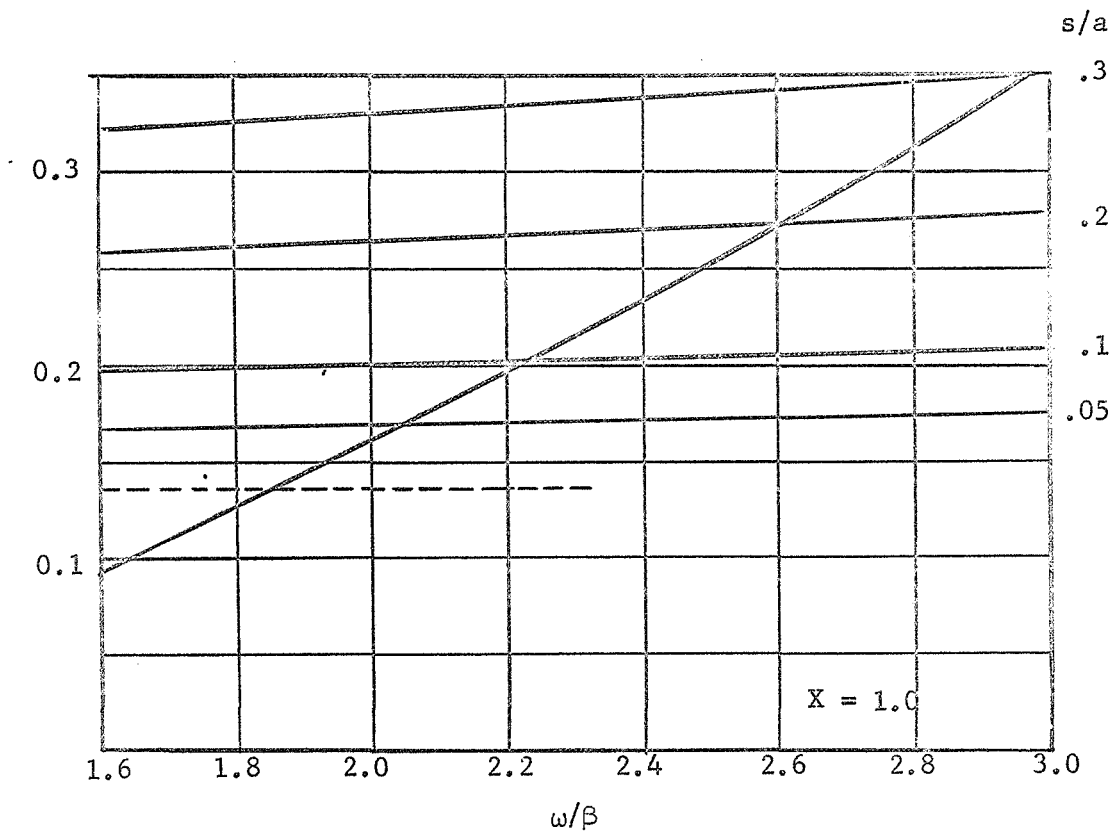

Figure A6

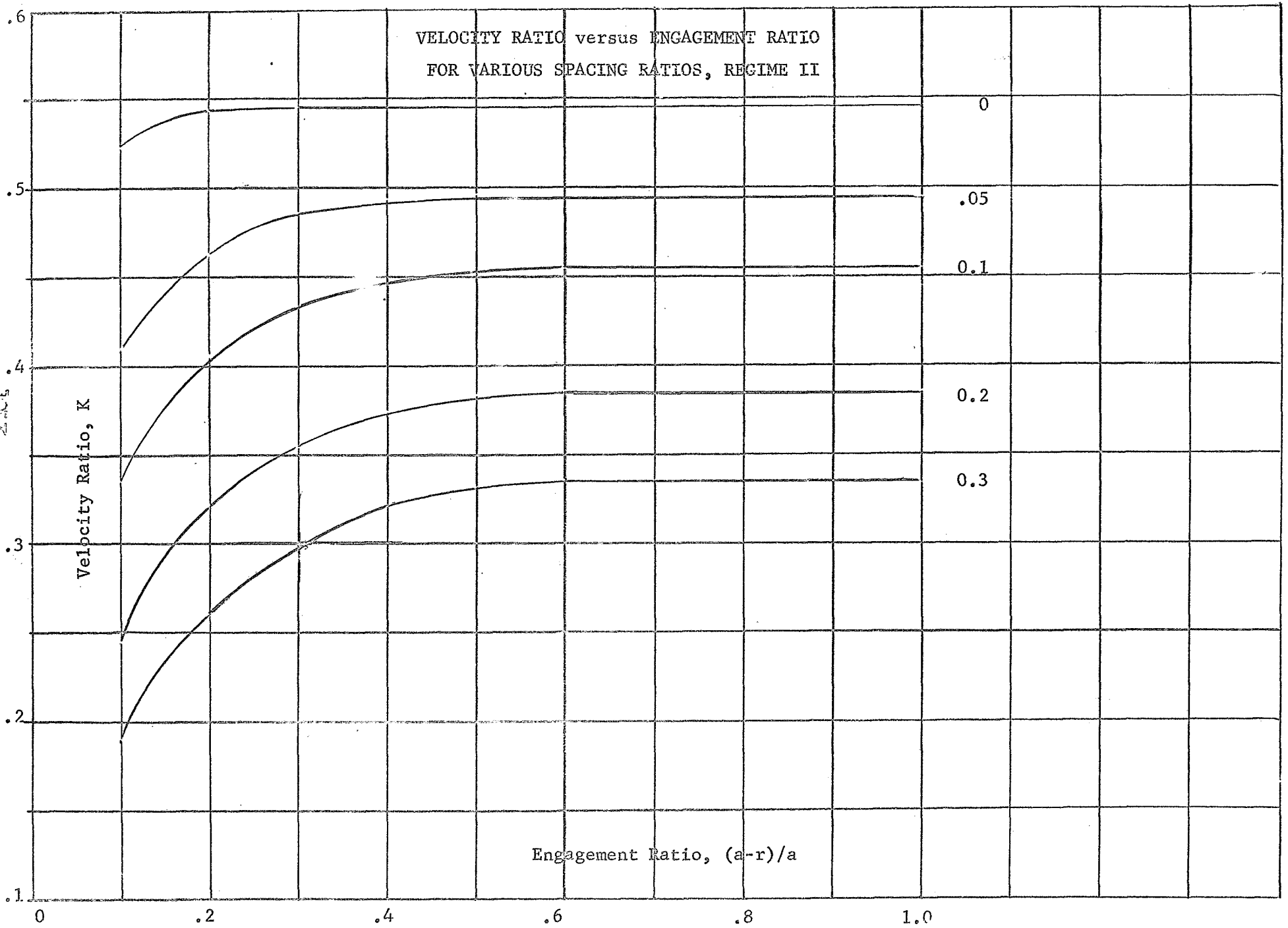
VELOCITY RATIO versus ENGAGEMENT RATIO
FOR VARIOUS SPACING RATIOS, REGIME II
Velocity Ratio, K
Engagement Ratio, (a-r)/a
.6
.5
.4
.3
.2
.1
0
.2
.4
.6
.8
1.0
0
.05
0.1
0.2
0.3

Figure A7

COMPARISON BETWEEN THEORETICAL AND EXPERIMENTAL
PREDICTION OF VELOCITY RATIO, AND MOMENT COEFFICIENT
ROTATING DISK, REGIME II

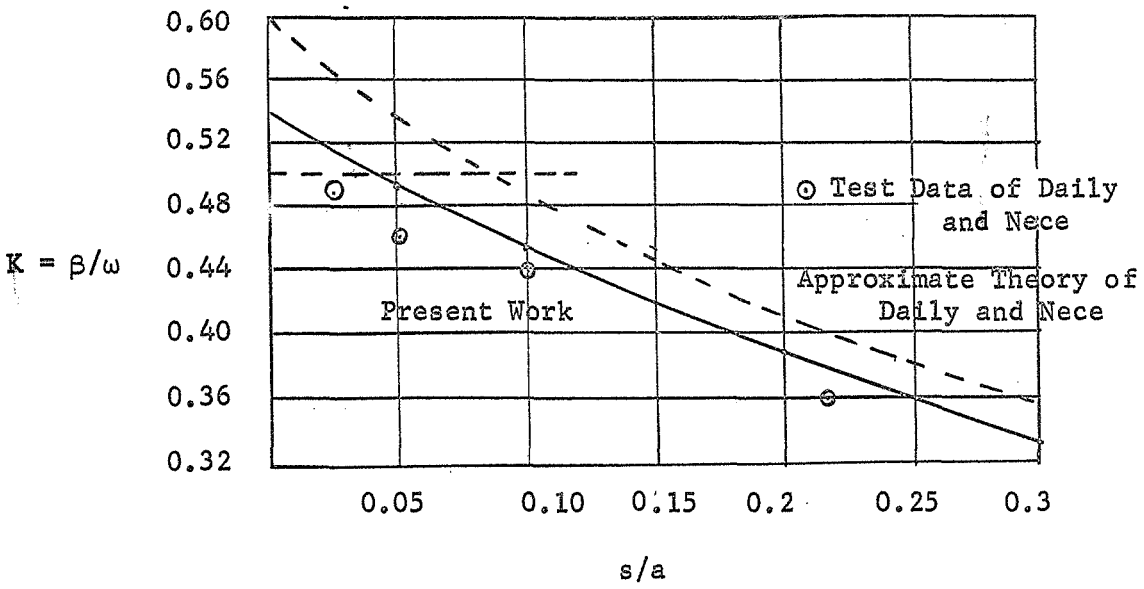

Figure A8

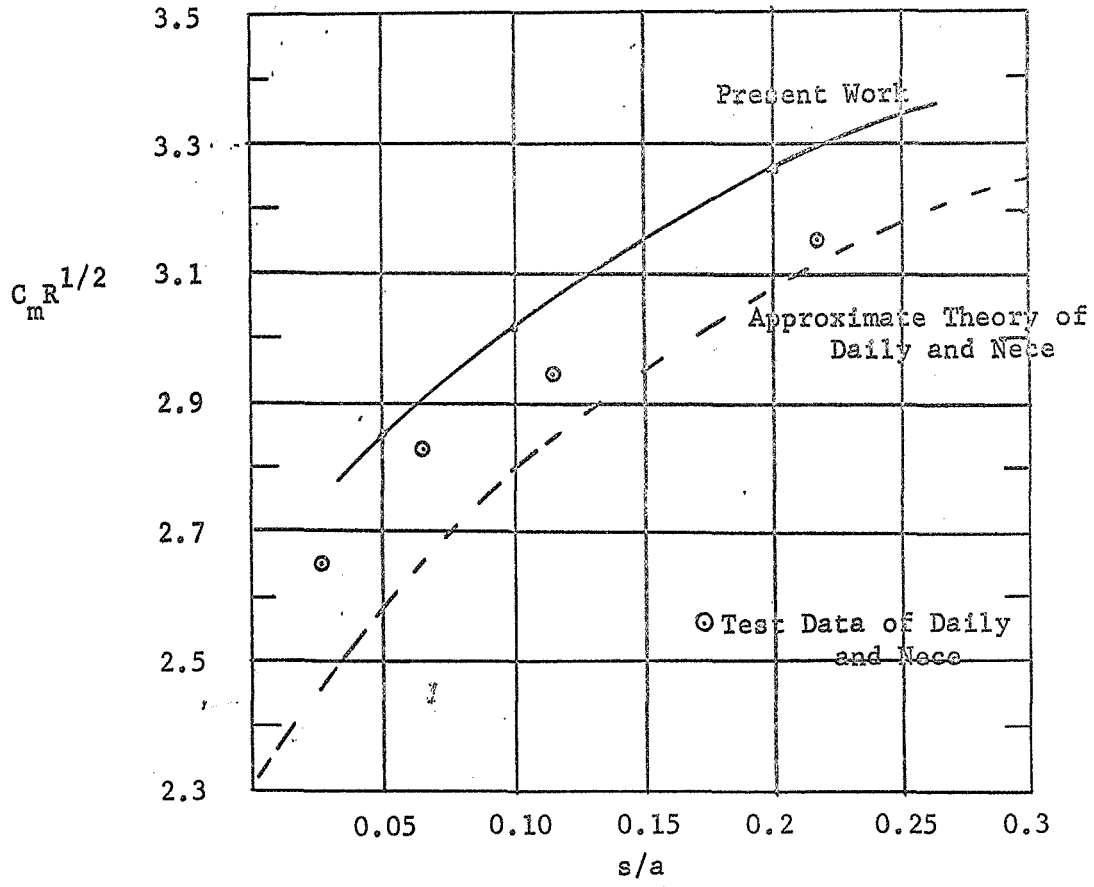

Figure A9

PRODUCT OF REYNOLDS NUMBER AND MOMENT COEFFICIENT
versus SPACING RATIO, ROTATING DISK, REGIME II

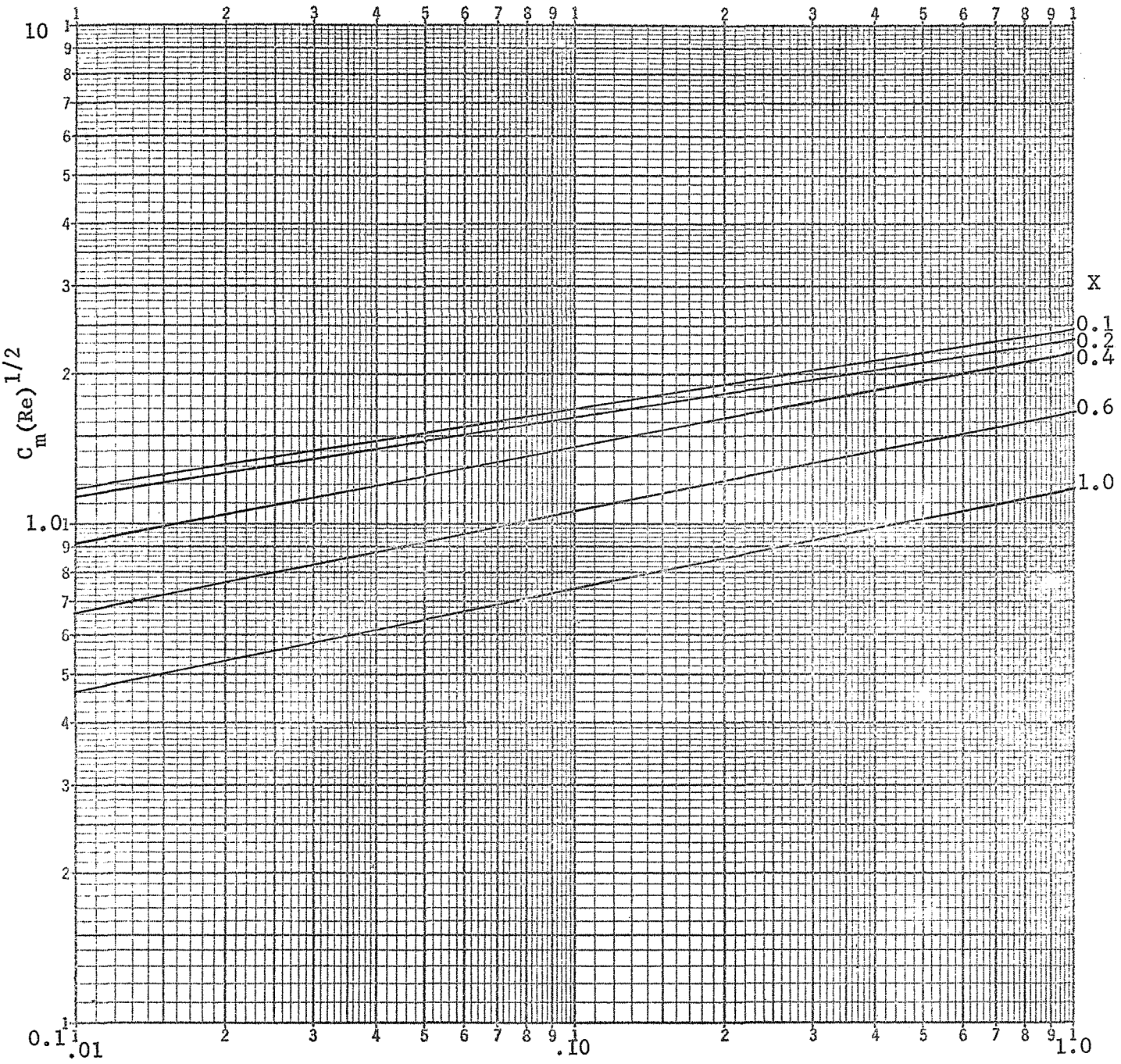

Figure A10

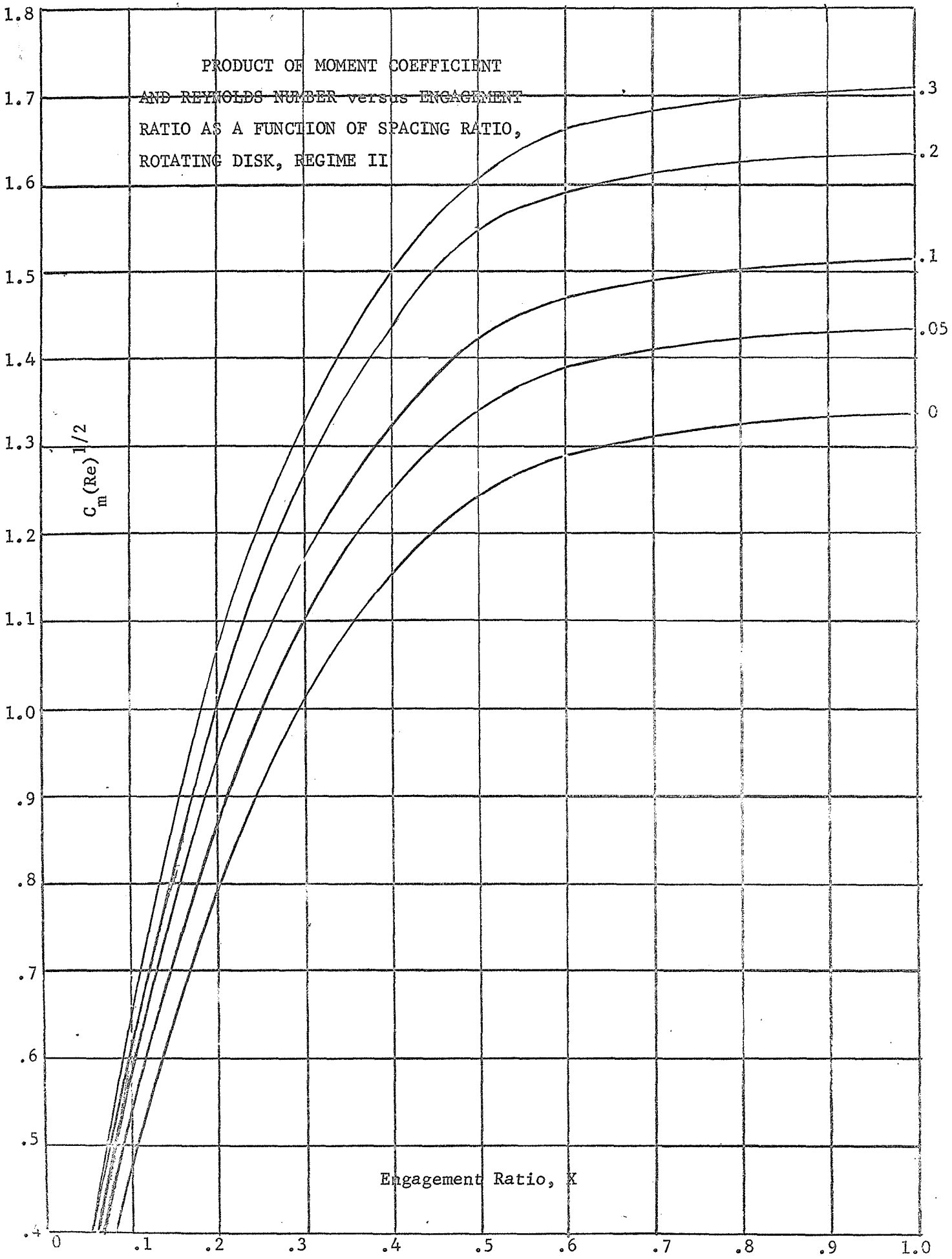
PRODUCT OF MOMENT COEFFICIENT
AND REYNOLDS NUMBER versus ENGAGEMENT
RATIO AS A FUNCTION OF SPACING RATIO,
ROTATING DISK, REGIME II
$C_m (Re)^{1/2}$
Engagement Ratio, X
1.8
1.7
1.6
1.5
1.4
1.3
1.2
1.1
1.0
.9
.8
.7
.6
.5
.4
0
.1
.2
.3
.4
.5
.6
.7
.8
.9
1.0
.3
.2
.1
.05
0

Figure A11

values of $C_m(Re)^{\frac{1}{2}} / (s/a)^{\frac{1}{10}}$ were calculated and a polynomial in X was fitted by sequential least squares to fit the following solution.

$$C_m = \frac{C_{X1} \ (s/a)^{\frac{1}{10}}}{Re^{\frac{1}{2}}} \tag{A47}$$

The polynomial in X was found to be

$$C_{X1} = .1528 + 6.74 \ X - 8.72 \ X^2 + 3.75 \ X^3 \tag{A48}$$

This is shown plotted in Figure A11.

This completes the theoretical analysis for the frictional torque on a rotating disk operating in Regime II with an arbitrary degree of wetting. The resulting equation, Equation A47, is in terms of the important physical variables of Reynolds number, spacing ratio and submersion ratio. Again, the special case for the totally wetted disk (X = 1.0) is shown in Figure A12 where $C_m Re^{\frac{1}{2}}$ is plotted for comparison to the experimental data and theory of Daily and Nece [8]. The agreement with the data is quite good especially at the lower values of spacing ratio.

There is a special situation which occurs in seal practice that deserves consideration at the point. Dynamic seals of the centrifugal type are made in several forms. One very important type is the rotating housing seal which is shown schematically in Figure A13. Note that in this case the physical situation involves rotation of the cylindrical wall also. This is important since one would expect an increase in the frictional moment and the velocity of the fluid core. For this reason, the analysis of Regime II was extended also to this case and is reported at this point.

The basic equations must be modified to account for the rotation of the cylindrical wall. The moment equation for the cylindrical wall (Equation A38)

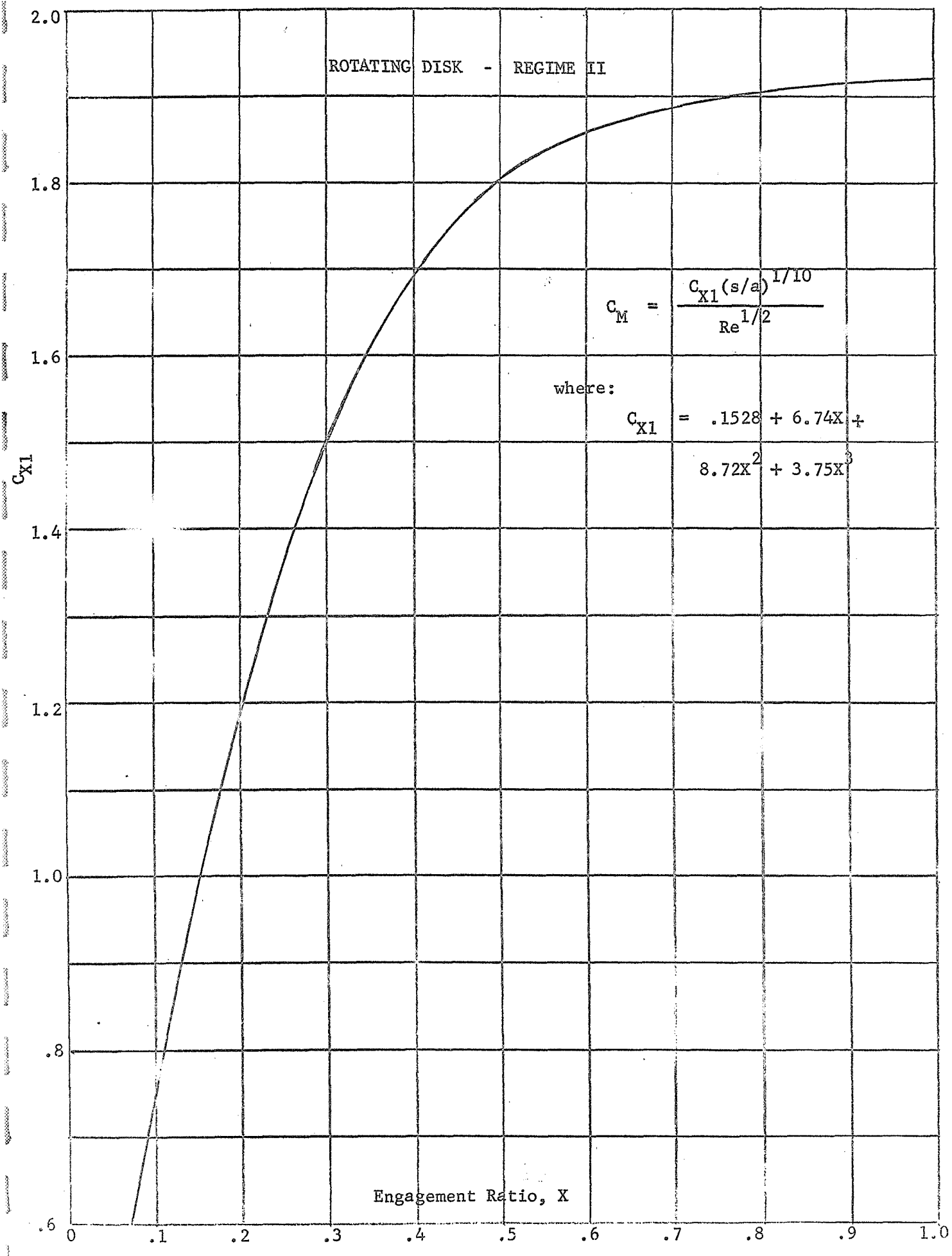
ROTATING DISK - REGIME II
$C_M = \frac{C_{X1}(s/a)^{1/10}}{Re^{1/2}}$
where:
$C_{X1} = .1528 + 6.74X + 8.72X^2 + 3.75X^3$
C_{X1}
2.0
1.8
1.6
1.4
1.2
1.0
.8
.6
0
.1
.2
.3
.4
.5
.6
.7
.8
.9
1.0
Engagement Ratio, X

Figure A12

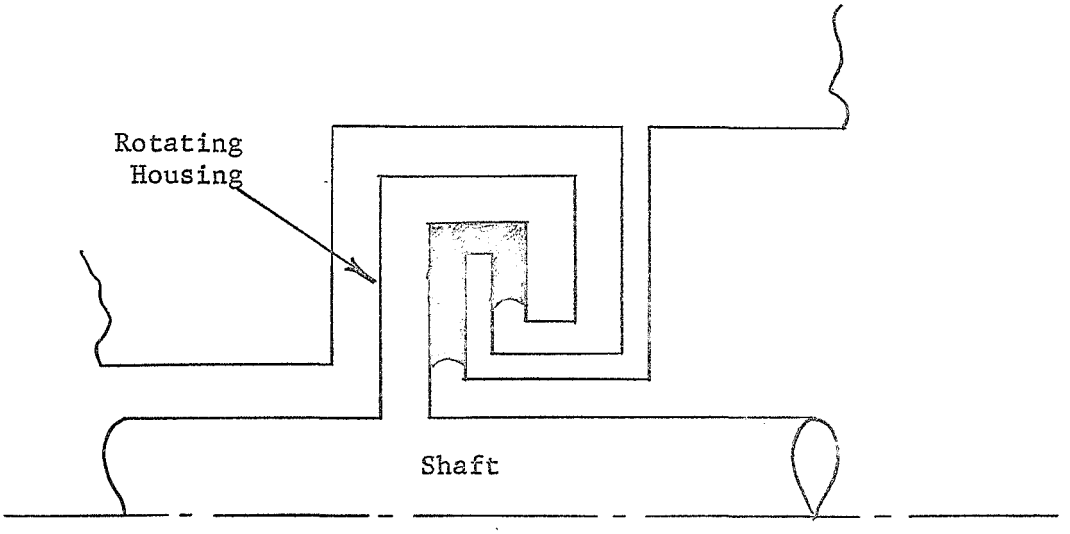

SCHEMATIC OF ROTATING HOUSING SEAL

Figure A13

is first modified by replacing β by $(\omega - \beta)$ to account for the rotation, therefore,

$$M_{cw} = 4\pi a^4 (s/a) \mu (\omega - \beta) (\beta/\nu)^{\frac{1}{2}} C_2 \tag{A49}$$

Summing the moments on the rotating parts

$$M_{RD} + M_{cw} = M_{ROT} = 4\pi a^4 (s/a) \mu (\omega - \beta) (\beta/\nu)^{\frac{1}{2}} C_2$$

$$+ \pi \mu (\omega - \beta) (\beta/\nu)^{\frac{1}{2}} a^4 C_2 C_3 \tag{A50}$$

$$M_{ROT} = 4\pi a^4 \mu (\omega - \beta) (\beta/\nu)^{\frac{1}{2}} \left[\left(\frac{s}{a}\right) C_2 + \frac{C_2 C_3}{4} \right] \tag{A51}$$

Equating the moments on the stationary and rotating parts

$$4\pi a^4 \mu (\omega - \beta) (\beta/\nu)^{\frac{1}{2}} \left[\left(\frac{s}{a}\right) C_2 + \frac{C_2 C_3}{4} \right] = 2\pi \mu \beta b^4 (\beta/\nu)^{\frac{1}{2}} C_1$$

Again, since $a \approx b$, this simplifies to

$$C_1 = 2\left(\frac{\omega}{\beta} - 1\right) \left[C_2 \left(\frac{s}{a}\right) + \frac{C_2 C_3}{4} \right] \tag{A52}$$

This equation has been plotted graphically for various submersion ratios and spacing ratios in the same manner as for the previous case. The results for X = 0.1 and 1.0 are shown in Figures A14 and A15 and the values of K as a function of X with (s/a) as a parameter are plotted in Figure A16.

The moment coefficient for this case is

$$C_m = \frac{2.4\pi a^4 \mu (\omega - \beta) (\beta/\nu)^{\frac{1}{2}} \left[\left(\frac{s}{a}\right) C_2 + \frac{C_2 C_3}{4} \right]}{\rho \omega^2 a^5} \tag{A53}$$

TYPICAL MOMENT EQUILIBRIUM PLOTS

ROTATING HOUSING, REGIME II

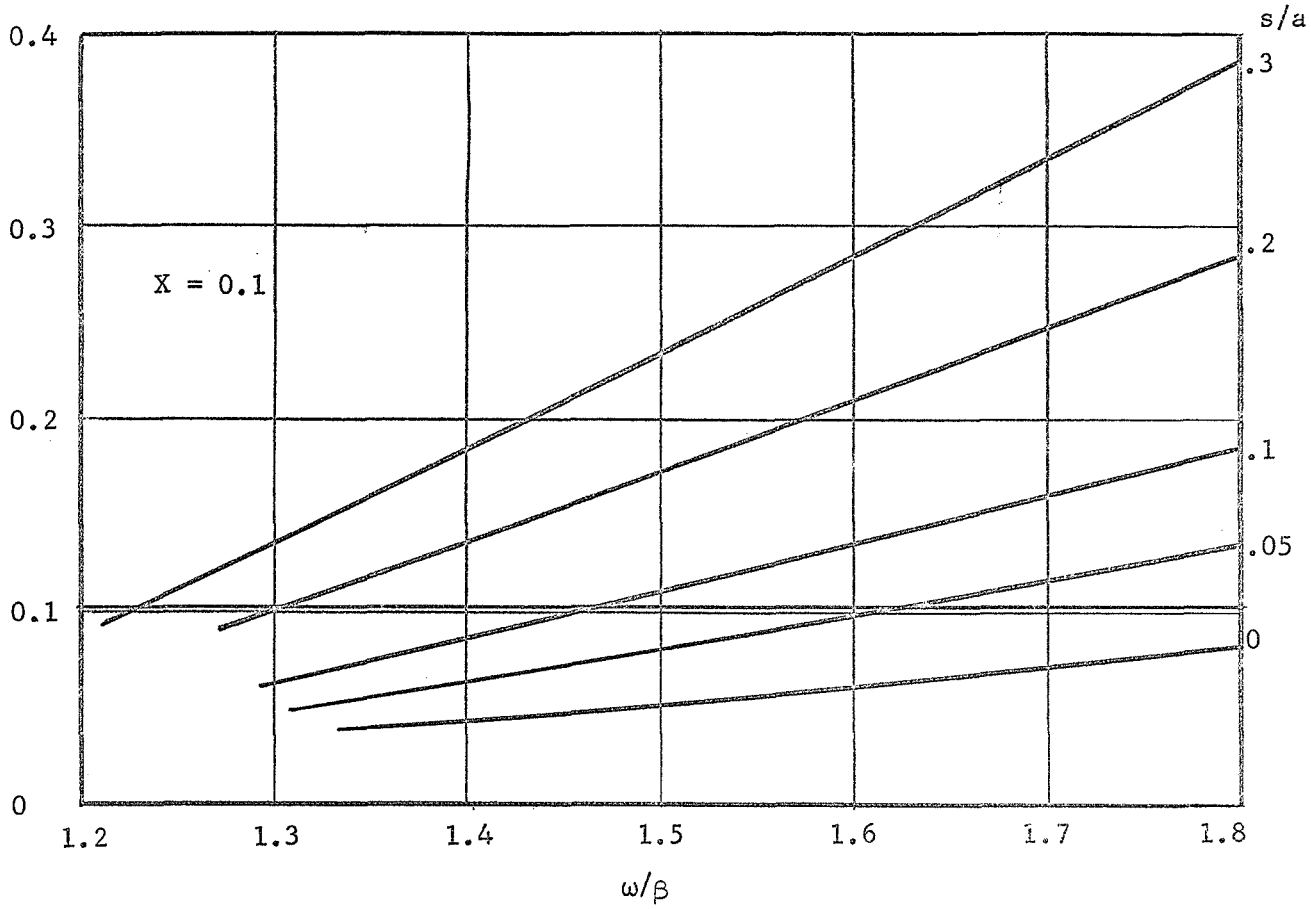

Figure A14

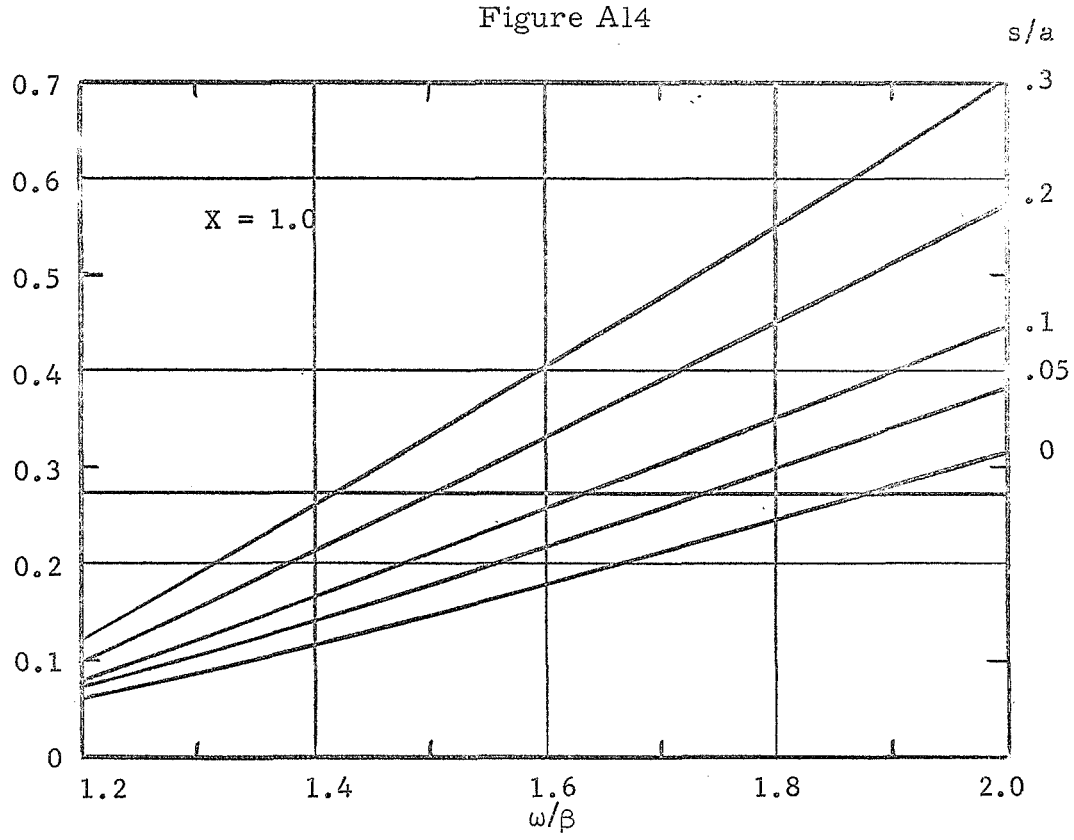

Figure A15

VELOCITY RATIO VERSUS ENGAGEMENT RATIO FOR VARIOUS SPACING RATIOS, ROTATING HOUSING, REGIME II

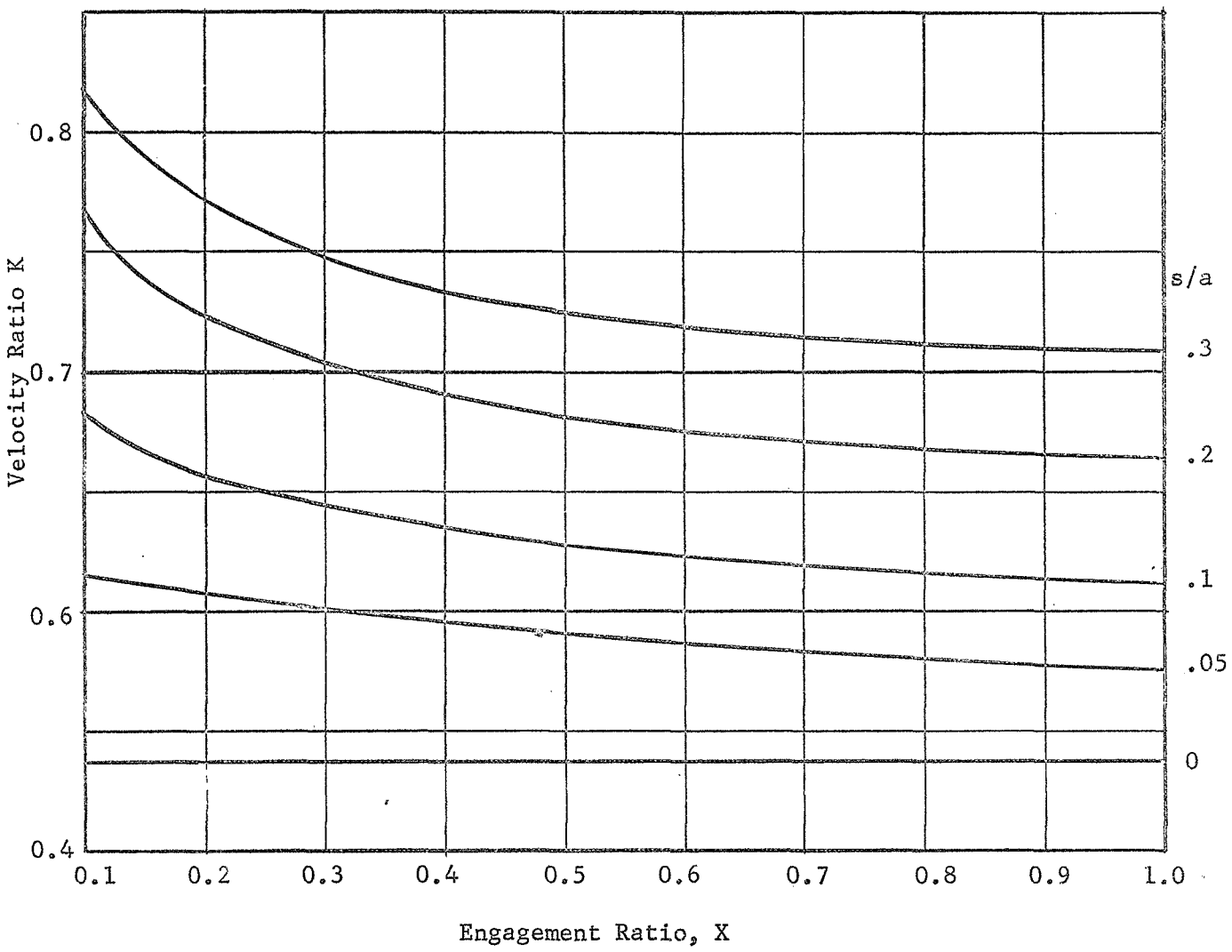

Figure A16

Simplifying this equation,

$$C_m = \frac{8\pi(1-K)(K)^{\frac{1}{2}}\left[\left(\frac{s}{a}\right)\right]C_2 + \frac{C_2 C_3}{4}}{Re^{1/2}} \tag{A54}$$

The value of $C_m(Re)^{\frac{1}{2}}$ was computed for the different values of X and (s/a). Figure A17 shows the variation with X while Figure A18indicates that $C_m Re^{\frac{1}{2}}$ to a close approximation varies as $(s/a)^{1/5}$. On this basis the value of $\frac{C_m Re^{1/2}}{(s/a)^{1/5}}$ was calculated and a sequential least squares fit was made for a solution of the form

$$C_m = \frac{C_{X2}\,(s/a)^{1/5}}{Re^{1/2}} \tag{A55}$$

The value of C_X was found to be

$$C_{X2} = .540 + 7.307\,X - 8.891\,X^2 + 3.682\,X^3$$

This function is plotted in Figure A19 as an aid in selecting values rapidly.

The frictional moment for either the rotating disk or the rotating disk-housing in Flow Regime II is now known for any degree of wetting and any spacing ratio. General conclusions that are drawn from this theoretical analysis are

1) The effect of submersion ratio, on the two important parameters of moment coefficient and fluid core velocity is most dramatic in the range from X = 0.1 to 0.5. For the rotating disk, a decrease in X will result in a decrease in K and C_m. This is to be expected since the reduced wetting will provide less frictional area through which the disk can drive the core of fluid. For the case with the rotating housing, i.e., cylindrical wall the reduction in wetting causes the fluid core to speed up while the moment coefficient is decreased. Here the driving torque applied to the

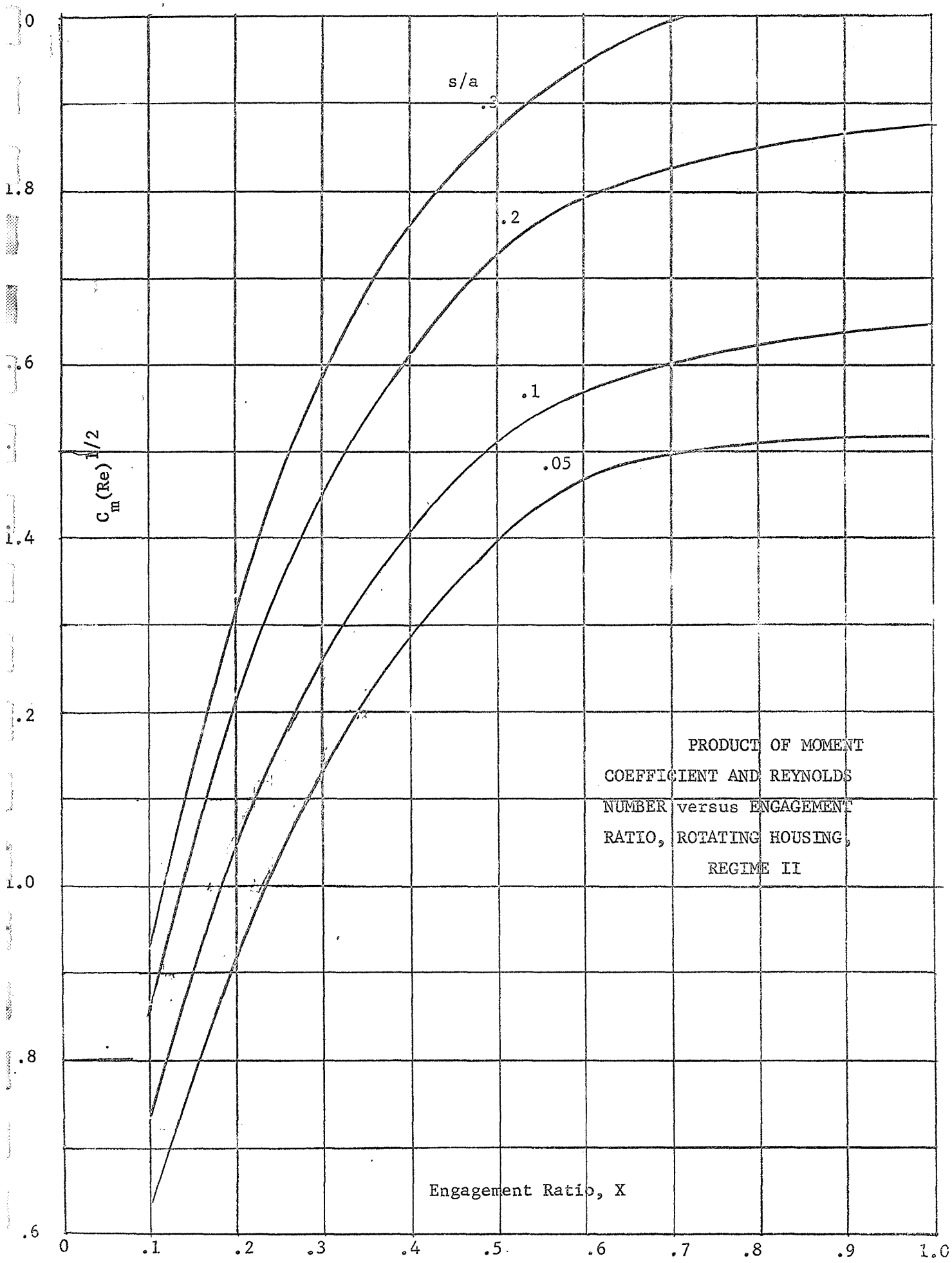
s/a
.3
.2
.1
.05
$C_m(Re)^{1/2}$
2.0
1.8
1.6
1.4
1.2
1.0
.8
.6
0
.1
.2
.3
.4
.5
.6
.7
.8
.9
1.0
Engagement Ratio, X
PRODUCT OF MOMENT COEFFICIENT AND REYNOLDS NUMBER versus ENGAGEMENT RATIO, ROTATING HOUSING, REGIME II

Figure A17

PRODUCT OF MOMENT COEFFICIENT AND REYNOLDS NUMBER versus SPACING RATIO, ROTATING HOUSING, REGIME II

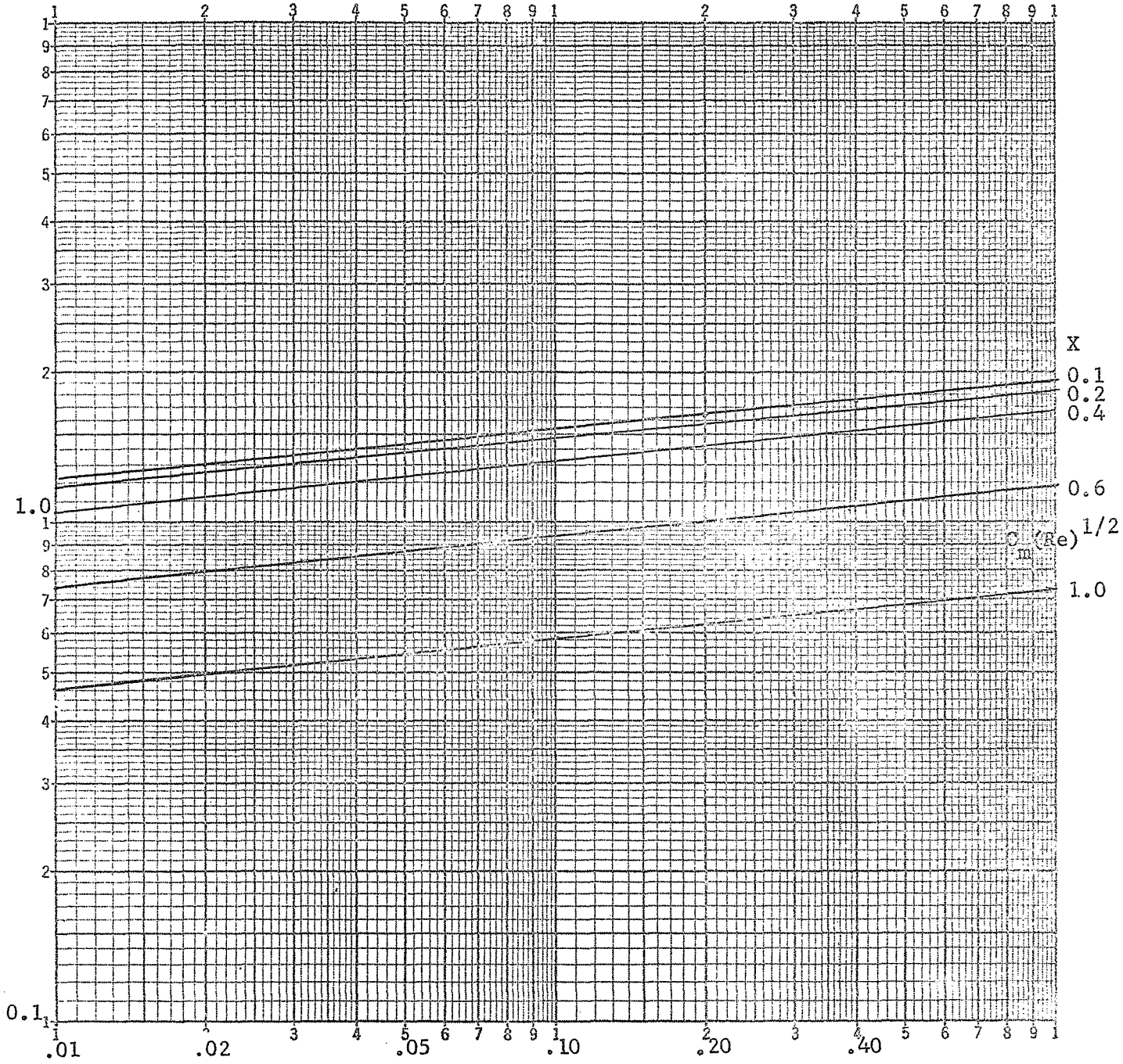

Spacing Ratio s/a

Figure A18

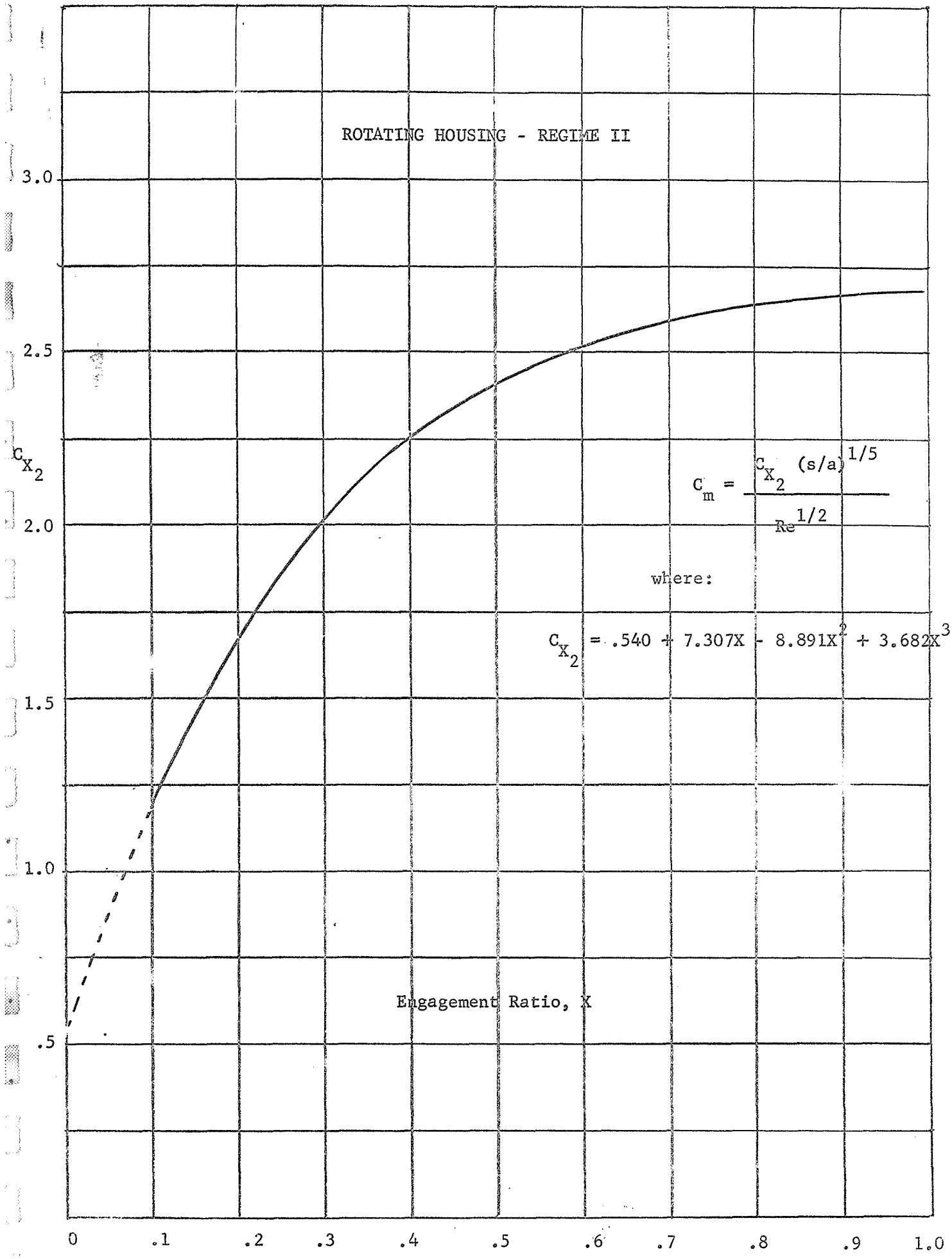
ROTATING HOUSING - REGIME II
3.0
2.5
2.0
1.5
1.0
.5
C_{X_2}
$C_m = \frac{C_{X_2} (s/a)^{1/5}}{Re^{1/2}}$
where:
$C_{X_2} = .540 + 7.307X - 8.891X^2 + 3.682X^3$
Engagement Ratio, X
0
.1
.2
.3
.4
.5
.6
.7
.8
.9
1.0

Figure A19

fluid by the rotating cylinder helps to speed up the core velocity as the retarding area on the stationary wall is reduced. This is an important result since the pressure generation for sealing is dependent on the core velocity, while it is desirable to have low power losses.

2) The effect of increasing the spacing ratio for the rotating disk is to increase the moment coefficient and decrease the core velocity. This is not a desirable situation for sealing, so that for the rotating disk the spacing ratio should be as small as possible, while still remaining in Regime II. For the rotating housing, an increase in spacing ratio results in both increased moment coefficient and core velocity. For the purposes of sealing this means that there is some trade-off point at which the maximum amount of sealing with a minimum power loss can be achieved.

B-3. Regime III Turbulent Flow - Merged Boundary Layers

This flow regime is the most difficult to handle for the totally wetted disk and this same difficulty exists for the case of the arbitrarily wetted disk. The problem resolves itself into the assumption of a very simple flow model with no secondary (radial) velocity components.

For this case, the spacing ratio is assumed to have a negligible effect (a good assumption) so that it is possible to directly equate the moments on the rotating disk and stationary wall. It is necessary to assume some turbulent velocity profile. Since the velocity profile assumed by Soo [7] yielded the most accurate results (7 - 15% high) for the moment coefficient of a totally wetted disk, this same velocity profile will be used here. Since the profile is symmetrical about the midpoint, with a fluid velocity of $\frac{\omega r}{2}$ at that point, the shear stresses and moments on both disk and wall will be equal. The shear stress relationship from the Soo analysis is

$$\tau_t = 0.03955 \; \rho \left(\frac{\omega r}{2}\right)^{\frac{7}{4}} \nu^{\frac{1}{4}} s^{-\frac{1}{4}} \qquad \text{(A56)}$$

The moment equation for the disk then becomes

$$M_{RD} = \int_R^a 2\pi r^2 dr \,.\, 0.03955 \; \rho \left(\frac{\omega r}{2}\right)^{\frac{7}{4}} \nu^{\frac{1}{4}} \; s^{-\frac{1}{4}} \qquad \text{(A57)}$$

Changing to the variable x this becomes

$$M_{RD} = - \frac{2\pi (0.03955) \rho \omega^{\frac{7}{4}} \nu^{\frac{1}{4}} a^{\frac{19}{4}}}{2^{7/4} \; s^{1/4}} \int_X^0 (1 - x)^{\frac{15}{4}} dx \qquad \text{(A58)}$$

The integral is evaluated as

$$\frac{4}{19} \left[1 - (1 - X)^{\frac{19}{4}}\right]$$

where the term in brackets is denoted as C_4 and is plotted in Figure A20 vs. X. Evaluating the numerical constants,

$$M = 0.01556 \; \frac{\rho \omega^{\frac{7}{4}} \nu^{\frac{1}{4}} a^{\frac{19}{4}} C_4}{s^{1/4}} \qquad \text{(A59)}$$

In terms of the moment coefficient, Equation A59 becomes

$$C_m = \frac{.0311 \; C_4}{\left(\frac{s}{a}\right)^{1/4} (Re)^{1/4}} \qquad \text{(A60)}$$

The term $\left(\frac{s}{a}\right)$ appears in the equation even though the frictional effect of the spacing ratio was not included in the analysis. This is similar to Regime I. Thus the moment coefficient for Regime III is now known as an explicit function of X, $\left(\frac{s}{a}\right)$ and Re. It is expected that this equation will

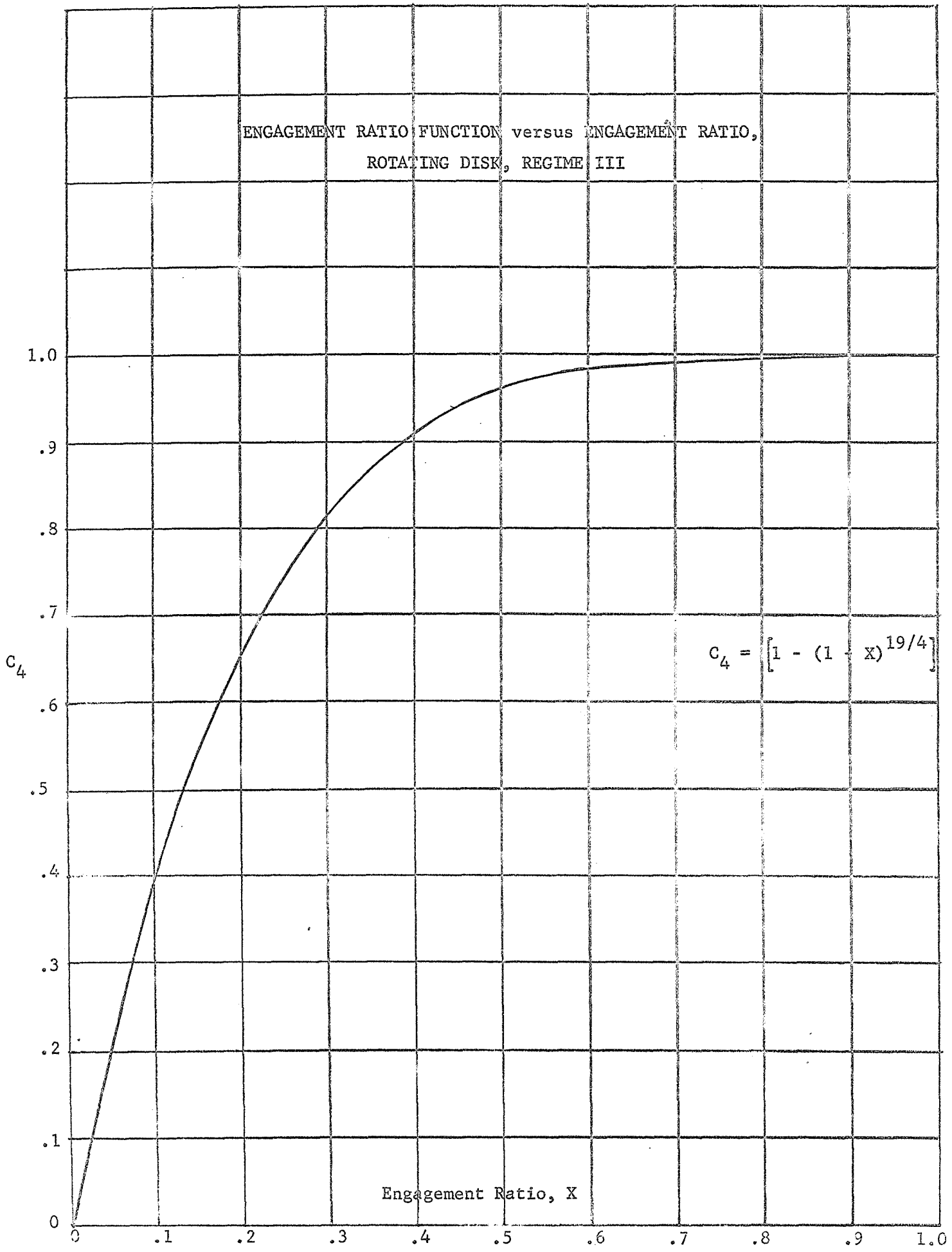
ENGAGEMENT RATIO FUNCTION versus ENGAGEMENT RATIO,
ROTATING DISK, REGIME III
$C_4 = \left[1 - (1 - X)^{19/4}\right]$
C_4
1.0
.9
.8
.7
.6
.5
.4
.3
.2
.1
0
Engagement Ratio, X
0
.1
.2
.3
.4
.5
.6
.7
.8
.9
1.0

Figure A20

yield results which are conservative (higher) for the moment coefficient.

B-4. Regime IV Turbulent Flow - Separate Boundary Layers

This case has been covered in detail by McCann [10] so that only the major results will be presented here. The solutions of that document were dependent on the model used by Schultz-Grunow, [5] similar to the Regime II development used here. The velocity distributions used were the typical power law profiles from the Schultz-Grunow analysis.

Both disk and wall $$v = v_o (\eta)^{1/7} (1 - \eta) \quad \text{(A61)}$$

Wall $$u = r\beta (\eta)^{1/7} \quad \text{(A62)}$$

Disk $$u = r(\omega - \beta)\left[1 - (\eta)^{1/7}\right] + r\beta \quad \text{(A63)}$$

Substitution of the velocity profiles into the momentum equations with the pressure use of the fluid core is the radial direction along with the following expressions for shear stress in the boundary layers for both disk and wall are the important assumptions.

$$\tau_r = .0225\, \rho \left(\frac{\nu}{\Theta}\right)^{1/4} r\beta^{3/4} v_o^* \left(\frac{v_o^{*2}}{r^2\beta^2} + 1\right)^{3/8} \quad \text{(A64)}$$

$$\tau_t = .0225\, \rho \left(\frac{\nu}{\Theta}\right)^{1/4} r\beta^{7/4} \left(\frac{v_o^{*2}}{r^2\beta^2} + 1\right)^{3/8} \quad \text{(A65)}$$

These are given here in terms of the stationary wall here, for the disk Θ is replaced by δ and β replaced by $(\omega - \beta)$.

The solution for the stationary case is of the form

$$M_{sw} = -2\pi \ (.0225)\ \rho b^{19/4} \cdot \nu^{1/4} \cdot \beta^{7/4} \int_0^X \frac{(1-x)^{15/4}}{d} dx \qquad (A66)$$

where d is a function of x. Graphical integration yields

$$M_{sw} = -2\pi \ (.0225)\ \rho\ \nu^{1/5} \cdot \beta^{9/5} \cdot b^{23/5}\ C_5 \qquad (A67)$$

where C_5 is dependent upon the value of X.

Similar consideration for the moment on the disk yield

$$M_{RD} = 2\pi^{5/23} (.0225)\rho \left(\frac{\nu}{\gamma}\right)^{1/4} \left(\frac{\omega}{\beta} - 1\right)^{7/4} \beta^{7/4} \cdot a^{23/5} \left[1 - (1-X)^{23/5}\right] \qquad (A68)$$

where $$\gamma^{1/4} = \left(\frac{\nu}{\beta}\right)^{1/20} \left(\frac{\omega}{\beta} - 1\right)^{1/4} \left[\frac{.0225}{\left(.313\frac{\omega}{\beta} + .504\right)\alpha}\right]^{\frac{1}{5}}$$

and $$\alpha\ 2 = \frac{1}{\frac{\omega}{\beta} - 1} \quad \frac{\left(\frac{\omega}{\beta}\right)^2 .0278 + \frac{\omega}{\beta}(.1944) - .222}{\frac{\omega}{\beta}(1.058 - .241)}$$

The expressions for $\gamma^{\frac{1}{4}}$ and α are evaluated as a function of K in Figures A21 and A22 .

The cylindrical wall friction is determined by assuming the shear stress for turbulent pipe flow where the boundary layer thickness is equal to that at the periphery of the disk.

$$\tau_t = .0225\rho \left(\frac{\nu}{\gamma}\right)^{1/4} a^{8/5} \beta^{7/4} \qquad (A69)$$

Rotating Disk, Regime IV

$$\gamma^{1/4}/(\nu/\beta)^{1/10}$$

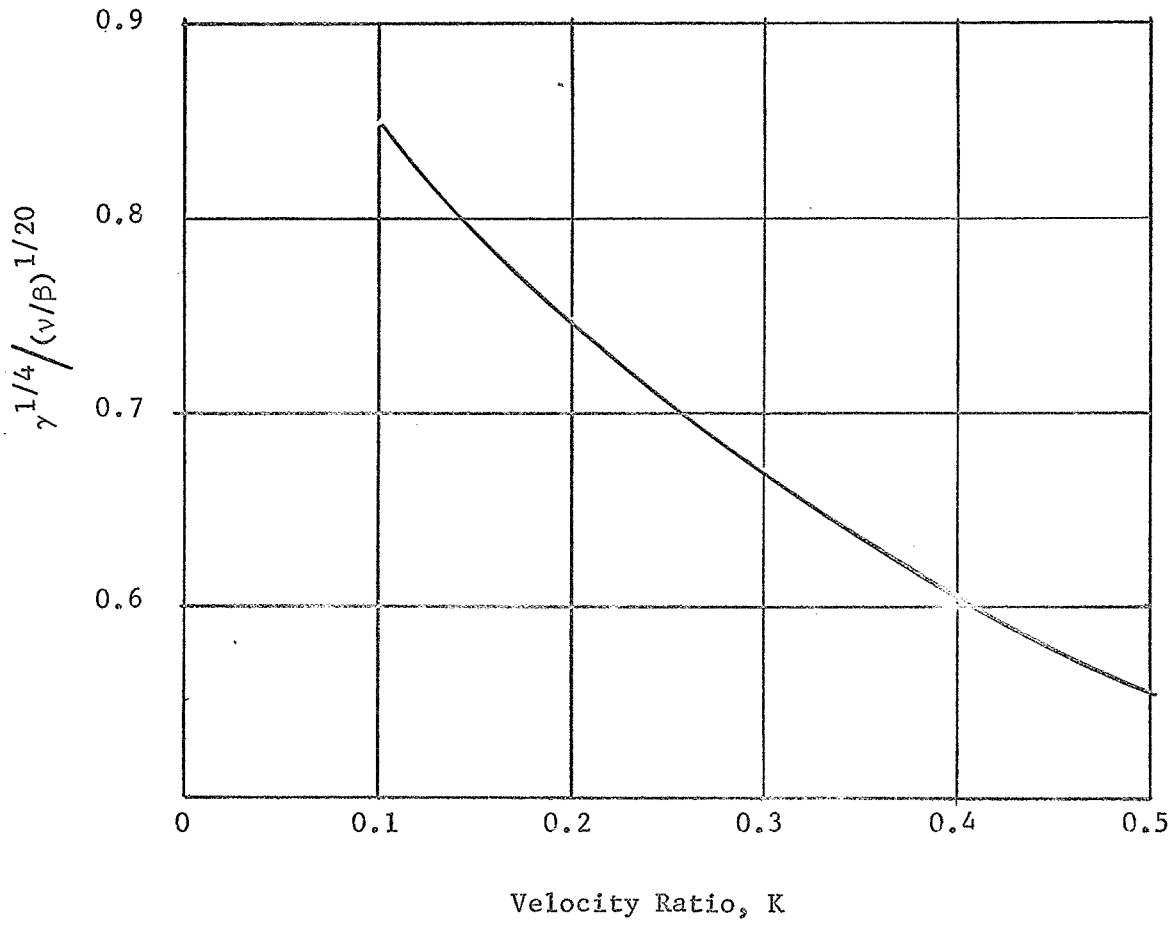

Figure A21

Rotating Disk, Regime IV

$$\alpha^2 = \frac{1}{\frac{\omega}{\beta} - 1} \quad \frac{(\omega/\beta)^2 \; .0278 + \omega/\beta \; (0.1944) - 0.222}{\omega/\beta \; (1.058) - .241)}$$

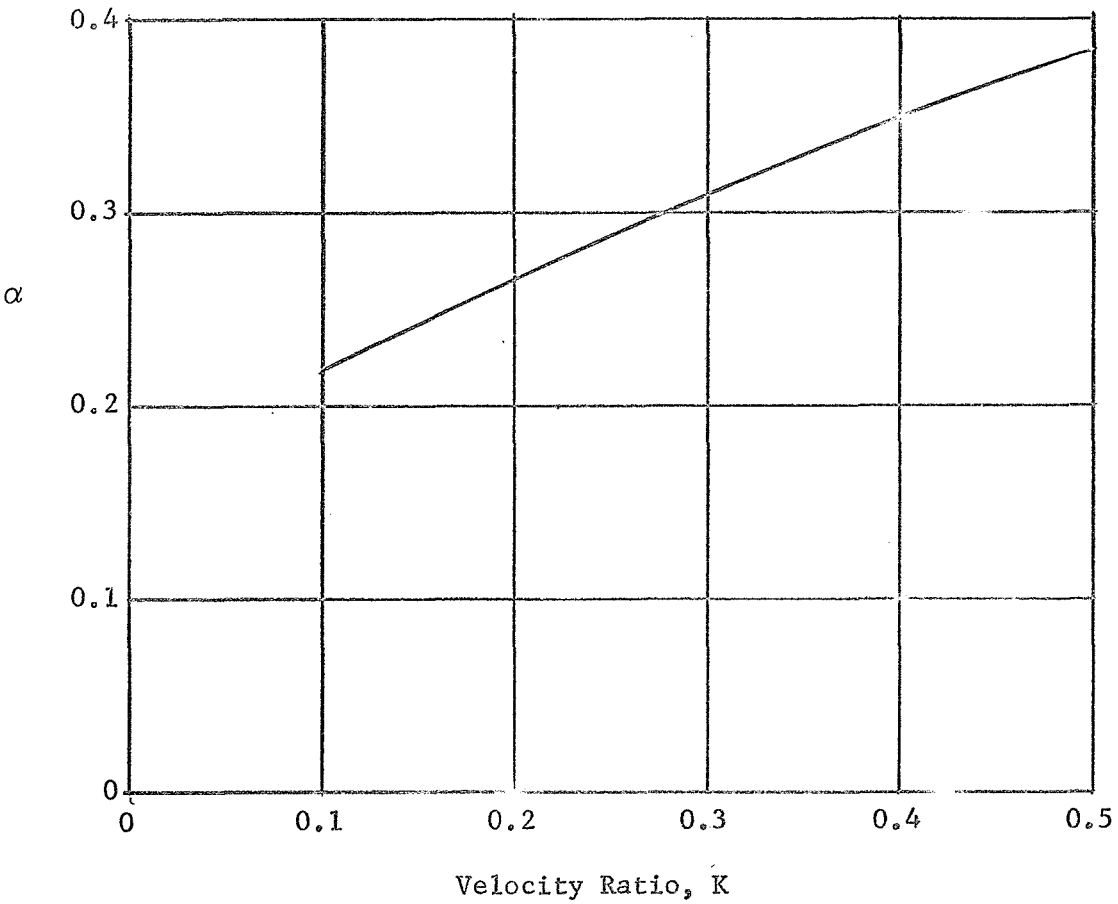

Figure A22

The moment on the cylindrical wall is then

$$M_{cw} = 2\pi\,(.0225)\,\rho\left(\frac{\nu}{\gamma}\right)^{1/4} a^{18/5}\; s\,(\beta)^{7/4} \tag{A70}$$

Equating the moments on the stationary and rotating parts for the rotating disk yields the values of K for different values of $\frac{s}{a}$ and X. Figure A23 shows the variation of K with the submersion ratio for various values of $\frac{s}{a}$.

The moment on the disk is now considered in terms of the moment coefficient.

$$C_m = \frac{.0615\,\dfrac{C_6}{C_7}\left(\dfrac{\omega}{\beta}-1\right)^{7/4}\left[\dfrac{1}{\left(\dfrac{\omega}{\beta}\right)^{9/5}}\right]}{Re^{1/5}} \tag{A71}$$

where

$$C_6 = \left[1-(1-X)^{23/5}\right] \quad \text{and}$$

$$C_7 = \left(\frac{\omega}{\beta}-1\right)^{1/4}\left[\frac{.0225}{\left(0.313\,\dfrac{\omega}{\beta}+.504\right)\alpha}\right]^{1/5}$$

Figures A24 and A25 show the variation of $C_m(Re)^{1/5}$ with submersion ratio and spacing ratio respectively. Since Figure A22 shows that $C_m(Re)$ is proportional to $\left(\frac{s}{a}\right)^{1/10}$ the following solution was assumed

$$C_m = \frac{C_{X3}\left(\dfrac{s}{a}\right)^{1/10}}{Re^{1/5}} \tag{A72}$$

A polynomial expression for C_X was fitted to the data by a least squares curve fit,

$$C_{X3} = .006 + .168\,X - .235\,X^2 + .107\,X^3$$

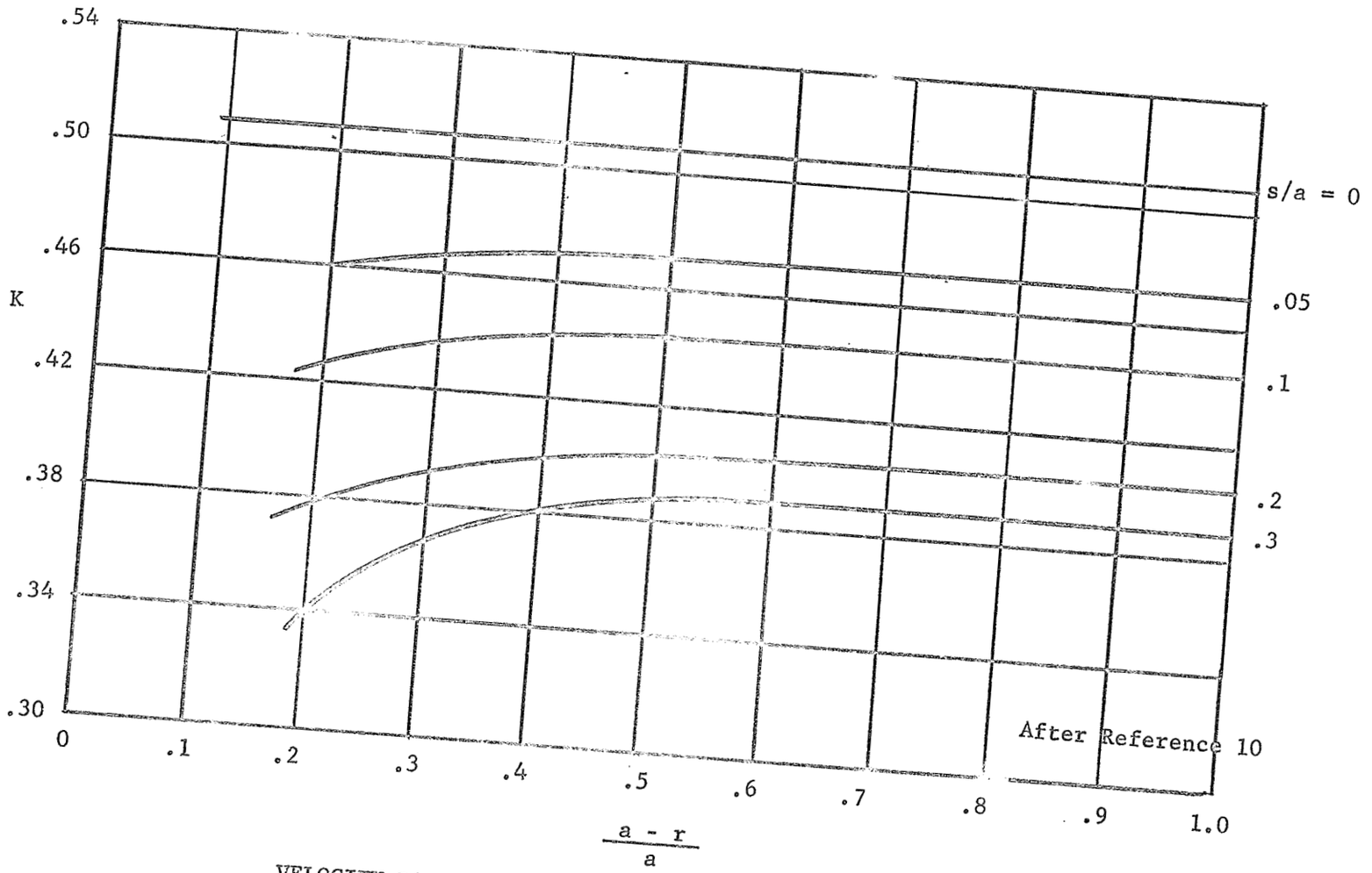

VELOCITY RATIO versus SUBMERSION RATIO
ROTATING DISK - STATIONARY HOUSING SEAL - REGIME IV

Figure A23

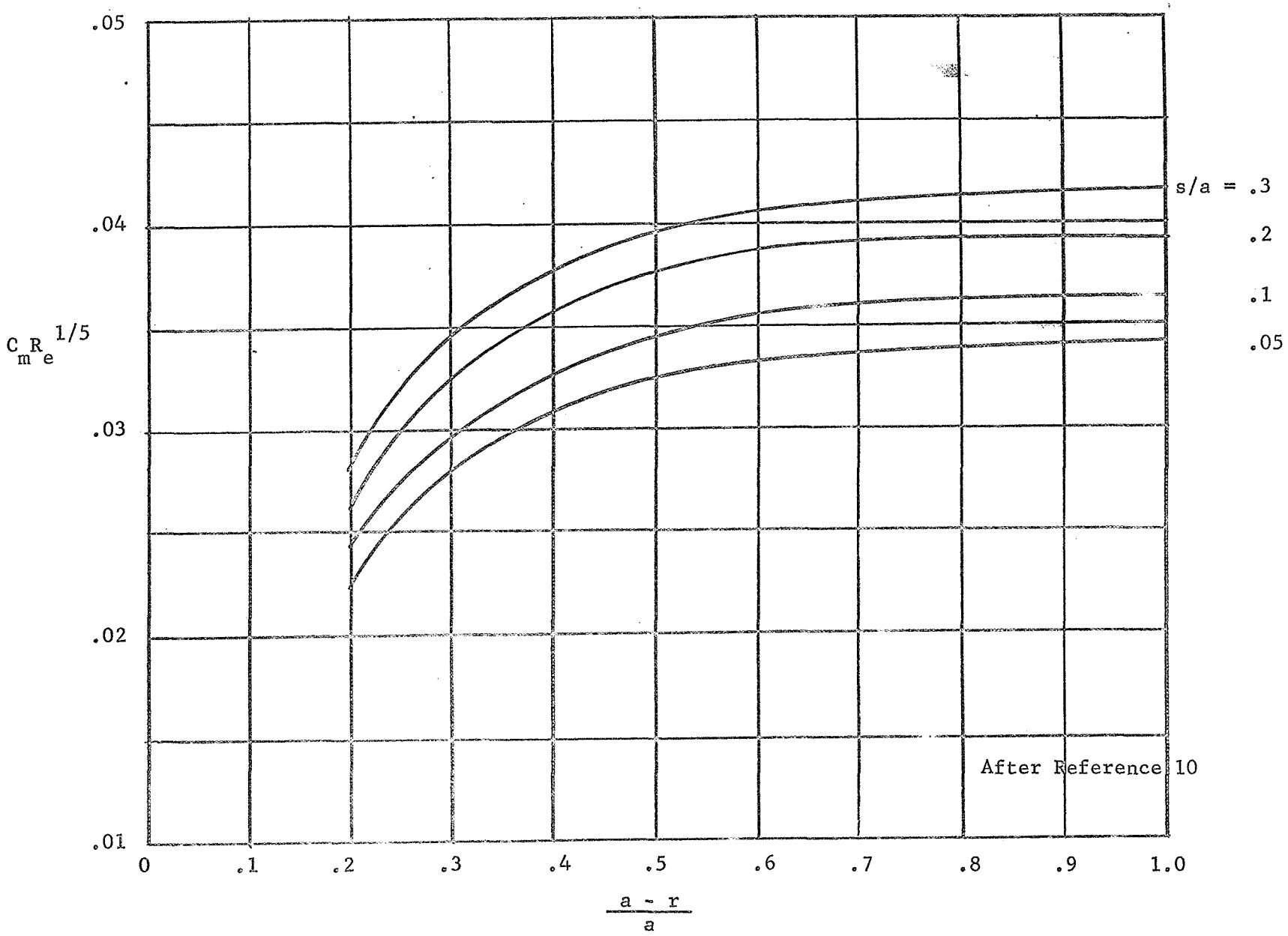

TORQUE COEFFICIENT versus SUBMERSION RATIO

ROTATING DISK - STATIONARY HOUSING SEAL - REGIME IV

Figure A24

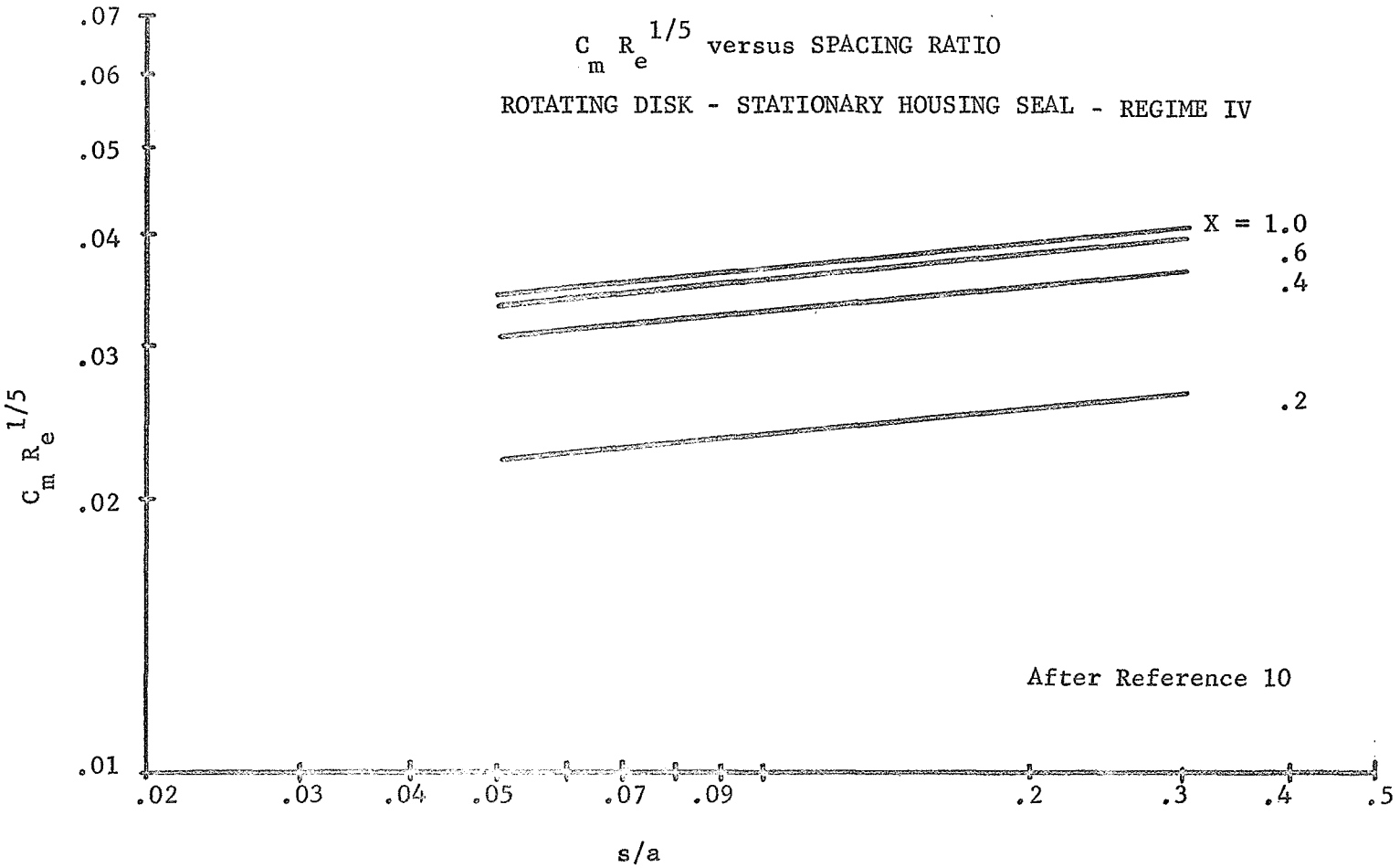
$C_m R_e^{1/5}$ versus SPACING RATIO
ROTATING DISK - STATIONARY HOUSING SEAL - REGIME IV
X = 1.0
.6
.4
.2
After Reference 10
.07
.06
.05
.04
.03
.02
.01
$C_m R_e^{1/5}$
.02
.03
.04
.05
.07
.09
.2
.3
.4
.5
s/a

Figure A25

McCann also considered the rotating housing seal where the cylindrical wall was assumed to rotate. The curves for K vs. X and s/a, $C_m (Re)^{1/5}$ vs. I and $C_m (Re)^{1/5}$ vs (s/a) are shown in Figures A26, A27 and A28 respectively. A solution was assumed,

$$C_m = \frac{C_{X4} (s/a)^{1/10}}{Re^{1/5}} \tag{A73}$$

and the polynomial in X was found to be

$$C_{X4} = 0.149 + .1813 X - .241 X^2 + .106 X^3$$

This completes the theoretical analysis for Regime IV. Caution should be used with the equation since they do predict C_m values approximately 10% below the experimental data of Daily and Nece for the case of the totally wetted rotating disk.

For review, the moment coefficient equations are restated here for all four flow regions

TABLE A4

Regime	Equation	
I	$C_m = \pi C_3 / (s/a) Re$	(A4)
	where $C_3 = [1 - (1 - X)^4]$	
II	Rotating Disk - $C_m = C_{X1} (s/a)^{1/10} / Re^{1/2}$	(A47)
	where $C_{X1} = .1528 + 6.74 X - 8.72 X^2 + 3.75 X^3$	

VELOCITY RATIO vs SUBMERSION RATIO

ROTATING HOUSING - STATIONARY DISK SEAL - REGIME IV

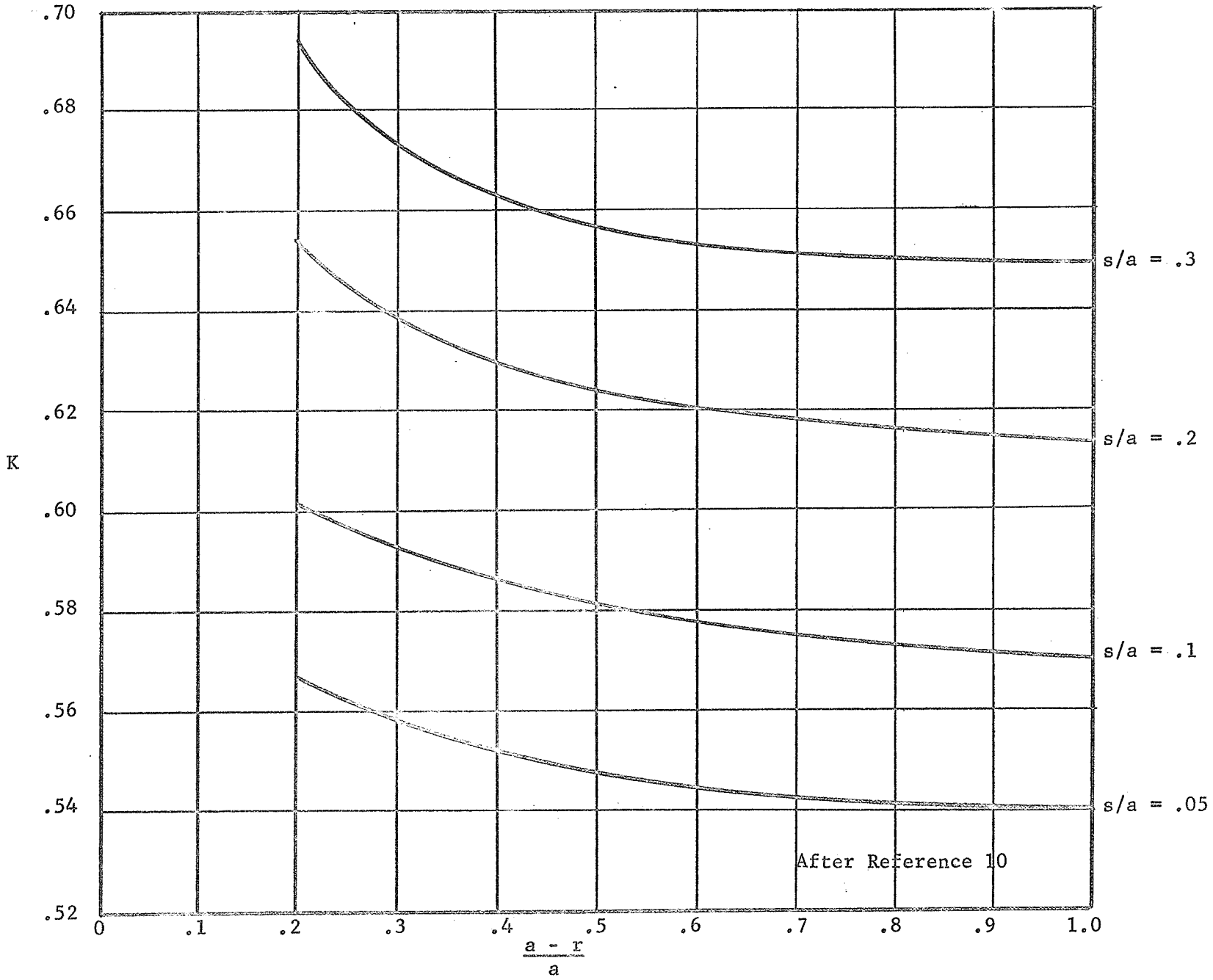

Figure

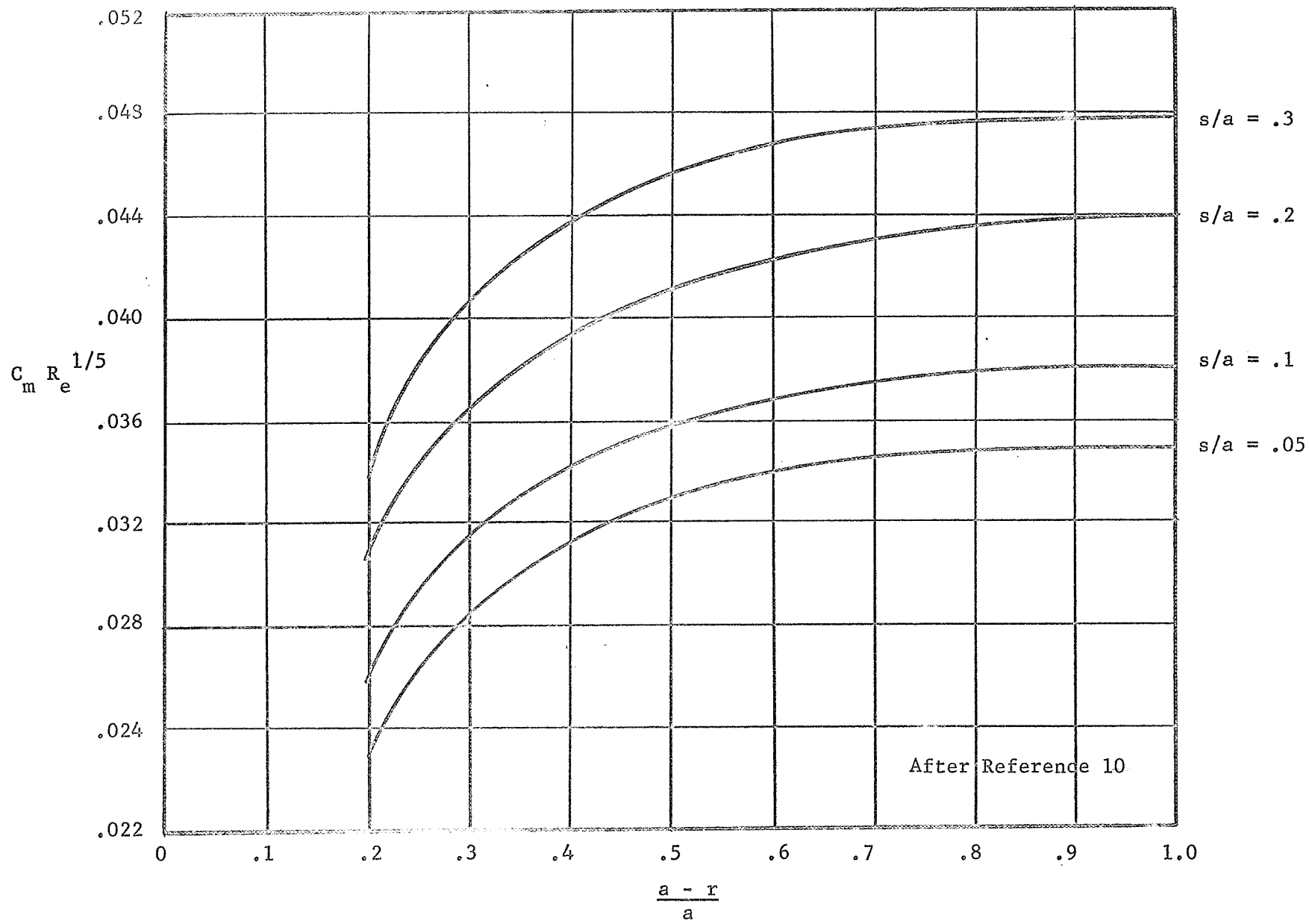

TORQUE COEFFICIENT vs SUBMERSION RATIO

ROTATING HOUSING STATIONARY DISK SEAL - REGIME IV

Figure A27

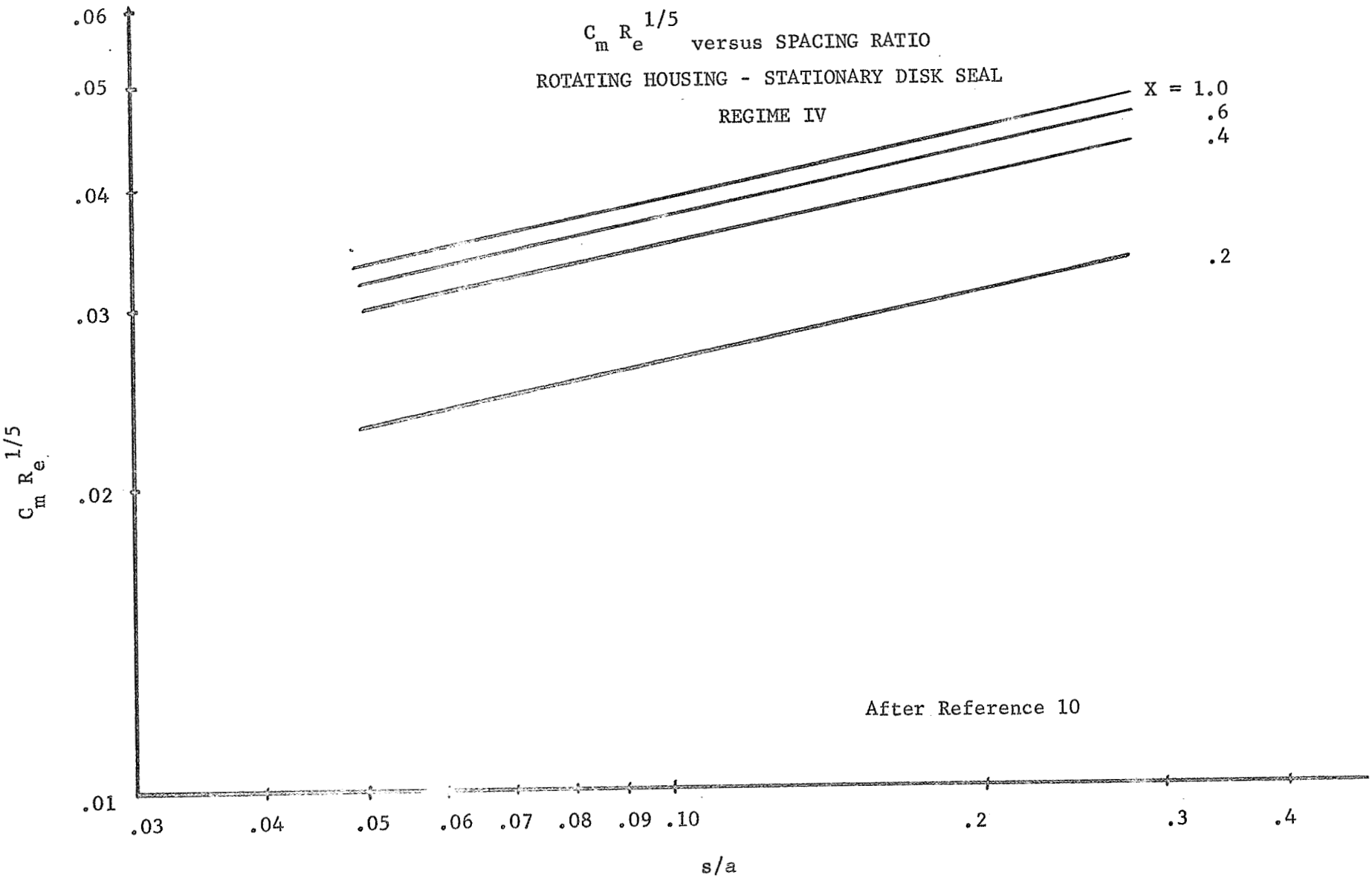
$C_m R_e^{1/5}$ versus SPACING RATIO
ROTATING HOUSING - STATIONARY DISK SEAL
REGIME IV
X = 1.0
.6
.4
.2
After Reference 10
$C_m R_e^{1/5}$
.06
.05
.04
.03
.02
.01
.03
.04
.05
.06
.07
.08
.09
.10
.2
.3
.4
s/a

Figure A28

TABLE A4 (continued

Regime	Equation	
II	Rotating Housing - $C_m = C_{X2} (s/a)^{1/5} / Re^{1/2}$	(A55)
	where $C_{X2} = .540 + 7.307 X - 8.891 X^2 + 3.682 X^3$	
III	$C_m = .0311 C_4 / (s/a)^{1/4} (Re)^{1/4}$	(A60)
	where $C_4 = \left[1 - (1 - X)^{19/4}\right]$	
IV	Rotating Disk $C_m = C_{X3} (s/a)^{1/10} / Re^{1/5}$	(A72)
	where $C_{X3} = .006 + .168 X - .235 X^2 + .107 X^3$	
IV	Rotating House $C_m = C_{X4} (s/a)^{1/5} / Re^{1/5}$	(A73)
	where $C_{X4} = .0149 + .1813 X - .241 X^2 + .106 X^3$	

B-5 Pressure Characteristics of Partially Wetted Enclosed Rotating Disks

The pressure characteristic is based on the assumption that the radial pressure gradient is equal to that experienced for a fluid mass rotating about its own axis with an angular velocity equal to $K\omega$.

The governing equation is therefore

$$\frac{dp}{dr} = \rho \, (K \, \omega)^2 r \qquad (A74)$$

For Regimes II and IV, the value of K is known for any given spacing and submersion ratio from Figures A7 and A23 respectively. For Regimes I and III the simple assumption made is that the average angular velocity of the fluid in the gap is equal to $\frac{\omega}{2}$ or, in other words, $K = .5$. Therefore, the differential pressure from $r = R$ to $r = a$ is given as

$$\Delta P = \rho/2 \; K^2 \; \omega^2 \; (a^2 - R^2) \qquad (A75)$$

Since $X = \frac{a - R}{a}$ Equation A75 can be simplified to

$$\Delta P = \rho/2 \, (K \, \omega \, a)^2 \left[1 - (1 - X)^2 \right] \qquad (A76)$$

The term in brackets is denoted as C_8 and is plotted in Figure A29 for reference. Equation A76 is now the generalized form for predicting the radial pressure head for a partially wetted rotating disk.

B-6 Flow Characteristics of Rotating Disks

The rotating disk can be considered as a small pump. Within the thin boundary layer on the disk the fluid moves radially and tangentially. If the disk is not enclosed, the fluid leaving the disk at the outer radius is dissipated in the surrounding medium. If the disk is enclosed the radial flow leads to a recirculation within the enclosing chamber. In many applications, such as scavenging a bearing cavity, or cooling a slinger seal, it is desired to use the rotating disk as a small pump. In these cases it is ncesssary to determine the head-flow characteristics of the rotating disk.

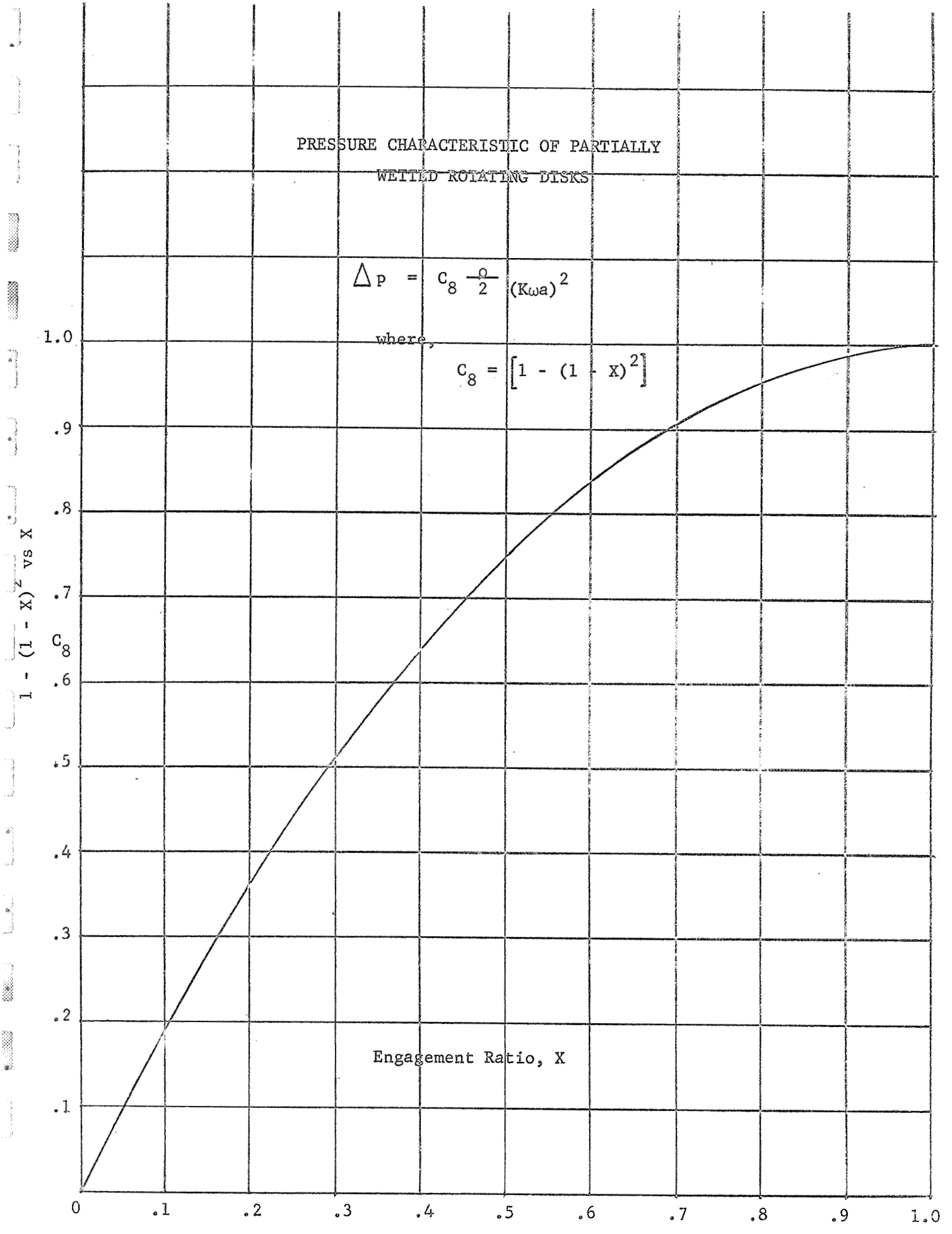
PRESSURE CHARACTERISTIC OF PARTIALLY
WETTED ROTATING DISKS
$\Delta p = C_8 \frac{\rho}{2} (K\omega a)^2$
where,
$C_8 = \left[1 - (1 - X)^2\right]$
C_8 vs X
$1 - (1 - X)^2$
Engagement Ratio, X
1.0
.9
.8
.7
.6
.5
.4
.3
.2
.1
0
.1
.2
.3
.4
.5
.6
.7
.8
.9
1.0

Figure A29

The quantity of fluid which is pumped radially by the disk as a result of centrifugal force is

$$Q = 2 \pi a \int_{o}^{\delta} u dz \tag{A77}$$

Since the solutions for flow regimes I and III assume no radial velocity it is not possible to calculate a flow capacity within the framework of the theory presented here. As a consequence, only cases II and IV are treated.

6a <u>Flow Characteristics - Regime II</u>

For Regime II, the radial velocity is given by

$$v = v_o \left[1 - (2 \eta - 1)^2\right] \tag{A23}$$

and the quantity of fluid pumped outward is

$$Q = 2 \pi a \int_{o}^{\delta} v dy = 2 \pi a v_o (2/3) \delta \tag{A78}$$

where

$$v_o = \frac{a}{\delta 2} \quad 2.5 \quad v \left[\frac{1 - \beta / \omega}{1 + 2/3 \beta / \omega}\right] \tag{A79}$$

The boundary layer thickness is given by

$$\delta = \sqrt{\frac{\nu}{\omega}} \left[\frac{(150)^{1/4}}{\sqrt{3}\left(\frac{2}{3} \beta/\omega + 1\right)^{1/2}} \left(\frac{6 - \beta/\omega}{1 + 7/3 \beta/\omega}\right)^{1/4}\right] \tag{A27}$$

Substituting for v_o in equation, we obtain

$$Q = \frac{2\pi a^2}{\delta} \frac{2}{3} \quad 2.5 \quad \nu \quad \frac{(1 - \beta/\omega)}{(1 + 2/3\ \beta/\omega)} \tag{A80}$$

and again for δ , the boundary layer thickness, the equation becomes

$$Q = \frac{10}{3} \pi a^2 \quad \nu \quad \frac{(1 - \beta/\omega)}{(1 + 2/3\ \beta/\omega)} \quad \frac{\sqrt{3}\,(1 + 2/3\ \beta/\omega)^{1/2}(1 + 7/3\ \beta/\omega)^{1/4}}{\sqrt{\frac{\nu}{\omega}}\ (150)^{1/4}\ (6 - \beta/\omega)^{1/4}}$$

$$\frac{Q}{\omega a^3} = \frac{10\ \pi \quad a^3\ \omega \quad 1 - \beta/\omega}{\sqrt{3}\ \sqrt{\omega \frac{a}{\nu}}\ (150)^{1/4}(1 + 2/3\ \beta/\omega)^{1/2}} \quad \frac{(1 + 7/3\ \beta/\omega)^{1/4}}{(6 - \beta/\omega)^{1/4}} \tag{A81}$$

which is of the same form as the expression for the flow on a free disk in laminar flow; that is, the dimensionless flow, $\frac{Q}{\omega a^3}$, varies inversely as the square root of the Reynolds number.

6 b. <u>Flow Characteristic Regime IV</u>

For Case IV, the McCann solution assumes that $\delta = \gamma\ r^{3/5}$ (A82)

and $v_o^* = \alpha\ (\omega - \beta)\ \gamma$ (A83)

Substituting in Equation A77 , and evaluation at $r = a$, we obtain

$$\frac{Q}{\omega a^3} = 2\ \pi \frac{\gamma}{(\nu/\beta)^{1/5}} \quad \frac{\alpha}{1\ R^{1/5}} \quad \frac{(1 - K)}{K^{1/5}} \tag{A84}$$

where α and $\gamma \; / \; (\nu \; / \beta)^{1/5}$ are presented in Figures A21 and A22. The boundary layer on the disk is then

$$\delta = \gamma \; a^{3/5} = \frac{\gamma'}{K^{1/5}} \; \frac{a}{R^{1/5}} \tag{A85}$$

The equation for the flow and the boundary layer thickness have the same form as for the free disk, but the multiplicative factor is now a function of K which, in turn, is a function of X and s/a.

Both Equations A81 and A84 are expressions for the natural circulatory flow which will be set up by a rotating disk. If the flow removed from the casing is much smaller than this flow, called the critical flow, the pressure distribution about disk will not be severely influenced. Daily and Arundt [11] show that for values of $\frac{Q}{\omega a^3} < .01$, that the pressure and velocity distributions are little affected by through flow.

6c. Effect of Flow on Power Loss

The approximate effect of through flow on the frictional loss can be considered by analyzing the rate of change of angular momentum imparted to the through flow. Thus, the friction torque can be expressed as a percentage of the zero throughflow case.

For Regimes II and IV the core is assumed to be rotating as a solid body with angular velocity β when there is no throughflow:

β / ω for the zero throughflow case is called K_o. The fluid is considered to enter the casing without any whirl and leave with angular velocity $K_o \omega r$. Obviously, K_o is a function of (s/a) and X from the previous analyses in Regimes II and IV and is assumed to be equal to .5 in Regimes I and III.

The increase in torque is given by

$$\Delta M = \Delta (\rho Q u r) \tag{A86}$$

$$\text{or} \quad \Delta M = \rho Q K_o \omega a^2 - 0 \tag{A87}$$

Since the moment coefficient $M_o = \dfrac{C_m \rho \omega^2 a^5}{2}$ then

$$\frac{\Delta M}{M_o} = \frac{\rho Q K_o \omega a^2}{\frac{C_m}{2} \rho \omega^2 a^5} = \frac{2 K_o}{C_m} \cdot \frac{Q}{\omega a^3} \tag{A88}$$

This increase in torque can be related to the original C_m expressions. For example, for the case of Regime II where

$$C_m = C_{X1} (s/a)^{1/10} / Re^{1/2} \tag{A47}$$

Then Equation A88 becomes

$$\frac{\Delta M}{M_o} = \frac{2 K_o (Re)^{1/2}}{C_{X1} (s/a)^{1/10}} \cdot \frac{Q}{\omega a^3} \tag{A89}$$

Thus the increase in torque is not only a function of the Reynolds number, the spacing ratio and the submersion ratio, but it also includes the dimensionless flow parameter $\left(\dfrac{Q}{\omega a^3}\right)$.

APPENDIX B

SCREW SEAL THEORY

A. SCREW SEAL GEOMETRY

The screw seal consists of a threaded shaft rotating in a close clearance sleeve. Figure B-1 gives the screw geometry and Figure B-2a shows a portion of a screw seal in which the rotational speed of the sleeve relative to the shaft is U. The component V tends to drag the fluid in the direction of the channel. The T component induces a transverse flow which is neglected in the analysis. Figure B-2b illustrates an element of helical channel with only the relative volocity component V existing on the sleeve with no pressure gradient.

B. SCREW SEAL SEALING CAPABILITY

It is shown in References 17 and 18 that in laminar flow the sealing capability is given by

$$\psi_\ell = \frac{\Delta \rho \delta^2}{\mu U L} = K_1 \qquad \text{(B1)}$$

where K_1 is a function of the screw geometry alone, that is,

$$K_1 = K\,(h/w,\ \delta/h,\ w/(w+w'),\ \phi) \qquad \text{(B2)}$$

By taking the partial derivatives of K_1 with respect to h/w, δ/h, $(w+w')$, ϕ, and setting the resulting equations equal to zero, values of w/h, δ/h, $w/(w+w')$, and ϕ can be found for which ψ_ℓ is a maximum. This has been done in the past by many investigators and a summary of optimum geometry is given in Reference 18 .

In turbulent flow the sealing coefficient is no longer a function of geometry alone, but is also a function of Reynolds number, that is,

$$\frac{\Delta \rho \delta^2}{\mu U L} = K_1 + K_2 \, Re_\delta^n \tag{B3}$$

The values of K_1 and K_2, also functions of geometry, have not been optimized for the turbulent flow case. For this reason, optimizations based on laminar flow analysis are also used for turbulent flow operation. Values of K_1 and K_2 for two geometries are available in Reference 18.

C. SCREW SEAL POWER LOSS

It is shown in Reference 18 that the screw seal power loss can be calculated by treating the loss as frictional dissipation by viscous shear in an annulus of clearance δ. The effect of the grooves is neglected. In laminar flow this loss, expressed in terms of a moment coefficient λ is given by

$$\lambda = \frac{4\pi}{Re_\delta} \tag{B4}$$

and in turbulent flow by

$$\lambda = \frac{.156\pi}{Re_\delta^{.43}} \tag{B5}$$

The test results of Reference 18 indicate a critical Reynolds number of 1000. The moment on the shaft is given by

$$M = \lambda \frac{\rho \, \omega^2 \, r^4 \, L}{2 \, g_o} \tag{B6}$$

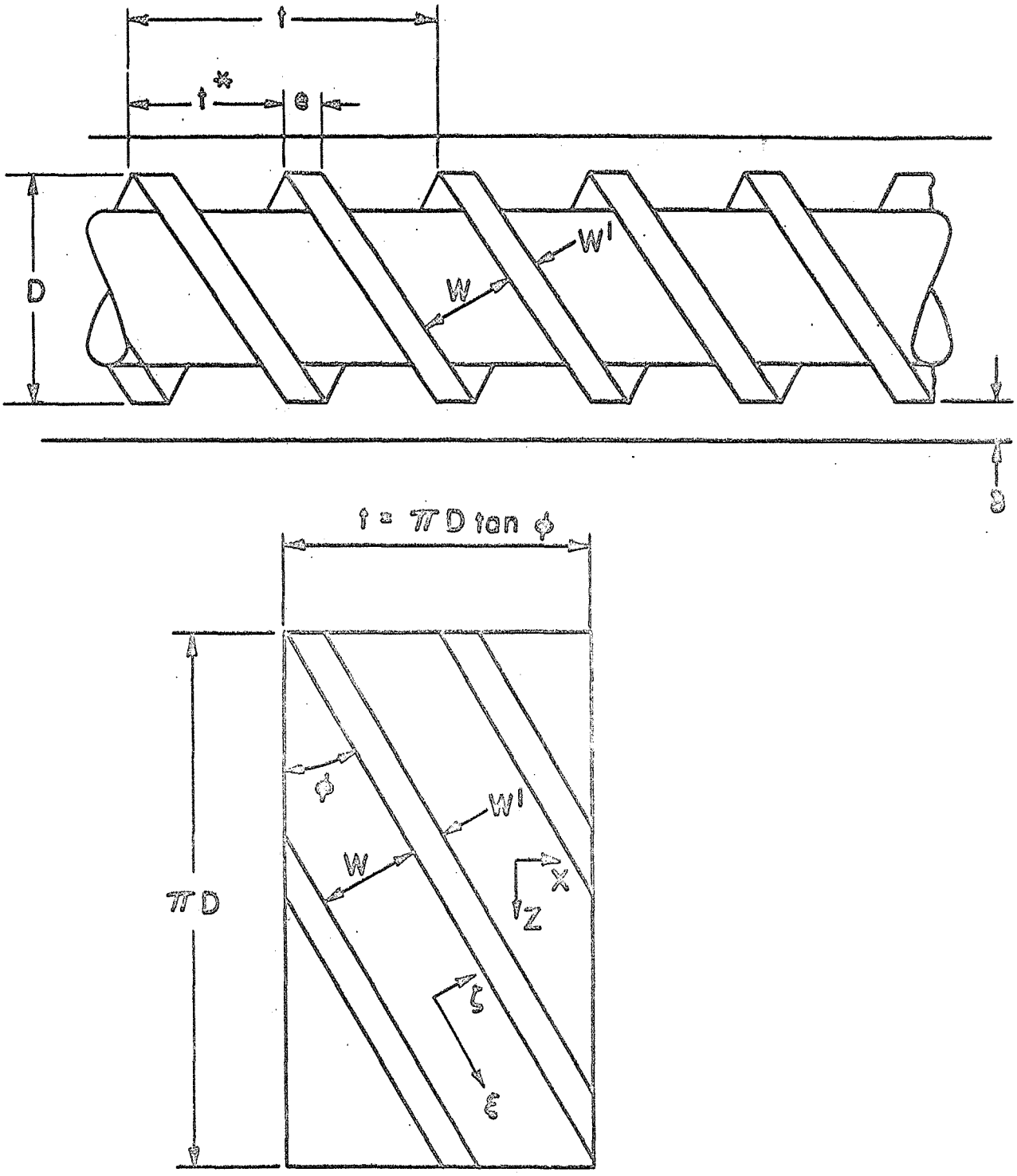

Figure B-1 Screw Geometry

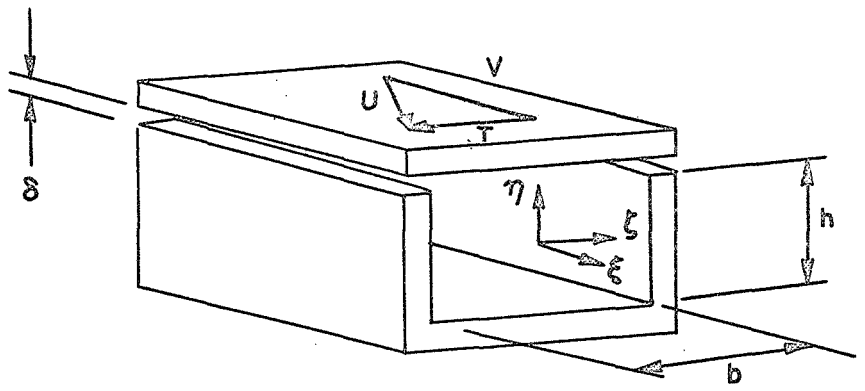

a. Portion of Screw Pump Channel

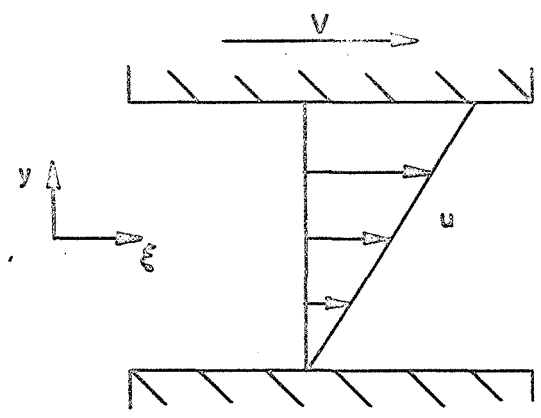

b. Couette Flow Approximation to Flow in Screw Pump Channel

Figure B-2

APPENDIX C

BEARING POWER LOSS

Exact prediction of ball bearing power loss is not possible. Some empirical power loss formulas are available. One such is the Styri equation:

$$T = 1.5 \times 10^{-5} w (D_1 + D_2)^2 N^{0.63} + 3.24 \times 10^{-5} P^{1.5}$$

where

w	=	bearing width, in.
D_2	=	O.D., in.
P	=	equiv. load, lb.
D_1	=	bore, in.
N	=	rpm
μ	=	viscosity, cp

Power loss versus equivalent load is shown in Figure C1 for various lubricant temperatures.

The amount of heat the oil can absorb for various temperature rises and flow rates are given in Figure C2.

BEARING POWER LOSS

vs

BEARING EQUIVALENT LOAD

Fluid: ET378
Speed: 12,000 RPM

STYRI Equation:

$$T = 1.50 \times 10^{-5} \omega (D_1 + D_2)^2 \mu N^{0.63} + 3.24 \times 10^{-5} P^{1.5} \text{ (in-lb)}$$

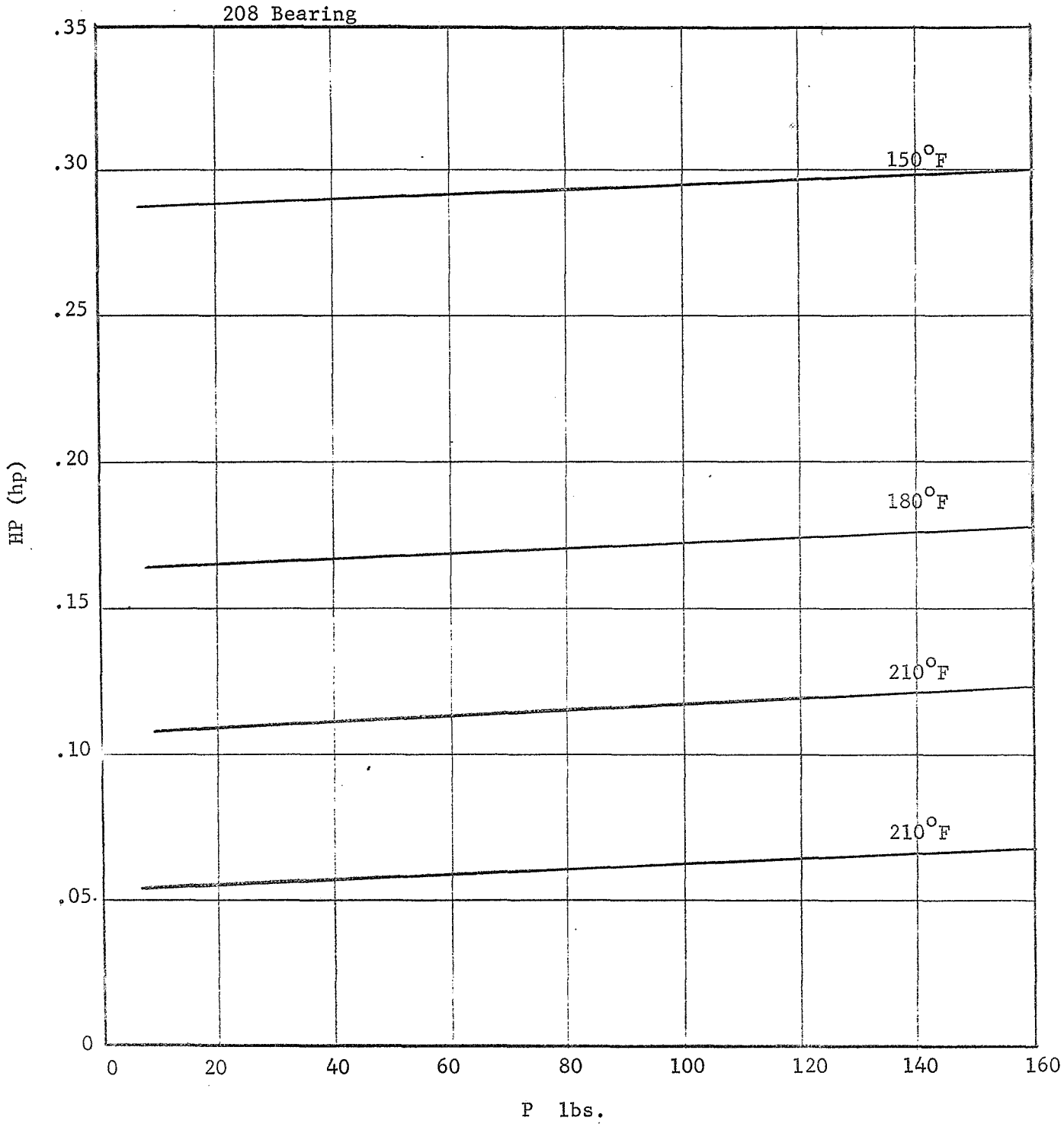

Figure C1

POWER ABSORBED BY OIL
FOR VARIOUS FLOW RATES
AND TEMPERATURE RISES

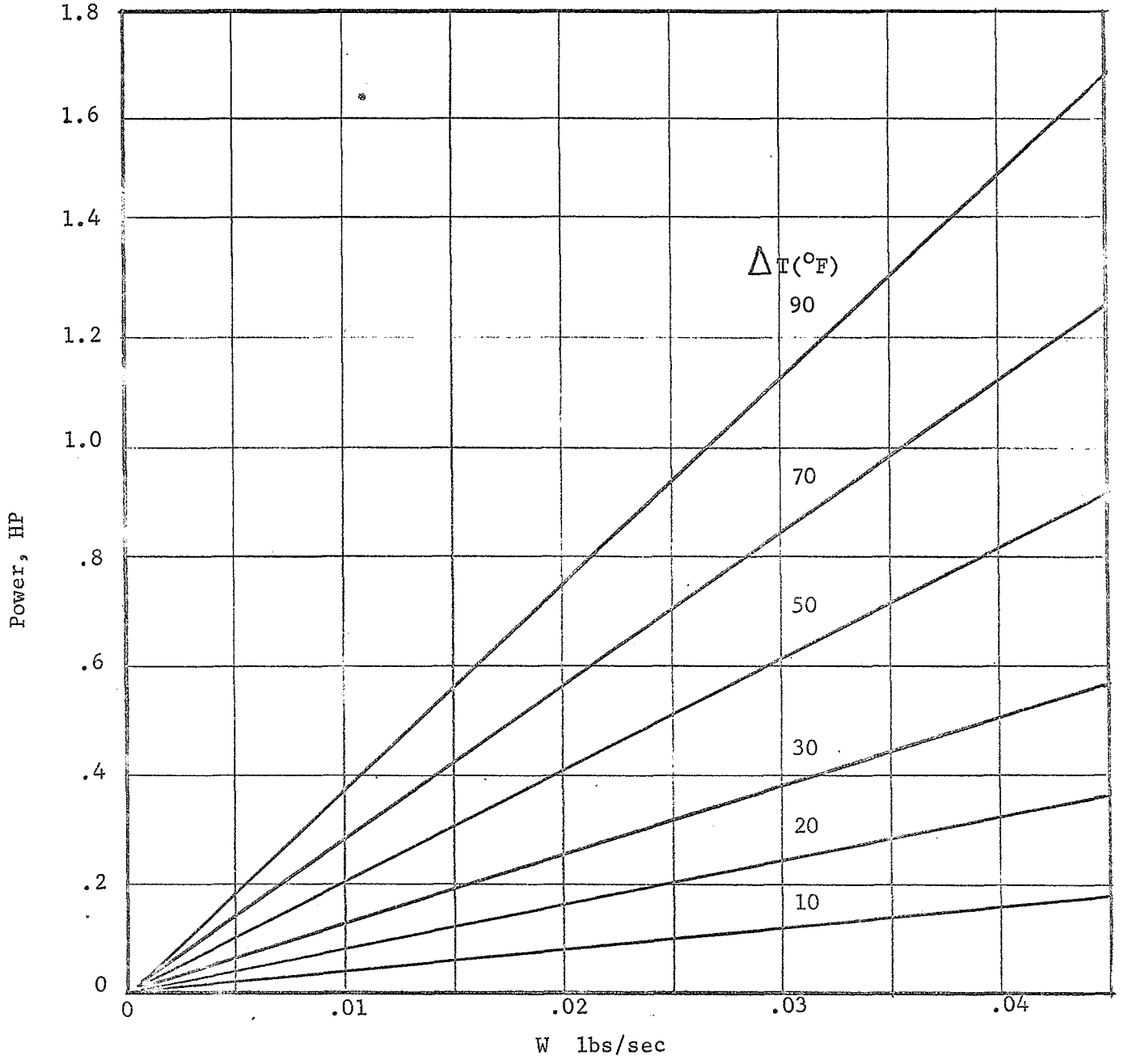

Figure C2

FIGURES

		Page
1.	Drawing of Plane Slinger with Screw Return	5
2.	Drawing of Housing-Disk Seal	7
3.	Drawing of Screw Seal	8
4.	Drawing of Rotor and Casing Assembly	19
5.	Photograph of Test Rig	20
6.	Lubrication System Schematic	24
7.	Instrumentation Schematic	25
8.	Oil Jet Ring Orifice Calibration Curve, Drive End	29
9.	Oil Jet Ring Orifice Calibration Curve, Anti-Drive End	29
10.	Torque-Meter Reading Versus Angular Displacement	30
11.	Torque Versus Quill Twist	31
12.	"As Built" Drawing Plane Slinger with Screw Return	33
13.	Typical Flow and Pressure Measurements, Plane Slinger with Screw Return	35-36-37
14.	Bearing-Seal Temperatures, DE, Plane Slinger with Screw Return	39
15.	Bearing-Seal Temperatures, ADE Plane Slinger with Screw Return	40
16.	Accumulated Leakage Versus Time Test No. 4, Plane Slinger with Screw Return	41
17.	Bearing-Seal Temperatures Versus Flow Rate, DE, Plane Slinger with Screw Return	42
18.	Bearing-Seal Temperatures Versus Flow Rate, ADE, Slinger with Screw Return	43
19.	Typical Flow and Pressure Measurements, Plane Slinger with Screw Return, Heat Input	45
20.	Bearing-Seal Temperatures Versus Heat Input, DE, Plane Slinger with Screw Return	46
21.	Bearing-Seal Temperatures Versus Heat Input, ADE, Plane Slinger with Screw Return	47
22.	"As Built" Dimensions Slinger without Screw Return	49

FIGURES (continued)

23. Accumulated Leakage, Plane Slinger without Screw Return 52
24. Preliminary Housing-Disk Seal Configuration 54
25. Picture of Interface Preliminary Housing-Disk Seal 55
26. Velocity Ratio Versus Speed, Preliminary Housing-Disk Seal 56
27. "As Built" Dimensions Housing-Disk Seal 58
28. Accumulated Leakage Versus Time Housing-Disk Seal 59
29. "As Built" Dimensions of Screw Seal 61
30. Pressure and Flow Data Screw Seal 63
31. Bearing-Seal Temperatures, Drive End, Screw Seal 64
32. Bearing-Seal Temperatures 65
33. Accumulated Leakage Versus Time, Screw Seal 67
A1. Slinger Seal Geometry 75
A2. Operating Flow Regimes for Rotating Disks 76
A3. Moment Characteristic versus Engagement Ratio, Regime I 80
A4. Function of Boundary Layer Growth, Stationary Wall, Regime II 87
A5. Typical Moment Equilibrium Plot, Rotating Disk, Regime II, X = 0.1 . . . 93
A6. Typical Moment Equilibrium Plot, Rotating Disk, Regime II, X = 1.0 . . . 93
A7. Velocity Ratio versus Engagement Ratio for Various Spacing Rations, Regime II 94
A8. Comparison Between Theoretical and Experimental Values of Velocity Ratio, Regime II 95
A9. $C_m(Re)^{1/2}$ As a Function of s/a 95
A10. $C_m(Re)^{1/2}$ As a Function of X 96
A11. Moment Characteristic Versus Engagement Ratio, Rotating Disk, Regime II 97
A12. Comparison of Theoretical and Experimental Values of Moment Coefficient, Regime II 99
A13. Schematic of Rotating Housing Seal 100
A14. Typical Moment Equilibrium Plot for Rotating Housing, Regime II, X = 0.1 102

FIGURES (continued)

A15. Typical Moment Equilibrium Plot for Rotating Housing, Regime II, X = 1.0 102

A16. Velocity Ratio versus Engagement Ratio 103

A17. $C_m(Re)^{1/2}$ versus X, Rotating Housing, Regime II 105

A18. $C_m(Re)^{1/2}$ versus s/a, Rotating Housing, Regime II 106

A19. Moment Characteristic versus X, Rotating Housing, Regime II . . . 107

A20. Engagement Ratio Function versus X, Regime III 110

A21. Function of ω/β versus K, Rotating Disk, Regime IV 113

A22. Function of ω/β versus K, Rotating Disk, Regime IV 114

A23. K Versus X as a Function of s/a, Rotating Disk, Regime IV 116

A24. $C_m(Re)^{1/5}$ versus X, Rotating Disk, Regime IV 117

A25. $C_m(Re)^{1/5}$ versus s/a, Rotating Disk, Regime IV 118

A26. K versus X as a Function of s/a, Rotating Housing, Regime IV . . . 120

A27. $C_m(Re)^{1/5}$ versus X, Rotating Housing, Regime IV 121

A28. $C_m(Re)^{1/5}$ versus s/a, Rotating Housing, Regime IV 122

A29. Pressure Characteristic of Partially Wetted Disks 125

B1. Screw Geometry 130

B2. Portion of Screw Channel 130

TABLES

Page

1. Bearing-Seal Operating Conditions 3
2. Plane Slinger with Screw Return Power Loss Tabulation 12
3. Oil Jet Ring Design 13
4. Housing-Disk Seal Power Loss Tabulation 14
5. Screw Seal Geometry 15
6. Screw Seal Power Loss Tabulation 16
7. Nominal Test Operating Conditions 32
8. Heat Balance, Plane Slinger with Screw Return 50
9. Comparison of Calculated and Measured Power 68
10. Leakage Data Summary 70

A1. Possible Flow Regimes for a Disk Rotating in an Enclosed Chamber . . 74
A2. Summary of Moment Coefficients for a Totally Wetted Disk 77
A3. C_1 versus X 88
A4. Summary of Moment Coefficients for the Partially Wetted Disk . . . 119

NOMENCLATURE

a = radius of disk (L)

b = radius of wall or width of disk (L)

c, d = coefficients in series solution - Eq. 34

$$C_1 = \left[0.0316 + \int_{.02}^{X} \frac{2(1-x)^3}{\Theta}\, dx\right]$$

$$C_2 = \left[\frac{(2 + 3\ \omega/\beta)^{1/2}}{(150)^{1/4}} \left(\frac{\omega/\beta + 7/3}{6\ \omega/\beta - 1}\right)^{1/4}\right]$$

$$C_3 = \left[1 - (1 - X)^4\right]$$

$$C_4 = \left[1 - (1 - X)^{19/4}\right]$$

$$C_5 = \left[0.0369 + \int_{.02}^{X} \frac{(1 - X)^{15/4}}{d}\, dx\right]$$

$$C_6 = \left[1 - (1 - X)^{2\ 3/5}\right]$$

$$C_7 = \left(\frac{\omega}{\beta} - 1\right)^{1/4} \left[\frac{0.0225}{(0.313\ \frac{\omega}{\beta} + 0.504)\ \alpha}\right]^{1/5}$$

$$C_8 = \left[1 - (1 - x)^2\right]$$

C_{X1} = $0.1528 + 6.74\,X - 8.72\,X^2 + 3.75\,X^3$

C_{X2} = $0.540 + 7.30\,X - 8.891\,X^2 + 3.682\,X^3$

C_{X3} = $0.006 + 0.168\,X - 0.235\,X^2 + 0.107\,X^3$

C_{X4} = $0.0149 + 0.1813\,X - 0.241\,X^2 + 0.106\,X^3$

C_m = disk torque coefficient = $\dfrac{2\,M}{\rho\omega^2\,a^5}$

C'_m = cylindrical wall torque coefficient $\dfrac{f\,\Pi\,b}{8a}$

D = diameter (L)

D_f = pipe friction factor

K = velocity ratio = β/ω

L = wetted length of seal (L)

M = frictional disk torque (L-F)

M' = frictional cylindrical wall torque (L-F)

p = pressure (F/L^2)

Q = volumetric flow rate (L^3/T)

r = radius (L)

Re = disk Reynolds Number

Re_δ = screw seal Reynolds Number

NOMENCLATURE (continued)

R	=	inner radius of fluid (L)
s	=	axial clearance between disk and end wall (L)
u	=	absolute tangential velocity component (L/T)
U	=	shaft surface velocity (L/T)
v	=	absolute radial velocity component (L/T)
v_o	=	reference radial velocity near disk (L/T)
v_o^*	=	*indicates reference to wall (L/T)
w	=	axial velocity component (L/T)
x	=	$\frac{a-r}{a}$ or $\frac{b-r}{b}$
X	=	submersion ratio $\frac{a-r}{a}$ or $\frac{b-r}{b}$
y	=	distance normal to wall (L)
z	=	distance normal to disk (L)
α	=	$v_o / (\omega - \beta) r$
β	=	angular velocity of fluid core (1/T)
δ	=	disk boundary layer thickness or radial clearance (L)
γ	=	$\delta / r^{3/5}$ $(L/L^{3/5})$
η	=	dimensionless distance from solid boundary
Θ	=	end wall boundary layer thickness (L)
μ	=	absolute viscosity $(F\text{-}T/L^2)$
ν	=	kinematic viscosity (L^2/T)

NOMENCLATURE (continued)

ξ	=	cylindrical wall boundary layer thickness (L)
ρ	=	density (M/L^3)
τ_r	=	radial component of shear stress (F/L^2)
τ_t	=	tangential component of shear stress (F/L^2)
ϕ	=	$v_o^* \Theta$ (L^2/T)
ω	=	angular velocity of disk (1/T)

Subscripts

cw	=	cylindrical wall
0	=	zero through flow
rd	=	rotating disk
rot	=	rotating portion
sw	=	stationary wall
st	=	stationary portion

REFERENCES

1. Von Karmann, T., "Über laminare und Turbulente Reibung," ZAMM, Vol. 1, No. 4, (1921)
2. Cochran, E.G., "The Flow Due to a Rotating Disk," Proceedings of the Cambridge Philosophical Society, Vol. 20, (1933-34)
3. Goldstein, S. "On the Resistance to the Rotation of a Disk Immersed in a Fluid," Proceedings of the Cambridge Philosophical Society, Vol. 31, Part II, (1935)
4. Bodewadt, U.T., "Die Drehströmung über festem Grunde," ZAMM, Vol. 20, (1940)
5. Schultz-Gronow, F, "Der Reibungswiderstand rotierender Scheiben in Gehäusen," ZAMM, Vol. 15, (1935)
6. Ippen, A.T., "Influence of Viscosity on Centrifugal Pump Performance," ASME Trans., Vol. 68, No. 8
7. Soo, S. L., "Laminar Flow Over an Enclosed Rotating Disk," ASME Trans., Vol. 80, No. 2
8. Daily, J.W. and Nece, R.E., "Roughness and Chamber Dimension Effects on Induced Flow and Frictional Resistance of Enclosed Rotating Disks," MIT Hydrodynamics Laboratory, Tech. Rept. No. 27, (1958)
9. Quarterly Reports, Space Power and Propulsion Section, G.E., "Dynamic Shaft Seals in Space," AF Contract No. AF 33(657)-8469, (1963-64)
10. McCann, J.M., "Theoretical Investigation of the Fluid Ring Seal," Space Power and Propulsion Section, G.E. Report No. DM 63-163, (1963)
11. Daily, J.W. and Arndt, R.E., "Enclosed Rotating Disks with Superposed Throughflow: A Survey of Basic Effects," MIT Hydrodynamics Laboratory Report No. 53, (1962)
12. Wood, G.M, Manfredi, D.V., and Gaynor, J.E., "Centrifugal Types of Dynamic Shaft Seals," ASME Paper 63-WA-167
13. Jones, F.C., "Preliminary Bearing Tests with a Through Flow Oil Feed," General Electric Report R56SE169, (1956)

REFERENCES (continued)

14. Moore, C.C., "Operational Data Including Frictional Horsepower Measurements on High Speed Ball Bearings," General Electric Co. Report R54TL068

15. "Development Component Specification Alternator, Brushless, Liquid-Cooled," Aerojet-General Corporation Specification AGC-10175, 2nd Preliminary, 6 August 1963

16. Development Component Specification Bearing, Ball, Angular Contact, 40 mm Bore, AGC Specification 10206, 28 June 1963

17. McGrew, J.M., and McHugh, J.D., "Analysis and Test of the Screw Seal in Laminar and Turbulent Operation," General Electric Company TIS Report 63GL66, April 1963

18. McGrew, J.M., "An Experimental Evaluation of Three Types of Visco Seals," General Electric Company TIS Report 63GL173

19. SNAP-8 Electrical Systems Monthly Reports

20. McGrew, J.M., "Bearing Evaluation and Critical Speed Calculations for the SNAP-8 Alternator," General Electric Report 64GL125

GENERAL ELECTRIC

Advanced Technology Laboratories

SCHENECTADY, NEW YORK

DISTRIBUTION LIST

TIS REPORT NO. 64GL126

	Copies
H. O. Slone Lewis Research Center NASA Cleveland, Ohio	5
P. H. Hudson Aerojet-General Corp. 9190 East Flair Drive El Monte, Calif.	5 + 1 repro.
G. Oiye Aerojet-General Corp. 9190 East Flair Drive El Monte, Calif.	1
C. T. Luddy 3001 East Lake Rd. DC Motor & Generator Erie, Pa.	3 + 1 repro.
R. H. Guedet 3001 East Lake Rd. DC Motor & Generator Erie, Pa.	1
J. F. Davis 3001 East Lake Rd. DC Motor & Generator Erie, Pa.	1
C. S. Renner 3001 East Lake Rd. DC Motor & Generator Erie, Pa.	1
T. Salmon - 3-65B 3001 East Lake Rd. DC Motor & Generator Erie, Pa.	1

	Copies
DC Motor & Generator Technical Library - 1-9 3001 East Lake Rd. Erie, Pa.	1
P. M. Tabor General Electric Dr. Room 242 Waynesboro, Virginia	1
D. A. Fisk Room 250 General Electric Dr. Waynesboro, Virginia	
T. F. Bruce Defense Programs Oper. 6607 West 80th St. Los Angeles, Calif.	1
J. M. McGrew Bldg. 37, R. 1020 Advanced Tech. Laboratories Schenectady, N. Y.	10
E. Ray Valley Forge Space Tech Center King of Prussia, Pa.	1
L. Lady Valley Forge Space Tech Center King of Prussia, Pa.	1
Herman Ernst Bldg. 701, N-13 Re-Entry Systems Space Power & Propulsion Dept. Interstate Highway 75 Evendale, Ohio	1

DISTRIBUTION LIST (Continued) TIS REPORT NO. 64GL126

	Copies
E. Schnetzer Space Power & Propulsion Dept. Re-Entry Systems Interstate Highway 75 Evendale, Ohio	1
A. Schnake Space Power & Propulsion Dept. Re-Entry Systems Interstate Highway 75 Evendale, Ohio	1

TITLE PAGE ONLY

W. R. Becraft
Space Power and Propulsion Eng.
Re-Entry Systems
Interstate Highway 75
Evendale, Ohio

A. E. Truran
Small Steam Turbine
166 Broad St.
Fitchburg, Mass.

M. E. Petersen
Bldg. 50, R. 360
Schenectady

E. P. Smith
Bldg. 41, R. 314
Schenectady

I. E. Andreason
3001 East Lake Rd.
DC Motor & Generator
Erie, Pa.

ATL

S. Neal

W. E. Gray

W. L. Zabriskie

H. Stern

G. R. Fox

J. P. Hanna

V. FITS AND CLEARANCES, TABLE

The following table lists the fits and clearances for the SNAP-8 alternator S/N 481485 through S/N 481491. The given design values apply only to the later prototype machines. All dimensions are in inches and are measured values where practical.

Snap-8 Alternator

Table of Fits and Clearances

Location	Design	S/N 481485	S/N 481486	S/N 481487	S/N 481488	S/N 481489	S/N 481490	S/N 481491
Inboard side of DE inboard slinger	.010/.008	.0242	.0254	.0241	.0094	.0096	.0088	.0094
Inboard side of ADE inboard slinger	.010/.008	.0242	.0267	.025	.0094	.0096	.0088	.0094
Outboard side of DE inboard slinger	.038/.030	.0426	.0423	.0419	.0337	.0327	.0342	.0330
DE bearing stop gap	.007/.005	.0140	.0128	.0153	.0054	.0068	.0055	.0063
DE Wavy washer assembly	.210/.206	.2162	.2155	.2173	.2072	.2102	.2084	.2092
Inboard side of DE outboard slinger	.028/.025	.029	.0269	.0265	.0275	.0226	.0235	.0228
Outboard side of DE outboard slinger	.031/.023	.0451	.0404	.0414	.0266	.0266	.0272	.0264
Outboard side of ADE inboard slinger	.038/.030	.0432	.0417	.0410	.0329	.0327	.0355	.0346
ADE bearing stop gap	.007/.005	.0138	.0155	.0153	.0053	.0051	.0051	.0063
ADE Wavy washer assembly	.210/.206	.2163	.2169	.2173	.2084	.2083	.2076	.2100
Inboard side of ADE outboard slinger	.028/.025	.0280	.0278	.0269	.0263	.0231	.0222	.0224
Outboard side of ADE outboard slinger	.031/.023	.0432	.0393	.0434	.0264	.0272	.0274	.0265
Radial clearance of DE outboard slinger	.019/.015	.0104	.0105	.0178	.0176	.0168	.0169	.0176
Radial clearance of DE inboard slinger	.019/.015	.0091	.0103	.0166	.0169	.0165	.0165	.0165
Radial clearance of ADE inboard slinger	.019/.015	.0085	.0098	.0163	.0168	.0166	.0168	.0170
Radial clearance of ADE outboard slinger	.019/.015	.0099	.01035	.0168	.0171	.0172	.0169	.0171
DE outboard screw seal	.005/.0013	.0043	.0044	.0035	.0032	.0025	.0027	.0028
DE inboard screw seal	.005/.0015	.0045	.002	.0025	.0032	.0034	.0027	.0030
ADE inboard screw seal	.005/.0015	.0045	.0019	.0030	.0035	.0034	.0033	.0036
ADE outboard screw seal	.005/.0013	.0042	.0042	.0041	.0027	.0028	.0028	.0027
Minimum radial air gap	.054	.0545	.0577	.0565	.0567	.0565	.0562	.0577
Maximum radial air gap	.067	.0605	.0625	.0605	.0623	.0614	.0617	.0613
Stator core in frame	-.006/-.002	-.0030	-.0050	-.0040	-.0055	-.0035	-.0030	-.0045
Field coil in frame	LL/.004	.0040	.0020	.0005	.0020	.0025	.0030	.000
Shroud over fins	LL/-.004	-.0030	-.0010	-.0010	-.0015	-.0020	-.0030	-.002
DE end shield in frame	LL/-.002	.0005	-.0011	-.0003	-.0003	-.0009	-.0009	-.001
ADE end shield in frame	LL/-.002	.00005	-.0007	-.0005	-.0009	-.0010	-.0008	-.0002
DE outboard screw seal in E.S.	.0005/-.0005	.00015	-.0001	.0004	.0001	-.00015	-.00005	-.0002
DE inboard screw seal in E.S.	.0005/-.0005	.0085	-.0001	-.0003	.00005	-.00013	.00005	-.00015
ADE inboard screw seal in E.S.	.0005/-.0005	+.00025	-.0002	-.0001	.0001	-.00003	-.00014	-.0002
ADE outboard screw seal in E.S.	.0005/-.0005	-.00042	-.00015	.0002	-.0001	-.00005	.00005	-.00015
DE collar on rotor	LL/-.001	-.00045	-.0002	-.0005	-.0002	-.0002	-.00015	-.0004
ADE collar on rotor	LL/-.001	-.00072	-.00015	-.0004	-.0002	-.0007	-.0001	-.00045
DE outboard slinger on rotor	LL/-.001	-.00070	-.00065	-.0005	-.00015	-.0007	-.0007	-.0008
ADE outboard slinger on rotor	LL/-.001	-.00045	-.00060	-.00050	-.00050	-.00080	-.00060	-.00055

Snap-5 Alternator
Table of Fits and Clearances

Location	Design	S/N 481485	S/N 481486	S/N 481487	S/N 481488	S/N 481489	S/N 481490	S/N 481491
DE ball bearing on rotor	-.0001/-.0005	-.00030	-.00040	-.00030	-.00035	-.00030	-.00027	-.00032
ADE ball bearing on rotor	-.0001/-.0007	-.00030	-.00035	-.00050	-.00035	-.00040	-.00025	-.00035
DE inboard slinger on rotor	LL/-.001	∓.00045	-.00065	-.0004	-.0004	-.0007	-.0002	-.00035
ADE inboard slinger on rotor	LL/-.001	-.00055	-.0006	-.0004	-.0003	-.0007	-.0004	-.0005
DE ball bearing in E.S.	.0007/.0001	.00023	.00028	.00028	.00035	.0003	.00031	.00033
ADE ball bearing in E.S.	.0007/.0001	.00032	.00016	.00028	.00036	.0003	.00028	.00026
DE set ring in E.S.	.0008/.0001	.00028	.00053	.0005	.00055	.0002	.00015	.00015
ADE set ring in E.S.	.0008/.0001	.00050	.00039	.00030	.00057	.00020	.00001	.00025
DE bearing stop in E.S.	LL/-.00050	-.00022	-.00014	-.00030	-.00025	-.00020	-.00025	-.00025
ADE bearing stop in E.S.	LL/-.0005	-.00020	-.00026	-.00030	-.00015	-.00030	-.00024	-.00025
Innershaft in rotor	.0002/∓.0004	-.00010	-.00010	-.00015	-.00020	-.00030	-.00020	-.0001

VI. FIELD COIL FIT

The following design calculation describes the field coil fit for the 2CM391A1 alternator (P/N 094162).

GENERAL ELECTRIC

REV NO.	TITLE Field Coil Fit	CONT ON SHEET	SH NO. 1
CONT ON SHEET SH NO.	FIRST MADE FOR 2C/139141		

Ingot iron frame 7.6×10^{-6} in/in/°F

Copper field coil 9.8×10^{-6} in/in/°F

Assume frame temp will be 130°C (266°F) from pg 46 of heat transfer calculations

Assume field coil temp will be 200°C (392°F) an unspecified worst condition

Basic diameter = 10.357"

Frame is 10.357" dia at 75°F

$$\begin{array}{r} 266 \\ -\ 75 \\ \hline DT = 191°F \end{array}$$

$$\frac{7.6 \times 10^{-6} \text{ in}}{\text{in °F}} \Big| \, 10.357 \text{ in} \, \Big| \, 191°F = .01505'' \text{ expansion}$$

$392 - 75 = 317°F$ DT

$$9.8 \times 10^{-6} \, \Big| \, 10.357 \, \Big| \, 317 = .0322'' \text{ expansion at } 200°C$$

Assume avg field coil temp is 160°C (320°F)
$320 - 75 = 245°F$

$9.8 \times 10^{-6} \times 10.357 \times 245 = .0248''$ expansion at 160°C

Assume avg field coil temp is 130°C (266°F

$9.8 \times 10^{-6} \times 10.357 \times 191 = .0194''$ expansion at 130°C

MADE BY S. J. Rollins	APPROVALS	DIV. OR DEPT.	VI 2
ISSUED 8-21-63		LOCATION	CONT ON SHEET SH NO.

GENERAL ELECTRIC

REV NO.	TITLE Field Coil Fit	CONT ON SHEET	SH NO. 2
CONT ON SHEET SH NO.	FIRST MADE FOR 2CM391 A1		

Component	Temp	Expansion from R.T.
Frame	130°C	.015"
Coil	130°C	.019"
Coil	160°C	.025"
Coil	200°C	.032"

Therefore, make the fit between the field coil and the frame .004" loose to something tighter whatever close tolerances will allow.

MADE BY J. Ballone	APPROVALS	DIV. OR DEPT.	CONT ON SHEET	SH NO. VI 3
ISSUED 8-21-63		LOCATION		

VII. WEIGHT

The Snap-8 alternator weighs 431 pounds. Of this, 196 pounds or about 45% of the alternator weight is electromagnetic weight. The following table compares the electromagnetic and structural weights of the pre-prototype and prototype machines. The component designated as "other" includes covers, caps, screws, washers, collars, shims, bearing stops, pins, key ring studs, a lock nut and other hardware.

The noticeable weight differences in the pre-prototype and prototype machine occur in the end shields, rotor and frame. The rotor weight was reduced by cutting out material to increase the saliency. The frame weight was increased to provide sufficient structural material for the trunnion mountings and increase the flux path of the stator.

The analysis of structural and electromagnetic weights for the frame and rotor is given in the Analysis section on page ___ Table #____. These represent calculated weights on the table while the other listed weights are measured values

TABLE

	Pre-prototype - 2CM391A1 - 481485			Prototype - 2CM391B1 - 481490		
Component	Electro-magnetic weight	Structural Weight	Total	Electro-magnetic weight	Structural Weight	Total
Rotor	56.40	7.60	64.00	52.525	7.60	60.125
Inner shaft		2.00	2.00		2.00	2.00
Slingers & Seals		13.80	13.80		13.80	13.80
DE End Shield		70.60	70.60		51.00	51.00
ADE End Shield		38.00	38.00		29.00	29.00
Bearings		1.76	1.76		1.76	1.76
Frame	37.10	79.90	117.0	55.00	119.00	174.
Stator Wound	101.00		101.00	101.000		101.00
Terminals	2.05		2.05	2.050		2.05
Other		9.79	9.79		11.165	11.165
Total	206.55	223.45	428.00	210.575	237.26	446.0

Page No.
Property of General Electric Company
Maintain one inch side margin

VIII. MATERIALS FOR CONSTRUCTION - PREPROTOTYPE ALTERNATOR

The materials are the same as the prototype with the following differences

(1) The rotor material was changed from 4130 to 4620 rotor material.

(2) The bearings were changed from single vacuum melt to triple vacuum melt steel.

(3) The end shields were changed from solid Inconel-X to the present composite construction.

Page No.
Property of General Electric Company
Maintain one inch side margins.

MATERIALS FOR CONSTRUCTION - PROTOTYPE ALTERNATOR - 2CM391B1

	Part Name	GE Spec	Commercial Designation
(1)	Frame Flange	B50CD188	HY-80 Alloy steel forging
(2)	Frame Shell	B30E4C	Low - Carbon, seamless steel pipe, ASTM designation A106 Grade A
(3)	Shroud	B30E4C	Low - Carbon, seamless steel pipe, ASTM designation A106 Grade A
(4)	Trunnion Inserts	B5F7H2	Hot-rolled heat treated chromium - molybdenum steel
(5)	End Shields, Hub	B50CD182-S1	Inconel-X forging
(6)	End Shields, Flange	B7A54	304 Chromium Nickel Steel Plate
(7)	Rotor	B50CD189	4620 Alloy Steel Forging
(8)	Seal Components		
	(a) Screw Seals	B5F7H2	Hot-rolled, heat treated chromium-molybdenum steel
	(b) Slingers	B5F7H2	Hot-rolled, heat treated chromium-molybdenum steel
	(c) Coating	A16B5	Polytetrafluoroethylene
	(d) Wavy Washers	B5F7H2	Hot-rolled, heat treated chromium-molybdenum steel
(9)	Bearings	Aerojet # 095355	Triple vacuum melt steel
(10)	Innershaft	B5E1AM	Nitriding steel bars chromium-aluminum
(11)	Stator Punching	B3E20-S5	M-19 Silicon Sheet Steel
(12)	Stator Wire	B50CD116-S7	Heavy coated aromatic polymide insulated magnet wire (rectangular)
(13)	Field Wire	B50CD117-S8	Heavy coated aromatic polyirmide insulated magnet wire (round)
(14)	Hermetic Terminals		
	(a) Main	Drwg #36B508481	Alumina ceramic body leads - OFHC copper metalizing-molybdenum manganese
	(b) Field	Drwg #36B508483	Alumina ceramic body leads OFHC copper metalizing molybdenum manganese sealing flange and tubes Grade A Nickel
	(c) Thermocouple	Drwg #36A227180	Alumina ceramic body metalizing molybdenum manganese, Alumel & Chromel lea

IX. INSTRUCTION MANUAL

An instruction manual describing the preprototype alternator with instructions pertinent to handling and storage, inspection, operating, maintenance, disassembly, cleaning and testing, are covered in this section.

Section IX

Report No.

GENERAL ELECTRIC

SNAP 8 ELECTRICAL SYSTEM

INSTRUCTION MANUAL FOR ALTERNATOR

AEROJET-GENERAL CORPORATION

P. O. BOX 296 - AZUSA, CALIFORNIA

Aerojet-General P/O OP359076, Work Order 0741-16-3000

NASA 5-417

OCTOBER 11, 1963

Prepared by:

C. H. FREEBERG

SNAP 8 ALTERNATOR

INSTRUCTION MANUAL
(PRELIMINARY OCTOBER 11, 1963)

MODEL 2CM391A1
(GENERAL ELECTRIC)

AEROJET P/O OP359076
WORK ORDER 0741-16-3000

AEROSPACE MOTOR AND GENERATOR PRODUCTS SECTION

GENERAL ELECTRIC COMPANY
DIRECT CURRENT MOTOR AND GENERATOR DEPARTMENT
ERIE, PENNSYLVANIA

GENERAL ELECTRIC COMPANY

INSTRUCTION MANUAL
(PRELIMINARY OCTOBER 11, 1963)

AIRCRAFT ALTERNATOR 2CM391A1

Contents:

	Page
Introduction	1
Description and Principles of Operation	1
Handling and Storage	4
Inspection, Preparation and Insulation	4
Operating Instructions	6
Maintenance	6
Disassembly	6
Cleaning	6
Testing	7
Generator Constants	8

Appendix A (Illustrations, Tables and Curves)

Appendix B (General Electric Company Acceptance Test Engineering Instructions)

These instructions do not purport to cover all details or variations in equipment nor to provide for every possible contingency to be met in connection with installation, operation, or maintenance. Should further information be desired, or should particular problems arise which are not covered sufficiently for the purchaser's purposes, the matter should be referred to the General Electric Company.

GENERAL ELECTRIC COMPANY
INSTRUCTION MANUAL
A-C GENERATOR 2CM391A1

1. INTRODUCTION

1.1 This manual contains descriptive information and instructions for the handling, storage, preparation, installation and maintenance of the Model 2CM391A1 A-C Generator manufactured by the Direct Current Motor and Generator Department, General Electric Company, Erie, Pennsylvania.

1.2 The Model 2CM391A1 A-C Generator is used as a turbine driven source of a-c electrical power. The rating is as follows:

80 KVA
.75 LAG to unity PF
3 Phase 6 Wire
223 AMPS
120/208 rms Volts
400 cps
12,000 RPM
Oil Cooled

1.3 Rotation - counterclockwise, when viewed from drive end.

2. DESCRIPTION AND PRINCIPLES OF OPERATION

2.1 Definitions

2.1.1 Drive End - Refers to the mounting flange end.

2.1.2 Anti Drive End - Refers to the end opposite the drive end.

2.2 Mechanical Features

The major components for the Model 2CM391A1 are -

2.2.1 The Stator Wound - consists of the frame, stator core wound, DC field coil and leads, terminal blocks and hermetic terminals, thermocouples and mounting trunnions.

2.2.2 The End Shield Assemblies each consists of a single row ball bearing, jet ring, inboard and outboard oil slinger and inboard and outboard screw seal. Also oil fittings, hermetic terminals for thermocouples and bearing preload spring.

2.2.3 The Rotor is a solid rotor construction with an inner shaft.

2.3 Special Mechanical Features

The generator is designed to be cooled with 1600 lb/hr of Dow Corning ET-378 at 210°F maximum inlet temperature. Each bearing will be cooled and lubricated with 200 lb/hr of ET-378 fluid at 210°F. Therefore, the generator has three separate oil circuits .

Drain ports are provided in the bottom of the generator to drain seal leakage oil and to provide access to the generator cavity for the purpose of pulling a vacuum. Two drains are installed in the generator frame at either end of the stator core. One drain is installed in the drive end end shield between the generator bearing and the turbine. One drain is installed in the anti-drive end cap.

A flexible quill shaft is provided to reduce loads on the drive spline in the event of misalignment in order to provide the longest possible spline life.

2.4 Special Electrical Features

The DC field coil is sandwiched between two stator cores with the field leads brought out through a slot in outside diameter of a stator core to hermetic terminals in the frame.

The main armature winding is a two circuit winding with equalizer connections to reduce magnetic forces on the bearing caused by eccentricity between the rotor and stators.

The generator has been designed to operate at low flux densities and low current densities to provide low losses and low winding temperatures.

2.5 Principles of Operation

2.5.1 Refer to Eléctrical Schematic Diagram, Dwg. 194E691, Appendix A.

2.5.2 The 2CM391A1 is a solid pole (4 pole) homopolar inductor generator. The generator is driven at 12000 RPM by being connected directly to a turbine which operates on a mercury vapor rankine cycle.

2.5.3 When operating, the solid rotor, which has its poles displaced at 90°, shifts the magnetic flux 90° as it passes through the stationary

stator core and frame. A field coil, energized with induced D-C power, magnetizes the frame. The magnetizing flux passes through the stator core. Coils placed in the stator core lie in the magnetic field and act as the armature windings.

As the rotor turns, the magnetic flux path moves, cutting the electrical conductors. This changing flux causes the current to flow in the stator coils.

2.5.4 The 400 cycle power output of the generator is controlled by the system voltage regulator. This is accomplished by sensing the generator output voltage and, in turn, controlling the amount of d-c power induced into the field coil.

2.5.5 Refer to Hydraulic Schematic Diagram, Dwg. 194E691, Appendix A.

2.5.6 Generator cooling is accomplished by the flow of ET-378 oil. The maximum temperature of the oil at the generator inlet is 99°C (210°F). The oil is supplied to the generator at 33 psi, with a back pressure of 20 psi at the generator outlet.

2.5.7 The cooling oil enters the generator cooling system through the oil inlet tube in the frame shroud. The cooling oil then circulates through a labyrinth of slots, machined longitudinally on the periphery of the frame, and is discharged from the generator cooling system through the oil outlet tube.

2.5.8 Generator bearing lubricating is accomplished by flow and slinger action in the bearing cavity. ET-378 oil is used for bearing lubrication and cooling. The oil used for bearing lubrication is taken from the cooling oil supply in parallel with the oil entering the generator cooling system, and is circulated through each bearing lubrication system.

The drive end bearing lubrication system consists of an inlet tube in the drive end end shield, which carries the oil to a hole in the drive end end shield to a jet ring in the bearing cavity where the oil is sprayed through four small holes to the bearing and through two small holes to the inboard slinger. The oil is scavenged from the bearing cavity by two slinger seals. The slinger seals are backed up by two screw seals running with a close clearance on the rotor shaft. The anti drive end bearing lubrication system is the same as stated above for the drive end.

3. HANDLING AND STORAGE

3.1 Handling

3.1.1 The generator must be handled with care. The shipping cover should be in place whenever the generator is not mated to the turbine.

DO NOT USE THE SHAFT EXTENSION, TERMINALS TERMINAL BLOCKS, OR OIL LINES AS HANDLES OR SUPPORTS AT ANY TIME. THE GENERATOR SHALL BE PROTECTED AGAINST ANY DAMAGING CONTACTS.

It is recommended that the generator be lifted by the eye bolts, transported or mounted on the generator oil shroud in a suitable v-block or cradle to avoid damage to any of the above mentioned components.

3.1.2 Caution Note

AT NO TIME MUST THE FINELY GROUND MOUNTING FLANGE SURFACE BE ALLOWED TO BECOME SCRATCHED, GOUGED, KNOCKED OUT OF FLATNESS, OR OTHERWISE DAMAGED. DO NOT USE SCREW-DRIVERS OR OTHER SIMILAR INSTRUMENTS TO DIS-ENGAGE THE GENERATOR FROM THE TURBINE.

3.2 Storage

3.2.1 Cover the generator with a plastic bag or similar covering to protect against contamination.

3.2.2 Store the generator in its shipping container to protect against physical damage.

3.2.3 The oil inlets and outlets shall be covered at all times to prevent dust or foreign objects from entering the system.

3.2.4 If required, the exterior of the generator can be wiped with a clean lint-free cloth, lightly moistened with trichloroethylene (Federal Specification P-S-661A), or other approved solvent, and blown dry with filtered compressed air.

3.2.5 The shipping cover shall be in place during all storage periods.

4. INSPECTION, PREPARATION AND INSTALLATION

4.1 Inspection

4.1.1 Generators in storage for longer than two years should be returned to the manufacturer for testing.

4.1.2 Generators in storage for less than two years should be inspected as follows:

4.1.2.1 Check generator nameplate to determine that the generator is proper for the application.

4.1.2.2 Visually inspect the generator exterior for damage, presence of safety wire, etc. Carefully remove the shipping cover and inspect the mounting flange surface and inner shaft for damage. Replace the cover.

4.1.2.3 Remove terminal covers and terminal hardware and inspect for possible damage, proper safety locking of attaching bolts, and clean terminal contact surfaces.

4.1.2.4 Measure the resistance of stator windings with a portable double bridge (Tool No. 9069199G2, Figure 3), or equivalent. See paragraph 9.2 for resistance values.

4.1.2.5 Check for insulation breakdown in the stator with high potential current limited tester (Tool No. 9892115G1, Figure 3). Refer to Electrical Schematic Diagram, Dwg. 194E691. Attach test probes, bring up voltage gradually, and apply voltage specified for one minute. There shall be no insulation breakdown. Return voltage to zero at completion of each test, and before disconnecting test probes. Refer to paragraph 9.2 for hi-pot values.

WARNING

HIGH POTENTIAL TESTING IS CONSIDERED HAZARDOUS. TO AVOID SERIOUS OR FATAL ELECTRIC SHOCK, DO NOT MAKE BODILY CONTACT WITH TEST PROBES OR GENERATOR PARTS DURING TEST.

4.2 Preparation

4.2.1 After inspection, replace the terminal hardware and terminal covers. Place the generator in a suitable v-block or cradle to prevent damage to vulnerable components.

4.3 Installation

4.3.1 Clean the generator and turbine mounting flange surfaces with a clean, lint-free cloth moistened with isopropyl alcohol, or equivalent solvent, and wipe dry.

4.3.2 Install the mounting flange sealing ring on the generator flange.

4.3.3 With the generator supported in a v-block or cradle, move it into position to mate with the turbine. The dowel pin at the top of the generator mounting flange must line up with the corresponding hole in the turbine. The generator shaft may have to be rotated slightly to enable the splines to engage.

4.3.4 When proper mating has been achieved, install nuts. Torque the nuts to the limits specified on GE drawing No. 194E691.

4.3.5 Make the electrical connections in accordance with the electrical system instructions. When tightening the terminal stud lock nuts, torque to the values specified in the table of Terminal Stud Torque Limits, Drawing 194E691. (DO NOT EXCEED THESE VALUES).

4.3.6 Reinstall terminal board cover gaskets and terminal board covers.

5. OPERATING INSTRUCTIONS

5.1 Since the generator operates as an integral part of the generating system, and is not operated independently from the system, refer to the system operating instructions.

6. MAINTENANCE

6.1 Recommended maintenance for the Model 2CM391A1 generator is limited to replacement of the terminal covers, terminal stud hardware, and such cleaning and testing as can be performed without major disassembly of the generator. For further maintenance, repair or overhaul, the generator shall be returned to the manufacturer.

7. DISASSEMBLY

7.1 Aside from terminal board maintenance, there will be no disassembly of the generator.

8. CLEANING

8.1 Trichloroethylene may be used on all metal parts. Wipe with clean cloth and dry.

9. TESTING

9.1 Preparation

9.1.1 Remove terminal board covers and terminal hardware.

9.2 Test per General Electric Engineering Instruction 718A302WM as required.

WARNING

POSSIBLE SERIOUS OR FATAL INJURY CAN BE INFLECTED BY FLYING PARTS WHICH MAY RESULT FROM MECHANICAL FAILURE. PERSONNEL SHALL BE PROTECTED AGAINST SUCH POSSIBLE INJURY. TO CONFINE FLYING PARTS, THE GENERATOR SHALL BE ADEQUATELY SHIELDED DURING OVERSPEED BY A GUARD FABRICATED BY THE USER TO SUIT THE TEST AREA AND THE TEST EQUIPMENT BEING USED.

10. 2CM391A1 GENERATOR CONSTANTS (CALCULATED)

Constant	Units	Generator
Frequency	cps	400
Base Values	Volts rms L-N Amps rms 1 Ø	120 V 223
Ra	P. U.	.0187 at 184°C
Xa	P. U.	.0962
Xad	P. U.	1.300
Xaq	P. U.	.791
$T_{d'o}$	Sec	0.506
R field	Ohms at 25°C	1.56 + - 0.10
R armature		
Excitation at 181°C		
If NL	amps	7.5
If 0.5L 0.9PF	amps	10.8
If 1.0L 0.75PF	amps	18.2
If 2.0 PU 3 Ø S6		19.0 amps

APPENDIX A

This appendix contains all illustrations, tables and curves referenced by figure numbers in the preceding portion of this data manual.

Contents:

Figure No.	Title
1	194E680, 2CM391A1 Alternator (Layout)
2	194E691, 2CM391A1 Alternator (Outline)
3	Special Tools and Test Equipment

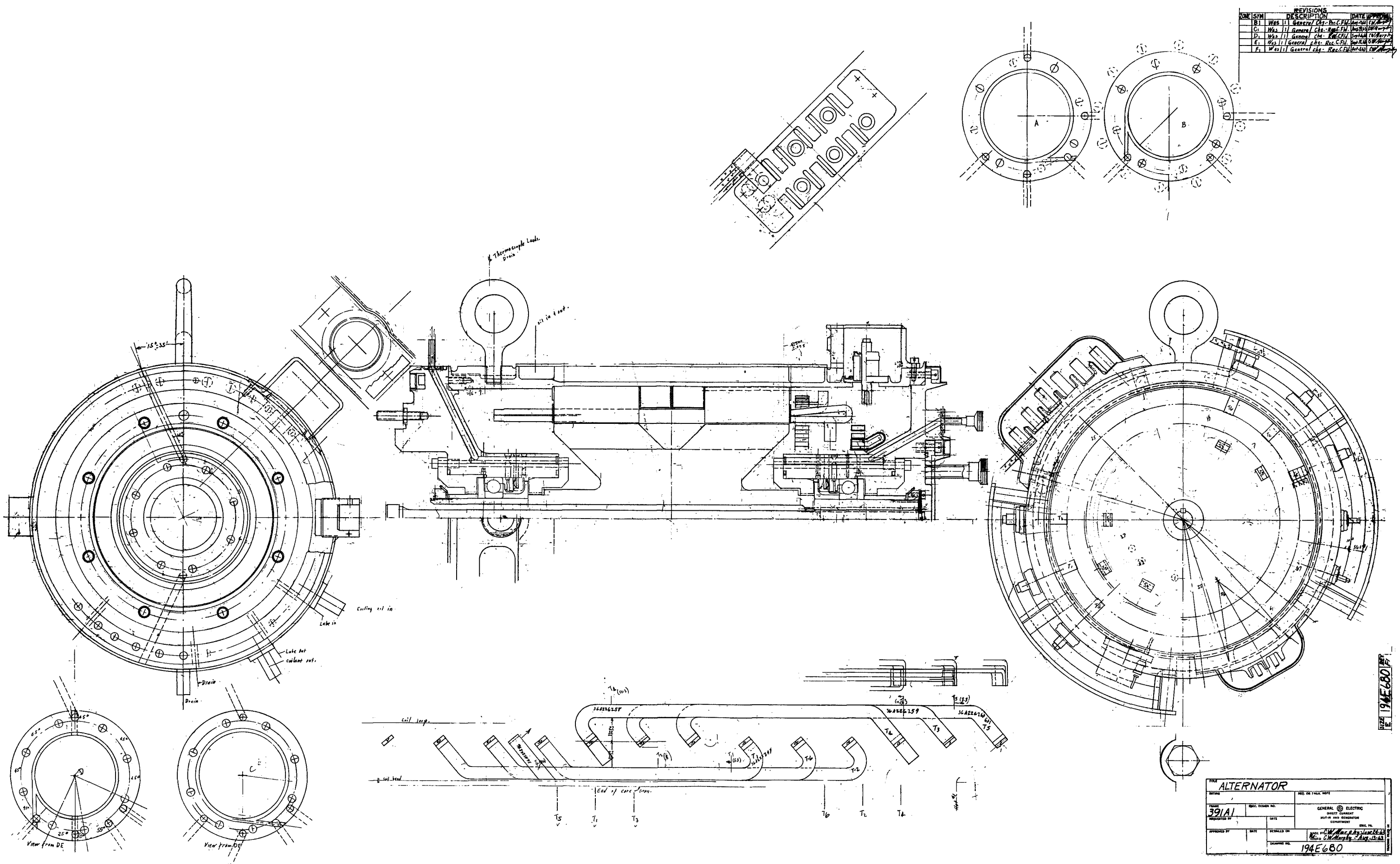

REVISIONS
ZONE SYM DESCRIPTION DATE APPROVAL
B1 Was 1 General Chg. Rec. C.Fld.
C1 Was 1 General Chg. Rec. C.Fld.
D1 Was 1 General Chg. Rec. C.Fld.
E1 Was 1 General chg. Rec. C.Fld.
F1 Was 1 General chg. Rec. C.Fld.
A
B
Thermocouple Leads
Drain
Cooling oil in
Lube in
Lube out
coolant out
Drain
Drain
Coil loop
Coil head
End of core iron
View from DE
View from DE
SIZE E 194E680 REV F1
TITLE ALTERNATOR
391A1
GENERAL ELECTRIC
DIRECT CURRENT
MOTOR AND GENERATOR
DEPARTMENT
DRAWING NO. 194E680

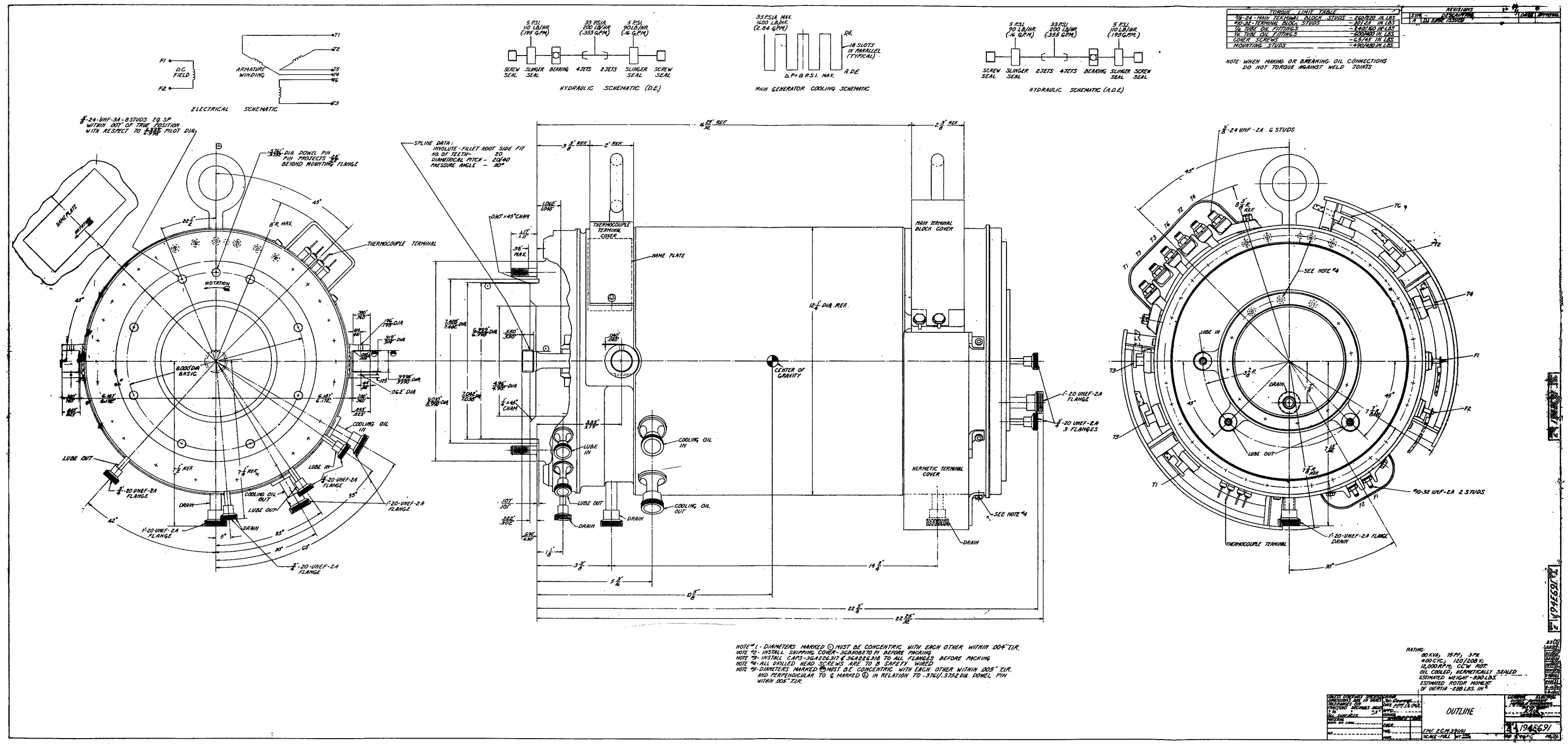
ELECTRICAL SCHEMATIC
D.C. FIELD
ARMATURE WINDING
HYDRAULIC SCHEMATIC (D.E.)
SCREW SEAL
SLINGER SEAL
BEARING
4 JETS
2 JETS
MAIN GENERATOR COOLING SCHEMATIC
18 SLOTS IN PARALLEL (TYPICAL)
HYDRAULIC SCHEMATIC (A.D.E.)
TORQUE LIMIT TABLE
3/8-24 - MAIN TERMINAL BLOCK STUDS - 240/270 IN LBS
#10-32 - TERMINAL BLOCK STUDS - 30/35 IN LBS
1/4 TUBE OIL FITTINGS - 140/160 IN LBS
1/2 TUBE OIL FITTINGS - 200/220 IN LBS
COVER SCREWS - 65/145 IN LBS
MOUNTING STUDS - 490/540 IN LBS
NOTE: WHEN MAKING OR BREAKING OIL CONNECTIONS DO NOT TORQUE AGAINST WELD JOINTS
REVISIONS
NAME PLATE
THERMOCOUPLE TERMINAL
ROTATION
8.000" DIA BASIC
LUBE OUT
LUBE IN
COOLING OIL IN
COOLING OIL OUT
DRAIN
THERMOCOUPLE TERMINAL COVER
MAIN TERMINAL BLOCK COVER
HERMETIC TERMINAL COVER
CENTER OF GRAVITY
SEE NOTE #4
SPLINE DATA: INVOLUTE - FILLET ROOT SIDE FIT
NO. OF TEETH - 20
DIAMETRICAL PITCH - 20/40
PRESSURE ANGLE - 30°
12 1/4" DIA REF.
1" - 20 UNEF-2A FLANGE
3/4" - 20 UNEF-2A 3 FLANGES
3/8" - 24 UNF-2A 6 STUDS
#10-32 UNF-2A 2 STUDS
RATING
80 KVA, 75 PF, 3 PH
400 CYC., 120/208 V.
12,000 RPM, CCW ROT.
OIL COOLED, HERMETICALLY SEALED
ESTIMATED WEIGHT - 330 LBS.
ESTIMATED ROTOR MOMENT OF INERTIA - 28 LBS. IN²
OUTLINE
CME 2CM39101
SCALE - FULL
1948691

TOOL NO.	DESCRIPTION
9069199G2	Double Bridge, Portable, 0-22 Ohms.
9892115G1	Tester, High-Potential, Current-Limited.

FIGURE 3. SPECIAL TOOLS AND TEST EQUIPMENT

GENERAL ELECTRIC COMPANY
INSTRUCTION MANUAL
A-C GENERATOR 2CM391A1

APPENDIX B

Contents:

EI Number	Title
EI 718A302WM	Generator Acceptance Test Specification

SIZE A 718A302 WM SHEET NO. 1 OF 7 SHEETS REV 0

SNAP-8 ELECTRICAL SYSTEM - GENERATOR ACCEPTANCE TEST SPECIFICATION MODEL NO. 2CM391A1

1.0 SCOPE

1.1 GENERAL - THIS SPECIFICATION DESCRIBES THE ACCEPTANCE TESTS TO BE CONDUCTED ON EACH PRE-PROTOTYPE SNAP-8 GENERATOR, MODEL NUMBER 2CM391A1.

1.2 DESCRIPTION OF UNIT - THE GENERATOR TO BE TESTED HAS A NOMINAL CONTINUOUS RATING OF 80 KVA, .75 LAG TO UNITY PF, 120/208 RMS VOLTS, 3-PHASE 6 WIRE, 223 AMPERES, 400 CPS AT 12000 RPM, COUNTERCLOCKWISE ROTATION FROM DRIVE END. THIS IS AN OIL-COOLED, BRUSHLESS, HOMOPOLAR INDUCTOR ALTERNATOR, DESIGNED TO MEET REQUIREMENTS OF AEROJET GENERAL SPECIFICATION AGC-10175. (PROTO WILL BE 4 WIRE.)

1.2.1 THE GENERATOR WILL BE TESTED UTILIZING AN ADAPTER WITH A 10 INCH MOUNTING FLANGE AND A DRIVING SPLINE. THE GENERATOR IS OIL-COOLED FOR BOTH TESTING AND APPLICATION.

1.2.2 FOR TESTING, AN EXTERNAL DC FIELD SOURCE WILL EXCITE THE GENERATOR FIELD WITH A DESIRED MAXIMUM CURRENT CAPACITY OF 20 AMPERES. EXCITATION VOLTAGE REQUIREMENTS SHALL NOT EXCEED 50 VOLTS DC.

2.0 REFERENCE DATA AND APPLICABLE SPECIFICATIONS

2.1 THE FOLLOWING DOCUMENTS FORM A PART OF THIS SPECIFICATION TO THE EXTENT SPECIFIED HEREIN.

2.1.1 APPLICABLE DOCUMENTS:

AGC-10175	AEROJET GENERAL A.C. GENERATOR SPECIFICATION
194E691	OUTLINE - 80 KVA INDUCTOR ALTERNATOR (2CM391A1)
MIL-G-6099A	GENERATORS AND REGULATORS, AIR-COOLED, AC GENERAL SPECIFICATION, DATED 4/15/58
AIEE #503	TEST CODE FOR SYNCHRONOUS MACHINES
MIL-G-10228A (CE)	GENERATOR SETS, ENGINE DRIVEN, METHODS OF TEST, DATED 1/8/58.
AGC-10174	AEROJET GENERAL VOLTAGE REGULATOR SPECIFICATION

REVIEWED BY C. F. Renner 10-8-63, RELIABILITY ENGINEER

REVIEWED BY W. R. David, Jr 10/8/63, QUALITY CONTROL ENGINEER

WBO-B2
LA-1
3EW(BW
3-9(BW)2
3-10(V
3-S(V
3-17(BW
KEY3
3E(BK)25
5B(50)
PRINTS TO

PREPARED BY S. J. Bellows DATE 10/8/63 APPROVED BY C. T. Luddy ISSUED 10-8-63

DC3-20 (9-59)

NEW PER S. J. BELLOWS, OCTOBER 8, 1963

REV 0

REV 0 718A302 WM SHEET NO. 2 OF 7 SHEETS SIZE A

3.0 TEST EQUIPMENT

3.1 FACILITIES

3.1.1 PRIME MOVER - THE PRIME MOVER FOR OPERATING TEST UNITS SHALL PROVIDE INPUT POWER FOR RATED OUTPUT AT NO LOAD AT 12000 RPM CONTINUOUS AND 13200 RPM FOR FIVE MINUTES.

3.1.2 ELECTRICAL LOADS - LOAD BANKS SHALL BE CAPABLE OF PROVIDING RESISTIVE AND REACTIVE, BALANCED AND UNBALANCED LOADS AS REQUIRED BY INDIVIDUAL TESTS.

3.1.3 BEARING AND SEAL LUBRICATION

3.1.3.1 LUBRICATION REQUIREMENTS:

(A) ET-378 OIL
(B) FLOW - .690 -.710 GPM (TOTAL); .345 -.355 GPM (EACH BEARING)
(C) FILTER - 5 MICRON NOMINAL AT INLET AND OUTLET
(D) TEMPERATURE - 210 +0.0 OR MINUS 10.0 °F AT INLET
(E) PRESSURE - 33.0 PLUS 0.0 OR MINUS 1.0 PSIA AT INLET

3.1.4 GENERATOR COOLING - THE COOLING FLUID, DOW CORNING ET-378, FLOWS THROUGH THE GENERATOR AT A MAXIMUM FLOW RATE 2.84 GPM. THE INLET PRESSURE AND TEMPERATURE IS 33 + 0.0 OR -1.0 PSIA AND 210 + 0.0 OR -10.0 °F, RESPECTIVELY. THE MAXIMUM PRESSURE DROP ACROSS THE MACHINE MUST NOT EXCEED 13 PSI.

3.1.5 VACUUM PUMPS WILL BE REQUIRED TO UPLL 1 PSIA PRESSURE OR LESS ON THE GENERATOR CAVITY AND OUTSIDE SEALS.

3.1.6 SPIN TEST - THIS FACILITY WILL BE CAPABLE OF SPINNING THE ROTOR AT A SPEED OF 18000 PLUS OR MINUS 2% RPM FOR A PERIOD OF FIVE MINUTES.

4.0 INSTRUMENTATION

4.1 CALIBRATION

4.1.1 ALL INSTRUMENTS SHALL BE CALIBRATED WITHIN THE PREVIOUS 30 DAYS FROM THE TIME THE TEST IS STARTED TO AN ACCURACY OF PLUS OR MINUS 1% FULL SCALE, AND PLUS OR MINUS 1/4% FULL SCALE FOR SYMMETRY OF CONSTRUCTION TEST.

4.1.2 WATTMETERS, AC AMMETERS, AC VOLTMETERS, AND CURRENT TRANSFORMERS SHALL BE CALIBRATED FOR USE AT 400 CPS.

4.2 ELECTRICAL QUANTITIES - FOLLOWING ARE THE ELECTRICAL QUANTITIES TO BE READ VISUALLY:

(A) LINE TO NEUTRAL VOLTAGE AND LINE TO LINE VOLTAGE, SWITCHED TO ALL LINES OR INDIVIDUAL METERS (0-250 VOLTS RMS AT 400 CPS).
(B) LINE CURRENT (0-500 AMPS RMS AT 400 CPS).
(C) TOTAL 3-PHASE POWER (0-100 KW).
(D) FREQUENCY (0-500 CPS)
(E) FIELD VOLTAGE (0-50 VOLTS DC)
(F) FIELD CURRENT (0-25 AMPS DC)

3-10(VN)
3-17(BW)
3EW(BW)
3-9(BW)2
3-S(VN)
WBO-B2
LA-1
3E(BK)25
5B(50)
PRINTS TO

NEW PER S. J. BELLOWS, OCTOBER 8, 1963

REV 0

PREPARED BY S J Bellows DATE 10/8/63 APPROVED BY C T Fuddy ISSUED 10-8-63

DC3-20 (9-59)

REV 0
718A302 WM SHEET NO. 3 OF 7 SHEETS
SIZE A

4.3 THE IRON-CONSTANTAN THERMOCOUPLE TEMPERATURES SHALL BE MEASURED WITH A BRISTOL MULTIPOINT RECORDER.

4.4. OSCILLOGRAPH TRACES SHALL BE RECORDED WITH A HONEYWELL HELLAND OSCILLOGRAPH.

4.5 HARMONIC VOLTAGE SHALL BE MEASRUED WITH A GENERAL RADIO WAVE ANALYZER.

4.6 HOT AC WINDING RESISTANCE SHALL BE MEASURED USING A SEELY BRIDGE IN CONJUNCTION WITH A G.E. DOUBLE BRIDGE.

5.0 STANDARD TEST CONDITIONS

5.1 THE TESTS WILL BE CONDUCTED UNDER ATMOSPHERE CONDITIONS WHICH EXIST IN THE TEST LABORATORY UNLESS NOTED OTHERWISE.

5.2 COOLING OIL:

(A) TYPE: ET-378
(B) RATE OF FLOW: 2.84 PLUS 0.0 OR MINUS 0.1 GPM
(C) INLET TEMPERATURE: 210 PLUS 0.0 OR MINUS 10.0 °F

5.2.1 BEARING AND SEAL OIL WILL FLOW ACCORDING TO THE CONDITIONS SPECIFIED IN PARAGRAPH 3.1.3.

5.3 ELECTRICAL RATING - CONTINUOUS FULL LOAD RATING AS SPECIFIED BY PARAGRAPH 1.2.

6.0 DATA RECORDING PROCEDURES

6.1 GENERAL - ALL DATA RECORDED VISUALLY MUST BE ENTERED ON THE DATA SHEETS WITHOUT CORRECTION. IF CORRECTIONS MUST BE MADE FOR CALIBRATION, SUCH DATA MUST BECOME A PERMANENT PART OF THE TEST DATA.

6.2 CALCULATIONS - CALCULATED DATA SHALL BE MARKED AS SUCH AND THE METHOD OF CALCULATION NOTED.

6.3 ENTRIES - MAKE ENTRIES ON THE DATA SHEETS NEAT AND LEGIBLE AND KEEP DATA SHEETS CLEAN. RECORD DATA ORIGINALLY ON THE DATA SHEETS.

7.0 ACCEPTANCE TEST - EACH GENERATOR SHALL BE SUBJECTED TO THE ACCEPTANCE TESTS LISTED BELOW:

TITLE OF TEST	PARAGRAPH NO.	REF. AGC-10175, PARA. NO.
EXAMINATION OF PRODUCT	7.1	-------
ROTOR OVERSPEED	7.2	3.3.19.1
RESISTANCE CHECK	7.3	-------
NO LOAD EXCITATION	7.4	-------
PERFORMANCE RATING	7.5	3.3.2
WAVE FORM	7.6	3.3.3

3-9(BW)2
3-EW(BW)
3-17(BW)
3-10(VN)
3-s(VN)
WBO-B2
LA-1
3E(BK)25
5B(50)
PRINTS TO

PREPARED BY S.J. Bellows DATE 10/8/63 APPROVED BY C.T. Fuddy ISSUED 10-8-63

DC3-20 (9-59)

REV 0 NEW PER S. J. BELLOWS, OCTOBER 8, 1963

ACCEPTANCE TEST (CONTINUED)

TITLE OF TEST	PARAGRAPH NO.	REF. AGC-10175 PARA. NO.
SYMMETRY OF CONSTRUCTION	7.9	3.3.4
EXCITATION	7.10	3.3.6
EFFICIENCY	7.7	3.3.7
ELECTRICAL CHARACTERISTICS	7.8	3.3.9
SHORT CIRCUIT CAPACITY	7.8.1	3.3.9.1
OPEN CIRCUIT TIME CONSTANT	7.8.2	3.3.9.2
SHORT CIRCUIT RATIO	7.8.3	3.3.9.3
VOLTAGE DROP	7.8.4	3.3.9.4
HOUSING LEAKAGE	7.13	3.3.15
COOLING	7.5	3.3.17
OVERSPEED/UNDERSPEED	7.11	3.3.19
DIELECTRIC STRENGTH	7.12	3.3.20

7.1 EXAMINATION OF PRODUCT - EACH GENERATOR SHALL BE INSPECTED IN ACCORDANCE WITH THE QUALITY ASSURANCE PROGRAM PLAN FOR THE SNAP-8 GENERATOR. PRIOR TO FINAL ASSEMBLY, INSPECTION AND TEST RECORDS OF EACH SUBASSEMBLY SHALL BE CHECKED TO DETERMINE CONFORMANCE TO APPLICABLE DRAWINGS. ASSEMBLY DATA SHALL BE CHECKED AND RECORDED, AS REQUIRED BY THE INSPECTION PLAN. AFTER COMPLETION OF TESTS, THE GENERATOR SHALL BE INSPECTED TO DETERMINE CONFORMANCE WITH OUTLINE DRAWING 194E691.

7.2 ROTOR OVERSPEED - THE ROTOR OVERSPEED TEST WILL BE CONDUCTED ON A COMPLETED ROTOR WITHOUT THE QUILL SHAFT AND PRIOR TO ASSEMBLY INTO THE GENERATOR. THE ROTOR WILL BE MOUNTED IN A HIGH SPEED TEST STAND AND HEATED BY RADIATION TO 550°F PLUS OR MINUS 50°F AT 12000 RPM. THE ROTOR SPEED SHALL THEN BE INCREASED TO 18000 RPM FOR FIVE MINUTES. AFTER COMPLETION OF THIS TEST, THE ROTOR BALANCE AND OD SHALL BE CHECKED AND RECORDED.

7.3 RESISTANCE CHECK - WINDING RESISTANCES SHALL BE CHECKED, CORRECTED TO 25°C AND SHALL FALL WITHIN THE LIMITS NOTED BELOW:

T1 TO T4	.00550 TO .00575 OHMS
T2 TO T5	.00550 TO .00575 OHMS
T3 TO T6	.00550 TO .00575 OHMS
F1 TO F2	1.49 TO 1.63 OHMS

7.4 NO LOAD EXCITATION - VARY THE FIELD CURRENT FROM 0 TO 30 AMPS RECORDING LINE-TO-NEUTRAL VOLTAGE IN 5 VOLT STEPS AT RATED SPEED. RECORD ALL PHASE AND LINE VOLTAGE AT RATED GENERATOR VOLTAGE. PHASE ROTATION SHOULD BE T1-T2-T3 WHEN ROTATION IS AS NOTED ON THE OUTLINE DRAWING.

3EW(BW)
3-9(BW)
3-S(VN)
3-10(VN
3-17(BW
WBO-B2
LA-1
3E(BK)25
5B(50)
PRINTS TO

PREPARED BY S.J. Bellows DATE 10/8/63 APPROVED BY C.T. Fuller ISSUED 10-8-63

REV 0
718A302 WM SHEET NO. 5 OF 7 SHEETS
SIZE A

7.5 PERFORMANCE RATING - TAKE A STABILIZED FULL LOAD HEAT RUN AS FOLLOWS:

1. THE GENERATOR CAVITY SHALL BE EVACUATED TO A PRESSURE OF 1 PSIA MAXIMUM. THE BEARING OIL FLOW SHALL BE ADJUSTED TO .345 TO .355 GALLONS PER MINUTE OF ET-378 OIL AT A PRESSURE OF 32-33 PSIA AND A TEMPERATURE OF 200° F - 210° F WITH THE GENERATOR SPEED SET AT 12000 RPM. EACH GENERATOR AND ADAPTER DRAIN SHALL BE PROVIDED WITH A VISUAL MEANS OF CHECKING OIL LEAKAGE. THERE SHALL BE NO MEASURABLE OIL LEAKAGE AT ANY OF THESE DRAINS. THE GENERATOR SCAVENGE SYSTEM SHALL PUMP THE OIL OUT OF THE BEARING CAVITY. THE DISCHARGE PRESSURE SHALL BE 4.75 TO 5.0 PSIA.

2. THE GENERATOR SHALL BE COOLED WITH 1600 POUNDS PER HOUR (2.84 GPM) OF ET-378 OIL AT AN INLET PRESSURE OF 33.0 PSIA. THE PRESSURE DROP THROUGH THE OIL SYSTEM SHALL NOT EXCEED 13.0 PSI WHEN THE OIL TEMPERATURE IS 210° F.

3. WITH THE SPEED SET AT 12,000 RPM, THE FOLLOWING LOAD SHALL BE APPLIED:

OUTPUT	80 KVA AT .75 PF LAGGING
VOLTAGE	120/208 VOLTS RMS
CURRENT	223 AMPS (REFERENCE)
FREQUENCY	400 CPS

THE MACHINE WILL BE CONSIDERED STABILIZED WHEN THE STATOR TEMPERATURE RISE AND THE FIELD TEMPERATURE RISE DO NOT INCREASE MORE THAN 2° C IN TEN MINUTES.

4. THE TEST SHALL BE CONTINUED FOR FIFTEEN MINUTES AND THE FOLLOWING DATA SHALL BE RECORDED:

(A) ELECTRICAL OUTPUT VOLTAGE, CURRENT, AND POWER
(B) GENERATOR SPEED AND FREQUENCY
(C) BEARING LUBE OIL INLET AND OUTLET PRESSURE AND TEMPERATURE (2" FROM GENERATOR CONNECTION), AND FLOW.
(D) GENERATOR EXCITATION (LIMITS - 20 AMPS MAXIMUM CURRENT, 20 VOLTS DC MAXIMUM)
(E) PHASE UNBALANCE (LIMIT - 1% MAXIMUM)
(F) WINDING HOT SPOT TEMPERATURE SHALL NOT EXCEED 392° F
(G) VIBRATION OF THE GENERATOR FRAME SHALL BE MONITORED DURING THIS TEST.

7.6 WAVE FORM - THE LINE-TO-LINE HARMONIC VOLTAGES SHALL BE MEASURED BETWEEN 400 CPS AND 10,000 CPS AT 0, 50%, AND 100% LOAD AT 1.0 PF. TEST CONDITIONS SHALL BE AS NOTED IN PARAGRAPH 7.5 EXCEPT LOAD. A GENERAL RADIO WAVE ANALYZER SHALL BE USED TO MEASURE THE INDIVIDUAL HARMONICS. THE TOTAL DISTORATION SHALL BE DETERMINED BY TAKING THE SQUARE ROOT OF THE SUM OF THE SQUARES OF THE INDIVIDUAL HARMONIC VOLTAGE PERCENTAGES AND SHALL NOT EXCEED 7%. THE VOLTAGE REGULATOR SHALL CONTROL THE OUTPUT VOLTAGE FOR THIS TEST.

3EW(BW)
3-9(BW)
3-S(VN)
3-10(VN)
3-17(BW)
WBO-B2
LA-1
3E(BK)25
5B(50)
PRINTS TO

PREPARED BY S. J. Bellows DATE 10/8/63 APPROVED BY C. T. Suddy ISSUED 10-8-63
DC3-20 (9-59)

REV 0 NEW PER S. J. BELLOWS, OCTOBER 8, 1963

7.7 EFFICIENCY - THE GENERATOR EFFICIENCY SHALL BE DETERMINED AT THE CONDITIONS NOTED IN PARAGRAPH 7.5. THE TEST MAY BE RUN CONCURRENTLY WITH THE PERFORMANCE RATING TEST. LOSSES OF THE VOLTAGE REGULATOR AND EXCITER SHALL NOT BE INCLUDED IN THIS DETERMINATION. AT THIS LOAD (FULL LOAD, .75 POWER FACTOR) THE EFFICIENCY SHALL EXCEED 87%. DETERMINE EFFICIENCY FOR 25%, 50%, 65%, 75%, 85%, 95%, AND 105% AT 1.0 PF.

THIS TEST WILL BE PERFORMED ON A 90 HP INDUCTION DYNAMOMETER. THE INPUT TORQUE WILL BE MEASURED ON A HOWE WEIGHTOGRAPH SCALE, WHICH HAS A CAPACITY OF 100 FOOT-POUNDS.

7.8 ELECTRICAL CHARACTERISTICS

7.8.1 SHORT CIRCUIT CAPACITY - WITH THE GENERATOR HOT AS A RESULT OF RUNNING AT RATED LOAD, A THREE PHASE AND SINGLE PHASE SHORT CIRCUIT SHALL BE APPLIED. THE GENERATOR SHALL BE CAPABLE OF DELIVERING 200% OF RATED CURRENT AT RATED SPEED FOR A MINIMUM OF FIVE SECONDS. RECORD EXCITATION FOR A THREE PHASE SHORT CIRCUIT AT ONE PER UNIT AND TWO PER UNIT CURRENT.

7.8.2 OPEN CIRCUIT TIME CONSTANT

(A) REQUIREMENT - THE ALTERNATOR, OPERATING AT STEADY-STATE TEMPERATURE, SHALL HAVE AN OPEN CIRCUIT TRANSIENT TIME CONSTANT (T-DO) NOT EXCEEDING 0.5 SECOND.

(B) TEST APPARATUS - A MINNEAPOLIS HONEYWELL VISICORDER SHALL BE USED TO RECORD ONE-PHASE VOLTAGE, FIELD CURRENT, AND FIELD VOLTAGE. A GOOD QUALITY KNIFE SWITCH SHALL BE USED TO SHORT THE FIELD WINDING. CARE MUST BE TAKEN TO REDUCE THE IMPEDANCE OF THE FIELD LEADS TO A MINIMUM. THE LEADS SHOULD BE SHORT AND THE KNIFE SWITCH SHOULD PROVIDE A GOOD CONTACT AREA WHEN CLOSED.

(C) TEST PROCEDURE - THE NO LOAD PHASE VOLTAGE OF THE GENERATOR SHALL BE ADJUSTED TO 120 VOLTS. THE VISICORDER SHALL BE USED TO RECORD THE SHORT CIRCUIT CURRENT OF THE FIELD USING A CHART SPEED OF 50 INCHES PER SECOND.

THE FUSE USED TO PROTECT THE FIELD EXCITATION SUPPLY SHOULD HAVE A CURRENT RATING SLIGHTLY ABOVE THE FIELD CURRENT REQUIRED TO PRODUCE RATED NO LOAD PHASE VOLTAGE.

THE METHOD OF CALCULATING THE DIRECT-AXIS TRANSIENT OPEN-CIRCUIT TIME CONSTANT IS DESCRIBED BY PARAGRAPH 1.910 OF AIEE TEST CODE FOR SYNCHRONOUS MACHINES, NO. 503.

7.8.3 SHORT CIRCUIT RATIO - THE RATIO OF THE FIELD CURRENT AT NO LOAD, RATED VOLTAGE (PARAGRAPH 7.4) TO THE FIELD CURRENT FOR A THREE PHASE ONE PER UNIT SHORT CIRCUIT CURRENT (PARAGRAPH 7.8.1) SHALL BE DETERMINED. THIS RATIO SHALL EXCEED 0.25.

3EW(BW)
3-9(BW)2
3-S(VN)
3-10(VN)
3-17(BW)
WBO-B2 LA-1
3E(BK)25
5B(50)
PRINTS TO

REV 0
718A302 WM SHEET NO. 7 OF 7 SHEETS
SIZE A

7.8.4 VOLTAGE DROP - WITH THE GENERATOR STABILIZED AT NO LOAD WITH RATED COOLING, A THREE PHASE, 1/2 PER UNIT LOAD AT .9 LAGGING POWER FACTOR SHALL BE SUDDENLY APPLIED. THIS TEST WILL BE CONDUCTED WITH THE REGULATOR DESIGNED TO MEET THE REQUIREMENTS OF AGC SPECIFICATION 10174. THE VOLTAGE SHALL NOT DROP BELOW 70% OF RATED VOLTAGE AS A RESULT OF LOAD APPLICATION DESCRIBED.

7.9 SYMMETRY OF CONSTRUCTION - THE DIFFERENCE BETWEEN THE HIGHEST AND LOWEST VOLTAGE AT THE GENERATOR TERMINALS SHALL BE MEASURED FOR EACH OF THE FOLLOWING TESTS:

7.4	NO LOAD EXCITATION	NO LOAD	
7.5	PERFORMANCE RATING	FULL LOAD	.75 PF
7.6	WAVE FORM	FULL LOAD	1.0 PF

THE DIFFERENCE BETWEEN THE HIGHEST AND LOWEST PHASE VOLTAGE SHALL NOT EXCEED 1.0% FOR THE NOTED TESTS.

7.10 EXCITATION - EXCITATION AT FULL LOAD .75 PF WILL BE CHECKED AS PART OF PERFORMANCE RATING PARAGRAPH 7.5. EXCITATION CURRENT SHALL BE 20 AMPERES MAXIMUM AND VOLTAGE SHALL BE 50 VOLTS DC MAXIMUM.

7.11 GENERATOR OVERSPEED/UNDERSPEED - RATED LOAD SHALL BE APPLIED TO THE GENERATOR AT 11,400 RPM AND 13200 RPM FOR FIVE MINUTES AT EACH SPEED. TEST CONDITIONS AND LIMITS SHALL BE IN ACCORDANCE WITH PARAGRAPH 7.5 EXCEPT FOR SPEED, FREQUENCY AND EXCITATION LIMITS.

7.12 DIELECTRIC STRENGTH - WHIEL THE GENERATOR IS HOT AS A RESULT OF TESTING, THE FOLLOWING VOLTAGES SHALL BE APPLIED FOR ONE MINUTE (OR 120% OF NOTED VALUES FOR 1 SECOND).

MAIN STATOR	PHASE TO PHASE	1416 VOLTS A-C RMS
	PHASE TO GROUND	1240 VOLTS A-C RMS
FIELD COIL	COIL TO GROUND	500 VOLTS A-C RMS

7.13 HOUSING LEAKAGE - THE DRIVE END OF THE GENERATOR SHALL BE ADEQUATELY SEALED WITH A TEST FIXTURE. THE LEAK DETECTOR SHALL BE CONNECTED TO ALL DRAIN PORTS SO THAT ALL GENERATOR CAVITIES MAY BE EVACUATED. WHEN THE REQUIRED PRESSURE IS ATTAINED, THE GENERATOR WILL BE ENCASED IN A BLANKET OF HELIUM BY A SUITABLE MEANS AND THE HELIUM LEAKAGE INTO THE GENERATOR SHALL BE DETERMINED. THE MAXIMUM ALLOWABLE LEAK RATE SHALL BE 1 x 10 -7 CUBIC CENTIMETERS (CC) OF HELIUM PER SECOND. THE TEST WILL BE CONDUCTED AT ROOM TEMPERATURE.

3EW(BW)
WBO-B2
LA-1
3-17
3-9(BW)2
3-S(VN)
3-TO(VK)
3E(BK)25
5B(50)
PRINTS TO

NEW PER S. J. LLOWS, OCTOBER 8, 1963

REV

PREPARED BY S.J. Bellows DATE 10/8/63 APPROVED BY C.T. Fuddy ISSUED 10-8-63

DC3-20 (9-59)

AEROJET-GENERAL CORPORATION